UNIVERSITAT DE BARCELONA

The Effect of Intermittent Hypobaric Hypoxia and Exercise on the Recovery of Induced Skeletal Muscle Damage in Trained Laboratory Rats: Performance Evaluation, Plasma Markers and M. Soleus Differential Gene Expression

El efecto de hipoxia hipobárica intermitente y ejercicio de la recuperación del daño muscular esquelético inducido en ratas de laboratorio entrenadas: evaluación de rendimiento, marcadores plasmáticos y expresión génica diferencial del M. Soleus

Juan Gabriel Ríos Kristjánsson

The Effect of Intermittent Hypobaric Hypoxia and Exercise on the Recovery of Induced Skeletal Muscle Damage in Trained Laboratory Rats:

Performance Evaluation, Plasma Markers and M. Soleus Differential Gene Expression

Juan Gabriel Ríos Kristjánsson

Doctoral Thesis, 2016

UNIVERSITAT DE BARCELONA

FACULTAT DE BIOLOGIA
DEPARTAMENT DE BIOLOGIA CEL·LULAR, FISIOLOGIA I IMMUNOLOGIA

THE EFFECT OF INTERMITTENT HYPOBARIC HYPOXIA AND EXERCISE ON THE RECOVERY OF INDUCED SKELETAL MUSCLE DAMAGE IN TRAINED LABORATORY RATS: PERFORMANCE EVALUATION, PLASMA MARKERS AND M. SOLEUS DIFFERENTIAL GENE EXPRESSION

TESIS DOCTORAL

Juan Gabriel Ríos Kristjánsson

UNIVERSITAT DE BARCELONA
FACULTAT DE BIOLOGIA
DEPARTAMENT DE BIOLOGIA CEL·LULAR, FISIOLOGIA I IMMUNOLOGIA

THE EFFECT OF INTERMITTENT HYPOBARIC HYPOXIA AND EXERCISE ON THE RECOVERY OF INDUCED SKELETAL MUSCLE DAMAGE IN TRAINED LABORATORY RATS: PERFORMANCE EVALUATION, PLASMA MARKERS AND M. SOLEUS DIFFERENTIAL GENE EXPRESSION.

EL EFFECTO DE HIPOXIA HIPOBÁRICA INTERMITENTE Y EJERCICIO EN LA RECUPERACIÓN DEL DAÑO MUSCULAR ESQUELETICO INDUCIDO EN RATAS DE LABORATORIO ENTRENADAS: EVALUACIÓN DE RENDIMIENTO, MARCADORES PLASMATICOS Y EXPRESIÓN GÉNICA DIFERENCIAL DEL M. SOLEUS.

Memoria presentada por:

Juan Gabriel Ríos Kristjánsson

Para optar al Grado de:

Doctor por la Universidad de Barcelona

Tesis realizada bajo la dirección del Dr. Ginés Viscor Carrasco del Departamento de Biología Celular, Fisiología e Inmunología, Facultad de Biología.

Adscrita al Departamento de Biología Celular, Fisiología e Inmunología, Facultad de Biología, Universidad de Barcelona, Programa de Biomedicina.

Dr. Ginés Viscor Carrasco

Sr. Juan Gabriel Ríos Kristjánsson

Barcelona, septiembre 2016

«The effect of intermittent hypobaric hypoxia and exercise on the recovery of induced skeletal muscle damage in trained laboratory rats: Performance evaluation, plasma markers and m. soleus differential gene expression.

El efecto de hipoxia hipobárica intermitente y ejercicio en la recuperación del daño muscular esquelético inducido en ratas de laboratorio entrenadas: Evaluación de rendimiento, marcadores plasmáticos y expresión génica diferencial del m. soleus»

El autor ha sido financiado por el Gobierno de España a través del Ministerio de Ciencia e Innovación — Subprograma Ayudas FPI-MICINN (BES-2011-044293) vinculado al proyecto nacional 'Efecto de la hipoxia hipobárica intermitente en la recuperación del daño muscular inducido en ratas de laboratorio' (DEP2010-22205-C02-01).

El autor realizó una estancia en el Centre of Human & Aerospace Physiological Sciences del King's College London, Inglaterra, como parte de la obtención de la mención europea para el grado de doctor.

Acknowledgments

When studying for my undergraduate degree in biochemistry, back at the University of Iceland, I had an interest in many aspects of sciences, and I took an elective practical module about experimental animals; thinking that realistically they would never be part of my future studies, given the limited opportunities. Little did I know at the time, that with continuing studies at the Department of Physiology at the University of Barcelona, I might have the ever-so unique opportunity to call myself a rat personal trainer, which I can see developing into a certification in rat lifestyle coaching.

First I would like to thank my tutor and supervisor, Ginés Viscor Carrasco, who somehow understood my gibberish Spanish and was open to taking me on board, yet, allowed me to grow independently. Without his guidance and his trust in my abilities, I would not have had the opportunities to develop my academic journey as far as I have and on so many different levels.

To my colleagues: Juana Valentin, David Rizo, Cristian Nuñez, Debora Coimbra, J Ramón Torrella, Teresa Pagès and Ginés Viscor, who put up with my extensively codified ideas and made my experience in the laboratory memorable.

To David Andrew Green, for taking a chance and accepting me into his team, for his trust in me and his advisory support, and making my experience at CHAPS/KCL an unforgettable part of my academic journey.

To my family: my parents, Kristján Eldjárn Jóhannesson and Helga Aðalbjörg Jóhannsdóttir; my sisters and brother, Aníta Eldjárn, Kristján Eldjárn, Karen Mist and 'adopted sister', Yesmine; for their patience, support and encouragement throughout the stressful times.

Moreover, especially to Karen Mist Kristjánsdóttir, Yesmine Olsson, Eva Guðríður Guðmundsdóttir and Lucy Robbins. Their able assistance, understanding and support have enriched my academic years exponentially.

Many thanks.

Table of Contents

List of Abbreviations

Ab	Antibody
ADP	Adenosine diphosphate
Ag	Antigen
ATP	Adenosine triphosphate
Ca^{2+}	Calicum (ion)
cDNA	complementary DNA
CK	Creatine kinase
DNA	Deoxyribonucleic acid
ELISA	Enzyme linked immunosorbent assay
Hb	Haemoglobin
HIF	Hypoxia-inudicble factor
IP	Intraperitoneal
LoD	Limit of detection
LoL	Limit of linearity
LoQ	Limit of quantification
Mb	Myoglobin
mRNA	messenger RNA
O_2	Oxygen (molecule)
PCR	Polymerase chain reaction
Pi	Inorganic phosphate
qPCR	Quantitative PCR
RNA	Ribonucleic acid
RoQ	Range of quantification
rRNA	Ribosomal RNA
RSD	Relative standard deviation
RT-qPCR	Reat time qPCR
SD	Standard deviation
SEM	Standard error of mean
Sess	Session [*specific for this dissertation*]
TnC	Troponin C
TnI	Troponin I
TnT	Troponin T
VEGF	Vascular endothelial growth factor
VO_2max	Maximum oxygen uptake

1 Introduction

1.1 Overture

The skeletal muscle is a very adaptable organ responding evidently to the level of stress, or lack of stress, under which it is put. One of the most classic examples that reflects the degree of which the skeletal muscle adapts concerns its response to exercise-training. With the stress load of exercise, the 'normal' non-exercise physiological equilibrium, homeostasis, of various systems in the body, are tipped off balance. A sufficient long-term level of exercise would then shift or optimise these systems to be in balance with the 'new' normal, which means that adaptation is in progress (Kraemer, Fleck and Evans, 1996; Lambert and Borresen, 2006). During this process, regardless of how relatively short or long it may be, the performing individual is potentially subject to some level of skeletal muscle injury.

The cause of the injury can be a combination of many different factors, some of which, differentiate between conditions, within which either elite athletes or recreational athletes are training or competing. One could say the training conditions, referring to the environment, the equipment, the trainer, the choice and setup of exercise programme, the periodic goals, etc. are more controlled and optimised for the elite athlete. Meanwhile, the recreational athlete whose drive might be principally of interest, enthusiasm and health benefits has less controlled training conditions and less optimised support system for guidance and prevention. Whilst these are relative parameters, it is quite reasonable to consider that the population of recreational athletes is more susceptible to a skeletal muscle injury in comparison with the population of elite athletes. Although the scope of this text is not to address the difference between these two groups *per se*, it is necessary to bear in mind the individual variability of performance along with different levels of what would be classified as a skeletal muscle injury. The optimisation or the lack of optimisation of the aforementioned training conditions also has its influence on how the variability is reflected within these two populations, even if the groups could be supposedly similar. These wide differences in muscle injuries amongst athletes (the degree of damage, the anatomical localisation, and the functional consequences) make it difficult to reach conclusive results from an epidemiological analysis.

In the following chapters of the introduction, we will start with looking at the physiology of the skeletal muscle, its exercise-training, injury and regeneration, but most importantly, the application of hypoxia in the recovery of a tissue damage. We will then later look at the practical aspects of using plasma markers, gene expression profiles and simple weight measurements to trace a recovery profile. Throughout the text and to conclude the introduction, we will consider various angles to raise experimental integrity, most of which can be employed via internal quality control

by the investigative team itself. The dissertation may seem to touch upon various topics; still, an experimental strategy in physiological research that utilises various scientific techniques needs to successfully orchestrate all aspects in a harmonised manner. — On those musical notes, this pretext is titled ‘overture’ and summaries that conceptualise bigger sections are titled ‘coda’.

1.2 The Skeletal Muscle: From Injury to Recovery

1.2.1 The Skeletal Muscle and Its Physiology in Brief

1.2.1.1 The Macro- and the Microscopic Anatomy of the Skeletal Muscle Contraction

The skeletal muscles are the contractile portions of an organism, attached through the fascia via tendons to the periosteum of bones and voluntarily produce movements or exert forces. The muscle structure is surrounded by different layers of the fascia, with the outermost layer being the epimysium encircling the organ as a whole and perimysium surrounding bundles (or fascicles) of several muscle fibres (or muscle cells), each composed of fused myocytes. Within the fascicles, endomysium separates individual cells and connects to the basement membrane which is closest to the cell membrane (or the sarcolemma) and acts as a supporting network. It carries capillaries that bring fresh blood with oxygenated haemoglobin and nutrients, etc. to the muscle fibres, which are left (to some extent) with waste products and deoxygenated haemoglobin molecules. It, furthermore, carries nerves with motor neurons that transmit action potentials to the fibres via synapses on the motor end-plate, and sensory neurons informing about the organ's postural and contractile status. The motor end-plate on the sarcolemma is optimised with receptors to react to the acetylcholine neurotransmitter, diffusing from the synaptic bulb of the neurone axon terminal and across the synaptic cleft. The receptors alter electrolyte composition of the immediate environment on both sides of the sarcolemma, the exosol and the cytosol, through the opening of specific ion channels, resulting in a depolarised membrane potential with the action potential propagating along the membrane.

The sarcolemma has dents of tubular network that extends the extracellular surface in contact with the cytosol (or the sarcoplasm) (Huxley and Taylor, 1958). The sarcoplasm contains glycogen (in glycogen granules), myoglobin to store and transport oxygen, creatine kinase to mobilise energy supplies, organelles such as the mitochondria, eccentrically localised nuclei and the Ca^{2+}-containing sarcoplasmic reticulum encircling the contractile organelles (the myofibrils). The myofibrils extend throughout the length of the muscle cell/fibre linked to the sarcolemma via dystrophin (a structural protein). Moreover, the myofibrils have interactive and highly organised protein compartments called sarcomeres arranged between the polarised ends of the myofibrils, within each organised filament protein structures lie, called myofilaments. Opposite ends of each sarcomere are marked by a dense protein plate called Z-discs. From both sides contractile proteins (the thin filaments), extend towards the middle of the sarcomere, though bluntly ending, supported and linked to the Z-disc by the structural proteins nebulin and α-actinin. Actin has binding sites for the other

contractile protein filament, myosin (the thick filaments), which is continuous through the middle of a sarcomere without extending the entire length from Z-disc to Z-disc. The repetitive hexagonal arrangement of actin filaments surrounding each myosin filament can be seen in a transverse section where the filament structures overlap within the sarcomere (Huxley, 1953). The myosin filaments are centrally linked and held in place via myomesin which forms the M-line of a sarcomere — in the middle where myosin is not overlapped with actin. The M-line is linked to both Z-discs with titin, which also stabilises the myosin filaments and, furthermore, attaches to α-actinin.

The interactions between the contractile proteins, actin and myosin, are the mechanical basis of a contraction occurring when myosin heads of the myosin filaments are linked to the binding sites on actin. These binding sites are mechanically regulated by tropomyosin which is regulated by the troponin complex (better explained in chapter 1.4.3.3) which, in turn, are regulated by Ca^{2+}. — Recall the existence of Ca^{2+}-containing sarcoplasmic reticulum. — The sarcolemma's action potential activates a voltage-dependent release of Ca^{2+} from the sarcoplasmic reticulum allowing it to bind to the troponin complex. The Ca^{2+}-binding facilitates the movement of tropomyosin away from the binding sites on actin for myosin. At this stage we have now coupled the cellular excitation (via the action potential) with the contractile properties; referred to as the excitation-contraction coupling (Ríos, Ma and González, 1991; Franzini-Armstrong and Jorgensen, 1994). The myosin head structure of myosin contains an ATPase and can bind ATP that is immediately hydrolysed (ADP + P_i) but hanging on to the phosphate, leaving the structure energised. When the myosin heads can bind to actin, forming the cross-bridges, they release the phosphate group, perform the power stroke, a 'forward' movement of the myosin head, which structurally opens and releases the ADP. The cross-bridges remain linked until another ATP molecule binds to the myosin heads, at which point, they detach from actin. In a structurally favourable position, the energised myosin head binds to the next binding site along the actin filament (Page and Huxley, 1963; Huxley and Simmons, 1971; Rayment *et al.*, 1993). The cross-bridges generate force as the movement cycle slides actin past myosin, on both ends, towards the centre of the sarcomere, bringing the Z-discs closer together, and the sarcomere shortens. For all these actions a sarcomere is called the basic functional unit of a myofibril.

1.2.1.2 The Contractile Attributes of the Skeletal Muscle

In a simplified manner, the muscle contractile function can be described with two variables, one that describes its length or the change in length and the other that describes the tension or the change in tension. The tension in the muscle is equal to the force it is generating which, in turn, is

proportional to the number of myofibrils and the contractile filaments overlapping length that are partaking in the contraction work (Huxley and Niedergerke, 1954; Gordon, Huxley and Julian, 1966). If the length of the whole muscle, or isolated myofibril, is kept constant during a contraction, that is, the contraction does not alter the immediate size, we are perceiving an isometric contraction which produces static muscle work. On the contrary, if the tension is kept constant during a contraction (via applied stable load) throughout a length-change, we perceive an isotonic contraction which produces dynamic muscle work. This behaviour is due to the presence of a series of elastic components (such as tendons) with a great mechanical compliance. The skeletal muscle, in addition to its contractile (plastic) components, namely the sarcomeres, is endorsed with both elastic and viscous components due to the physical properties of the other tissues surrounding the myofibrils. The elastic components are connected in series or parallel to the contractile apparatus. The parallel elastic elements provide the muscle with passive elastic properties derived from their membranous components (from sarcolemma to fascia), whereas, the series elastic components give it a passive elasticity derived from the action of contractile elements on tendons when the muscle is stretched. The viscous components (nervous tissue, capillaries) hinder the movement of the muscle but are still essential for a correct function of the system. These structural arrangements combined render the muscle with remarkable biomechanical properties (Levin and Wyman, 1927; Mathur *et al.*, 2001).

The dynamic range of a striated muscle is quite straight forward (or backwards, for that matter). We can produce a concentric action, where the sarcomeres are shortening, and the fibres are producing a force that overcomes an external resistance. Alternatively, the opposite occurs with an eccentric action, where the fibres are producing force but the external resistance, moving in the opposite direction of the shortening of the sarcomeres (Rivera-Brown and Frontera, 2012) slows down or prevent the lengthening of muscle fibres. The fibres, furthermore, contract and relax at different speeds due to different cellular composition and how quickly the ATPase in the myosin heads hydrolyses ATP (Karp, 2001). Red fibres are more capillarised, with a higher concentration of myoglobin and have more and larger mitochondria; thus, mainly generate ATP via aerobic cellular respiration. The combination of these factors, along with generally smaller cellular diameter, makes the fibres more fatigue-resistant. Their myosin head-ATPase rate is relatively slow, resulting in a slower paced contraction cycle, hence, bear the name of slow oxidative fibres (type I). Fast oxidative-glycolytic fibres (type IIa) are also red in their appearance as they have similar properties as the type I fibres, apart from being slightly larger in diameter and having high intracellular glycogen content meaning that they, furthermore, generate ATP via anaerobic glycolysis. Moreover, the myosin heads have an ATPase that hydrolyses ATP at a greater rate in comparison with type I fibres

(Bottinelli *et al.*, 1994; Capitanio *et al.*, 2006), making type IIa contract at higher speed. Lastly, in contrast to fibre types I and IIa, fast glycolytic fibres (type IIb) are white in colour and sparsely capillarised. They have high intracellular glycogen levels and form ATP via glycolysis as their main metabolic route, having simultaneously low myoglobin content and few mitochondria, thus, adapted for intense anaerobic work but fatigue quickly. These fibres are the largest in diameter, containing many myofibrils which endorse them with more powerful contractions in comparison with the other fibre types, and a fast contraction as the myosin head-ATPase hydrolyses ATP even quicker than in fibre type IIa (Bottinelli *et al.*, 1994). The majority of skeletal muscles are heterogeneous because they contain all of these three main types of fibres and, furthermore, hybrid fibre types (for example, type IIx between type IIa and IIb). The proportions between the fibre types reflect the general action carried out by the muscle as a whole (Pette and Staron, 2000). The postural muscles are rich in slow fibres, whereas muscles recruited only for quick and potent actions usually have a large portion of the fast contracting fibres.

1.2.2 Exercise-Training and Skeletal Muscle Injury

1.2.2.1 Different Types of Skeletal Muscle Exercise-Training

Skeletal muscle can be markedly affected by exercise training reflected in both structural and biochemical changes along with other physiological characteristics such as: altered blood flow; increased heart rate, breathing rate and sweat rate; secretion of stress hormones and increased body temperature; and increased oxygen consumption and glycolytic flux (Lambert and Borresen, 2006). The nature of the exercise, regarding duration and intensity, conducts the level of different changes, potentially occurring as an adaptation to different types of physical stress (Coyle, 2000; Garber *et al.*, 2011), making the end goal a key factor in determining the structure of the exercise-training. Still, in the work of Häkkinen *et al.* (2003), whilst the authors reiterate the divergent nature between the two variables, duration and intensity, for endurance-focused training or strength-focused training respectively; they also emphasise that they do not have to be worked on entirely separately. The preferred parameter to evaluate endurance training is generally the maximum oxygen uptake, $\dot{V}O_{2,max}$. In the work of Bassett and Howley (2000), the authors review the limiting factors for $VO_{2,max}$, which are indeed the central and peripheral training-related changes (mentioned above). The central factors concern the pulmonary system's diffusing capacity to saturate the arterial blood with O_2; the maximal cardiac output via the stroke volume and the velocity of the blood flow; and the oxygen carrying capacity of the blood via the concentration of haemoglobin (Hb) which carries the O_2. The peripheral factors concern the characteristics of the skeletal muscle

in terms of the PO_2 diffusion gradient over the surface of the O_2-delivering red blood cells and the sarcolemma facilitated by the mitochondrial O_2 uptake (Honig, Connett and Gayeski, 1992) which, in turn, is influenced by the increased mitochondrial mass by means of exercise (Essig, 1996). Furthermore, the surface area and the transit time is augmented with increased capillary density as a response to training (Saltin, 1985).

Continuous or repeated eccentric work of a muscle that is generally unaccustomed to the work is likely to be felt weak as a primary consequence of a muscle damage. Whilst pain, tenderness, swelling and stiffness 'may be secondary manifestations of acute inflammation triggered by some aspect of the muscle damage' (Armstrong, Warren and Warren, 1991 and Smith, 1991 cited in Allen, 2001, p. 311).

1.2.3 The Physical Damage in Exercise-Induced Skeletal Muscle Injury

A clear definition of what accounts for skeletal muscle injury is somewhat still a debate. In their review, Brancaccio, Lippi and Maffulli (2010) divide the types of injury into two groups: indirect and direct damage. Whilst the authors generally assign the indirect type as the result of clinical and pathological conditions, such as drug use, hyperthermia, electrolyte alterations or pathogenic infections; they classify the direct muscle injury as more trauma and exercise related. The direct muscle injury is, in turn, defined as a loss of muscle function caused by the physical disruption of muscle structures involved in producing or transmitting force (Proske and Allen, 2005; Slater *et al.*, 2005; Tiidus *et al.*, 2008). With a focus on the exercise-induced injuries, the physical disruption of the skeletal muscle fibre can be defined even further depending on where the damage takes place in the macro- or the microstructure. Although this is also true for trauma-induced injuries, we will leave those for more macro-level disruptions whilst the exercise-induced damage is often recognised to be more subtle.

When considering the microstructure, or the cell structure, the spotlight is naturally directed towards disruption within the functional units of the contraction, the sarcomeres, or proximal disruptions that cause relaying effects. The notion of sarcomere disruption is certainly not a new one. Embedded within normal units, displaced sarcomeres have been observed along with disrupted Z-disks and half-disrupted sarcomeres, reported in the work of Newham *et al.* (1983) — and throughout the years, the increased mechanical loading and longer muscle fibre length have been linked to a higher sarcomere disruption in a single eccentric-contraction studies (Brown and Hill, 1991; Talbot and Morgan, 1998). Furthermore, damages to other cytoskeletal elements also facilitate the disruption of the sarcomeres, given that they contribute to the integrity of the

myofibrillar structure, for example, the disruption of desmin (Lieber, Thornell and Fridén, 1996) and dystrophin (Komulainen *et al.*, 1998). The sarcolemma is also likely to get disrupted, potentially allowing the intracellular components to seep into the blood which can be detected as markers of injury, as further discussed in Chapter 1.4. Studies have, furthermore, revealed that fast glycolytic fibres (type IIb) are more easily disrupted in comparison with slow fibres (type Ia) in particular. The reason relates to both the rigorous effects in fast fibres from metabolic inability to regenerate ATP and perhaps more cytoskeletal structural support within the slow muscle fibres (Friden, Sjostrom and Ekblom, 1983, cited in Patel *et al.*, 1998; Patel et al., 1998).

Research started to focus on eccentric-contraction induced injury once studies revealed that the damages it causes were greater in comparison with concentric-contraction induced injury (Davies and White, 1981; Friden, Sjostrom and Ekblom, 1983, cited in McCully and Faulkner, 1985). McCully and Faulkner (1985), further established this notion when they demonstrated the link between the higher level of force loss and histological damage to eccentric contraction in comparison with concentric and isometric contraction. Since then, the mechanical properties of eccentric contraction have been found to play the key role in injuries (Warren *et al.*, 1993) and, as an experimental model, are now considered particularly injurious for skeletal muscle.

Given that the disruption of parts of the skeletal muscle fibres appears to be fairly scattered, even when the eccentric-contraction model is used, it seems quite puzzling that relatively more decreased force measures do not seem to be proportional to the overall structural damage. Investigators have observed that the eccentric-contraction model also alters the structure of the T-tubules (Takekura *et al.*, 2001; Yeung *et al.*, 2002), which in turn might impair the excitation-contraction coupling. This might, moreover, contribute to loss of calcium homeostasis, given that the 'coupling lies in the junctions between the T-tubules and the sarcoplasmic reticulum' (Ingalls *et al.*, 1998). With a focus on the coupling alterations, Warren *et al.* (2001) claim they are indicative of playing a key role in strength loss with an injury.

1.2.3.1 Repairing the Damaged Skeletal Muscle Fibre

As mentioned above, when skeletal muscle suffers an exercise-induced injurious event some muscle fibres lose part of their internal structural integrity and the sarcolemma can be disrupted. Local nuclei die as part of the fibre's localised necrosis, leaving a 'gap' filled up with haematoma initiating inflammatory reaction (Carlson and Faulkner, 1983; Hurme *et al.*, 1991). Neutrophils enter the injured area releasing free radicals, that target the cellular debris for phagocytosis, and secrete pro-inflammatory cytokineases, promoting the inflammation (Wiedow and Meyer-Hoffert, 2005).

Migrating macrophages release digestive enzymes that break down extracellular matrix and debris, which is also aided by the fibre's own lysosomes. The disrupted sarcolemma activates satellite cells, which are myogenic precursor cells, located between the sarcolemma and the basal lamina, and they start to differentiate into myoblasts. The cells align themselves on the basal lamina and fuse into myotubes and continue to differentiate and synthesise myofibrillar proteins (Hawke and Garry, 2001; Chargé and Rudnicki, 2004). With time the nuclei start to get pushed towards the periphery and will start to appear like a mature skeletal muscle fibre. To begin with, the fibre will not be able to contribute to the contraction force as before damage, still, as mentioned earlier, it is very adaptable, and Donovan and Faulkner (1987) discovered that regenerating fibres adapt even more rapidly in comparison with the already existing ones.

Some biochemical pathways of inflammation, in relation to regenerating muscle fibre, are specific to the general actions of leukocytes, for example, in common with their 'actions' in wound healing. In Chapter 1.5.2, these processes behind the regeneration of a skeletal muscle fibre and the inflammation will be revisited in relation to their gene expression profiles.

1.2.4 Hypoxia and Exercise as Rehabilitation to Actively Improve Skeletal Muscle Fibre Regeneration

Active rehabilitation via exercise has been backed up with experimental evidence (Kannus *et al.*, 2003; Järvinen *et al.*, 2005), to be beneficial to the regeneration of the injured skeletal muscle. Although immediate immobilisation is necessary after injury, mobilisation should start as soon as possible, refraining from high-intensity exercise to avoid re-rupture. The early onset of exercise is crucial to the induction of the appropriate molecules and the correct orientation of the regenerating myofibres (Kääriäinen *et al.*, 2001; Kannus *et al.*, 2003; Järvinen *et al.*, 2005) along with augmented mobilisation of progenitor cells with exercise (Möbius-Winkler *et al.*, 2009). Hence, totally passive rehabilitation is therefore not recommended (Hurme and Kalimo, 1992; Kääriäinen *et al.*, 2000) although immobility will not impede the cell from regenerating.

Furthermore, intermittent hypoxia exposure has been observed to augment the angiogenic effects (Panisello *et al.*, 2008) and to increase mobilisation of circulating stem cells (Serebrovskaya *et al.*, 2011). However, Viscor *et al.* (2009) demonstrated that circulating stem cells count could be improved significantly after acute hypoxia in combination with muscle electrostimulation. These findings point towards the potential benefits of the aforementioned factors which could improve the regeneration process of an injured skeletal muscle. Let us have a closer look at what is meant by hypoxia and what that entails.

1.2.4.1 Hypoxia

Hypobaric Hypoxia and Normobaric Hypoxia

Starting with atmospheric pressure and how altitude and temperature affect it in comparison with a sea level reference (normobaria); one needs to consider that with altitude the atmosphere gets thinner and, therefore, the overall pressure exerted by the gas molecules is, in turn, reduced (hypobaria). This means that atmospheric pressure decreases as a function of increased altitude. Furthermore, as the gas molecules weigh down on and compress the ones beneath them, the change in the atmospheric pressure with altitude is steeper closer to the surface of the earth. Moreover, as pressure decreases with lowering temperature, the decreasing rate of atmospheric pressure with altitude is enhanced even further as temperatures drop with altitude as well. These variables are described in the ideal gas law incorporating the classic Boule's and Charles' laws regarding the relationship between pressure, volume and temperature. The atmosphere, being a mixture of several molecules, has its proportion of oxygen (O_2) at about 20.95% and, apart from the water vapour, its gas composition is remarkably stable with altitude. Thus, with respect to the gases of physiological importance (oxygen, carbon dioxide and nitrogen) the concentration is uniformly decreasing but not the fractional concentration between these molecules. The atmospheric pressure is the sum of the partial pressures exerted by these individual gases, each exerting pressure in relation to its own concentration (as per Dalton's law). (Schmidt-Nielsen and Duke, 1997; West, Schoene and Milledge, 2007).

In general terms, hypoxia refers to a low quantity (or concentration, for a more relative reference) of O_2, that is, a reduced partial pressure of O_2. With altitude, as the barometric pressure decreases (hypobaria) reflecting the reduced total atmospheric pressure, the partial pressure of O_2 has simultaneously decreased, that is, hypobaric hypoxia. Normobaric hypoxia is essentially a play on lowering the O_2 concentration on a sea level atmospheric pressure. The consequence of either application would be reduced inspired pressure of oxygen resulting in hypoxemia within the body, meaning, less oxygenated arterial blood delivered to tissues, therefore, less oxygen for cellular respiration. An experimental analogue for hypobaric hypoxia requires reducing the total barometric pressure with air suction of a confined space with regulated vacuum pumps. The concentration of each gas molecule is equally reduced, hence the partial pressure of O_2 is reduced. The analogue setup for normobaric hypoxia would aim to reduce the concentration of O_2 alone (resulting in the drop of its partial pressure) but replacing it with an inert gas (for example nitrogen) to maintain the total barometric pressure at normobaric levels. Exposure to these conditions, natural or experimental (simulated), just as when performing exercise, is an exposure to a physiological stress

and a cascade of reactions which take place with the intention to keep homeostasis. The nature and the level of the response are dependent on the duration and the intensity of the exposure, where here, the intensity refers to the O_2 partial pressure difference with reference to a normoxic value of about 150 mm Hg (Conkin and Wessel, 2008).

The Types and the Effects of Hypoxia Exposure

A short one-time exposure is normally classified as acute hypoxia and triggers immediate physiological responses. A chronic hypoxia exposure is a prolonged exposure (and as long as it does not induce pathological effects) promotes acclimatisation in natural circumstances. The corresponding adaptation in laboratory condition is referred to as acclimation (Schmidt-Nielsen and Duke, 1997; Hochachka and Somero, 2002). An intermittent hypoxia exposure refers to alternating between hypoxic and normoxic conditions, and in controlled settings, seeking the benefits of favourable adaptations to the hypoxic environment with exposures that are short but relatively intense (Beidleman *et al.*, 2004). It is, furthermore, necessary to consider non-atmospheric related types of hypoxia experiences on a tissular level, even though those can be caused or in combination with external factors (such as atmospheric pressure change). Let us consider, for example, reduced or restricted blood flow (ischemia) causing insufficient delivery of O_2 to tissues. Restricted blood flow due to contracting big muscle groups can create a hypoxic environment for smaller tissues during exercise, and furthermore, the metabolic need for O_2, enforced by high-intensity exercise, can also be considered a form of hypoxic stress. Moreover, tissues that are relatively poorly capillarised also have a hypoxic gradient towards the cells furthest away from the capillaries.

The systemic effects of hypoxia exposure are several. The cardiac output increases, mainly due to increased heart rate, which is a physiological adjustment driven by a remarkable autonomic sympathetic response, accompanied by increased ventilatory exchange (Jouett *et al.*, 2015). This sympathetic drive also leads to increased haemoconcentration due to both the evaporative water loss caused by increased ventilation and the augmented diuresis. Although the most prominent effects are tachycardia and hyperventilation, increased haemoconcentration also helps to maintain the oxygen delivery to tissues by increasing the oxygen transport capacity of the blood (Grover, Weil and Reeves, 1986).

After this 'emergency' responses onset, if hypoxia exposure persists, several responses are initiated at endocrine level and also as a consequence of the hypoxia direct effects on the cells through a complex cascade of intracellular signalling pathways. These pathways are elicited by the hypoxia-

inducible factor (HIF) that acts as a master switching molecule in order to modify the gene expression of the cell if hypoxia conditions persist.

Furthermore, in conditions of an altitude around and higher than 2500 m, the condition of acute mountain sickness can develop in humans (Harrison *et al.*, 2013). This is the reason for which most of the altitude training centres around the world are sited between 2000-2500 m above sea level.

1.2.4.2 Intermittent Hypoxia Exposure

The adaptive physiological responses of the training method of live high-train low are becoming increasingly renowned for enhancing endurance performance by athletes (Wilber, 2001; Richalet and Gore, 2008; Millet *et al.*, 2010). The analogues to simulate the altitude for performers are either via normobaric hypoxia exposure or hypobaric hypoxia exposure.

It is still under debate whether the two analogues elicit the same physiological responses given that the fundamental stimulus is presumed to be the partial pressure of oxygen (Self *et al.*, 2011). Although, there is growing evidence suggesting that tissues might be under more oxidative stress in hypobaric hypoxia (Faiss *et al.*, 2013; Coppel *et al.*, 2015). However, the duration and the hypoxic level of exposure that should comprise the intermittency has not been standardised and varies somewhat between studies (Coppel *et al.*, 2015). Nevertheless, other studies focusing on the effects of intermittent hypoxia exposure on the myocardium and skeletal muscles demonstrated capillarisation increase (Panisello *et al.*, 2007) and oxidative metabolism shift of active fibres (Esteva *et al.*, 2009). These results make the idea of potential benefits of intermittent hypoxia exposure programs during skeletal muscle injury recovery a favourable application.

1.2.5 Rodents as Experimental Models for Exercise-Induced Injury

In order to either study the type or level of skeletal muscle injury and subsequent regeneration with or without rehabilitation interventions, one needs to start by acquiring the occurrence of the injury itself. The experimental setup with humans running downhill on a treadmill, considers the performer to eccentrically contract the muscles that brake off the running movement to avoid falling over. Above, we have established that the eccentric-contraction model results in more injured muscle tissue and in their work Newham *et al.* (1983) have also demonstrated that concentric contraction resulted in minimal injury. This is useful to bear in mind when intending to implement active rehabilitation, as the concentric contraction of the injured muscle will potentially aid the regeneration whilst minimising possible re-rupture.

Rodent models are popular for investigating skeletal muscle injury. Whilst rabbits are more used for trauma injury-models, mice and rats are popular for exercise-contraction injuries, having them running on a treadmill. The damage induction with rats (and mice) have been demonstrated to occur both during downhill and uphill running for 60-200 min and at speed between 0.25 and 0.42 m/s (Armstrong, Ogilvie and Schwane, 1983; Kasperek and Snider, 1985; Peeze *et al.*, 1989; Van der Meulen *et al.*, 1993; Kasuga *et al.*, 1999; Tiidus *et al.*, 2001). However, Taylor, Caldwell and Rowntree's (1972) study support the fact that downhill running is a more energy-efficient eccentric contraction. Notably, m. soleus seems to suffer tissue damage during both of these types running, still, not the only muscle. Nevertheless, there are contradictory speculations as to why the muscle responds in both conditions with respect to its stretched length in the hind limbs whilst a rat runs (Newham *et al.*, 1988; Komulainen, Kytola and Vihko, 1994; Gosselin, 2000).

1.2.6 Coda

The physiological groundwork has been laid down, and it is now time to look at an experimental model and how one can recreate recreational athletes. Whilst it is a loose term for an investigation, 'recreational' athlete, the conditioning needs to be stable and repeatable, or at the very least, be known. After all, the effect of a specific induction of muscle damage is likely to be different based on the previous condition of the 'wounded'. Still, irrespective of the different level of skeletal muscle injury occurring in everyday athletes or intentionally induced in experimental models, the subsequent chapters will address how the damage is assessed or measured indirectly. The meaning of indirect measuring is not to be confused with the above-explained difference between direct and indirect injury, as the assessment will indeed involve direct injuries.

1.3 Training Conditioning

1.3.1 Run-training for Rats

Rats are relatively intelligent in comparison with other, smaller rodents. As runners, they are prone to short voluntary bursts of discontinuous running (Squibb, Collier and Squibb, 1977). Perhaps, unless there is a continuous threatening reason, their proneness reflects a natural tendency of stopping and checking if there is anything to run away from. Smaller rodents are likely to evaluate their environment differently, and the difference is reflected in different types of treadmills designed for rats versus those designed for mice, for example, when carrying out run-training. Whilst a moving treadmill belt beneath the mice is, perhaps, stimulant enough to keep them running, rats do need an additional stimulus to keep them on the moving belt.

The majority of treadmills designed for rats rely on mild electric shock to keep them running. The electric shock is mediated via a metal grid (Fig. 1-1), located just behind the treadmill belt, and a shock is received every time the grid is touched. The word 'shock' in this context, might come across as quite harsh. However, the intensity of the stimulus is relatively low and of accepted level, and perhaps should rather be considered as 'uncomfortable' than 'harmful'. Although that would refer to physical implications, whilst emotional stress linked to the shock might mirror a different reaction pattern. Nevertheless, the intensity should, in theory, serve the purpose of making the rats recognise what they should be avoiding doing. Then, given that the treadmill belt and the metal grid are walled off, a rat will, therefore, either touch the grid and receive electric shocks or stay on the moving belt and run.

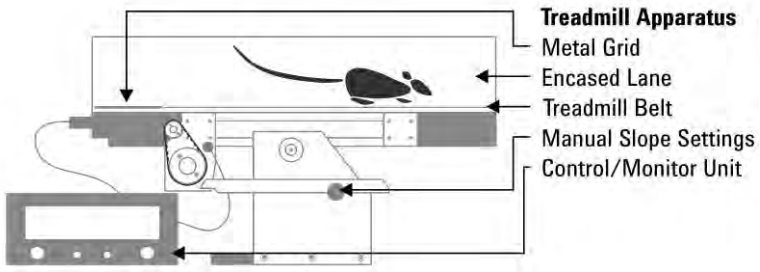

Fig. 1-1. Schematic drawing of a treadmill for rats based on Harvard Apparatus (USA).

Some manufacturers also design the treadmill apparatus with a controlling hardware that counts the number of shocks and the duration of each shock. These parameters can then be used to evaluate how a rat has been running considering how many electric shocks it has received and for

how long time. The logic is extremely straight forward. A rat that is a good runner might receive the occasional electric shock, still, will have a relatively low electric shock count summing up to a short duration. In contrast, a rat that has not been running well and is continually touching the metal grids will have a higher shock count with an accumulating duration reflecting that count. A duration of an electric shock is normally a question of a fraction of a second — unless the rat can withstand the intensity and decides to stay on the grids for a bit.

1.3.1.1 The Training Sessions

Naturally, there is no one way of constructing a training session on a treadmill. The design simply has to fit its purpose. Although, it is fair to say that the use of the word 'simply' in the context of designing a series of training sessions, can mean 'a wild stab in the dark'. It is relatively easy to judge if a rat is a really good runner or a terribly bad runner, and by that measure, if a protocol is appropriate or not. However, unless one could speak the squeaky language of rats, that is as far as reliability goes in terms of estimating the success of a training session. Clearly, it is not ethically sound, when working with laboratory animals, to base the design on a simple trial and error. Furthermore, what do we do with rats that are between being good and bad runners? Do we consider them as outliers? — If so, where do we draw the line of acceptance?

When looking through the literature it is safe to say that the majority reports sparsely on the training setup, and any comments on selecting the rats based on their success as runners is even poorer. Therefore, one could easily make the assumption that either throughout or by the end of the training period all the rats in a given study, pretty much ran with identical success. In Table 1-1 a comparison of training session on treadmill is listed. Although the parameters have been adjusted to the same units and all calculated parameters are demonstrated, although not specifically reported in this by each author, the information is still fairly fenestrated, especially with the mindset of inter-laboratory reproducibility. Nevertheless, published references like these are the only once available for one to be able to create a new protocol.

1.3.2 The Problems with Treadmill-Running

The treadmills for rats are normally not just walled off to the sides but rather boxed in, with air ventilation holes, in order to prevent the rat from potentially jumping away. As such, a closed system, the electric shock is the only direct implementation to make sure that the rat runs properly on the belt, without opening the encasing. A rat that is very stressed out by the combination of running and receiving electric shock, might momentarily 'freeze' on top of the grid. Increasing the intensity might work to get the rat to pop of the grid, but not necessarily, and some the rat needs

Table 1-1. An example of studies with rats running on treadmill and the provided protocol information.

Study reference	Objective	Sess/d	t, d	v, m/s	θ	t_{Sess}, min	t_{Total}, min	s_{Total}, m	$w_{Rat,Ini}$, kg	Observation
Mayer, Vitale and Mashayekh, 1954	interval	1	45	0.45	-	60	2700	72450	-	*overestimated values*
Griffiths, 1954	exhaustion?	-	-	-	-	-	-	-	0.250	*6 of 10 rats learned to run well*
Griffiths, 1956	exhaustion?	-	30	-	-	-	-	-	0.185	-
Parizkova and Stankova, 1964	-	1	200	0.30	-	50	10000	180000	-	-
Levitt and Webb, 1965	exhaustion	1	70	-	-	60	4200	-	provided	*49-70-h session*
Sembello and Gladfelter, 1974	5 min	1	0	0.44	-	30	0	0	-	-
Gerald, 1978	exhaustion	1	1	0.31	8°	45.5	45.5	855.4	-	-
Gerald, 1978	exhaustion	1	1	0.45	-	76	76	2036.8	-	-
Mattson *et al.*, 2000	-	1	48	0.45	10°	60	2880	77760	-	-
Moraska *et al.*, 2000	-	1	40	0.49	10%	60	2400	70080	-	-
Wisløff *et al.*, 2001	-	1	39	0.15	0°	15	585	5265	-	-
Wisløff *et al.*, 2001	-	1	65	0.60	30°	60	3900	140400	-	-
van Lunteren and Moyer, 2003	-	1	40	0.30	15°	60	2400	43200	-	-
Sakakima *et al.*, 2004	-	1	6	0.40	10°	40	240	5760	-	*'low-frequency running'*
Sakakima *et al.*, 2004	-	1	18	0.40	10°	40	720	17280	-	*'middle-frequency running'*
Sakakima *et al.*, 2004	-	1	36	0.40	10°	40	1440	34560	-	*'high-frequency running'*
Yoshimura *et al.*, 2005	-	1	20	0.67	6°	20	400	16000	-	-
Tsumiyama *et al.*, 2014	-	1	1	0.63	0°	56	56	2128	-	-
Tsumiyama *et al.*, 2014	exhaustion	1	1	0.70	−16°	64	64	2688	-	-

Explanations: Sess/d: session/day; t: time; v: speed; θ: slope; s: distance; w: weight.

to be manually pushed off. To push a rat of the grids, requires opening the encasing, and at that point rats can potentially escape. Furthermore, especially when rats are stressed, the leave faeces and urine on the treadmill belt, whilst running, which if touches the metal grids will be accounted for as an electric shock by the apparatus. To take that even further, droplet or solids stuck on the metal grid, will come across in the resulting electric shock parameters as if the rat in question was staying on the metal grid for considerable time. All of these actions reduce the reliability of the shock count parameters for the usage of estimating successful running — especially this runs through without any observations.

Up until now, there does not seem to be any ultimate solution. Some of the design elements of the treadmill have been approved, whereas older features gave the rats opportunity to clutch on and hang on to the walls, in order to avoid running. However, those improvements only address part of the problem. Other issues are related to the metal grids specifically; the counting apparatus does not differentiate between a rat that is continually touching the bar, or a piece of faeces, stuck on the bar. Addressing that can be troublesome without disturbing the running rat or affecting the session, if the access to and around the metal grids is not made easy.

1.3.3 Coda

It is technically difficult to implement a solution that fully replaces or addresses the problems. Some of the issues are not really problems that can be fixed, and therefore require continuous attention if the electric shock counts, from the basis of determine how well the rat has been running during a session. It is necessary to have tools that allow us to get the most out of what we have, especially when it comes to using experimental animals. It is easy to say to discard rats that run, but aren't really good runners – in order to have a more selective subject group. However, the reality is that unless the rats are specifically bread to fit the group, it certainly becomes an ethical issue if the selection of subject rats relies on discarding them, rather than refining the number of rats in the experiment from the onset.

1.4 Plasma Marker Assay

1.4.1 The General Concept of Plasma Markers in Relation to Muscle Damage

The general idea of plasma markers is to recognise molecules present in the blood stream that reflect distinct biological conditions, sometimes referred to as biomarkers in plasma. The reference to plasma *per se* is in which part of the whole blood the markers are located. Although, plasma is formally described as the separate blood liquid part in a separated anticoagulated whole blood whilst serum would refer to the same blood liquid of separated whole blood but after coagulation — hence serum does not contain fibrinogen (a protein that assists in the blood clot making).

When defining skeletal muscle damage, one needs to be aware of the fact that the level of damage can be of various extent. On a cellular level, one could define it as tares or ruptures of the skeletal muscle fibres. Depending on the degree of the skeletal muscle damage, it is then related to how many tared or ruptured fibres are involved, and if localised or not, which might also depend on the skeletal muscle as an organ, i.e. its anatomical position and function. A damaged skeletal muscle fibre that is tared will have part or fractions of its intracellular components seeping into the interstitial compartment and then entering the blood tissue network surrounding it. The intracellular compounds can now be found in the blood stream for some time relative to their size, and the degree of the muscle damage, until they are cleared by the kidneys or gradually broken down in the liver. It is, therefore, logical that if the blood is sampled after a skeletal muscle damage has been induced, its analysis will reveal some quantity of some of the fibre's intracellular components in the plasma. These components, from now on and throughout the dissertation, denominated as plasma markers, can be isolated from a plasma sample, identified and quantified. The quantity found in the blood will then depend on the degree of the damage, both on an individual fibre level and how many fibres are involved, and furthermore, which point in time after the damage, the blood sample is reflecting. Depending on the muscle fibre compound in question, its outbound flow is reflective of it being 'free', adhering, or as part of the structural elements of the fibre. If the severity of the damage is not adverse or catastrophic, a decreasing quantity in blood over time can then be used as an indirect measure of the recuperation process of the damaged structure.

1.4.2 Selecting the Appropriate Plasma Markers for Skeletal Muscle Damage

Logically, the blood will contain whatever needs to be transferred in it, irrespective of the occurrence of skeletal muscle damage. Therefore, any accompanying action with the muscle damage is also likely to be reflected in the blood in a similar way. Thus, it is necessary to select plasma markers that are unique to the tissue type of the muscle in question. If the actions that lead to the damage of skeletal muscle expectedly (or unexpectedly) caused some sort of damage to the cardiac or the smooth muscle cells; any marker common to muscle cells, in general, would give misleading quantity when judging the effects on skeletal muscle alone. Both being striated, skeletal and cardiac muscle cells have more intracellular components in common (structural, mechanical or metabolic) in comparison with smooth muscle cells. Thus in the process of selecting a marker, specificity is, therefore, key, although, not necessarily realistic in assay production.

In the case of skeletal muscle damage, the simplest scenario would be that the selected marker (or the component) is usually not found extracellular to the skeletal muscle fibre, i.e. a blood sample would not contain it until the tares involved in a skeletal muscle damage would then make it detectable via proceeding samples. Therefore, a clear indication of a skeletal muscle damage, until the liver would eventually have broken down these components, and after that not be detectable in blood anymore. Another clear indication that the damage has been repaired. Still, one needs to consider that tissues go under regeneration as part of normal biological maintenance. A growing individual has higher cell turnover frequency. These and other basal processes, which in our simple scenario we consider normal (or not damaged or non-healthy cell) also return components into the blood with regularity to be broken down. Depending on the component in question (role and 'normal' intracellular quantity) it both could or could not be detected in a plasma assay which, in turn, depends on the timing and the sensitivity of the assay. One can logically assume that the quantity released into the blood after damage is higher in comparison with what happens in normal cell turnover. Hence understanding the role of the marker chosen is necessary to be able to give the interpretation of the analysis any proper meaning.

1.4.3 Myoglobin, Creatine Kinase and Troponin-I in Plasma to Detect Skeletal Muscle Damage

In the following, the three components; myoglobin, creatine kinase and troponin-I; will be defined as muscle injury markers, and are indeed commonly relied on as plasma markers for the indication of muscle damage. Myoglobin and troponin-I are specific to striated muscle tissue. Whilst myoglobin is generally speaking non-specific for this purpose; troponin-I is expressed in different isoforms whether it is in skeletal or cardiac muscle cells. Creatine kinase is expressed in various tissues in general, where different isozymes are expressed in skeletal or cardiac muscle cells.

1.4.3.1 Myoglobin

Myoglobin (Mb) is a relatively small cytoplasmic globular protein made of 153-aminoacyl residue with the molecular weight of approximately 17 kDa. Two main isoforms have been identified, Mb1 and Mb2, with additional three in humans (Mb3, Mb4, Mb5), although none of them appears strictly specific to striated or skeletal muscle tissue (Rossi-Fanelli and Antonini, 1956; Fraser *et al.*, 2006; Perkoff *et al.*, 1962 in Gussoni *et al.*, 2011). Having ancestral relations with haemoglobin and both containing the O_2-binding haem ring, Mb is classically known to store and facilitate oxygen diffusion in the cardiac muscle cells and the oxidative myofibres of skeletal muscle (fibre types I, IIa and IIx, specifically) (Wittenberg, 1970; Ordway and Garry, 2004). Still, Frauenfelder *et al.* (2001) suggested the role of Mb to be of an allosteric enzyme due to its other functions of binding and reacting to CO and NO_2^-. The structural properties of Mb make its O_2 affinity much stronger than that of haemoglobin which underpins its role as oxygen carrier (Garry and Mammen, 2007), as, without it, O_2 diffusion inside the muscle cells is not enforced by an intracellular gradient sufficient for an adequate delivery to the mitochondria. After observing electron micrographs of gold-labelled Mb in rat cardiac cells, Hochachka (1999) postulated that a random intracellular distribution of Mb is 'to assure a similar [O_2] everywhere in the cytosol (and simultaneously to minimize or even destroy intracellular O_2 gradients)' (p. 669). Although, he does recognise and underline the fact that skeletal muscle cells might demonstrate different Mb recruitment in relation to different fibre types and their muscle's overall workload whilst cardiac cells are biochemically more homogenous (Hochachka, 2000). Meanwhile, ultrastructural immunohistochemical techniques have positioned Mb in concentration near the A-band and the I-band in skeletal muscle fibres (Mitsui *et al.*, 1994); bands which define the interdigitating thick and thin protein filaments, respectively, of the functional units (sarcomeres) within the fibres.

1.4.3.2 Creatine Kinase

Creatine Kinase (CK) is an enzyme the size of about 40-43 kDa in molecular weight, with three tissue-specific isozymic forms; MM, BB, and MB (a heterodimeric between MM and BB) (Grossman and Mollo, 1979; West *et al.*, 1984; Pickering *et al.*, 1985), as well as two mitochondrial isoforms (Eder *et al.*, 1999). The CK-MM isoform is found in muscle; both skeletal and cardiac, associated with the M-line structure of the myofibril (Wallimann, Turner and Eppenberger, 1977) the CK-MB is exclusive to myocardial tissue.

The CK-BB isoform is designated to brain tissue, where it is mainly found, although, it could be designated as the non-muscle isoform (Grossman, 1983; Eder *et al.*, 1999). CK catalysis the rephosphorylation of ADP, using phosphocreatine, to maintain the ATP energy requirements within the cell (West *et al.*, 1984; Grossman, 1990; Wallimann *et al.*, 1992), which Hochachka (1999) refers to as 'buffering' the ATP concentration, e.g. as 'during large-scale changes in muscle work' (p. 662) necessary for the ATP-hydrolysis in the cross-bridge cycle.

1.4.3.3 Troponin-I

Troponin-I (TnI) is a striated muscle-specific structural protein with the molecular weight of about 20-23 kDa. The TnI is known to have three isoforms 'encoded by three distinct genes that are differentially expressed in cardiomyocytes, fast skeletal muscle fibers, and slow skeletal muscle fibers' (Hastings, 1997, p. 206). Regarding peptide count, the cardiac isoform is about 30-60 units longer than the other two, which only demonstrate minor structural differences (Wilkinson and Grand, 1978; Brotto *et al.*, 2006). As part of a 3-polypeptide troponin complex, when the complex does not have Ca^{2+} bound to it, the TnI inhibits the actomyosin interaction which is the fundamental mechanical link needed for the cross-bridge cycle of a contraction (Farah and Reinach, 1995; Hastings, 1997). When the muscle cell action potential triggers the Ca^{2+}-release from the sarcoplasmic reticulum and its cytosolic concentration subsequently increases; Ca^{2+} binds to the TnC, the calcium-binding unit of the troponin complex. This binding leads to conformational changes in TnI and together with TnT, the 3rd part of the complex, pushes linked tropomyosin away from the myosin binding sites on actin, freeing the way for myosin to interact (Reinach *et al.*, 1997; Perry, 1998).

Table 1-2. The Charactersitics of Myoglobin, Creatine Kinase and Troponin-I.

Molecule	Size (kDa)	Type	Skeletal muscle isozyme	Cardiac muscle isozyme	Other important isozymes	Reference
Myoglobin (Mb)	≈17	Cytoplasmic globular protein	Mb1 (non-specific)	Mb1 (non-specific)	Mb2 (brain-specific)	Rossi-Fanelli and Antonini, 1956; Hochachka, 1999, 2000; Fraser *et al.*, 2006
Creatine Kinase (CK)	40-43	Enzyme	CK-MM	CK-MB and CK-MM	CK-BB (in non-muscle tissue)	Walliman, Turner and Eppenberger, 1977; Grossman and Mollo, 1979
Troponin-I (TnI)	20-23	Structural protein	Fast-TnI and Slow-TnI	Cardiac-TnI (maybe slow-TnI)	Not specific for striated muscle tissue.	Wilkinson and Grand, 1978; Hastings, 1997; Brotto *et al.*, 2006

1.4.4 Detecting Markers in a Sample

The identification and quantification of compounds in a solution can be carried out in many ways, and for biomarkers, the use of chromatographic analysis and mass spectroscopy are relatively standard. However, carrying simple assays such as ELISA is both straight forward and easily applicable in routine physiological laboratories, both for the confirmation of a markers existence in the given sample and for quantification. As much as an ELISA can be designed in several ways, it can be carried out in several manners as well. Between different variations and combinations of direct and indirect with sandwich, competition and inhibition types of ELISA, the general setups are not within the scope of this text. However, as a reference, the direct sandwich ELISA will be introduced.

1.4.4.1 Direct sandwich ELISA

The general description is based on a monoclonal antibody of the compound of interest being incubated to a hard plastic surface. The monoclonal aspect marks the specificity needed to distinguish the particular compound from the potential mixture of others in the subsequent acquisition of a sample. With the addition of a sample solution, the compound will bind to the antibody on the plastic during incubation. All unbound and other sample matrix material is, at this point, washed away. A second batch of the compound's antibody is now added. These antibodies normally have the following two characteristics: (**i**) The antibody is polyclonal, which is still specific to the compound but recognises multiple epitopes on the compound to ensure that each compound has a bound antibody during incubation. Furthermore, (**ii**) this polyclonal antibody is enzyme-linked. The enzyme plays the key part in subsequent recognition of the antibody-compound links. Then, another washing away of all unbound and excess material is carried out. At

this stage, the compound of interest, in the original sample, that has bound to the monoclonal antibody on the plate, has now also an enzyme-linked antibody bound to it, or, to reference the technical terminology (Aydin, 2015)— the compound is sandwiched in between the two types of antibodies. A substrate solution, specific for the enzyme linked to the antibody, is now added to the plate. A by-product of the substrate-enzyme reaction is a compound that gives off colour, which can be colourimetrically recognised. The incubation time needed for this step needs to take two factors into consideration; (**i**) the amount of substrate needs to be sufficient for any potential maximal Antibody-Compound-Antibody Sandwich on the surface area of each well. Also the amount of substrate has to be in sufficient excess quantity, to make sure that there is no competition for the amount of substrate, and that the substrate has reached or covered all potential areas where an enzyme might be available. (**ii**) At the same time, as the enzyme continually leaves of the coloured by-product with mildly excess substrate available; the reaction needs to be stopped as well for the colour emerging to be representative and proportional. A stop solution is added, which reacts with the substrate and the substrate by-product, leaving the unbroken substrate not available for the enzyme to react with, and changes the colour of coloured by-product. This new colour can also be recognised colourimetrically, and its amount can be quantified as the involved reaction is in proportion to the existence of the antibody.

1.4.4.2 Technical Considerations for Colorimetric Assays

The colourimetric identification is based on a wavelength absorption for the compound in question. However, the compound in question for the absorbance measurement is not the same as for the compound of interest in the sample. The existence can be back traced in a way that the compound in question only exists if elements in the stop solution have formed it with the by-product from the enzyme reaction. The enzyme reaction only takes place if the enzyme is available. In turn, the enzyme is only available if the enzyme-linked antibody is bound to the compound of interest from the sample. Moreover, the compound of interest from the sample is only there if it has bound to the antibody on the plastic surface of the well plate. However, we still do not know the quantitative relationship between one compound of interest with one active enzyme on its enzyme-linked antibody, and how many by-product compounds the one enzyme has formed that are simultaneously and unavoidably measured. If the enzyme was inactivated after one reaction, the relationship would be fairly straight forward. All these factors lead us to how a calibration curve is needed to reflect on this relationship between the concentration of the compound and its absorption. On a specific range, one can find a linear relationship, and define the limits of linearity. However, both because of matrix effects on the well plate and as the quantity of substrate is in excess; the relationship might become curved. Instrumental detector saturation can also be

reflected in a non-linear relationship; in either case, it is necessary to dilute the samples so it falls within the range of quantification of the calibration curve. The relationship between the limits of linearity and range of quantification are explained below.

1.4.4.3 The Calibration Curve

The key parameters to define the calibration curve and how it can be used for quantification are expressed in the following: The limit of detection (LoD), the limit of quantification (LoQ), the limit of linearity (LoL) and the range of quantification (RoQ). The LoD is where the measurement response can be said to be due to the compound of interest (Hayashi *et al.*, 2004). Consider an absorbance reading of a blank sample that is always fairly similar, still, slightly variable. If the background, the blank, has high variation, it becomes problematic to decide what one is truly measuring in a sample with a very diluted concentration of the compound of interest, that has an absorbance really close to the blank. Therefore, the limit is usually determined by the absorbance variation from the repeated measurements of the blank sample as a reference; more precisely, the value of 3-times its standard deviation. If the blank is chemically simple, and the measured volume is as constant as it can be between different repetitions, the LoD becomes an indication of the instrumental precision; however, in practice, it is likely that variations in the volumetric procedure play an over-shadowing role. Once the LoD has been established, we objectively need to decide at what point it can be said that we have detected the compound of interest, with a small absorbance value, though higher than that of the blank, and when possible we can relate the amount absorbed to the quantity of the compound. The quantification can be troublesome in diluted samples if one is supposed to deduct the absorbance value of an extremely varying blank for the rest to represent the compound of interest. The LoQ is also determined by the absorbance variation of the blank, still, 10-times its standard deviation, and formally determines at what point the smallest measurement response can be quantified with some certainty (Proctor, 2008). When a calibration curve is constructed with several known but distinct levels of concentration of the compound of interest, the absorbance-concentration relationship is usually limited to linearity. Between the different concentration points, the linearity is usually determined by the best fit with a linear slope using least mean square, where the acceptance mark is referenced to where the R^2 is higher than 0.999. The outermost concentration points of the curve that give this for determining LoL. Whilst the lower end of the range of quantification starts with the determined LoQ, the upper end is usually determined as 10% RSD from the upper LoL. In practice, this means that although several concentration points are used to make up the calibration curve, the LoQ and LoL define which of them can ultimately be used for reference which is the RoQ.

1.4.5 The Sample-Matrix Effect

The matrix effect of a sample on a well plate array is usually dealt with by a sample-blank. Still, a blank only estimates the general effects that the matrix may have on the absorption. The effect might be visible in a different manner especially in the lowest range of the compound concentration; affecting the readability, to put it simply (Hibbert, 2007). The reading is typically represented in a different linear relationship (less steep slope) in the lowest concentration points in comparison with the higher concentration points where the linear relationship is most evident; and, furthermore, being in many cases denoted as the initial curve before the linearity, or below the lower limit of linearity. Although, classically, this initial linear relationship is considered as outside linearity and therefore discarding any quantification of samples that fall within these ranges of concentration; the way to discard them is more formal, and, in fact, this initial relationship can be used, and only seems curved in comparison with the rest due to the matrix effect. However, what marks which low-concentration sample can be quantified is the LoQ. The definition of the LoQ is also debatable, but is a clearer reference point, and perhaps more realistic, than only the lower limit of linearity based on the middle linear relationship (the evident bit on a graph). Another type of the matrix effect is how the medium affects the measurability of the compound of interest in general (even if the blank is determined). This measurability can be determined by spiking a sample that is without any compound of interest and compare it with a calibration curve, which normally does not have the initial sample matrix involved. The yield calculation between the two then determines how the initial sample matrix, affecting the first steps of the assay, might be involved in the results.

1.4.6 Coda

As it is evident regarding the experimental environment, any application (physiological or otherwise) set up with the intention to cause skeletal muscle damage supposedly to be detected via plasma marker assay, will have several barriers to overcome in its procedural design. The analytical aspect of it will depend on practical skills, the equipment accuracy and, of course, the sensitivity of the assay itself. Still, even if these aspects would greatly affect the downstream results, they would generally only be viewed as part of the systematic error. The true complex factor involves the underlying biology in terms of its validity and variability. If for arguments sake, we assume that a given plasma marker is valid to reflect muscle damage and its quantification measures are correctly representative for the level of the damage; the plasma marker alone could only confirm the existence of a muscle damage in general. The identification of which muscle or muscles are involved could not be truly confirmed even if we could guesstimate it by the physical setup of the experiment. Similarly, as many skeletal muscle damage plasma markers are the same

as for cardiac muscle damage, one needs somehow to eliminate the existence of the latter in the results. One method of doing this is to select more than one plasma marker. This, indeed, is a commonly used strategy simply to ensure the probability of detecting the muscle damage, as a reason for the appearance of different markers in the blood stream is still not fully clear. However, the same strategy could logically be used simultaneously to measure the existence of cardiac muscle damage, as some markers are more specific to cardiac muscles cells, to either rule that possibility out or in. Of course, in practice, the rationale behind the experimental setup along with financial limits might suggest rather focusing on additional and different skeletal muscle damage measurements; some of which are introduced in the following chapters.

1.5 DNA Microarray Gene Expression

1.5.1 The Central Dogma of Molecular Biology

Changes in physiological circumstances require molecular responses on a cellular level. These molecular alterations can further promote the gene transcription for the synthesis of a protein that, further on, plays its part in the response. These molecular alterations affect the gene transcription by facilitating the bond of transcription factors to their specific regions on the DNA. These regions are promoters and are located upstream of a protein-coding gene. The transcription factor can act as an activator or repressor that respectively enhances or suppresses the transcription of the downstream gene. The same type of transcription factor can affect several genes, perhaps, enhancing the transcription of some and suppressing others. When the transcription factor is an activator, it can bind RNA polymerase II, forming the transcription initiation complex. If the transcription factor is a repressor, this complex will not form. The transcription takes place when the RNA polymerase II catalyses the formation of a pre-mRNA (pre-messenger RNA) by opening and unwinding a small portion of the double-stranded DNA, using the 3'-to-5'-direction strand as a template along the DNA, to from a pre-mRNA strand in the 5'-to-3'-direction. The transcription ceases with an end code of the gene region in the DNA itself. Any non-protein-coding portions of the pre-mRNA are now spliced away, forming the mRNA (messenger RNA). The mRNA is transported out of the nucleus and to the ribosomes. It is in the ribosomes that the mRNA strand is translated to a protein chain with the help of tRNAs (transfer RNA) that match representative amino acids, coded by every 3-base pairs in the mRNA strand. As with the transcription, the translation ceases with a stop code in the mRNA strand. The protein, either by itself, modified or as part of a bigger protein structure, relatively directly or indirectly participates in a biochemical process or processes in response to the molecular action it serves. The synthesised protein is what we can consider a functional gene product, and up until this point, from the commencing point of transcription, we say that the protein-coded gene has been expressed.

1.5.2 Gene Expression Profiles

With the accumulated scientific knowledge, many protein-coding genes in vertebrate species have been identified, via the measurements of the resulting corresponding up- or downregulated protein, as part of molecular pathways. The set of genes that can potentially express mRNA as part of a particular pathway, or a set of parallel pathways, can be referred to as the representing gene expression profile. A gene expression profile can also refer to the changes in the expression of a particular gene as a function of time. For an experimental setup involving exercise-induced skeletal

muscle damage and its recovery, perhaps with hypoxia, one could consider four different profiles: genes that are expressed as a response to skeletal muscle damage, hypoxia signalling, vascular endothelial growth factor signalling, and, perhaps, wound healing.

1.5.2.1 Skeletal Muscle Pathway

Skeletal muscle's role in voluntary movement contributes greatly to energy metabolism and its regulation via glucose uptake and storage by insulin. Complications from aging and metabolic diseases like diabetes and metabolic syndrome contribute to muscle wasting (atrophy). However, recent research hypothesises that metabolic defects in skeletal muscle contribute to the aetiology of diabetes and metabolic syndrome, suggesting that skeletal muscle has a larger role in these disease states than initially expected. Large heterogeneous protein complexes including titin or dystrophin facilitate muscle contraction by connecting the skeletal muscle cytoskeleton to the extracellular matrix (Conover, Henderson and Gregorio, 2009). Muscular dystrophies arise from inherited mutations in the genes encoding components of these complexes, and gene expression changes disrupting their normal contractile function dysregulate signalling pathways that control muscle growth. Potential therapies for muscle wasting include generation of new muscle cells (myogenesis) or increasing the mass of current muscle cells (hypertrophy). Thus, muscle-specific biological and pathophysiological processes are interrelated and cannot be studied in an isolated manner.

1.5.2.2 Hypoxia Signalling Pathway

Oxygen is required for aerobic energy metabolism processes such as oxidative phosphorylation. Low oxygen conditions activate the hypoxia signalling pathway in eukaryotic cells, primarily via the hypoxia inducible factor (HIF) (Bunn and Poyton, 1996). HIF heterodimers consist of a constitutively-expressed beta subunit and one of 3 alpha subunit isoforms whose expression is tightly regulated. The presence of oxygen activates prolyl hydroxylases to hydroxylate HIF, leading to its polyubiquitination and degradation. Under low oxygen conditions, prolyl hydroxylase inactivity allows the HIF to accumulate in the cytoplasm until translocation to the cell nucleus and there initiating target gene expression (Chi *et al.*, 2006). Hypoxia-inducible target genes mediate multiple biological functions, such as angiogenesis, haematopoiesis, and the maintenance of vascular tone to provide or replenish tissues with blood and oxygen.

1.5.2.3 Vascular Endothelial Growth Factor (VEGF) Signalling Pathway

Genes involved in signal transduction and cell signalling downstream of vascular endothelial growth factors and their receptors are critical for regulating new blood vessel formation, also known as angiogenesis, arteriogenesis, or vasculogenesis (Lyons *et al.*, 2010). Angiogenesis and VEGF Signalling go hand-in-hand with sprouting and splitting (intussusception) angiogenesis, vascularization, neovascularization, revascularization, pruning and vascular remodelling in response to the developmental and hypoxia or ischemic signalling pathways.

1.5.2.4 Wound Healing Pathway

Wound healing progresses via three overlapping phases: inflammation, granulation and tissue remodelling. After mechanical injury, a blood clot forms and inflammatory cells infiltrate the wound, secreting cytokines and growth factors to promote the inflammation phase (Gordon, 2003). During the granulation phase, fibroblasts and other cells differentiate into myofibroblasts, which deposit extracellular matrix proteins. Simultaneously, angiogenesis occurs, and keratinocytes proliferate and migrate to close the wound (Hoffmann, Gloe and Pohl, 2001). In the final tissue remodelling phase, apoptosis eliminates myofibroblasts and extraneous blood vessels, and the extracellular matrix is remodelled to resemble the original tissue. Dysregulation of this last tissue remodelling phase leads to fibrosis.

1.5.3 Gene Expression Analysis with Probe Arrays

In order to measure representative changes in gene expression for a specific moment in time, one needs to acquire a sample from a tissue of interest and process the mRNA transcribed by the cells in the tissue. The mRNA material is prepped to be potentially hybridised to single-stranded bits of DNA (called probes), each representative of a different gene of interest. The mRNA material needs to be properly extracted from the sample to avoid any interferences in the subsequent analysis. With a reverse transcriptase, the mRNA is converted to its complementary DNA (cDNA) which is also single stranded. The extracted mRNA is in relatively low quantity due to a small processing-sample size; hence, the corresponding amount of cDNA needs to be amplified with a PCR and is done so in a presence of a label (usually a fluorescent dye). The amplification process is necessary for the subsequent step. Remember, that the labelled cDNA molecules are of many kinds (as many as different mRNA were expressed in the sampled tissue), but are still all amplified. A lot of these different but representative labelled cDNA molecules are incubated with an amplified probe of interest (each separately) to allow hybridisation to take place and then unbound materials are washed away. If the labelled cDNA hybridises to a probe, we know that the corresponding gene

has been expressed in the sample. Furthermore, the intensity of the label (for example, the intensity of the fluorescent light emitted) can be measured and is proportional to the quantity of labelled-cDNA bound to the same type of probe. As various expressed mRNAs from the sample are in different quantity to start with, their labelled cDNA molecules after amplification will maintain these type-proportional differences and the amplified amount is proportional to the label intensity. This relationship is fundamental to the quantification used in quantitative real-time PCR (both qPCR and RT-qPCR).

PCR arrays are prepared to have as many different probes needed to represent a gene expression profile. For example, the number of different genes can be just under 96 or 384 to fit standard well plate capacity. However, the number of genes in a profile is not limited by a well plate *per se*, rather, it is a matter of practicality. Ultimately, depending on the genes used to make up that particular profile to fit on a well plate; if no hybridisation does take place, the chosen profile (and its composition) is not prominent in the physiological condition of the tissue from which the sample was taken – which, in turn, could make it a limiting assay with that respect. DNA microarrays have a much larger number capacity for different genes/probes and can mount up to as many as to represent the entire genome of an organism (20000-50000 probes per array, for example). Therefore, once the label intensity measure for each gene is obtained, selected genes can be collectively evaluated with reference to any known gene expression profiles if so desired. However, both of these technical applications to measure the gene expression mentioned here, only provide a relative level of expression for each gene, but not the initial concentration of the corresponding mRNA. Still, the difference in the expression level can be used to interpret the effect on different genes and also between the various experimental conditions.

1.5.4 Data processing for Differential Gene Expression

Many applications for the DNA microarray setup offer different cDNA labels for different samples to be compared. The 'classic' setup applies the two-colour detection, where one sample contains cDNA molecules labelled with fluorescent dye Cy3 (green) and the cDNA molecules from the compared sample are labelled with the fluorescent dye Cy5 (red). Each colour corresponds to a different wavelength and can, therefore, be measured separately. When the intensity of the two colours have been normalised, the comparison can be made numerically, and furthermore, visually, by overlying an image scan for each colour with each other. Each probe-type location on the array will appear in the colour of the labelling dye of the sample that dominates the hybridisation. If both samples are present, the resulting colour will be yellow.

However, to formally process these data, we need a more sophisticated approach. Applying t-statistics is the most straightforward with the objective of comparison, especially when looking at the differential expression on a gene-to-gene basis. Between two groups, the difference in the average expressions of each (for example, experimental group versus control group; control being the reference group) is presented in a $\log_2$-scale and is called the fold change ($\log_2$(FC)). If the value of the fold change is negative, the expression has been downregulated in comparison to the reference group, whereas the value of the fold change being positive, the expression has been up-regulated. The t-test provides the ratio of the difference between the groups' average expression and the variability of the groups. However, to normalise the variability between individual genes, a modified version of the t-test, called moderate t-test, furthermore, replaces any gene-specific variance by a common variance that represents all the genes analysed. Finally, the p-value of the t-test hypothetically determines how likely the same t-value is to be observed if the gene was not differentially expressed between the two groups. One can use the p-value as an arbitrary level of significance; for example, a p-value≤0.05 indicating that the difference is significant in 95% of the cases.

There are many different ways to represent the data of relative changes in gene expression. Some of them complement each other. However, the choice ultimately depends on the setup and the purpose of the experimental study and which type of interpretation is needed. With the focus on differential expression and correspondence with gene expression profiles, which means both wanting to look at many groups and many genes at a time; the volcano scatter plot and the gene list plot (in particular) are useful.

1.5.4.1 Practical Use of the Gene List Plot

When looking at groups of genes, for example, a gene expression profile, where the focus is on the differential expression and not on the absolute values, the gene list plot is very straightforward. The plot can be constructed in many ways. The fold change values can be presented per each gene, typically listed in rows, and per each comparison of groups in columns. The fold change is usually visually expressed by bars (with pooled standard deviations as error bars) heading towards the right in a positive direction if reflecting an up-regulation and heading towards the left in a negative direction of reflecting a down-regulation. Reference lines to mark certain fold change values are used as a visual aid to ease a general estimation.

1.5.4.2 Genome Overview with the Volcano Scatter Plot

A volcano plot is visually very appealing to guesstimate the number or the layout of the expression of many genes with reference to their p-value. Each dot in the graph represents one gene and is

plotted as its log_{10}-transformed p-value as a function of the fold change (logFC) landing the gene either on the down- or up-regulated section of the x-scale. The y-axis, the p-values, are in reverse order where one can conveniently mark the significance threshold value horizontally. If the majority of the expression values are not significant, they will be clustered below the horizontal threshold, whilst the significant range stretches upwards scattering the significantly expressed genes that are generally marked with the gene symbol if far from the main cluster. This plot can be used to rank the genes in their order of significance. However, for complex experimental setup, it has its limits, as one graph only compares two sample groups at a time, and is therefore perhaps more useful for intermediate data analytical steps.

1.5.5 Experimental Interferences

Gene expression analysis is very sensitive to all sorts of variability and deviations that can potentially take place during the entire experimental process. One of the fundamental factors that represents biological variability is evident when comparing the use of in vivo tissue samples vs in vitro cell cultures. When using experimental animals, an intention to the onset of biological differences is reduced by using genetically similar strains. However, the 'unwanted' biological difference can take rise from the difference in handling and living conditions, nutritive conditions, gender and age, and even different anaesthetic agents have been demonstrated to have their effects (Champy *et al.*, 2004). Although, some of the factors are more pronounced depending on the tissue sample of interest, standardising the experimental protocols becomes essential, especially if the experiment runs for a considerable time.

It is, furthermore, crucial to consider the tissue heterogeneity, especially if the experimentally affected cells are relatively localised within the organ, in which case a 'global' homogenised sample from the tissue can easily dilute any difference in the gene expression between the cells. Still, even if all these factors are controlled or managed, the practical aspects of the sampling itself have a big role in the quality of the sample. Samples can be processed immediately after tissue dissection, but in large experiments that is rarely practical and the samples need to be frozen. The length of the period from the time the fresh sample is acquired until it is snap frozen is critical regarding degradation of the mRNA and also for cross contamination with other samples via laboratory material. It is recommended that samples stay fresh no longer than 30 minutes (if to be frozen) and should be stored at −80 ºC reducing any freeze-thaw cycles. These factors are also very prominent in the RNA extraction itself, and it is important that the quantity of any isolated RNA be of high quality. The type of tissue can be a factor in the RNA yield, with fibrous tissue like skeletal muscle

having expected yield of 1-2 µg per 1 mg of sample, in comparison with 4 µg per 1 mg of cardiac muscle and 5-10 µg of 1 mg of liver tissue. Factors like these play a significant role in isolation, and it becomes a question of judgement whether the processed sample should be run through its extraction filters fewer times for higher yield or more times for higher purity as there is a minimum working quantity for the downstream microarray preparations. Therefore, the quantity and quality of the RNA is systematically assessed, based on potential degradation (28S:18S rRNA test), purity (A260/280 and A260/230 tests), and used as a point of reference for normalisation for the subsequent analysis.

1.5.6 Coda

As with many types of samples, one needs to be aware of the fact that gene expression measurement with arrays is a snapshot. The timing of this snapshot is crucial in order to gain a real insight into the consequences of physiological changes on a cellular level thus the main question concerns when they occur. Recently, the timing has been challenged as research has demonstrated that genetically identical subjects can have very different and random fluctuations in the expression of individual genes, ultimately suggesting basal stochastic characteristics (Raj and Van Oudenaarden, 2008) and even chemical memory (Tian, 2013). Still, these characteristics seem to differ between genes as well, which underpins the need to recognise the genes for an in-depth gene expression analysis. For any given physiological experiment, the choice of pathways with its representative gene expression profile could be both more or less extensive. One needs to be reasonable concerning the definition of a pathway (or pathways) and the corresponding gene expression profiles and the physiological conditions they are supposedly reflecting. The definition of a pathway is far from being set in stone regarding which genes make up the expression profile. The profile can be dependent on the definition of the physiological condition as well. Many genes have now been accepted to be responsible for protein synthesis in a particular biochemical reaction. Still, many gene participations would need to be verified even further and probably others that are unrecognised.

2 Thesis Aim

The general aim of this thesis is to see if intermittent hypobaric hypoxia exposure, alone or followed by a short duration of low impact rehabilitation exercise, has any effect on the recovery profile of the skeletal muscle damage elicited in m. soleus by a downhill-eccentric exercise-induction in treadmill-trained rats. The recovery after the induction of muscle damage was monitored via indirect measurements at four different time points throughout a 2-week rehabilitation period with a passive recovery as the control condition. The exercise-training protocols modelled to simulate that of human recreational athletes.

The indirect measurements used in the experimental work for this dissertation are: (**a**) Skeletal muscle damage-plasma markers; and (**b**) Differential expression of theoretically-representative gene expression profiles in the rat's hind limb m. soleus, as the muscle downhill eccentric-injury model protocols are widely considered effective.

Secondary measurements to ensure the experimental conditions are: (**c**) An intuitive treadmill-running rat's performance score (AEY-score), to estimate the quality of the treadmill training both before, during and after the exercise-induction of skeletal muscle damage. (**d**) The rat body weight logs, the lung and heart weight fraction and the Fulton index, to differentiate between sedentary, hypoxic and exercising rats. Lastly, (**e**) the internal quality control actions for procedures and analysis to ensure the validity of the results.

Given the following experimental conditions are true …

(**i**) The rats are considered trained (as 'recreational athletes') before the induction of skeletal muscle damage.

(**ii**) The downhill-running protocol is sufficiently effective to induce skeletal muscle damage (at least, noticeable in the rat's soleus muscle).

(**iii**) The intermittent hypobaric hypoxia exposure programme elicits physiological changes (acclimation) that improve the recovery of injured tissues.

(**iv**) The hypoxia exposure followed by a light treadmill exercise is different from the hypoxia exposure alone.

The following general and simplified expectancy variables should be …

(**A**) The AEY-score to demonstrate a consistent training performance allowing to discard a potential outlier affecting subject variability during and after training periods — Or, on the contrary, providing a tool that estimates the exercise-implication (individual behaviour) of animals on the treadmill.

(**B**) The skeletal muscle damage plasma markers could be detectable just after the training period (indicating muscle turnover), still, be markedly increased after the injury-induction protocol and be gradually reduced over the recovery period in the case of passive recovery. The intermittent hypoxia exposure should have some form of reduced plasma marker profile. If the addition of rehabilitation exercise favours the recovery, the plasma marker profile should be more reduced. However, there is a possibility of counteractive injury is some, in which case, the plasma-marker profile should have a differing pattern.

(**C**) The differential expression within the chosen gene profiles for the m. soleus, should be reflected in upregulated or downregulated genes, in response to exercise, tissue damage, hypoxia and hypoxia followed with exercise, and tissue regeneration or reparation. Different types of gradual changes should be visible throughout the injury-recovery period with reference to a passive recovery.

(**D**) The body weight log should reflect leaner rats if trained, in comparison with sedentary rats. The effect of the intermittent hypoxia exposure is not expected to have considerable effects on the weight due to the frequency and the duration of the sessions.

(**E**) Exercise is expected to slightly increase the Fulton index, with reference to sedentary subjects. Hypoxia is considered to be more effective than exercise to increase the index. After becoming 'recreational athletes', it is possible, to a certain extent, that the physiological changes are reflected in a higher index. Skeletal muscle damage alone is not considered to have any effect on this parameter. The intermittent hypoxia sessions might increase the index but likely to be only visible at the end of the measured recovery period. As the addition of rehabilitation exercise is not designed for endurance purposes, it is not likely to have any additional effects on the index during the recovery period.

3 Material and Methods

3.1 The Experimental Pretext

The funded research project, bearing the translated name 'Effect of intermittent hypobaric hypoxia on induced muscle injury repair in laboratory rats', makes the foundation for the work accounted in this dissertation. Several practical issues arose during the commencement of the project, requiring execution modifications regarding some parts of the experimental foci. The initial setup aimed to test an equal count of both male and female treadmill-trained Sprague-Dawley rats, divided into two experimental groups, and one control group, with each gender contributing 15 rats in each group ($N_{Rat}=45\times2_{gender}$). After inducing skeletal muscle damage with downhill treadmill running, the tissue recovery would be monitored for two weeks. During the recovery period, four sampling days would be included, [1, 3, 7, 14] days after the injury induction and one sampling day prior as a reference.

The main sample types of interest would be blood samples, to measure plasma markers with ELISA and blood cells with cell counting, and skeletal muscle tissue, for immunohistochemical and biochemical and quantitative gene expression levels (qRT-PCR) with interest in four different gene profiles. Acquiring the muscle tissue samples would mean sacrificing the animal in question. Therefore, apart from the reference day (prior to damage-induction), from the 1st post injury sampling (day 1) to the 4th post injury sampling (day 14), 3 male and 3 female rats would be sacrificed for the muscle tissue sampling; gradually decreasing the number of rats throughout the period. The blood sampling was planned to be acquired from every rat during each sampling day until it was sacrificed for the other sample acquisition.

3.1.1 The Experimental Caveats

When establishing the most appropriate blood sampling routine, regarding a specific sample volume or an invasive technique that would not have any potential post-sampling physiological effects – the techniques tried were not sufficiently efficient, especially regarding the quantity needed for the downstream analysis. The minimum volume needed would involve more invasive techniques and would interfere with the rat's normal physiology.

The decision was made to sacrifice the rats at each sampling to acquire the sufficient blood sample, counting on plasma marker ELISAs as a quick way to establish the existence of skeletal muscle damage for further studies. As the rats would be sacrificed in each sampling, the compensation would be exploring the rats with acquiring more types of sample. Spreading the rats, $N_{Rat}=45\times2_{gender}$, equally between all sampling days for each group, would mean n=3 per gender.

The results from this setup would be subject to little conclusive meaning, and to compensate, one gender was dropped (the female rats, keeping the more simplistic male rats), raising the count per sampling days and groups (subgroups) to n=6. The count would still stay within the approved N_{Rat}=90 (for the established protocols). To compensate for the extensive log of more samples per rat, the subgroup count was pushed to n=7, to raise statistical significance, simplifying the pre-injury subgroups (explained in the following chapters).

These changes are necessary to bear in mind, as to why only one gender was chosen, and more importantly, the expectancy of biological variability when looking at the overall picture, since from one point of view, the samples are discontinuous by nature. The focus, therefore, shifts to the necessity of rigorous technical integrity, to reduce the addition of other types of uncertainty. Furthermore, changes in the experimental setup altered the previous balance between more simple and advanced analytical techniques due to financial budgeting. The changes weighed down on the samples dedicated to qRT-PCR for four expression pathways; requiring the reduction of N_{Rat} or number of gene profiles. It was considered more valuable switching to whole genome expression analysis and pool data concerning any expression pathway of interest at the expense of reducing the subject number per subgroup.

3.2 The Experimental Backbone

3.2.1 The Ethical Approval

The relevant experimental procedures of the research project, DEP2010-22205-C02-01, were approved by the Experimental Animal Ethics Committee of the University of Barcelona (Comitè Ètic d'Experimentació Animal de la Universitat de Barcelona) (Appendix A.1, p. 167). The animals received humane treatment, fulfilling the Spaniard and European directives for the care of animal used for scientific purposes (Directive, 2010/63/EU).

3.2.2 The Experimental Subjects

3.2.2.1 The General Subject Accounting

During the course of 2.5-3 years, overall 5 female and 152 male Sprague-Dawley rats (strain: RjHan:SD, Janvier Labs, France) went through the entire experimental process. These were outbred albino rats with the Tyr^{c}/Tyr^{c} genotype. The rats went through the process generally in lots of 10 (min 5, max 13) to comply with the housing limitations and the experimental equipment availability. The experimental schedule was specifically constructed around general working days and other critical factors, to ensure repeatability between lots. Each lot always arrived on a Wednesday to the certified facility for experimental animals (Faculty of Biology, University of Barcelona) at the weight of 0.10 kg each (about 28 days old, Appendix A.2, p. 168). After six days in quarantine (the following Tuesday), the rats were moved to the experimental laboratory to immediately commence the first day of the experimental process, weighing 0.156(±0.009) kg. The first rats used were the 5 female rats and only served as a part of the trial tests (reasons explained in Chapter 3.1.1). From that point onwards, only male rats were used. Parts of the overall experimental project have a different subject count for logistical reasons, where 'N' will be symbolling an overall count for subjects, data sets or combined data sets; and where 'n' will be symbolling subgroup count or relevant partial count.

3.2.2.2 The Subject Identification Integrity

On their arrival to the experimental lab, each rat was numbered on the tail close to the base, with a marker; with the strategy in mind of using odd numbers for male rats and even numbers for female rats. These numbers were assigned in a logical order from 0-99 and then reused. This number, the working number, was remarked each week to avoid fading of the marks. The number was always written horizontally from the base towards the end of the tail, to secure a one-way-of-reading and avoiding potential ambiguity. The number was, furthermore, carefully registered and linked to the rat's home cage, along with the rat's unique ID number (a 9-digit code). The working number (on

the tail), used during the rat handling phase, was never used simultaneously with the ID number, which was applied at the moment of anaesthesia in the sampling procedure. The link registry between the two numbers was kept hidden and only used by two agents exclusively at the moment of anaesthesia. In this way, all agents that worked with the rats during the handling phase were only exposed to the working number; and from the moment of sampling and subsequent analysis, were only exposed to the 9-digit ID number without knowing the connection between the numbers until made accessible on the databases post all data analysis. The reason for this setup was to keep any biased opinion due to any given rat's behaviour separate from potentially affecting the downstream processes that took place during and after the sampling.

3.2.2.3 Housing and Care of the Rats

Throughout the entire run of the experimental project, the same protocol was used to monitor, maintain and clean the animal housing on a regular basis. The facility's room temperature and relative humidity ranged between 20-25°C and 45-55% respectively. The rats were housed at maximum three rats per cage (dimensions [length × width × height]: [465×215×145] mm), were fed a standard diet (15-mm diameter granulates) and water *ad libitum* and were regularly checked for stress signs, judging from their physical appearance and body weight monitoring. The weight logging consisted of a 3-times/week registry, in addition to other one-time weight registries needed, for each animal, until its end in the experimental process. Results from the weight accounting are presented in Chapter 4.1. Furthermore, the rats were handled regularly following an in-house handling protocol to ensure a routine and calm environment, especially for the anaesthetic manoeuvring (Appendix B.1, p. 169).

3.2.3 Instrumental

3.2.3.1 The Rat Exercise Treadmill

An encased five channel treadmill with an adjustable running plane (5°/ramp-setting from −15° to 25°) and its accompanying treadmill controller (LE 8710, Harvard Apparatus, United States), were used for the run-training. The instrument allows the running to be stimulated with an adjustable light electric shock (ranging from 0.2-2 mA), received when touching metal grids, located behind the back end of the treadmill belt. The encasing of the treadmill separates the five channels/lanes. The lid of the encasing is located in the back, above the metal grids, and air holes on the walls behind the metal grids and at the front, for each lane, enable free flow of air inside the encasing. For each lane, the monitor on the treadmill controller displays: (**i**) the number of electric shocks generated, (**ii**) the accumulated time of electric shocks, and (**iii**) the calculated distance considering

the set velocity and the time lapsed with the time spent receiving the electric shock deducted. The velocity setting gives a range of 0.05-1.50 m/s (0.18-1.08 km/h), with changes made collectively for all lanes, controlled with a start/stop button. When the button is on start, all running recordings are continuously displayed on the monitor. When the button is pushed to stop, the last recordings remain onscreen until the button is hit again or the reset button is pushed. The system offers the ability to connect the controller to a PC to automatically acquire the recordings in digital form. However, this function was not available for the project. The detailed description of this instrument plays an important role in issues concerning handling and monitoring the rats whilst on the treadmill.

3.2.3.2 The Hypobaric Chamber

A steel based grid creating the interior space of [0.6×0.6×0.9] m (length × depth × height), encased in 5 cm thick plexiglass blocks on each side, forms the custom-made hypobaric chamber (constructed 2008, Dept. Physiology & Immunology, University of Barcelona). An additional exterior steel grid positions the plexi blocks and junctions are sealed with silicon. Three holes run through the plexi blocks, each on a different side: (**1**) for the tube connection to the rotary vane pump (Trivac D4B, Oerlikon Leybold Vacuum, Germany), a vacuum pump which lowers the chamber's internal air pressure by suctioning the air out; (**2**) as an inlet for the passive pressure sensor (Penningvac PR25, Oerlikon Leybold Vacuum, Germany), which provides a continuous internal air pressure reading on the monitor operating unit (Combivac IT23, Oerlikon Leybold Vacuum, Germany); and (**3**) for the air valve (Vacuum lock valve DN16, Oerlikon Leybold Vacuum, Germany) with adjustable opening, enabling the manual control of the air flow. The vacuum pump, theoretically, can create a vacuum inside the chamber. However, the strength of the internal steel grid has only been tested to withstand an imploding force to the internal pressure of 526 hPa (395 torr), which simulates the altitude of slightly higher than 5000 m above sea level. Keeping the air valve closed during the running of the vacuum pump, allowing the internal pressure to decrease, until a reached set point. Opening the air valve slightly (which increases the internal pressure), with the pump running (which decreases the internal pressure), can be adjusted to maintain stabilised pressure, simultaneously allowing a steady influx of fresh air through the chamber.

3.2.4 The Experimental Strategy and Protocols

3.2.4.1 The Experimental Strategy

From the experimental point of view, the project was divided into two phases, connected by the point of sampling: (**i**) the rat handling phase, a pre-sampling phase which included the experimental protocols with the objective of creating the desired physiological conditions; and (**ii**) the analytical phase, a post-sampling phase, which included the sample analytical protocols and data handling procedure, to measure and interpret the resulting physiological conditions.

The Rat Handling Phase

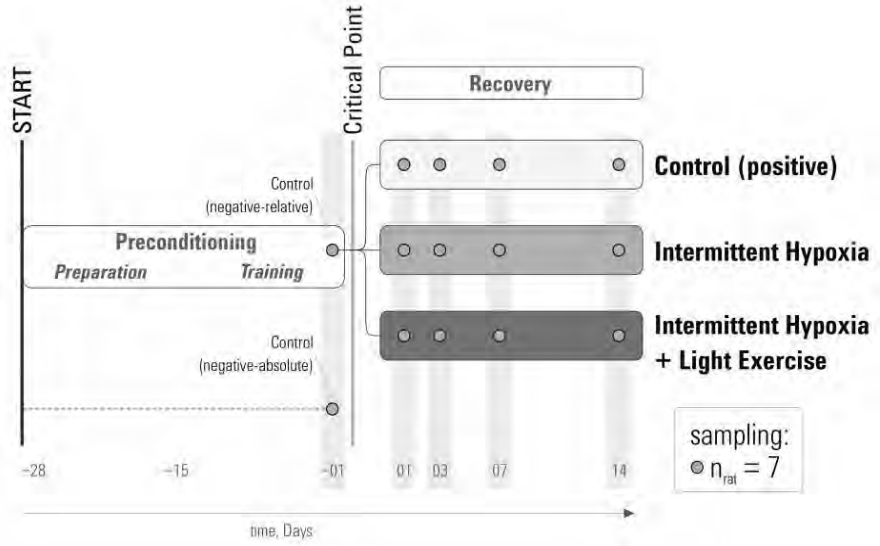

Fig. 3-1. The rat handling phase of the experimental procedure commencing with a countdown, from Day −28 to Day −1, representing the preconditioning period until the day of the experimental critical point (Day 0). Thereafter, a count-up, from Day 1 to Day 14, representing the recovery period.

Fig. 3-1 shows the schematic setup of the rat handling phase of the experimental procedure. Each rat handling phase started on a Tuesday (Day −28), the first day of the preconditioning period, which was composed of two stages. First (**i**) the preparation stage of 10 working days (2 weeks, minus 1.5 weekends), with the objective of conditioning the rats to get used to the stress of being inside the encased treadmill and then to run continuously; and then (**ii**) the training stage, of 10 working days (2 weeks, minus 2 weekends), ending with 1 additional relaxing day (always on a Monday), with the general objective of increasing stamina on the treadmill.

The day marking the critical point of the experiment (Day 0, always on a Tuesday) reflected carrying out the eccentric exercise-induction of skeletal muscle damage on the treadmill. Lastly, the recovery period, lasting 1-14 days (2 weeks, minus 2 weekends), is where the rats were divided into the

experimental groups, where each reflected the different application of recovery methods to induce the experimental physiological conditions of interests, ending with sacrificing the rats on different days during the period.

3.2.4.2 The Experimental Groups

With the aim of investigating the effect of two physiological applications on trained rats with induced skeletal muscle damage, two experimental groups were planned out: (**i**) The group of hypoxia, [H]-group, subject to intermittent hypobaric hypoxia sessions during the working days in the recovery period; and (**ii**) the group of hypoxia+exercise, [E]-group, subject to the same hypoxia sessions as [H]-group, but, immediately followed by an additional light rehabilitation training on the treadmill. (**iii**) The positive control group, [C]-group, (positive to training followed by the induced muscle damage) experienced no additional physiological application, i.e., had a passive recovery during the recovery period. (See Chapter 3.2.4.3 for negative controls.)

3.2.4.3 The Sampling Frequency

For each experimental group, [C], [H] and [E]-groups, sampling took place on 4 different days throughout the recovery period; on Day 1, Day 3, Day 7 and Day 14. The subgroups with reference to the day count were identified as following: In the control [C]-group, C{01}, C{03}, C{07} and C{14}; in the hypoxia [H]-group, H{01}, H{03}, H{07} and H{14}; and in the hypoxia+exercise [E]-group, E{01}, E{03}, E{07} and E{14}.

The Negative Controls

For a physiological reference, an additional control subgroup was strategized, R{−1}, with rats that after having gone through the preconditioning period, training on the treadmill, were sacrificed on Day −1; before the induction of muscle damage on Day 0. This control group was relatively negative; negative to the induced muscle damage, still, positive to the preconditioning.

For an analytical reference, another additional control subgroup was strategized, A{−1}, with sedentary rats throughout the preconditioning period and were sacrificed on Day −1, before the muscle damage induction. This control group was absolutely negative; negative both to the induced muscle damage and to the preconditioning.

A detailed schedule, lining out the actions carried out for each subgroup, with reference to the name of periods, stages, weeks and days, is provided in Appendix C.1, p. 189.

3.2.4.4 The Experimental Subject Counting

Rats were randomly allocated to the different scheduled subgroups throughout the entire duration of the research project, with the following accounting in mind: Each of the 14 subgroups (experimental and negative controls) consisted of n=7 male rats or N_{Rat}=98 in total for the study. (This count does not include n=4 rats that were discarded throughout the rat handling process).

Over the preconditioning period, the N_{Rat}=98 weighed on average 0.156(±0.009) kg and 0.24(±0.01) kg at the start and the end of the preparation stage, respectively, and then, 0.27(±0.01) kg and 0.38(±0.02) kg at the start and the end of the training stage, respectively. The weekend between the stages bridged the weight gain. Of those rats, N_{Rat}=84 exercised according to the muscle damage protocol, on Day 0, weighing 0.39(±0.03) kg at the start of the day and 0.36(±0.02) kg at the end of the day. These rats commenced the recovery period on Day 1 weighing 0.37(±0.03) kg, with the average weight gain of 0.0063 kg/d throughout the period.

3.2.4.5 The Experimental Protocols

The General Structure of the Exercise Schedule

During the preconditioning period, the rats generally did sessions of continuous exercise 5 days per week (d/week), but not on the weekends. From Week 1 to Week 4, they started with one session per day (1 Sess/d), always around 09:00 hours, from Day −28 to Day −25. During the rest of the period they did 2 Sess/d. On a day with two sessions, the former session was carried out around 09:00 hours and the latter session around 17:00 hours, with the goal of minimum 6-h rest in between them. On Day 0, the day of muscle damage induction, they carried out two sessions with a 4-h rest in between. Lastly, during the 14-d recovery period, Week 5 and 6, the assigned rat group did 1 Sess/d (around 13:00 hours), but never on the weekends.

The General Phases of a Treadmill Session

All exercise protocols were generally divided into 5 phase-settings (from 0 to IV), as per Fig. 3-1, addressing the floor angle of the treadmill, θ, in °, the speed, v, in m/s, the acceleration, a, from one speed setting to another, in (m/s)/min, and the duration, t, in min. (**0**) Phase 0-setting involved no treadmill velocity, still, with an active electric shock function. (**I**) Phase I-setting consisted of a 5 min acceleration to a specific velocity mark. (**II**) Phase II-setting involved a 2-3 min lower acceleration to a higher velocity mark in comparison with phase I (this phase was only used in the preparation stage, see below). (**III**) Phase III-setting, the main exercise phase of each exercise session, where the set/objective velocity was kept stable. Lastly (**IV**) phase IV-setting, which included a 1-2 min rest at the end with no velocity, still, with the electric shock function active. A detailed qualitative registry

of each rat's performance, with specific analytical emphasis on phase III, makes up part of the result data in this dissertation (see Chapter 3.3).

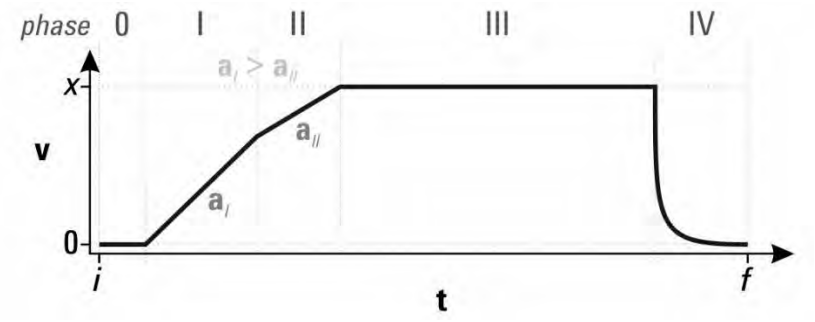

Fig. 3-2. The general phase-settings for one treadmill session reflected in velocity, v, as a function of time, t. A typical session initiating at t=i and ending at t=f with the velocity objective of v=x in phase III, starts and stops with no velocity in phases 0 and IV respectively. The velocity change from v=0 to v=x is carried out with acceleration rate a_I on phase I and a_{II} on phase II, where $a_I > a_{II}$.

The Preconditioning Period — Treadmill Protocol During the Preparation Stage

The formal day count for the preparation stage was between Day −28 and Day −16, covering Week 1 and Week 2 of the experimental process. This stage had ten working days (days with sessions): Day −28 to −24 of Week 1, Tuesday to Saturday; and Day −22 to −18 of Week 2, Monday to Friday. The objective of this stage was to reduce stress by conditioning the rats to the environment of the treadmill and for that the rats would run continuously on a θ=0°-planar surface — preferably avoiding receiving electric shocks from the grids. Day −28 and −27 solely consisted of the rats being on the treadmill without running (phase 0-settings). From Day −26 onwards, the treadmill phase III-settings started at v=0.30 m/s, t=10 min/Sess and were gradually changed throughout the preparation stage with 2 Sess/d until the settings matched the training stage protocol (See protocol in Appendix B.2, p. 170).

The Preconditioning Period — Treadmill Protocol During the Training Stage

The formal day count for the training stage was between Day −15 and Day −1, covering Week 3 and Week 4 of the experimental process. This stage had ten working days: Day −15 to −11 and Day −8 to −4, both from Monday to Friday Week 3 and 4 followed by an additional day of rest on Monday of the 5th week, Day −1. The rats always had two identical sessions per day with phase III-settings at θ=0°, v=0.45 m/s, t=30 min, with a minimum of 6-h rest between the sessions on each day (See protocol in Appendix B.3, p. 172).

The Muscle Damage Protocol on Day 0

This protocol was specific on Day 0 (always a Tuesday) and represents the critical point of the experiment to induce skeletal muscle damage with eccentric exercise/running on the treadmill. The

protocol is carried out twice with a minimum of 4-h rest between the sessions. The rats ran downhill with a slope of θ=−15° declination, v=[0.50-0.70] m/s until exhaustion. Each rat was immediately removed from the treadmill if muscle damage became visible in the running style; and, if no signs were visible, removed from the treadmill at the point of exhaustion (See protocol in Appendix B.4, p. 174).

The Recovery Period – Intermittent Hypobaric Hypoxia Sessions

The recovery period had the formal day count of Day 1 to Day 14, covering Week 5 and Week 6, with overall ten working/session days, starting on a Wednesday and ending on a Tuesday, two weeks later. The rats allocated to the groups of hypoxia [H] and hypoxia+exercise [E], were placed inside their cages into the hypobaric chamber for 4-h sessions at a simulated altitude of 4000 m above sea level, i.e. at 616 hPa (462 torr). Each session started and ended with 12-15 min to adjust the pressure gradient in addition to the 4 hours. The sessions were carried out in the morning, starting at around 08:00-09:00 hours only on the working days. During each session, the rats were monitored closely, registering a qualitative status rapport for each rat every 30 min, to secure their wellbeing and on standby to terminate the session immediately if necessary. On a day of sampling, the rats always finished their session first (See protocol in Appendix B.5, p. 176).

The Recovery Period – Treadmill Protocol

The rats of the hypoxia+exercise [E] group, immediately (<30 min) after each hypoxia session (described above), continued with a light rehabilitation exercise on the treadmill. The rats ran uphill with θ=5°, inclination, at v=0.30 m/s for t=15 min in the treadmill phase III-settings. The idea was to imitate the condition of humans doing exercise inside a hypobaric chamber. However, as the rat treadmill did not have wireless control, the analogue setup was limited regarding those conditions (See protocol in Appendix B.6, p. 178).

Running Encouragement Whilst on the Treadmill

The mild electric shock (intensity range: I=[0.2–2] mA) that the rats received if lagging in the running and touching the metal grid was a useful stimulus to encourage running, still, also the most efficient resource for stimulus throughout all the weeks of training. Therefore, the use of the electric shock was regulated with gradually changing minimum and maximum intensity limits throughout the weeks. For the ten working days of the preconditioning stage, the intensity limits ranged from I_{min}=0.2 mA at the beginning to I_{max}=1.0 mA at the end of the stage. For the ten working days of the training stage, the intensity limits ranged from I_{min}=0.8 mA to I_{max}=1.8 mA. During the muscle damage protocol on Day 0, the intensity limits ranged from I_{min}=1.2 mA to I_{max}=1.8 mA. Lastly, for the light exercise protocol, used throughout the recovery period, intensity limits ranged from

I_{min}=1.0 mA to I_{max}=1.6 mA. A log was kept to monitor the changes made in the applied intensity, which was always adjusted to the worst performing rat in each training lot. Following the log, it was made sure that throughout all the exercise sessions, the intensity was never lower than the last change made (for the training lot in question), still, kept within the described minimum and maximum limits for each period/protocol. The training agents were, furthermore, instructed to knock on the back wall of the treadmill, or simply give the rats a little push (with their hands), to strategically reduce the use of the electric shock, hence, making the electric shock more effective if nothing else worked. At the end of each training session, the good rat performers (subjective-qualitative estimate), always received a bit of chocolate as a reward linked with the sound of a bell. Each rats' reaction to the chocolate was logged to possibly identify stress or tiredness (No data provided in this dissertation).

The Control Group Protocol

During the preconditioning period, the absolute negative control rats, A{−1} (n=7), always stayed in their cages close to the treadmill during sessions until Day −1. The relative negative control rats, R{−1} (n=7), were randomly allocated to the group on Day −1 after participating in the treadmill protocols like the other rats. The positive control rats, [C]-group (n=7 ×4 subgroups), randomly allocated to their group, participated in the treadmill training like the other rats until Day 1, at the start of the recovery period. The [C]-rats always waited in their cages on top of the hypobaric chamber, during the sessions, to reduce the difference in the stress stimulus provoked by the noise from the vacuum pump.

3.2.5 The Sampling Procedure

The project's sampling procedure (The S33+ Sampling Process, in Appendix C.2, p. 190) intertwined the preparation stages of all provisional analytical assays, some of which that do not form part of this dissertation — however, the level of integrity and quality assurance still does.

3.2.5.1 The Material used in the Sampling Procedure

Chemicals

0.05% (v/v) Chlorine solution for surface sterilisation; 0.5 M NaOH-solution and 70% (v/v) Ethanol-solution for sterilisation of surgical material. 0.9 g/dL NaCl-solution for tissue bath; 30 g/dL Urethane solution, with a 0.9 g/dL NaCl as diluent, for irreversible anaesthesia (solution-batches older than 6 days were not used); Cocktail combination with 42.9% of 100 mg/mL Ketamine solution and 57.1% of 20 mg/mL Xylazine solution, for long reversible anaesthesia; Isolfurane as backup anaesthesia. Isopentane and liquid N_2 for tissue storage.

Material

Three-part (1-mL and 2.5-mL) syringes with 23 G needle (Blue) for the anaesthesia; 3-part (5.0-mL) syringe with 21 G needle (Green) for retrieving blood. 4-mL tubes to receive blood: K_3-EDTA and Na-heparin treated. Surgical equipment: surgical blades (No. 10A and 21A) and handles, pincettes and scissors. Surgical gauzes for drying and plastic plates and bags for tissue storage.

3.2.5.2 Maintaining the Subject Identification Integrity

Just before initiating the sampling with anaesthesia, the working number on each rat in the sampling lot was hidden with its corresponding unique 9-digit ID (as a barcode), to 'blind' the agents carrying out the sampling procedure (see Chapter 3.2.2.2). Furthermore, within each lot, the rats in the sampling lot were put under anaesthesia in a random order. The 9-digit ID codes displayed during the sampling would therefore never appear in a logical order, to further confuse any preconceptions of which rat was in sampling. Moreover, during the sampling routine, 2-3 rats could coincide in the process as far as being in the sampling laboratory at the same time. To avoid any mix-up between the dedicated plastic and storage material for each rat, the random anaesthetic order (to confuse the 9-digit number logic) was given a logical Roman operating number (I-X, depending on the lot size) accompanying each rat throughout the sampling routine. Pre-sampling, each roman number was applied to a set of plastic and storage material dedicated to one rat in the sampling. This action, furthermore, controlled the identification of each pre-weighed material and gave a clear separation as to which material should be in use for any given rat.

3.2.5.3 The Anaesthesia and the Blood Sampling

Rats were weighed about 1 hour before the sampling process to calculate the anaesthetic dose. To reduce the stress for each rat at the point of anaesthesia, the necessary handling, formed part of the regular handling protocol, used throughout the rat handling phase (see Chapter 3.2.2.3). Sacrificing each rat in its sampling, an irreversible anaesthetic agent (Urethane dose 1000 mg/kg rat body weight) was injected IP (right side) (Parasuraman, Raveendran and Kesavan, 2010). In the case of the solution seeming to end up in the fat tissue, thus not having sufficient anaesthetic effect, the additional dose was injected IP (left side) to the maximum of total Urethane dose of 1500 mg/kg rat body weight. Signs of adequately deep anaesthesia was generally reached after around 5 min, at which point the rat was re-identified (visually) with its registered ID code. The coded rat was moved into the operating laboratory and prepared for blood sampling via the vena cava, opening the abdominal area for further dissection (Parasuraman, Raveendran and Kesavan, 2010). About 3-4 mL of blood sample went into a pre-weighed syringe and was weighed to estimate the

density. The sample was distributed according to the estimated need of 1 mL into a heparin-treated test tube for rheological analysis (requiring the density measure) and the rest of the whole blood into an EDTA-treated test tube for a general blood cell count, plasma analysis and stem cell analysis. The plasma analysis with plasma markers makes up part of the result data in this dissertation (see Chapter 4.3).

Reversible Anaesthesia

As the original idea was to sample each rat for blood several times, the reversible anaesthesia needed to be used (until eventually sacrificed with an irreversible anaesthesia) with a combination of the dose of 60 mg/kg Ketamine and 16 mg/kg Xylazine (IP injection). In these trials, if a rat did not show sufficient level of anaesthesia after the expected amount of time, the anaesthetic level was assisted by having the rat inhale isoflurane. With this anaesthesia, the blood sampling was carried out via the saphenous vein or the tail vein (Parasuraman, Raveendran and Kesavan, 2010).

3.2.5.4 The Dissection of Skeletal Muscle Tissue

After the blood sample was acquired the dissection of the skeletal muscle started. From the rat's left side: m. tibialis anterior, m. gastrocnemius, and m. soleus. Except for m. soleus, the muscles were cut into approximately even distal and proximal parts. All tissue samples were coded and weighed, and immersed in 1 mL of isopentane, and then stored in liquid N_2 until the point of histochemical analysis (not part of this dissertation). From the rat's right side: m. tibialis anterior, m. gastrocnemius, m. soleus, m. extensor digitorum longus, m. quadriceps femoris. The sampling objective focused on fractioning each muscle to the maximum of three ≈200-mg samples and the rest of the tissue in the fourth fraction (if applicable). Each tissue fraction was individually weighed and coded, put in a sampling bag, fast frozen in liquid N_2 and stored at −80 °C until the point of biochemical analysis (on all muscles) and gene expression analysis (only on certain m. soleus samples). The gene expression analysis on m. soleus makes up part of the result data in this dissertation (see Chapter 4.4).

3.2.5.5 The Dissection of Other Organs

After the dissection of the skeletal muscles of interest had concluded, other organs (the diaphragm, cardiac muscle, lungs, and brain) were dissected, coded and weighed. The fresh weight of the lungs and the heart were used for a normalised developing-weight comparison. All the samples were then fast frozen in liquid N_2 and stored at −80 °C until the point of biochemical analysis (not part of this dissertation).

3.2.5.6 The Weight Statistics

The weight fractions of the lungs and specific parts of the heart, the right ventricle and the combined left ventricle and septum, were calculated as:

$$\frac{w_x}{w_{Rat}}$$

Equation 3-1

where, w_x, symbols the weight of organ or organ part in question, and w_{Rat}, symbols the rat body weight. Furthermore, weight ratio between the ventricles of the heart, to obtain the Fulton-index, FI, was calculated as per the following formula:

$$FI = \frac{w_r}{w_{(l+s)}}$$

Equation 3-2

where, w_r symbols the weight of the heart's right ventricle and $w_{(l+s)}$ symbols the combined weight of the heart's left ventricle and septum. One-way ANOVA with Turkey's Test was used to analyse the weight ratios of all the subgroups in the study with the threshold of significance at $p \leq 0.05$.

3.2.6 The Trial Tests and the Developmental Actions

Certain testing was needed to establish the custom experimental protocols that involved the rats, actions of which led to marked changes in the experimental strategy and procedures. The first 10 rats, beginning with 5 female and then 5 male, were used to develop the rat experimental protocols and establish adequate sampling techniques. (From this point onwards, only male rats were used for the subsequent actions). The following 20 rats and the samples acquired from those, were used to establish the final versions of the rat experimental protocols, including carrying out the muscle damage protocol (see Chapter 3.2.4.3) only once. Furthermore, the sampling and the analytical processing techniques were established with those rats.

3.2.7 The Data Processing & the Management System

As part of an internal quality control setup for the project, all actions relating to the experimental and analytical procedures were carefully logged to ensure traceability and reliability of the results, using MS Excel. The acquisition of the sample data was obtained (real time) using tailored VBA-tailored programming, where the entire sampling process was carefully registered using unique 9-digit ID barcodes for each and every sample or sample fraction. All logging included hour, date and which agent carried out the action. The acquired log was imported into a VBA-tailored post-sampling database which managed all analytical data and traceability and status; managing the

logs on sample banks, keeping information on localisation and utilisation for the count of freeze-thaw cycles with reference to an hour, date and agent involved.

3.2.8 Non-Conformity Issues

A deviation report system was used throughout the experimental and analytical trials to register all non-conformity issues that occurred. The issues were divided and categorised into small deviations and big deviations. Small deviations included incidences that did not comply with given protocols, in a way that they did not require the action of stopping a procedure (experimental or analytical). Big deviations, on the other hand, included incidences that did require partially or fully stopping a procedure (experimental or analytical) until it was temporarily or permanently resolved by a supervising agent.

The agent that experienced the incidence filled out a deviation report and forwarded it to the relevant supervising agent responsible for the procedure in question. Once a solution was provided, the supervising agent added the resolution to the report for completion. The reports were made accessible for the research group to see, and therefore all agents were updated in detail on the actions that took place.

3.2.9 The General Statistical Approach

The given values for each subgroup are generally expressed as the average accompanied with its standard deviation; unless otherwise noted. Linear T-statistics were used to evaluate regression and linear F-statistics for comparison with the threshold of significance at $p \leq 0.050$. The general route of F-statistics was with 1-way ANOVA due to the general experimental setup, whilst the post hoc tests were dependent on the analytical/sampling procedure involved. The main analytical descriptions in the following subchapters, outline the specific statistical involvement.

3.2.10 Software Packages

The data management was carried out using Microsoft Excel 2007, 2010 and 365 (version 12, 14 and 15, respectively, Microsoft Corporation, USA) with an update throughout the years. All basic statistical calculations were carried out in Excel spreadsheets. The additional statistical analysis of ANOVA and post-hoc tests were carried out using SigmaPlot (version 11 and 12, Systat Software Inc., USA).

3.3 The AEY Performance Score

3.3.1 The Innovative Premise

The AEY Performance Score came about as a secondary (backup) measure for the experimental project, addressing the need to qualitatively quantify a rat's performance, based on its running style and actions, whilst running on the treadmill. In its development, the style was based on three registry criteria, each with a resulting score value. The criteria were each designated its letter, A, E, Y; as the IATA airport code, AEY, for the town of Akureyri, from where the two agents come, who designed and defined the qualitative style codes and the related code of quantification.

3.3.2 The Subject Count and the Developmental Stages

Being a secondary measurement, developed at the onset of the experimental project, the registry notes cover N_{Rat}=130 overall. In retrospect, the development occurred in 4 stages, in the following order: (**i**) The commencement stage, N_{Rat}=20; (**ii**) the formation stage, N_{Rat}=36; (**iii**) the qualitative assessment and quantification stage, N_{Rat}=65; and (**iv**) the re-testing stage, N_{Rat}=10.

3.3.3 The Equipment

For the score, the following items were used: The rat treadmill and accompanying controller used during the training of the rats as per Chapter 3.2.3.1. Extensive registry protocols to log all actions. VBA tailored MS Excel spreadsheet to receive imported data, and to apply calculations according to the quantification protocol.

3.3.4 The Registry Protocols

3.3.4.1 Commencement- and Formation Stages (the 'Historical' Pretext)

The Commencement Stage

During the commencement stage, the agents were still getting to know the practical limitations of using the treadmill. These limitations were based on reoccurring artefacts that obscured the performance parameters, exclusively the two that were related to the electric shock count displayed on the treadmill controller. These artefact-incidences were generally based on either faeces or urine, disposed of by the running rats, touching the metal grid momentarily or for a longer time. If the displayed values (electric shock-related) from the monitor were the only values for future references, one could believe that the rat in question was touching the metal grid instead of

running continuously. The registry of these incidences gradually changed from informal observations to a categorised registry as part of a monitoring protocol during the treadmill sessions, where the artefacts and the error in the electric shock related parameters line out the criteria for the Y-part of the score.

The Formation Stage

During the formation stage, the A- and E-part of the score became gradually defined as the training treadmill protocols had been defined. The first observations involved a slacking tail of a rat that was running continuously. The tip of the tail seemed to be touching the metal grid and potentially affecting the reading from the treadmill controller (with increasing the electric shock count), although the rat could be considered a good runner. Moreover, throughout the stage, a trend was noticed by the experimenters. The rats seemed, in general, to be lifting their tails so the tip would not touch the metal grid, quite evidently, in the early part of a session. However, drawing closer to the end of a session, the tails were slack and perhaps touching the treadmill belt. Therefore, it seemed that the position of the tail could be somewhat telling of how tired the rat was during a session. These observations eventually formed the E-part of the score.

Simultaneously, still more complex in defining, the informal registry of how a rat was running became developed. Between a 'good' performer and a 'bad' one, a running on the treadmill belt without touching the metal grid, as opposed to a rat continuously touching the metal grid, the electric shock count was adequately representative to distinguish the two. Relatively clever rats, however, still managed to partially avoid running with some logical or clever ways without touching the metal grid. Many of these ways required physical involvement by the experimenter (sometimes continuously throughout a session or series of sessions) as increasing the intensity of the electric shock had no influence on these situations. On the same note, the registry from the treadmill controller alone would indicate a rat like this as a good runner, whilst in reality, the rat might not have been training, and therefore, although going through all training sessions it could potentially be an outlier subject. This turned out to be more common than expected, thus, the physical positioning and actions of the rats when on the treadmill, eventually formed the A-part of the score.

3.3.4.2 The Qualitative Assessment and the Quantification Stage

At the beginning of this stage, all classifications for a qualitative assessment of all three criteria of the score were ready, and formal systematic registry was initiated (see protocol description in Chapter 3.3.4.3). The quantification stage took place after all the rats in the experiment had gone through the training, applying calculations on all the systematic qualitative assessment registry afterwards. In hindsight, this meant that the development of the quantification protocol was

independent of the assessment acquisition, thus more objective (see protocol description in Chapter 3.3.5). Still, some sub-classifications were gradually defined and incorporated during the qualitative assessment stage. However, the quantification method strategically does not differentiate between them, making sure the entire assessment would be equally valid, and furthermore, keeping the score criteria open for unforeseen classifications.

3.3.4.3 The AEY Registry

The treadmill protocols' phase III (Chapter 3.2.4.5), representing steady velocity, was utilised to carry out the qualitative assessment. Throughout the entire phase III of each session, for each rat, in every session, the three criteria (A, E, Y) were assessed at the end of every 5 minutes, except in long duration of the muscle damage protocol, at the end of every 10 minutes. Fig. 4-7 and Fig. 4-8 (pp. 80-81) in the Results (Chapter 4.2.1), show the resulting classification marks with a diagram and description, along with the assigned score value for each of the three score criteria. Note that the score value was not available at the actual time of the assessments. A typical registry and subsequent calculations can be found in Appendix C.5 (p. 192).

During each registry period (RP) of 5 min (or 10 min), the rat could show many different styles, especially corresponding to the A-criteria. In the case of many styles (within the same criterion), the most representative were registered only once with the most dominant style underlined, which later, was taken into account in the quantification protocol.

3.3.4.4 The Stage of Re-testing

As all the rats for the research project had been sacrificed once the quantification was in place, rats for a small deviating project were used to quickly retest the data processing efficiency. These rats (see Chapter 3.3.2), with an extended exercise protocol for preconditioning up to 5 weeks, provided the opportunity to quickly retest the methodology and applying the automatised calculations for the score. No data on measuring the efficiency of the procedure is provided. Furthermore, these rats are not incorporated into any other analytical aspect presented in this dissertation.

3.3.5 The Quantification Protocol

3.3.5.1 Turning the Classifications into Scores

Each score criterion would be represented with its resulting score value, but all of them had a style or classification that was considered the most favourable and representative of a theoretically ideal rat running on a treadmill. In a case of an ideal rat, the score value would be reflected in a score roof of 1.00 within each score criterion. Other styles of situations that were less favourable, with

reference to the ideal rat, would reduce the score value until it would be representing a theoretically most unfavourable situation, reflected with a scoring floor of 0.00 within each score criterion.

In the A-criterion, the rat commenced each session with the roof value 1.00, by default. Only one style was considered to represent the ideal runner and reduced this '1' by the value of 0.00 (i.e. no effect). Meanwhile, the other styles were given negative values, i.e. styles with unfavourable traits of various degree, which reduced the default value according to the following formula:

$$[A]_{RP} = 1 + \frac{\sum \alpha_{mark}}{n_{\alpha}}$$

(Equation 3-3)

where, the sum of the score value for each registered mark, $\Sigma(\alpha_{mark})$, divided by the number of A-criterion marks, n_{α}, added to '1' would give the A-score, $[A]_{RP}$, for any given registry period (RP), of (normally) 5 minutes. As each mark is only registered once within each registry period, an underlined dominant mark was treated as occurring twice, both in the score value sum and the mark count. Many of the unfavourable styles were visually different but assigned with a similar negative value. This meant that the score would not be designed to end up with a value that could be back traced to a specific average style, rather, the resulting value would be indicating how good a runner the rat was on the scale from 0 and 1.

In the E-criterion, based on the tail position, the score value was obtained differently, with only 4 (+1) possible style assignations. One tail position was considered the most favourable, with the roof value of 1.00. With two intermediate positions, given the score values of 0.75 and 0.50, and the most unfavourable position of the tail with the score value of 0.25, the score floor value of 0.00 was to reflect on an unfavourable A-criterion situation where marking the tail position would be impossible or redundant. The score for a registry period was calculated as:

$$[E]_{RP} = \frac{\sum \varepsilon_{mark}}{n_{\varepsilon}}$$

Equation 3-4

where, $\Sigma(\varepsilon_{mark})$, is the sum of the score value for each registered mark and, n_{ε}, the number of E-criterion marks, giving, $[E]_{RP}$, the E-score for any given registry period of (normally) 5 minutes.

The Y-criterion, representing artefacts in the electric-shock parameters, commenced with the score roof value of 1.00, by default. This meant that if no incidence took place that would reduce the validity of the electric shock parameters, the Y-score would remain as 1.00. Any registered incidence would then have the effect that the score value would be lower. However, classifying different incidences with regards to influence on the score did not have any reasonable backing. Throughout

the historical observational registry, four main types of incidences covered the majority, and each was given the same reducing value of −0.15. Moreover, only the count of type of incidence (with reference to these four main types) would affect the value, giving the lowest score of 0.40, if all of them would occur during registry, according to the following formula:

$$[Y]_{RP} = 1 + \sum \upsilon_{mark}, \qquad n_{\upsilon}\text{-specific}$$

Equation 3-5

where, the sum of the score value for each type of registered mark, $\Sigma(\upsilon_{mark})$, is added to '1', resulting in the Y-score for any given registry period, $[Y]_{RP}$, of (normally) 5 minutes. As each type of observation was generally followed by a detailed description in the registry, they could vary in terms of content. It was not considered reasonable to code the situation further. Therefore, the Y-score only served to tell how much attention should be given to this part of the monitoring registry. However, if during monitoring registry, incidences were continuously reoccurring, and considered to have a major effect on the readings of the treadmill monitor, a specific registry mark would always change the sum of score values, $\Sigma(\upsilon_{mark})$, to −1.00. This specific registry was independent of other registered marks in the registry period, reducing the $[Y]_{RP}$ to the score floor value of 0.00 to differentiate numerically from the lowest calculated score of 0.40.

3.3.5.2 Averaging Out the Scores

To represent an entire session regarding each score criterion, the score from each registry period within a given session was averaged out according to the following formula:

$$[\bar{X}]_{Sess} = \frac{\sum_{i=1}^{N} [X]_{RP,i}}{N_{RP}}$$

Equation 3-6

where, for each score-criterion X (either A, E or Y), the average session score (or the session score, $[X]_{Sess}$) was calculated by summing up the scores from the registry periods, $[X]_{RP}$, divided by the number of registry period, N_{RP}. With similar logic, a group of session scores could be added up and divided by the session count included, to represent the average score for a given period.

3.3.5.3 The Representation of the AEY Score

The AEY score was designed to be represented as **[**A;E;Y**]** to pool the three criteria together, where a theoretical best rat would have the score of **[**1;1;1**]** and the theoretically worst rat would have the score of **[**0;0;0**]**. Furthermore, as each score (averaged out or not) can represent different protocols, the score should always be accompanied by a represented analysed timeframe and information

about the training setup (θ, v, t, etc.) to evaluate the possibilities of any comparison if the score would be used for other protocols.

3.3.5.4 The Data Overlook and Comparison

The AEY scores were primarily pooled to weekly averages with quartile calculations for a descriptive overview of the scores involved, where the lower and upper fences marking ≈2×SD could potentially differentiate the outliers. The use of the standard deviation (SD) and the standard error of mean (SEM) was applied to describe the variability and to estimate the homogeneity of the entire subject pool.

3.4 The Plasma Markers of Muscle Damage

3.4.1 The Subject Count

The total of N_{Rat}=20 was used to establish the eccentric exercise protocol for muscle damage induction; and after that, N_{Rat}=98 with the established experimental procedure. These 98 male rats were distributed with the objective of n=7 for each experimental subgroup as per Chapter 3.2.4.5.

3.4.2 The Equipment and the Reagents

Centrifuge (CM-6MT, ELMI Ltd, Latvia); ELISA kits: Rat CK-MM [2112-2], Rat Myoglobin [2110-2-N], Rat Skeletal Muscle Tn-I [2020-2-SK] (Life Diagnostics Inc., USA), each kit contained antibody-coated 96-well plates and all necessary reagents; Microplate spectrophotometer (Infinite 200, Tecan Group Ltd, Switzerland), exported readings to an MS Excel spreadsheet; Vortex mixer (VX-200, Labnet International Inc., USA); Plate agitator (Reciprocal 30, Labnet International Inc., USA); Tips and Precision pipettes [10, 20, 100, 200, 300(multi)-µL] (Research Plus, Eppendorf AG, Germany); 0.5-mL microtubes; 5-mL polypropylene test tubes; 0.5-L squirt bottle; distilled H_2O.

3.4.3 The Sampling

Whole blood was received via the principal sampling procedure (see Chapter 3.2.5.3), and centrifuged at 2300 rcf (3531 rpm) for 15 min. The plasma was evaluated according to haemolytic appearance (Chapter 3.4.3.1) and then aliquoted into microtubes. Each tube contained about 120 µL of plasma, enough to carry out one run of assays on both ELISA kits, to not influence the quality of the total plasma volume (from each rat) with freeze-thaw cycles if a second run was needed. Plasma aliquot in a microtube (from the same rat) was registered with a unique 9-digit sampling ID each. Strictly within 60 minutes after sampling, all microtubes were stored at −80 °C until the ELISAs were carried out. A diagram of the procedure is shown in Appendix C.6 (p. 193).

3.4.3.1 The Plasma Haemolytic Appearance Evaluation

A custom made key was constructed to evaluate the plasma with reference to its colour to indicate the level of haemolysis. This was carried out as a precautionary step in the case of haemolysis affecting any type of downstream plasma analysis. The haemolytic evaluation key and matching CMYK colour code are shown in Appendix D.1 (p. 194).

The distribution of non-outliers and outliers from the plasma assay results were checked against their evaluation with the key code, after, identifying any potential outliers with the A15 estimation and, thereafter, with quartile calculations.

3.4.4 The ELISA procedure

Each kit came with its protocol from the manufacturer (Appendix B.7, p. 180), which was followed exactly except using 3 wells (3 replicas) for reading each sample and concentration points within the kit's calibration curve, as opposed to relying on 2 replicas. The fundamental reliability of measurement was determined by looking at relative standard deviation between the readings from the three replicas, according to the general formula:

$$RSD = \frac{SD}{\bar{x}}$$

Equation 3-7

where the relative standard deviation, RSD, is equal to the standard deviation, SD, divided by the average reading between the replicas. The average was considered to be good if RSD≤0.05 and acceptable if RSD≤0.10. Any average reading with an RSD>0.10 was either: (**i**) 'cleaned' if one reading point could be considered an anomaly and omitted (noting the subsequent quantification with an observation for the interpretation); or (**ii**) the sample was repeated (in the case of procedural error) or omitted entirely. Find further explanation in Chapter 3.4.6.

3.4.5 Verifying the Use of the Muscle Damage Protocol

The Rat Myoglobin and Rat Troponin-I kits were used for the first 20 rats to specifically evaluate the effectiveness of inducing muscle damage with the muscle damage protocol (which, at first, only included one session (1 Sess/d) on Day 0, but not two sessions (2 Sess/d) as per Chapter 3.2.4.5). The Rat Troponin-I kit, however, also demonstrated calibration curves with too high RSD values in general, and therefore to avoid any further uncertainty, the Rat Myoglobin and the Rat Creatine Kinase kits were used instead, thereafter, for the N_{Rat}=98. This was the same point at which all protocols were established including using the muscle damage protocol as 2 Sess/d.

3.4.6 The Data Analysis

All calibration curves were run in triplicate on each well plate to reduce any potential ambiguity and to provide the minimum basis for statistical analysis. The validity of each calibration curve was referenced to the coefficient of determination, R^2, and was accepted if R^2>0.999, preferably R^2>0.9999. However, due to marked matrix effect in the lowest concentrations, the curve was

fractioned and experimental samples referenced to the linear fit that corresponded to the fraction part of the curve in question.

Once all experimental samples had been quantified, after the RSD-'cleaning' or a re-run if necessary, the concentration values allocated to each experimental subgroup were revised in two separate ways: (**i**) based on the quartile calculations, using the 1.5×IQR (Interquartile range) to detect the outliers, and then with the Grubb's method (Ellison, Barwick and Farrant, 2009); and, in the case of detected outliers, (**ii**) the values of the outliers were reduced with the A15 estimation (Ellison, Barwick and Farrant, 2009). The comparison between the subgroups was based on two facts: (**a**) that the subgroups of negative control (absolute and relative) did not strictly follow the time line with respect to the critical point of muscle damage, whilst the other subgroups did (where 2-way ANOVA would be appropriate); and (**b**) given the fact that the time factor (after the critical point) was separated by using different rats at each time point, and not the same rats throughout. — Therefore, the resulting statistical tests to determine the significance between the groups utilised was 1-way ANOVA accompanied with Turkey's test post-hoc analysis for multiple comparison, with significant difference referenced to $p<0.05$.

3.5 The Gene Expression in Muscle Damage

3.5.1 The Subject Count

The total of N_{Rat}=42 male rats was used for the differential gene expression analysis to represent the 14 subgroups, each with n=3. The selection of the n=3 from n=7 per subgroups was primarily based on the size/quantity restraints of the analysed tissue, the m. soleus, in the sample processing as per Chapter 3.5.3.

3.5.2 The Equipment and the Reagents

Homogeniser (Polytron PT 3100, Kinematica AG, Switzerland); Dispersing aggregate (PT-DA 07/2EC, Kinematica AG, Switzerland); Analytical balance (GF-200, A&D Instruments Ltd, United Kingdom); Thermobath (Certomat 886 362/8 WR, B. Braun AG, Germany); Centrifuge (CR3i, Thermo Electron Corporation, USA); RNA extraction kit (RNeasy Fibrous Midi Kit, QIAGEN GmbH, Germany), the kit contained specific filters, plastic ware and reagents; Solutions not included in the kit: Absolute Ethanol, 2 M DTT(dithiothreitol)-solution. For cleaning and sterilisation: 1 M NaOH solution, 70% (v/v) Ethanol solution, DEPC-treated water. Sterile consumables: filtered tips and precision pipettes [20, 200, 1000 µL] (Research Plus, Eppendorf AG, Germany); Surgical knife; 15-mL sample tubes]; 25-G needles; 1-mL 3-piece syringe; 15-mL falcon tube; 0.5-mL cryogenic microtubes (to store analytical samples).

3.5.3 The Sampling

Frozen m. soleus tissue samples, prepared in the main sampling procedure (See chapter 3.2.5.4) were used as the most likely candidate of skeletal muscle to have induced muscle damage after the experimental application. Due to economic restraints, the downstream analysis only allowed for n=3 per each of the 14 experimental subgroups. The combined sample requirements for the RNA extraction kit and the subsequent downstream analysis, restricted the selection even further with using tissues of 200-250 mg, and not much less, for the RNA extraction, still, the highest RNA yield possible for the subsequent microarray analysis. The selected rats within each group were therefore based on getting the highest quantity of an m. soleus tissue sample (w_{max} = 250 mg) followed by rat having the next numerically lighter tissue, etc. The laboratory was then sterilised for the subsequent sample process.

3.5.4 The Sample Processing

3.5.4.1 The Homogenisation

The samples were homogenised in a 15-mL sample tube on ice in the DTT-RLT buffer from the RNA extraction kit. The homogenisation was carried out in 3 cycles of 10-15 s at full speed (with pauses to check any stuck material that potentially wouldn't get properly homogenised). After the final cycle, the buffer was applied on the dispersing aggregate to remove all tissue residues back into the sample tube, aiming to end up with the final ratio of 1 mL of buffer per every 100 mg of tissue. The tubes were store at −80 °C until the RNA extraction was be carried out.

3.5.4.2 The RNA Extraction

The RNA extraction was carried out as per the instructions from the manufacturer of the kit, with some necessary on-site adaptations (See protocol, Appendix B.8, p. 186). The extraction kit was chosen for being optimised for fibrous tissues and included genomic DNA removal step that could potentially contaminate the downstream analysis. In theory, the kit would yield 5-10 µg of RNA per 10 mg of muscle tissue; with maximum 250 mg tissue capacity per sample (as mentioned above). The downstream analysis required a minimum of 200 µg of RNA per sample. Hence the primary criterion for selecting the n=3 samples was not to jeopardise the quality of the analytical results. The extracted RNA solution samples were stored at −80 °C until the microarray analysis was carried out.

3.5.4.3 The Gene Expression Analysis

The microarray gene expression analysis was carried out by Bioarray S.L. (Alicante, Spain) using a SurePrint G3 Rat Gene Expression Microarray (ID 028279, Agilent Technologies, USA). The quality and quantification controls, coverage, hybridization and scanning and the quality analysis of the processed arrays, was carried out according to the official protocol for Two-Colour Microarray Based Gene Expression Analysis, version 6.5 (Agilent Technologies, 2010).

3.5.5 The Data Analysis

The Bioarray research service provided all statistical data; carrying out the normalisation, relative quantification of the genes with differential expression. The analysis was carried out using the open source software Bioconductor which is based on the R programming language. All possible comparisons between the experimental subgroups for differential gene expression was calculated, and the significance expressed with a direct p-value and adjusted p-value for false discovery rate (FDR), $p \leq 0.05$ for a significant difference. For the adjusted p-value from the multiple testing to be

more representative, the number of included genes was decreased from the 30003 genes (almost the entire rat genome) to 742 genes. The 742 genes, collectively represented 12 expression pathways thought to be, at least, relevant to the experiment in question. These pathways were chosen according to the literature summary from SABiosciences/QIAGEN (Qiagen, 2012) and consisted of: Hypoxia signalling, Skeletal muscle myogenesis & myopathy, Angiogenesis, Angiogenetic growth factors, EGF/PDGF signalling, Inflammatory Cytokines & Receptors, mTOR signalling, Mitochondrial energy metabolism, Oxidative stress, Stem cell transcription factors, VEGF signalling, and Wound healing.

The resulting analysis only represented the significant differential expression, fold change values, amongst all the subgroup comparisons, with reference to four expression pathways: Skeletal muscle myogenesis & myopathy, Hypoxia signalling, VEGF signalling and Wound healing; and adjusted to the 740 genes, mentioned above. The entire gene symbol and code list that mark the data analysis can be found in Appendix D.2 (p. 195).

4 Results

4.1 The Weight Measurements

To accompany the following results in this chapter, as a reminder, the rats were divided into groups with reference to the experimental Day 0, where the use of eccentric exercise (via downhill running) was intended to induce skeletal muscle damage. Thereafter, the rats were allocated to three groups defined by the recovery applications: the [C]-group, the positive controls with passive recovery; the [H]-group, recovery with intermittent hypobaric hypoxia sessions; and the [E]-group, which had the same recovery type as the [H]-group, followed by light rehabilitation exercise sessions.

Within each group, the subgroups are defined by the corresponding [C], [H] or [E] and the day of sampling {Day No.}. The negative control groups were sampled one day prior to Day 0, representing sedentary and trained rats, A{−1} and R{−1} respectively.

4.1.1 The Body weight of the Rats

The routinised rat handling protocols (Chapter 3.2.2.3) ensured a 3-times/week weight registry for each rat. However, throughout the working period of the project, more rats than the study's N_{Rat}=98 make up these registries. These rats are part of the initial phases, participating and the establishments of protocols, etc., and explains why the N_{Rat} is fairly fluid in this dissertation, depending on which data set is being presented. However, unless it is specified, the following results only involve the study's main N_{Rat}=98.

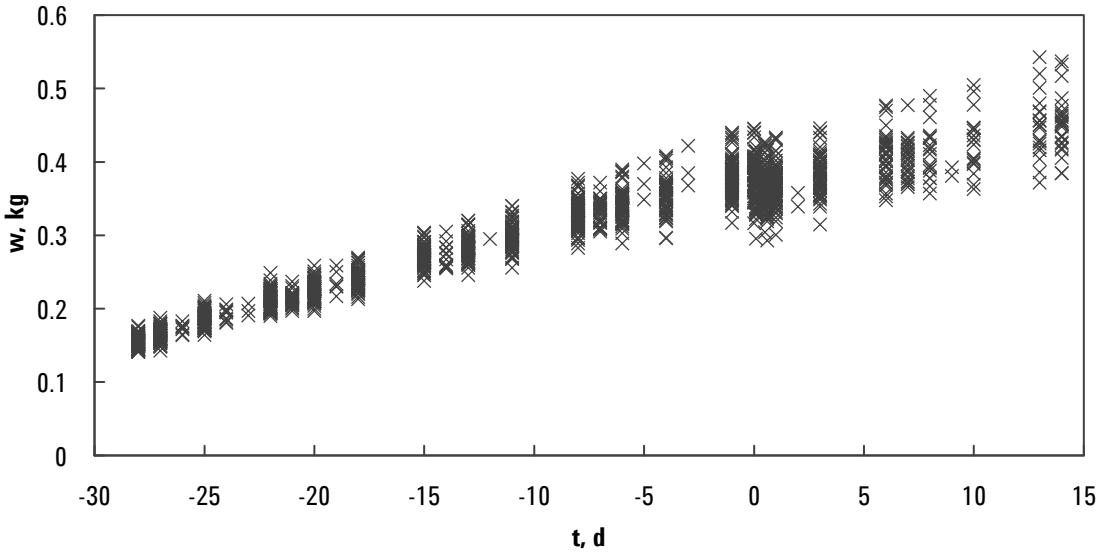

Fig. 4-1. The rats' body weight log (N_{inital}=98), in kg, throughout the experimental procedure, in days, with a weight registry of 3 times/week. The days reflect: the preconditioning period (Day −28 to −1); the day of skeletal muscle injury induction w/ 4 weight registries (Day 0); the recovery period (Day 1 to 14), where the N is dropping due to sampling.

In Fig. 4-1, the overall weight log presents the rat's body weight, in kg, as a function of time, in days. The day count starts with a negative number, from Day −28 to Day −1, marking the preconditioning on the treadmill, until the experimental critical point on Day 0. During this period the rats are young and growing; coincidently commencing at the age of ≈28 days on Day −28. The dense section on Day 0 represents four weight registries, before and after both downhill running-sessions on the day, mirroring a slight weight drop due to the strenuous exercise. The 2-week recovery period (from Day 1 to Day 14) continues to reflect a general increase in the body weight. All subgroups are embedded in the graph without showing any statistical distinction from the tendency of the average body weight profile, irrespective of being either entirely sedentary like the A{−1}-group or exercising throughout like the E{14}-group. (Still, closer analysis is presented below).

Table 4-1. The development of rats' body weight throughout the different periods of the experimental process.

Periods/Stages	Time, week	Days	Sampling days	N_{Rat}	$w_{initial}$, kg (±SD)	dw/dt, kg/d
Preparation (P)	1	−28 to −23		98	0.156 (±0.009)	9.6×10^{-3}
	2	−22 to −16		98	0.21 (±0.01)	8.7×10^{-3}
Training (T)	3	−15 to −8		98	0.27 (±0.01)	7.3×10^{-3}
	4	−7 to −1	Day −1	98	0.33 (±0.02)	7.3×10^{-3}
Day of injury protocol	Day 0	0		84	0.39 (±0.02)	-2.6×10^{-2} [a]
Recovery (R)	5	1 to 7	Day 1, Day 3, Day 7	84	0.37 (±0.03)	6.6×10^{-3}
	6	8 to 14	Day 14	21	0.42 (±0.04)	6.7×10^{-3}

[a] Extrapolated rate from measurements throughout Day 0.

Table 4-1 lists an overview of the weight statistics in relation to the different periods of the experimental procedure (Chapter 3.2.4.1), representing the weight (with standard deviation) at the start of the defined periods and the corresponding regression, i.e. the average weight rate (dw/dt). The subject count, N_{Rat}, changes in relation to how many rats have been sacrificed on each day of sampling, prior to the subsequently registered weight in the table. The overall tendency of the weight rate is indicative of a reduced increase; excluding the temporary weight loss on Day 0, that mirrors a small displacement, as shown in Fig. 4-1.

Upon closer examination of the recovery period (Day 1 to Day 14), despite the overall weight tendency having slightly slowed down, each group, [C], [H] and [E], show a significant increase. Still, the only significant inter-group difference happens on Day 14, as shown in Fig. 4-2. Day 14, represents the point of which the differences between the groups are the greatest, in practice, and the average weight of E{14}, 0.43(±0.03) kg, is significantly lower ($p=0.006$) than average weight of C{14}, 0.47(±0.04) kg. This relatively lower weight of E{14} is confirmed by the fact that it is not significantly higher than that of E{07}. However, E{07} has significantly higher weight than both E{01}

(p=0.008) and E{03} (p=0.030). At the same time, C{14} and H{14} each have significantly higher average weight than all its corresponding subgroups, where the comparisons between C{14} and C{01}/C{03}/C{07} all have p<0.001 and the comparisons between H{14} and H{01}/{H{03}/H{07} all have p≤0.005. The negative control groups, absolute A{−1} and relative R{−1}, are not significantly different from each other having the average weight of 0.39(±0.03) kg and 0.37(±0.02) kg respectively.

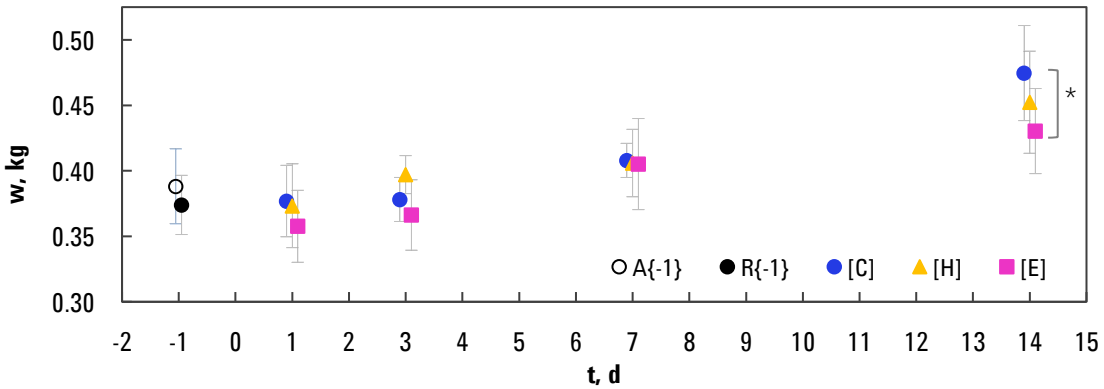

Fig. 4-2. The rats body weight-changes, in kg (±SD), after downhill-exercise induction of skeletal muscle injury on Day 0, between: [C] Control groups with passive recovery, [H] Hypoxia groups with hypoxia sessions, and [E] Hypoxia+Exercise groups; throughout Day 1 to Day 14. The negative controls, sedentary and trained rats, A{−1} and R{−1} respectively, are referenced from Day −1. Considering the time factor, only [E]-group and [C]-group have statistically different(*p=0.006) average weight, on Day 14, using 1-way ANOVA with Turkey's test.

4.1.2 The Weight Fractions of the Lungs and the Heart Compartments

The following weight fractions are always obtained with reference to the rat body weight for comparative purposes, except for the Fulton index (Chapter 4.1.2.1) which represents a different weight ratio. When comparing the three groups, [C], [H] and [E], during the recovery period, the average lung's weight fraction is only significantly higher in E{03} at 0.5(±0.1) $\times 10^{-2}$ in comparison with E{14} (p=0.020) and C{14} (p=0.017), both of which ratios are 0.36(±0.05) $\times 10^{-2}$ (Fig. 4-3). Moreover, the [E]-group is showing the overall greatest deviations, especially in E{03}, in comparison with the other groups, whilst the tendencies of [H] and [C] groups are relatively more stable regarding the statistical variation.

The weight fraction of the heart's left ventricle and septum combined (Fig. 4-4) is overall without any significant changes within each group, [C], [H] and [E], throughout the recovery period. However, on Day 14, H{14} and E{14} with the ratios of 0.22(±0.05) $\times 10^{-2}$ and 0.18(±0.01) $\times 10^{-2}$ respectively, are significantly different from each other (p=0.008) which does support the tendency of decrease between H{03} and H{14}. The pattern of, perhaps, gradually increasing weight fractions

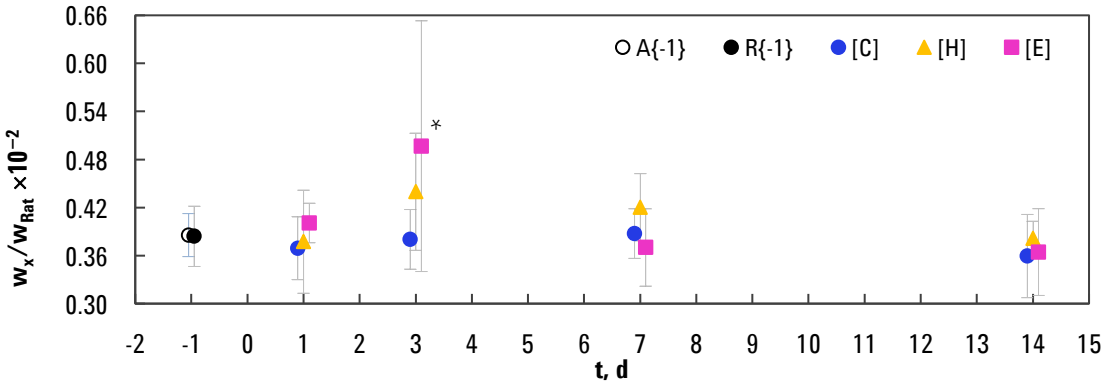

Fig. 4-3. The average lung weight fraction ($\times 10^{-2}$, ±SD) to the rat body weight, w_{Rat}, during the recovery period (Day 1 to Day 14) for the [C] Control groups, the [H] Hypoxia groups, and the [E] Hypoxia+Exercise groups, after an induction of muscle damage on Day 0, with absolute A{−1} and relative R{−1} negative controls on Day −1. Only the [E]-group on Day 3 appears statistically different from the [C] ($p=0.017$) and the [E]-groups ($p=0.020$) on Day 14, using 1-way ANOVA with Turkey's test.

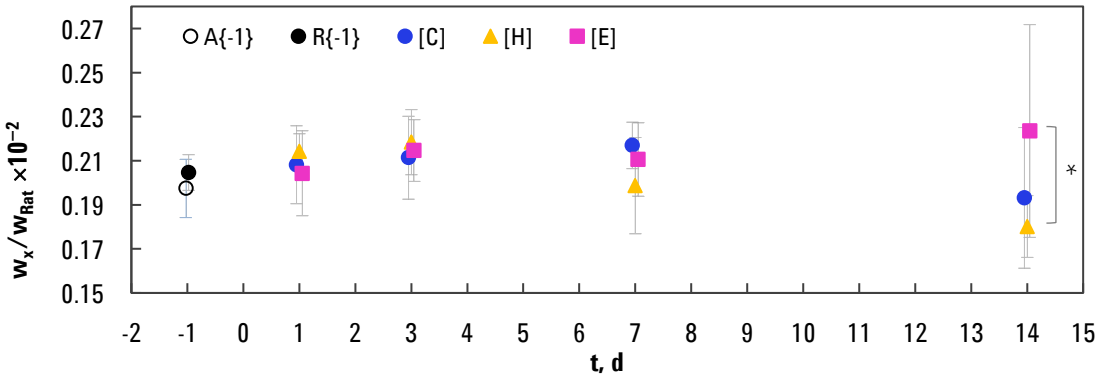

Fig. 4-4. The average weight fraction ($\times 10^{-2}$, ±SD) of the heart's left ventricle and septum together to the rat body weight, w_{Rat}, during the recovery period (Day 1 to Day 14) for the [C] Control group, the [H] Hypoxia group, and the [E] Hypoxia+Exercise group, after an induction of muscle damage on Day 0, with absolute A{−1} and relative R{−1} negative controls on Day −1. The only significant difference can be observed between the [H] and [E]-groups on Day 14 ($p=0.008$) using 1-way ANOVA with Turkey's test.

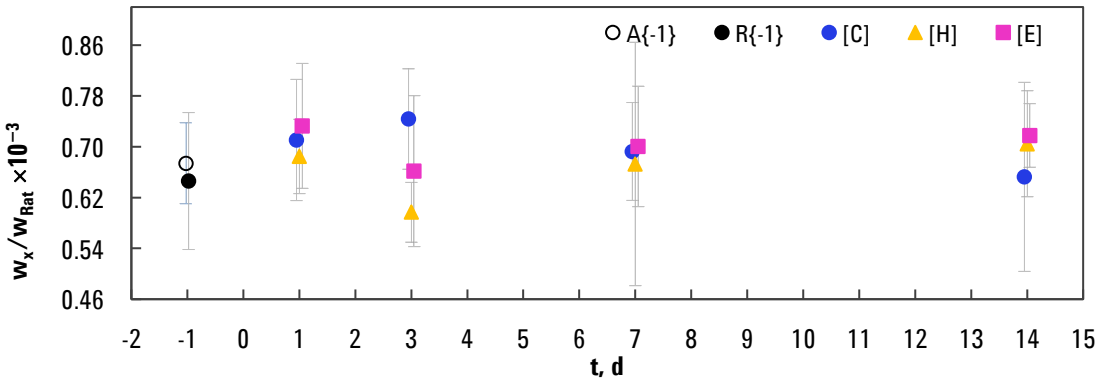

Fig. 4-5. The average weight fraction ($\times 10^{-3}$, ±SD) of the heart's right ventricle to the rat body weight, w_{Rat}, during the recovery period (Day 1 to Day 14) for the [C] Control group, the [H] Hypoxia group, and the [E] Hypoxia+Exercise group, after an induction of muscle damage on Day 0, with absolute A{−1} and relative R{−1} negative controls on Day −1. Any possible tendencies are without any significant backing (using 1-way ANOVA with Turkey's test).

within the [E]-group in general, that is shared by the [C]-group until after Day 7, is made less valid by the generally large variations within E{14} and C{14}.

The heart's right ventricle weight fraction (Fig. 4-5), appears to be mirrored by some tendency changes within each group [C], [H] and [E], throughout the recovery period. However, no group turns out to be significantly different from one another, and the ratios are, furthermore, oscillating more closely to and within the variability of A{−1} and R{−1} combined, or around the ratio of 0.69×10^{-3}.

4.1.2.1 The Fulton Index

The Fulton index (Fig. 4-6) describes the weight ratio between the heart's right ventricle and the combined weight of the heart's left ventricle and septum. The change in the index, theoretically, can be due to altered heart's right ventricle alone, due to the heart's left ventricle and septum alone, or due to parallel or opposite changes in both. In significant terms, the H{14}, index of 0.40(±0.01), is generally higher than that of the other [H]-groups ($p<0.05$), and is most likely to be due to the only significant difference, decrease, in the H{14}-weight ratio of the heart' left ventricle and septum (Fig. 4-4). However, the variability in the heart's right ventricle weight ratio seems to be reflected more markedly in the Fulton index, in general, when looking through the non-significant patterns within each group, [C], [H] and [E].

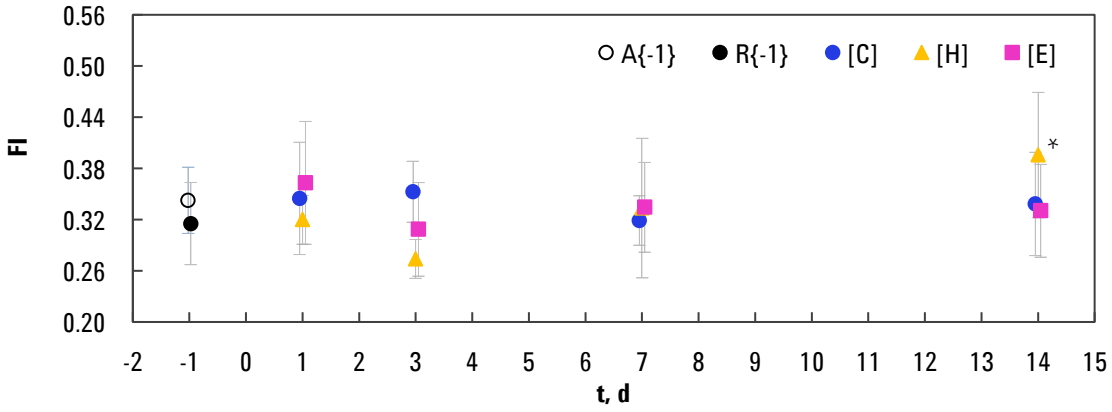

Fig. 4-6. The average changes in the rats Fulton Index, FI (±SD), during the recovery period (Day 1 to Day 14) for the [C] Control group, the [H] Hypoxia group, and the [E] Hypoxia+Exercise group, after an induction of muscle damage on Day 0, with absolute A{−1} and relative R{−1} negative controls on Day −1. The [H]-group on Day 14 is significantly different from the other [H]-groups on Day 1 ($p=0.045$), Day 3 ($p<0.001$) and Day 7 ($p=0.005$); and from the R{−1} ($p=0.042$), the [E]-group on Day 3 ($p<0.014$) and the [C]-group on Day 7 ($p=0.041$); using 1-way ANOVA with Turkey's test.

4.2 The AEY Performance Score

4.2.1 The Resulting Score Tables

The marks within the three criteria of the performance score, [A:E:Y], were quantified to fit a score scale from 0 to 1. The value of 1 in each criterion would be representing the theoretically good and well-trained runner-rat in a treadmill exercise session with no instrumental artefact affecting any accompanying numeric evaluation. The value of 0 in each criterion would be representing a rat that is impossible to get to run, making the E-criteria redundant, and the instrumentation would be mirroring the situation with continuous artefacts in the accompanying numeric evaluation. After an experienced-based approach to quantify the negative impact of each marked situation during the training sessions, the resulting tables with the marks and their accompanying score values, α, ε and υ for A, E and Y-criteria respectively, are presented in Fig. 4-7 and Fig. 4-8. The logical orders of marks are not necessarily represented with gradually changing score value, rather, representing the historical development.

4.2.1.1 The A-Score Criteria with the α Score Values

The A-criteria is demonstrated in Fig. 4-7 and covers the position of a rat running on a treadmill. The main positions of a rat that is running continuously involve continuously not touching the metal grid, and therefore resulting in low or no electric shock count by the treadmill apparatus, mark-A, or continuously touching the metal grid, represented by a high electric shock count, mark-C. In both cases, the rat could be a fairly good runner. Hence, the α_A (the score value for mark-A) is 0.00, reflecting no deduction with reference to the hypothetical good rat, and $\alpha_C = -0.30$, reflecting some deduction. If a rat is continuously moving from the back of the treadmill belt to the front, away from the metal grids, stopping until its get closer to the metal grids again, etc. the rat is not showing continuous running. In this case, the α_D ranges from −0.15 to −0.30, depending on the way it moves back and forth, i.e. how much running the rat is actually doing.

In essence, marks-B, E, F, G and L, describe a rat that is avoiding running, still, positioning itself in a way that it does not receive electric shocks. Getting into these positions is likely to be somewhat indicative of a level of intelligence, but, affected by the speed of the moving belt. However, the value of α reflects how easily a rat could sustain or get away with the position, and the easier it seems to be, a lower α value was assigned. Mark-B has a very low score value, $\alpha_B = -0.70$, where a rat that cheats running by supporting itself on the front wall of the treadmill encasing only moving the with the hind limbs. Still, even if a rat described by marks-E, F and G, is sliding on the treadmill

belt, as demonstrated in the diagrams, and is not running at all in the position, it is not likely the rat can hold it like that for too long; and the marks all have the same score value, $\alpha=-0.50$. Mark-L, $\alpha_L=-0.50$, reflects a particular situation where a rat discovers the treadmill belt is not covering the entire floor surface (the peripheral parts of the treadmill, if applicable). The rat discovers it can position one side of its body on the moving part, forced to move along with the limbs of the other side of body.

Marks-H, I and J, describe a rat that is 'preoccupied' (in the loosest sense), where both rats of mark-H are trying to walk backwards away from the metal grid to avoid shock ($\alpha_H=-0.80$) and a rat of mark-I, standing on the electric shock metal grid without repositioning itself ($\alpha_I=-0.90$). However, mark-J, $\alpha_J=-0.05$ is simply reflecting a rat that is for the most part running but seems very distracted by the surroundings (perhaps due to stress). In fact, mark-J rats normally run quite well, hence the α is only hinting some difference.

Mark-K, M and N rats, ($\alpha=[-0.40, -0.65, -0.65]$ respectively) rest the whole or part of their bodies onto the treadmill whilst running — Maybe not with the potential tactic of avoiding running, rather, these styles of running were more evident in the developing registry when the rats came across as really tired. Furthermore, this is more likely to happen in exhaustive sessions or when the treadmill belt is positioned with an inclination or declination. The negative impact of the marks also reflects how much 'running' the rat is doing in these positions.

Lastly, any rat, that for any given reason is not capable of running, however, for some reason is still evaluated, could be given the α-score of -1.00. (There is no specific mark defined for that registry).

4.2.1.2 The E-Score Criteria with the ε Score Values

The E-criteria is demonstrated in the left side column in Fig. 4-8, where the marks value the tail's position of a running rat. Holding the tail lifted (most likely, away from the metal grids) has a (+) mark and is considered as full score criteria, $\varepsilon_{(+)}=1.00$. When the rat does the opposite, and the tail hangs onto the treadmill belt, (−) mark, the score value is $\varepsilon_{(-)}=0.25$. The intermediate positions, (+/−) and (−/+) marks, are reflected with $\varepsilon_{(+/-)}=0.75$ and $\varepsilon_{(-/+)}=0.50$ respectively, although, exact position is somewhat subjective. The position of the tail in these conditions might be indicative of how tired the rats are, as it might change throughout a session. However, that logic is only applicable from resulting score value between 1.00 and 0.25, as the (0)-mark serves to indicate if evaluating the position of the tail is irrelevant or impossible, in relation to the A-criteria, for example with marks-G, H and I, and possible with marks-C and E. Moreover, in a confined area, the tail might be forced to simply bend due to the limits of the encasing.

AEY Performance Score; Schematic Setup.

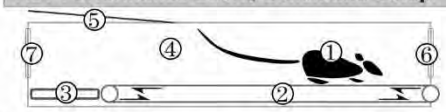

① A rat, running forward against the movement of ② the treadmill belt, with ③ an electric shock-providing metal grid at the back; in ④ an encased treadmill lane with ⑤ a hinge top lid, and ⑥ a front- and ⑦ a back air-opening to allow free air flow.

A-score Criteria with α score values.

Mark	Diagram	Description	Score
A		The rat runs continuously without touching the metal grid.	0.00
B		The rat runs but supports itself on the front wall with its fore limbs whilst only moving the hind limbs.	–0.70
C		The rat runs but continuously touches the metal grid.	–0.30
⊖D D ⊕D		The rat moves away from the metal grid to the front of the treadmill and stops until its has been moved back with the treadmill belt. Movement by: (–)D, running; D, galloping; (+)D, with a big jump.	⊖D –0.15 D –0.25 ⊕D –0.30
E		The rat hangs on to the front air-opening and therefore avoids running.	–0.50
F		The rat manages to slide in a brake against the movement of the treadmill belt and avoids running.	–0.50
G		The rat is somehow able to position itself (usually on its back) sliding still on the treadmill belt and avoids running.	–0.50
⊖H ⊕H	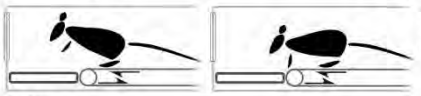	The rat walks backwards close (or really close) to the metal grid: (–)H, on hind limbs only; (+)H, on all four legs.	–0.80 (both)
I		The rat stands on the metal grid, receiving electric shock, and does not reposition itself onto the treadmill belt.	–0.90
J		The rat runs forward but is really distracted at the same time.	–0.05
K	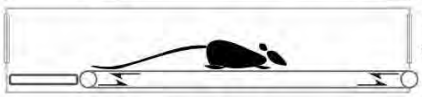	The rat rests the whole body on the treadmill belt whilst it runs or walks forward.	–0.40
L	*(front view)* *no image*	The rat uses the peripheral non-moving floor part (not covered by the treadmill belt) to avoid running. Essentially, one body-side is moving.	–0.50
M		The rat runs with only using the hind limbs to move and skating with the fore limbs.	–0.65
N		The rat runs with only using the fore limbs to move and dragging the hind limbs behind.	–0.65

Fig. 4-7. The AEY performance score, A-score criteria, describing a rat's position whilst running on a treadmill, each represented with a mark, a diagram, a description and a representative score value, α.

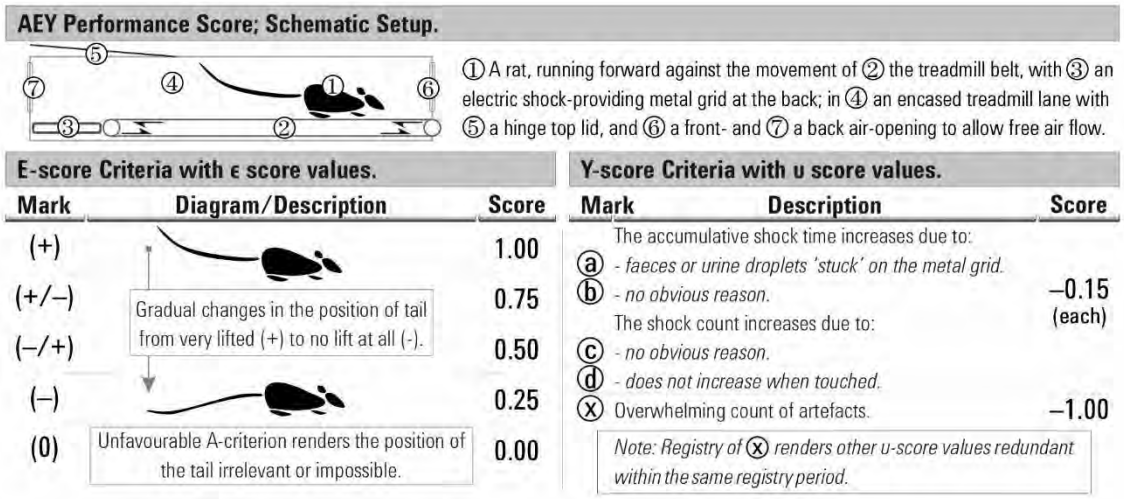

Fig. 4-8. The AEY performance score, E-score and Y-score criteria, describing a position of a rat's tail whilst running on a treadmill (E-criteria) and type of general incidences effecting electric shock parameters with the treadmill (Y-criteria). Each criterion is represented with a mark, a diagram or a description, and a representative score value, ε and υ for E and Y score respectively.

4.2.1.3 The Y-Score Criteria with the υ Score Values

The Y-criteria is demonstrated in the right side column in Fig. 4-8, where each mark describes a general type of incidence that could affect either the electric shock count or the accumulative time the shocks take. The score values for these most regular type incidences, ⓐ, ⓑ, ⓒ and ⓓ-mark, $\upsilon = -0.15$ for each mark. Therefore, the υ does not numerically distinguish between the types of incidences, for the reason that the impact of one and the same type can vary extensively. Instead, as the υ values are summed up, the resulting score value does only describe how many types of incidences occurred, with the maximum count of four different types, giving an overall intermediate score between 1 and 0.40. However, in the case of too many artefacts rendering the descriptive electric shock parameters invalid, the registry could be marked with ⓧ, $\upsilon_{ⓧ} = -1.00$, overriding the existing υ values (as the resulting Y-score is not defined for negative values), resulting in the score of 0.00. As such, the Y-score is simply a reverse indication of how much attention, or how much truth, is in the accompanying electric shock count from the treadmill apparatus.

4.2.2 Hypothetical References

Any resulting AEY-score is calculated as explained in Chapter 3.3.5, using the defined score value for any given mark. However, the objective was not to make a score value traceable to a mark, as the steps of averaging out the score values make that redundant even if the score values were different for each mark within each score criterion. Still, to form some idea of how the values represent different rats, a hypothetical data, based on the registries are presented in Table 4-2.

Table 4-2. Hypothetical data for four different rats in a session where the speed is kept constant.

Registry Period	1st-[5 min]			2nd-[5 min]			3rd-[5 min]			4th-[5 min]			6th-[5 min]			$[X]_{ave,RP}$		
Condition	**A**	**E**	**Y**	**A**	**E**	**Y**	**A**	**E**	**Y**	**A**	**E**	**Y**	**A**	**E**	**Y**	**A**	**E**	**Y**
1	A	(+)		A	(+)		A	(+)		A	(+/−)		A	(+/−)	ⓐ	1.000	0.900	0.970
Electric shock:			*11*			*2*			*0*			*0*			*3*	*Shock count: 16*		
																Shock time: 6 s		
2	A, B	(+)		A, B, E	(+)		B, C	(+)		C, G	(+)		A, B	(+)		0.578	1.000	1.000
Electric shock:			*15*			*5*			*7*			*10*			*3*	*Shock count: 40*		
																Shock time: 23 s		
3	A, C	(+)	ⓐ	A, C, I	(+/−)		−D, A	(−/+)		C, +D	(−/+), (−)	ⓐ	K, C	(−)	ⓐ, ⓑ	0.767	0.575	0.880
Electric shock:			*32*			*22*			*13*			*26*			*37*	*Shock count: 130*		
																Shock time: 295 s		
4	C, −H, I	(0)	ⓓ	C, I	(+/−)	ⓓ, ⓒ	C, −H, I	(−/+), (0)	ⓓ, ⓧ	C, J, D	(−/+)	ⓐ, ⓧ	+D, C, +H, I	(0)	ⓐ	0.499	0.225	0.480
Electric shock:			*27*			*67*			*0*			*40*			*53*	*Shock count: 187*		
																Shock time: 345 s		

The electric shock count is divided to represent the count occuring in each registry period. In practice, the number is likely to represent an accumulating count throughout.

The hypothetical data (Table 4-2) is based on five 5-min registry periods within a session where the speed is kept constant. Four conditions are described, i.e. four different rats — The rats are not necessarily running together: (**i**) Condition 1 with [A;E;Y]=**[**1.000**;**0.999**;**0.970**]**, describes a rat that shows a good running style, does not to appear to be very tired and only one type of incident that reduced the validity of the electric shock count. (**ii**) Condition 2 with [A;E;Y]=**[**0.578**;**1.000**;**1.000**]**, describes a rat that shows ways of avoiding running and therefore does not appear to be particularly tired. Therefore, without any case of incident affecting the electric shock parameters, by reading from them alone, they indicate a good runner. (**iii**) Condition 3 with [A;E;Y]= **[**0.767**;**0.575**;**0.880**]**, describes a rat that seems generally tired and is somewhat struggling, with several incidences that have affected the validity of the electric shock parameters. Lastly, (**iv**) Condition 4 with [A;E;Y]=**[**0.499**;**0.225**;**0.480**]**, describes a rat that, for whatever reason, seems to find the session difficult, confusing, etc. The A-marks suggest that the rat is constantly touching the metal grids. However, the registry has many incidences that affect the electric shock parameters that, again, would indicate a good runner if they were considered alone (although, the incidences *per se* are not related to how the rat is running).

These references are by no means a gold standard for the conditions described, and only serve to bring the score into some perspective. They also emphasise the fact that it is important to understand the setup of a session, and interpret the resulting score considering all the parameters.

4.2.3 The Scope of Comparison

The rats, N=65, that make up the quantitative AEY data, only represent a portion of the experimental subject count, N_{Rat}=98, randomly distributed between the subgroups that ever trained on the treadmill, from the point of incorporating the AEY systematic registry.

4.2.4 The Preconditioning Period

The preconditioning period, composed of 4 weeks, where during the former two weeks (the preparation stage) the rats trained with a gradually changing protocol, and during the latter two weeks (the training stage) the rats trained with a non-changing protocol. All days of training had 2 Sess/d, except in Week 1, where the only day with two sessions was the last day. Furthermore, these experimental weeks were all separated by a weekend of rest between them. It became noticeable, especially in the latter two weeks, that there was an overall performance cycle in the running of the rats, both between Mondays and Fridays and between morning and afternoon sessions.

In Fig. 4-9, the quartile analysis of average session-scores, separated into morning and afternoon sessions are displayed on a week basis throughout the preconditioning period. Bearing in mind that Week 1 has only one afternoon session, tendency indications in the quartile distributions are somewhat visible. The A-score seems to improve throughout the entire period with gradually less distribution of the score range, indicating that the running styles are generally more refined with scores changing from 0.7(±0.1) to 0.94(±0.09). This tendency is though flatter and closer to a score value of 1.00 in the afternoon sessions, changing from 0.9(±0.1) to 0.96(±0.05). The E-scores hint to an opposite trend throughout the period, compared with the A-scores, where the score seems to be dropping with time, from 0.97(±0.08) to 0.8(±0.2). in the morning sessions, and from 0.96(±0.09) to 0.8(±0.1) in the afternoon sessions. Furthermore, between the morning and afternoon session, the E-scores are markedly lower, in general, indicating that the rats hold their tail in a lower position. The Y-scores, displayed on a narrower scale, show a relatively flat curve throughout the period both in the morning session and in the afternoon (both around score value of 0.99(±0.01)). However, with the exception of the one afternoon session on Week 1, the distribution of the score is slightly less dispersed in the afternoon.

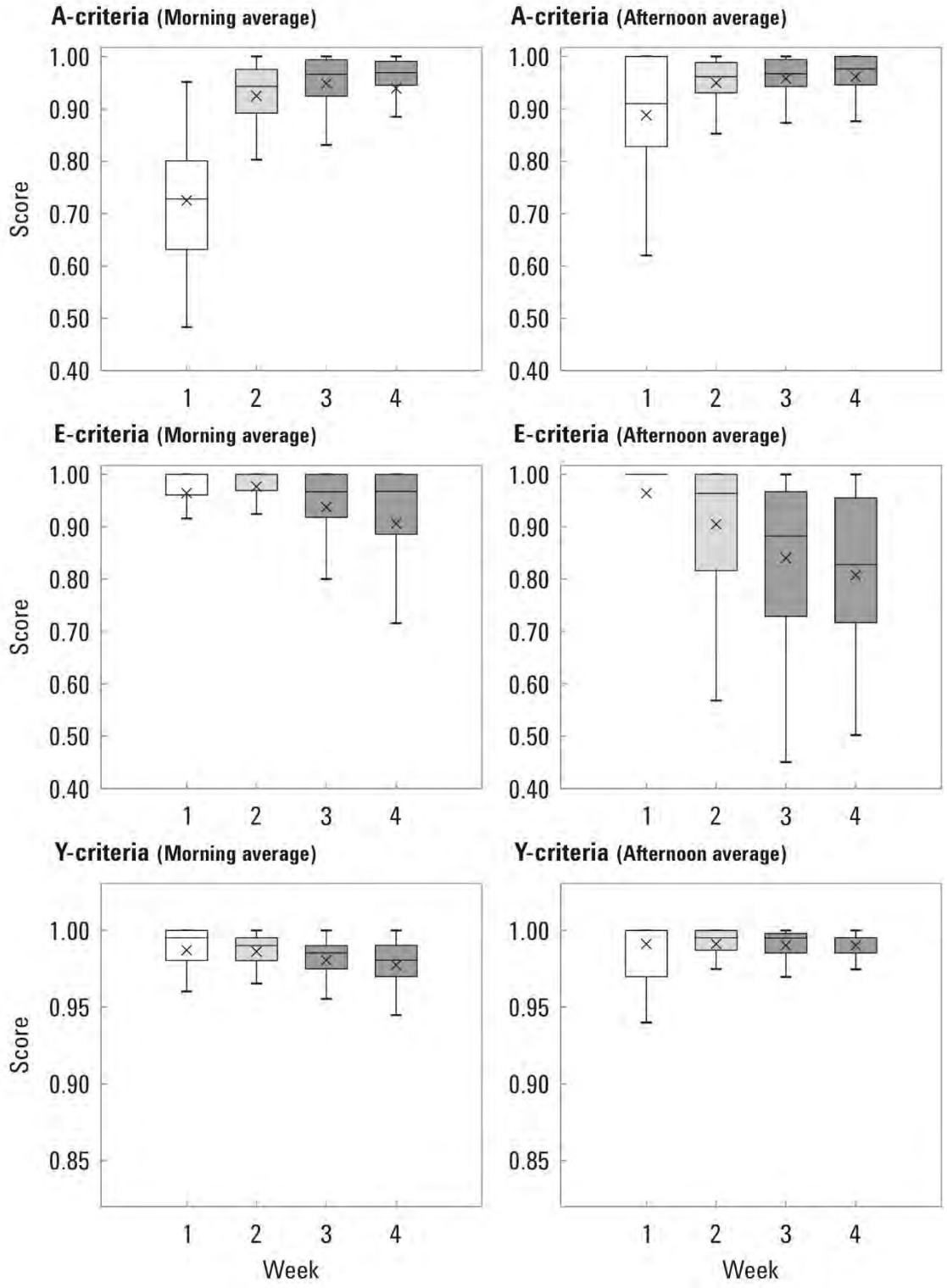

Fig. 4-9. The average session AEY score throughout the preconditioning period (N_{Rat}=65) separated into morning (09:00h) and afternoon (17:00h) sessions. The average score within corresponding quartiles is marked with an "x". Each week has 2 sessions per day, except Week 1 with only one afternoon session.

4.2.5 Throughout the Experimental Procedure

After the preconditioning period, the exercise sessions to induce muscle damage on Day 0 were very different from what the rats had previously experienced. Apart from running downhill and at a slightly higher velocity, the duration of each session that day was to each rat's exhaustion, with a minimum 4-h of rest in between them. In Table 4-3, the representative duration of both sessions on Day 0 is presented, both with reference to the entire experimental procedure (N_{Rat}=84) and the AEY-score evaluation (N_{Rat}=61). Irrespective of the subject count, here in question, the average time of the former session was two times longer than of the latter session, 120(±20) min and 60(±20) min respectively. The remaining rats that carried out exercise during the recovery period, from Day 1 to Day 14, which were exclusively in the [E]-group hypoxia+exercise. Again, although the setup did not change throughout the period, the sessions were entirely different from before; slower, shorter, uphill, and only 1 Sess/d. The rats in the [E]-group that were evaluated for the AEY-score, started at N_{Rat}=23 on Day 1, N_{Rat}=16 on Day 3, and N_{Rat}=12 on Day 7, and N_{Rat}=5 on Day 14.

Table 4-3. The average duration of the eccentric-exercise sessions in minutes, on Day 0.

Session	t_{ave}	SD	t_{max}	t_{min}
Included in the experimental procedure, N_{Rat}=84:				
Former	123	22	168.0	58.0
Latter	62	23	132.2	25.1
Included in the AEY-score evaluation, N_{Rat}=61:				
Former	123	24	168.0	58.0
Latter	64	25	132.2	25.1

In Fig. 4-10, the quartile analysis of the weekly training day scores (or working day scores) is presented throughout the experimental period. Whilst the weeks of the preconditioning period (Week 1 to Week 4) are separated by weekend-resting, the weeks of the recovery period (Week 5 and Week 6) start on a Wednesday; locating the weekend resting 'in the middle'. The recovery period is, therefore, split into three bits, to normalise the overall view: (**i**) Throughout the preconditioning period, the A-score showed a tendency of a score increase from 0.8(±0.1) in Week 1 to 0.95(±0.07) in Week 4, and with the tendency of decreasing variability. On Day 0, with a very distinct protocol, the A-score dropped to 0.75(±0.09). However, through Week 5 and Week 6, the score increased from 0.8(±0.1) to 0.92(±0.08). In general, the A-score seems to get more refined with the reuse of the same type of protocol. (**ii**) The E-score demonstrates a different overall pattern through the entire experimental period. From Week 1 to Week 4, the score dropped from 0.97(±0.05) to 0.86(±0.09) with some increasing variability. On Day 0, the score dropped to 0.3(±0.1), and thereafter, through Week 5 and Week 6 it increased from 0.85(±0.09) to 1.00.

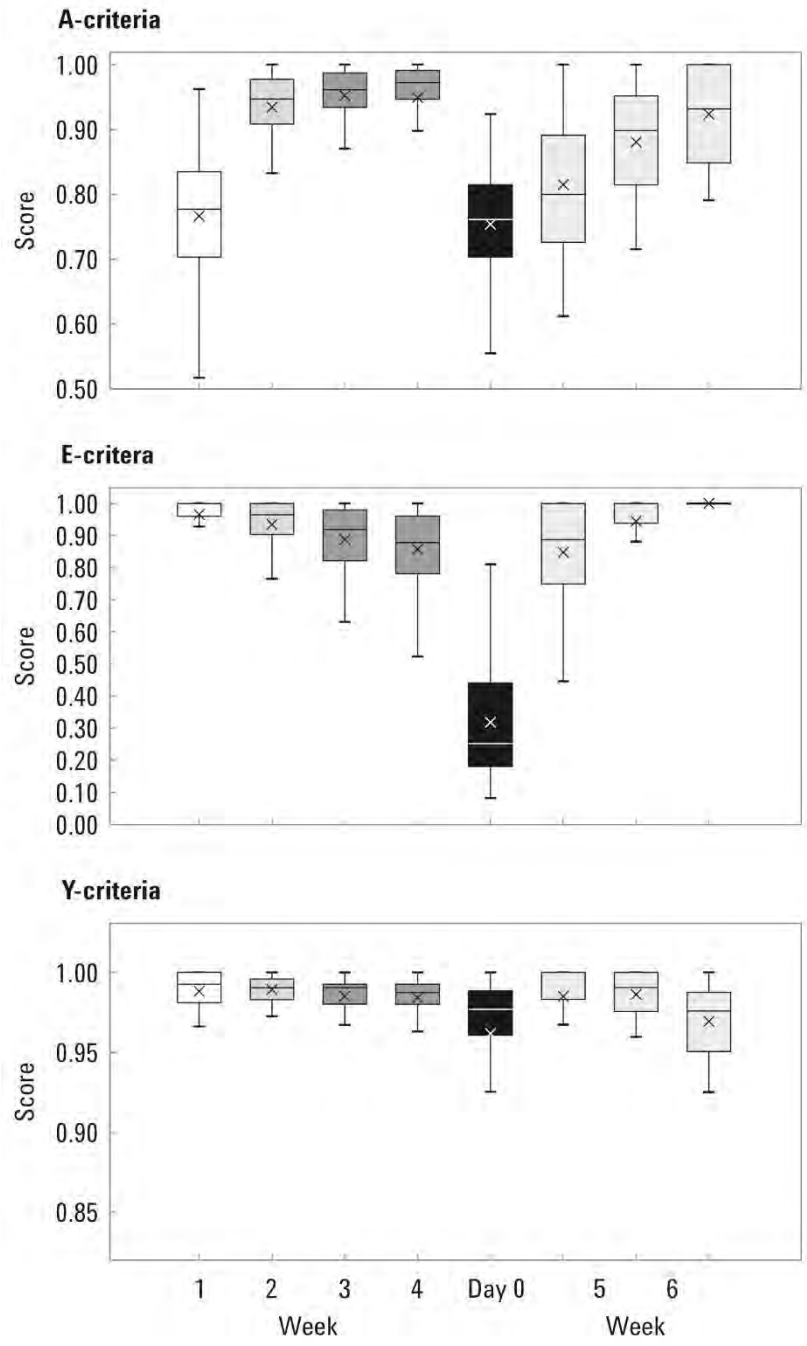

Fig. 4-10. The average training day AEY score throughout the preconditioning period (Week 1 to Week 4, N_{Rat}=65), Day 0 (N_{Rat}=61) and the recovery period (Week 5 to Week 6, N_{Rat}=23→5). The average score within corresponding quartiles is marked with an "x". Before Day 0, each week is separated by weekend-resting. After Day 0, the experimental weeks are not determined by weekend-resting.

In general, the E-score tendencies seem to be related to the supposed level of exercise difficulty in each protocol or throughout time periods. The preconditioning period starts off very easy in terms of session parameters but gets heavier with time, and perhaps more difficult to sustain. The sessions on Day 0 are really difficult and leave the rats very tired, and perhaps remain tired for the next days.

However, during the recovery period, with a very easy but different protocol, the first-day experience (at the start of Day 1) might be quite clumsy, but thereafter the score is really high. Furthermore, the N_{Rat} is decreasing throughout the period which might have its statistical effect. (**iii**) The Y-score is quite flat throughout the preconditioning period, around 0.98-0.99, and shows a slight drop on Day 0 to 0.95(±0.05) which is likely to have to do with the augmented possibility of incidences with a longer session. During Week 5 and Week 6, however, the decreasing number of subjects makes the average incidences disproportional in comparison with the rest.

4.2.6 Comparing the Preconditioning

Although the rats evaluated and given the quantified AEY score do not have an even distribution in terms of the subject count for each experimental group, their average value might serve as a hint as to how homogenous the rats were regarding the training.

Table 4-4. The average AEY score for the evaluated rats over Week 4 and Day 0.

		Week 4			Day 0		
Group		**A**	**E**	**Y**	**A**	**E**	**Y**
R{−1}	*ave.*	0.9	0.8	0.99			
n=4	*SD*	*0.1*	*0.1*	*0.01*			
	SEM	*0.05*	*0.07*	*0.005*			
[C]-group	*ave.*	0.95	0.8	0.99	0.75	0.3	0.96
n=19	*SD*	*0.07*	*0.1*	*0.01*	*0.08*	*0.2*	*0.05*
	SEM	*0.02*	*0.03*	*0.003*	*0.02*	*0.04*	*0.01*
[H]-group	*ave.*	0.95	0.9	0.98	0.73	0.3	0.94
n=19	*SD*	*0.06*	*0.1*	*0.01*	*0.08*	*0.2*	*0.07*
	SEM	*0.01*	*0.03*	*0.003*	*0.02*	*0.04*	*0.01*
[E]-group	*ave.*	0.95	0.9	0.99	0.77	0.4	0.97
n=23	*SD*	*0.08*	*0.1*	*0.01*	*0.09*	*0.2*	*0.03*
	SEM	*0.02*	*0.03*	*0.002*	*0.02*	*0.04*	*0.006*

Table 4-4 lists which experimental group the rats, receiving a quantified AEY evaluation, eventually belonged. Furthermore, it reflects on the average AEY score for the sessions in Week 4, and the average AEY score for the two sessions on Day 0. Within each score criterion, the average values are all on a similar level, with fairly uniform variability between each group — both in the Week 4 calculations and on Day 0. On a similar note, the SEM shows similarity throughout which numerically strengthens the idea of homogeneity. Given this similarity, the uniformly low SEM strengthens the idea of homogeneity even further. For the purpose of predicting uniformity, the Y-score has less input for evaluating the subjects, still, is more relevant for the evaluating the treadmill apparatus.

4.3 The Plasma Markers

The key elements of the developmental phase of the eccentric exercise protocol for muscle damage are presented in the following chapter where N=20 rats provided data plasma marker data. Thereafter, in Chapter 4.3.2, the plasma marker data with reference to the actual experimental phase are introduced with N_{Rat}=98 (n=7/subgroup).

4.3.1 The Developmental Phase

4.3.1.1 The Procedural Results

The Results Determining the Muscle Damage Protocol

The initial eccentric exercise protocol to induce skeletal muscle damage was designed as a one session per day (1 Sess/d)-exercise protocol. However, lacking in literature results to demonstrate its potential impact on a healthy skeletal muscle, specifically estimated via plasma markers, required some trials to ensure how to best develop the protocol efficiently. After all, the rats would train on the treadmill through the fairly extensive preconditioning period, a necessary lead up to Day 0, and a faulty muscle damage protocol would clearly render the post physiological applications redundant.

Fig. 4-11 shows the quantified levels of TnI in plasma over the recovery period (from Day 1 to Day 14) in rats with a passive recovery after the 1 Sess/d-muscle damage protocol. (The recovery process is equivalent to the definitive [C]-group). The overall profile indicates a descending pattern from a concentration level about 15(±2) ng/mL on Day 1. However, no TnI was measured in some of the rats' plasma. Furthermore, the general range of deviation on Day 3, 7 and 14, greatly reduced the credibility of the concentration on Day 1 being particularly high and potentially reflecting muscle damage.

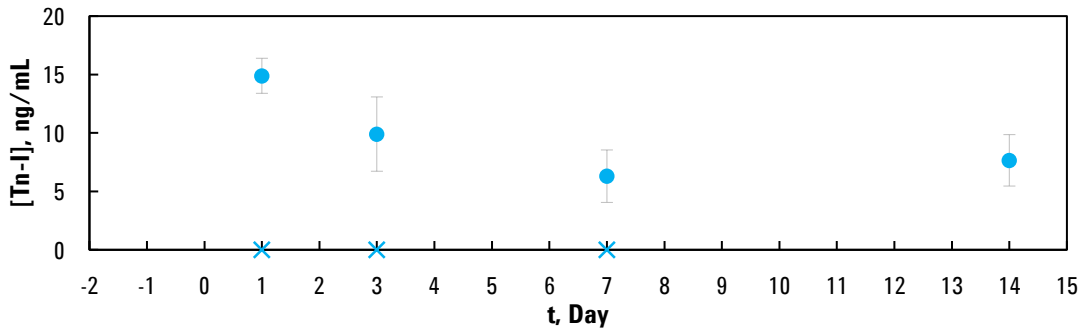

Fig. 4-11. The plasma concentration of skeletal muscle troponin-I during a passive recovery period (Day 1 to Day 14) after a one session of eccentric-exercise to exhaustion on a treadmill. Each average(±SD) data point has n=4 rats included from Day 1 to Day 7, except for the markings at 0 ng/mL with n=1, and n=5 on Day 14.

Under the same conditions, the quantified profile of myoglobin in plasma is shown in Fig. 4-12. The profile, although with the overall tendency of decreasing concentration from 30(±20) ng/mL to 15(±8) ng/mL, does not reflect a refined regression. Furthermore, the overall standard deviation is even greater than for the TnI values, comparing their RSD ranging between 2%-35% for the TnI measurements and 35%-100% for the Mb values.

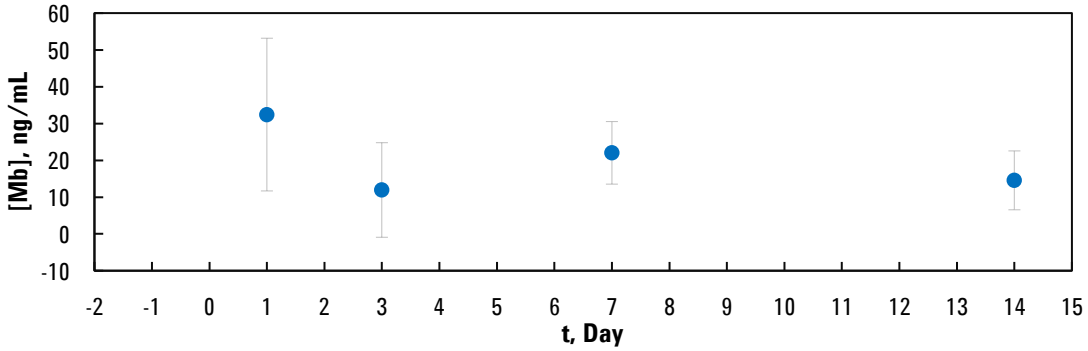

Fig. 4-12. The plasma concentration of skeletal muscle myoglobin during a passive recovery period (Day 1 to Day 14) after a one session of eccentric-exercise to exhaustion on a treadmill. Each average(±SD) data point has n=5 rats included.

The Calibration Curves

The calibration curves, with reference material provided by the ELISA kit manufacturer, were thoroughly analysed for each assay — And, although the resulting quantification of the samples in Fig. 4-11 and Fig. 4-12 did not *per se* raise any assay quality issues, despite not displaying particularly favourable results, the curves alone looked 'suspicious'; the TnI curve in particular.

In Fig. 4-13, a representative TnI calibration curve is demonstrated; not coming across as a promising quantification reference. The calibration curve was run twice (always in triplicate) with the first kit used and once with the second kit (the run displayed in here), all of them giving similar results. The overall linear fit calculates at R^2=0.9781, way below the acceptance threshold. Furthermore, excluding the highest concentration level, 50 ng/mL, which seems to put the curve off-trend, the curve seems to have the general potential of being non-linear with R^2=0.9204.

In Fig. 4-14, a representative Mb calibration curve is demonstrated; coming across a lot more promising in comparison with the TnI calibration curve. Although, here, the highest concentration level, 100 ng/mL is designed to be included in the RoQ (range of quantification), it calculates with R^2=0.9937, which is a poor linear fit for a calibration curve. However, in contrast to the TnI calibration curve, there is considerably less uncertainty when it comes to analysing the Mb calibration curve.

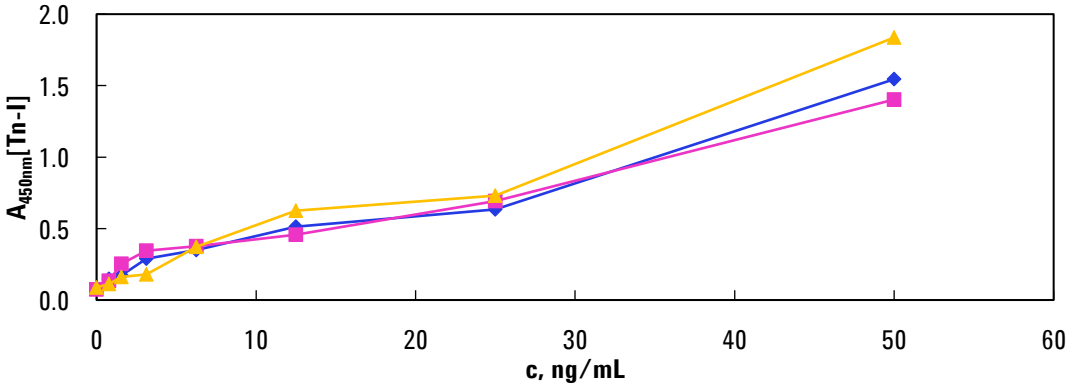

Fig. 4-13. The TnI calibration curve divided into the profiles of its three well-replicas. The overall linear regression giving the slope m=0.02815 and the intercept b=0.13289 and the fit R^2=0.98094. The range of the relative standard deviation between the replicas RSD=[0.038-0.313]. Excluding the highest concentration point yields y=0.023423x+0.15818 with R^2=0.920359.

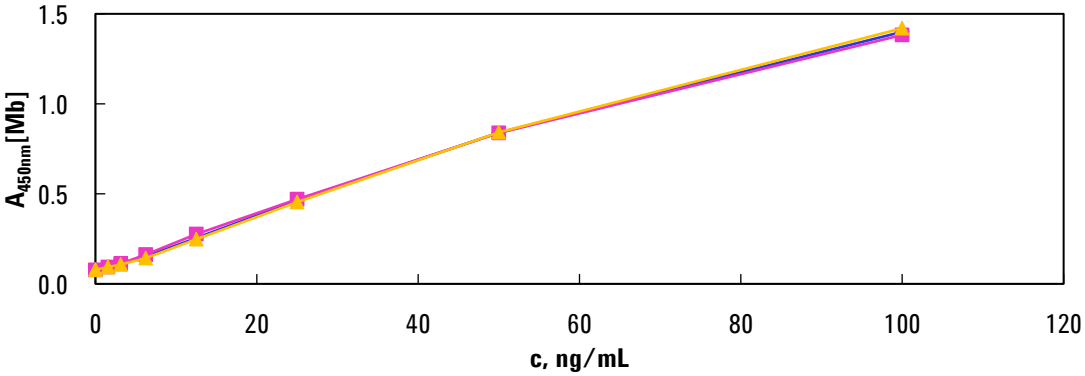

Fig. 4-14. The Mb calibration curve divided into the profiles of its three well-replicas. The overall linear regression giving the slope m=0.013562 and the intercept b=0.088306 and the fit R^2=0.993739. The range of the relative standard deviation between the replicas RSD=[0.001-0.066]. Excluding the highest concentration point yields y=0.015486x+0.06748 with R^2=0.999233.

Table 4-5. The parametric overview for quickly evaluating the TnI and the Mb calibration curves.

TnI-calibration curve							**Mb-calibration curve**						
Theoretic		Measured		Calculated			Theoretic		Measured		Calculated		
Conc. ng mL^{-1}	**Dilution factor**	**Absorb. A_{450nm}**	**Replicas RSD**	**Conc. ng mL^{-1}**	**Recovery %**	**Dilution factor**	**Conc. ng mL^{-1}**	**Dilution factor**	**Absorb. A_{450nm}**	**Replicas RSD**	**Conc. ng mL^{-1}**	**Recovery %**	**Dilution factor**
50.00	2	1.594	0.14	51.91	104%	2.65	100.00	2	1.401	0.01	96.78	97%	1.75
25.00	2	0.685	0.07	19.62	78%	1.39	50.00	2	0.840	0.00	55.43	111%	2.01
12.50	2	0.531	0.16	14.15	113%	1.71	25.00	2	0.462	0.02	27.57	110%	2.18
6.25	2	0.366	0.04	8.27	132%	1.69	12.50	2	0.260	0.06	12.66	101%	2.68
3.13	2	0.271	0.31	4.90	157%	2.18	6.25	2	0.152	0.07	4.73	76%	2.94
1.56	2	0.196	0.26	2.25	144%	-	3.13	2	0.110	0.02	1.61	52%	4.35
0.78	N/A	0.132	0.14	-0.05	N/A	N/A	1.56	N/A	0.093	0.00	0.37	N/A	N/A
0.00	N/A	0.081	0.08	-1.83	N/A	N/A	0.00	N/A	0.079	0.01	-0.72	N/A	N/A

TnI-calibration curve is expressed with the linear regression of y=0.028158x +0.13289.

Mb-calibration curve is expressed with the linear regression of y=0.013562x +0.088306.

Table 4-5 summarises the differences between the two calibration curves, for TnI and Mb quantification. The 'measured' section of the table shows the variability between the absorbance values of the three replicas, where the TnI curve has the majority of data points with RSD>0.10, whilst the Mb-curve has only two data points with RSD>0.05 yet RSD<0.10. The 'calculated' section of the table show each curve re-quantified with reference to the average linear regression they reflect, and the difference ratio (the recovery) between the two. The updated dilution factor then gives an idea how linear the regression between the data points is truly.

In essence, the Mb calibration curve in Fig. 4-14 can be considered valid for quantification as long as the overall curve is roughly fractioned around the points it is bending, re-estimating the linear regression within each new fraction. The changes in the recovery and the dilution factor of the recalculated curve help to find the points of bending. Unknown samples are then quantified with reference to within which fraction they fall. The need for estimating the curves in this way is not uncommon in samples with matrices that can influence the absorbance reading. The matrix effect is noticeable when the compound of interest is very diluted and requiring a closer point of view of the calibration curve. The first 3 to 4 data points on the Mb calibration curve do show a different tendency (if extrapolated) in comparison with the rest.

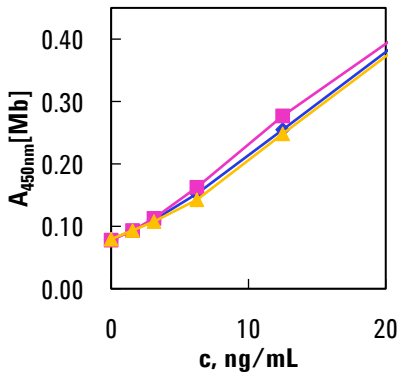

Fig. 4-15. The reference-sample matrix effect visible in the lowest concentration levels of the Mb calibration curve giving them collectively a slightly different regression rate.

4.3.1.2 The Decisions Before the Next Step

Despite using the TnI and Mb plasma markers with only a few rats, the results were still indicative enough to take the next step of changing. In that process, three decisions were taken: (**i**) The rats could run a little bit faster in the muscle damage protocol, judging from the monitoring registry. Thus, introducing a speed range during the steady-velocity phase (phase III), mainly to affect the rats the ran the longest in a training lot, when the other rats had already been removed from the treadmill. (**ii**) To carry out the muscle damage exercise session two times on the same day, with the

minimum of a 4-h break in between sessions. Still, options were limited to make each session *per se* harder for the rats. (**iii**) To discontinue the use of the manufacture's troponin-I ELISA for the muscle damage, due to two bad experiences, and take a 'risk' with a different one, as the subject count needed to be reset when starting using creatine kinase plasma marker ELISA instead accompanying the myoglobin ELISA.

4.3.2 The Experimental Phase

The following overall data reflects what has been referred to as the experimental procedure in the previous chapters, with all the established treadmill protocols and group setup unchanged. In the context of the plasma markers, this period refers to using only Mb and CK as muscle damage plasma markers, with the aforementioned two sessions of eccentric exercise to induce muscle damage on Day 0. With the N_{Rat}=98 (n=7 per each of the 14 subgroups), the quartile calculations did not identify any outliers — however, the Grubb's method identified two according to the quantified plasma marker data, one in subgroup E{03} in the Mb analysis, and one in subgroup R{−1} in the CK analysis. The comparative statistical analysis was run both before and after smoothing out the outlier with statistical A15-estimation.

4.3.2.1 Myoglobin Concentration in the Plasma

The Intra-Experimental Group Comparison

Two negative controls are thought to set the scene regarding relevant thresholds for the experimental groups, from Day −1. The average plasma concentration in the absolute group measured A{−1}=50(±40) ng Mb/mL, and the average concentration in the relative group measured R{−1}=40(±40) ng Mb/mL. The RSD for each were about 83% and 100% respectively, and no statistical analysis would differentiate between the two, given their averages are too close to each other. Moreover, since the variability was that great, an outlier could not be determined with our methods could not determine one.

Fig. 4-16 shows the plasma concentration of Mb for the [C]-group during the recovery period. On Day 1, the subgroup C{01}=200(±100) ng Mb/mL has the highest average concentration, and the only one that is significantly different from all the other positive controls, overall with $p \leq 0.034$; and also significantly different from the negative controls ($p \leq 0.018$). The other subgroups do not demonstrate any significant difference between them. The overall pattern commences with the variable basal concentrations on Day −1 and reaches its significant peak on Day 1, after the induction of muscle damage. The concentration level starts dropping back to the basal level on Day 3 (C{03}). There seems to be a slight tendency after the drop reaches its minimum on Day 7

(C{07}=40(±20) ng/mL) for an increase, mirrored on Day 14 (C{14}=50(±20) ng/mL). However, this intra-basal range tendency does not have statistical backing.

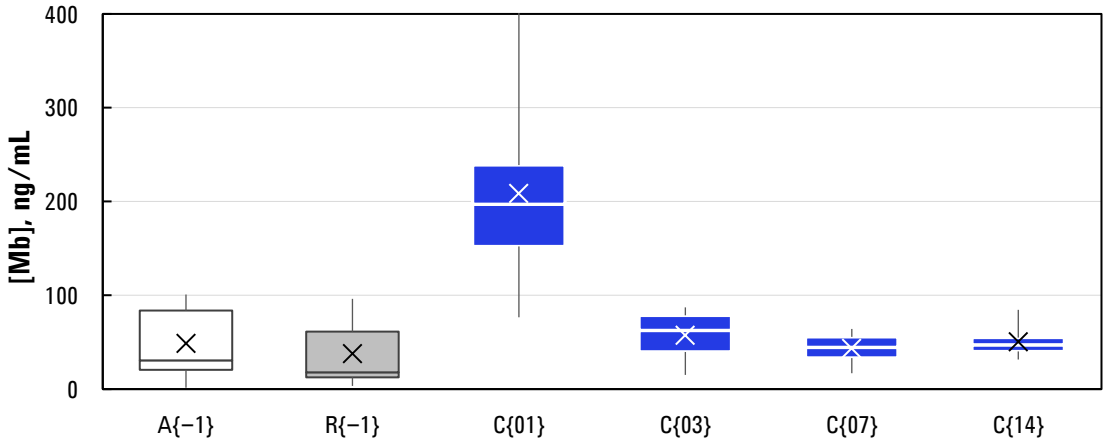

Fig. 4-16. The plasma concentration of myoglobin [Mb] in rats, with quartile distribution (average as 'X'), of the [C] positive control groups (C{01}, C{03}, C{07} and C{14}) during a 14-d passive recovery after eccentric-exercise induced skeletal muscle damage. The C{01} with 200 (SD:100) ng Mb/mL is significantly from the rest of the (p≤0.034), including the absolute and relative controls, A{−1} and R{−1} respectively (p≤0.018), sampled prior to the muscle damage. Analysis with: 1-way ANOVA with Turkey's test (p<0.05).

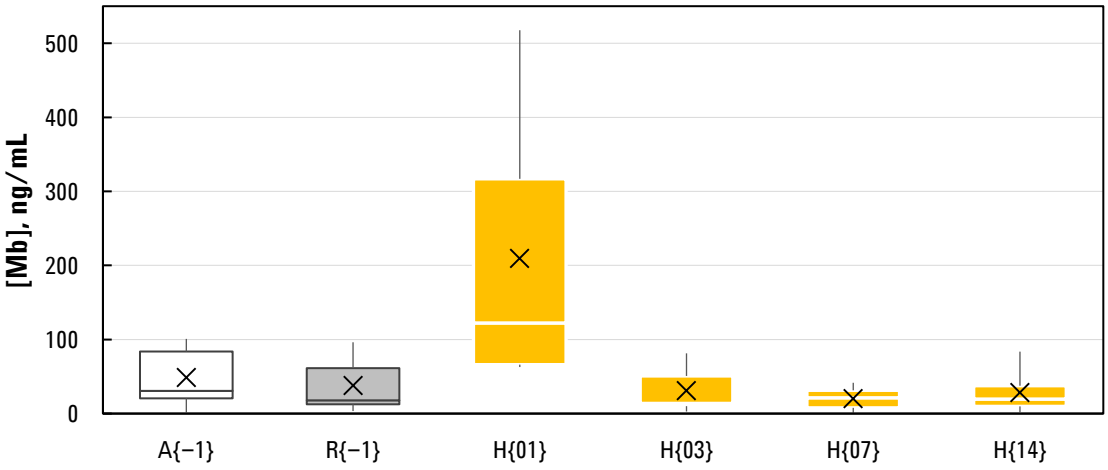

Fig. 4-17. The plasma concentration of myoglobin [Mb] in rats, with quartile distribution (average as 'X'), of the [H] hypoxia groups (H{01}, H{03}, H{07} and H{14}) during a 14-d recovery, with intermittent hypoxia, after two eccentric-exercise sessions on a treadmill. The H{01} with 200 (SD:200) ng Mb/mL is significantly different from the rest of the subgroups (p≤0.004), including the absolute and relative controls, A{−1} and R{−1} respectively (p≤0.017), sampled prior to the muscle damage. Analysis with: 1-way ANOVA with Turkey's test (p<0.05).

The hypoxia group, [H], Fig. 4-17, shows a very similar pattern as the [C]-group; perhaps, slightly more exaggerated profile. From the basal range on Day −1, the concentration reaches its peak on Day 1 (H{01}=200(±200) ng Mb/mL) and is the only significantly different subgroup from the rest in the [H]-group, with overall p≤0.004, and the negative controls (p≤0.017). After Day 1 the concentration falls to the basal range, and even to the range's lower concentration levels, reaching

its minimum on Day 7 (H{07}=20(±20) ng/mL). Just like the non-significant tendency between the [C]-groups, the concentration seems to have slightly risen again on Day 14 (H{14}=30(±30) ng/mL).

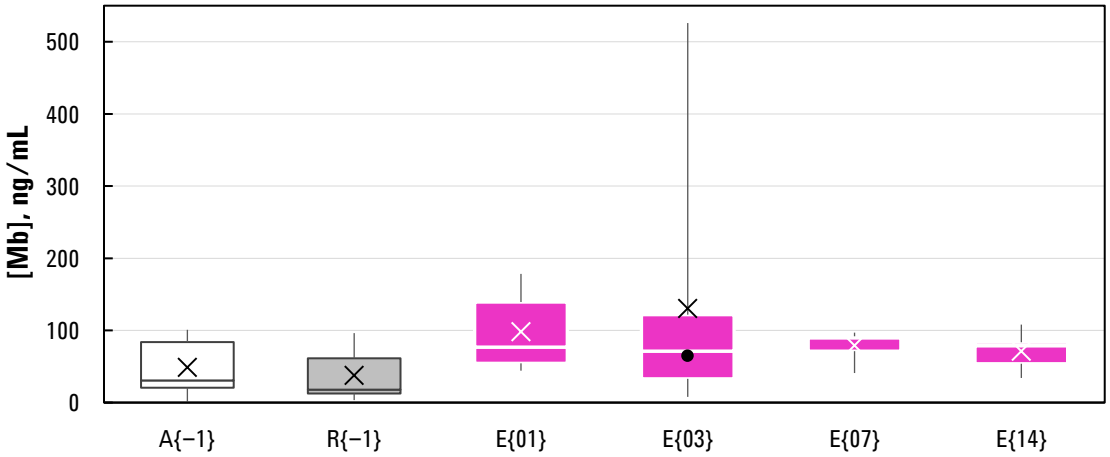

Fig. 4-18. The plasma concentration of myoglobin [Mb] in rats, with quartile distribution (average as 'X'), of the [E] hypoxia+exercise groups (E{01}, E{03}, E{07} and E{14}) during a 14-d recovery, with intermittent hypoxia and light exercise, after two eccentric-exercise sessions on a treadmill. The E{03}=100(SD:200) ng Mb/mL, was detected with an outlier (Grubbs method) and adjusted according to A15 estimation resulting in E{03}'=90(SD:70) ng Mb/mL (new average as black circle). No groups are significantly different from each other, neither before and after outlier-treatment: Analysis with: 1-way ANOVA with Turkey's test ($p<0.05$).

The Mb plasma concentration pattern within the [E]-group (Fig. 4-18) is markedly different from the rest, and it does not have any significant difference between any of the subgroups (including the negative controls). Therefore, strictly statistically, the tendency is fairly planar. Furthermore, on Day 3, E{03}=100(±200) ng Mb/mL, has the former outlier of two in the entire experiment. Upon reducing the outlier's effect on the average and the variability, with the statistical A15 method, the new concentration calculates as E{03}'=90(±70) ng/mL. The average is on a similar scale, but the deviation has reduced greatly. However, it still does not affect the significance in the comparison, but, adds on a more reliable criterion to the tendency, especially when compared to E{01}=100(±60) ng/mL. The adjusted non-significant Mb-pattern, starting at the basal range, rises on Day 1 and gradually decreases until Day 14.

The Inter-Experimental Group Comparison

Fig. 4-19 mirrors a panoramic image of all the experimental groups and the representative plasma [Mb] concentration. With a focus on the inter-inter-experimental group comparison, C{01} and H{01} are the only subgroups significantly different from all the other subgroups not belonging to Day 1. Still, between themselves, C{01}, H{01} and E{01} are not significantly different from another. If a statistical A15-'fine tuning' is applied, the position of C{01} and H{01} becomes clearer, as C{01} becomes significantly different from all the hypoxia+exercise (E) subgroups, and H{01} becomes

significantly different from them as well except E{01}. This is a good indication of the inter-pattern on Day –1: as C{01} and H{01} have the highest concentration values, still not significantly different from each other, and C{01} is significantly different then E{01} which has a lower concentration value, and H{01} and E{01} are not significantly different. The pattern seems to be C{01}>H{01}>E{01} (in terms of myoglobin concentration), and the rest of the subgroups have a somewhat planar tendency and at the same concentration level as the control negative subgroups.

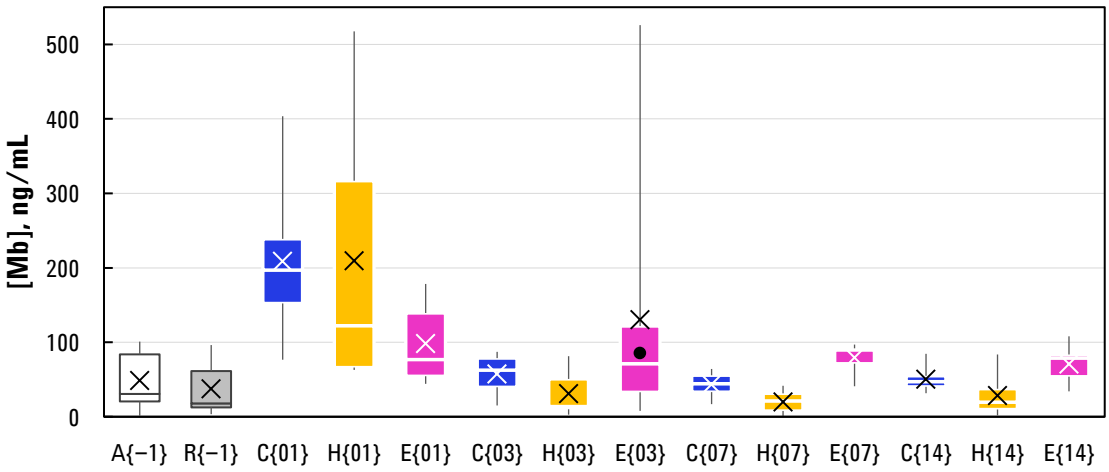

Fig. 4-19. The plasma concentration of myoglobin [Mb] in rats, with quartile distribution (average as 'X'), with the attention on inter-experimental group comparison of the [C] control, [H] hypoxia and [E] hypoxia+exercise, on the four sampled recovery days {01, 03, 07 and 14} after two-eccentric exercise sessions. C{01} and H{01} are significantly different from each other's corresponding subgroups ($p \leq 0.005$ and $p \leq 0.031$, respectively). C{01} is significantly different from all [E]-groups ($p \leq 0.007$) and H{01} in comparison with [E]-groups ($p \leq 0.036$), except with E{01}. Analysis with: 1-way ANOVA with Turkey's test ($p < 0.05$), includes A15-outlier adjustment on group E{03}.

4.3.2.2 Creatine Kinase Concentration in the Plasma

The Intra-Experimental Group Comparison

Starting with the reference groups, or the negative controls from Day −1. The average plasma concentration in the absolute group was measured at A{−1}=400(±300) ng CK/mL, and the average concentration in the relative group at R{−1}=170(±80) ng CK/mL. The groups are no significantly different from each other, and their corresponding RSD is about 80% and 50% respectively. One outlier could be detected in R{−1}, with the Grubb's method, which was smoothed out using the A15 estimation resulting in R{−1}'=140(±30) ng CK/mL, which did not affect the non-significance. However, the absolute negative group, with such high variability, and no determined outliers, was never significantly different from any of the other subgroups in the following results.

Fig. 4-20 shows the plasma concentration of CK for the [C]-group during the recovery period. On Day 1, the subgroup C{01}=800(±400) ng CK/mL has the highest average concentration, and the only one that is significantly different from the other positive controls, overall with p≤0.027; and also significantly different from R{−1} (p=0.011). The other subgroups do not demonstrate any significant difference between themselves. Excluding the aspect of A{−1}, the overall pattern commences with the reference basal level on Day −1 and reaches its significant peak on Day 1, after the induction of muscle damage. Thereafter, the concentration drops back to the upper part of the basal level and stays around 200-210 ng CK/mL from Day 3 to Day 14.

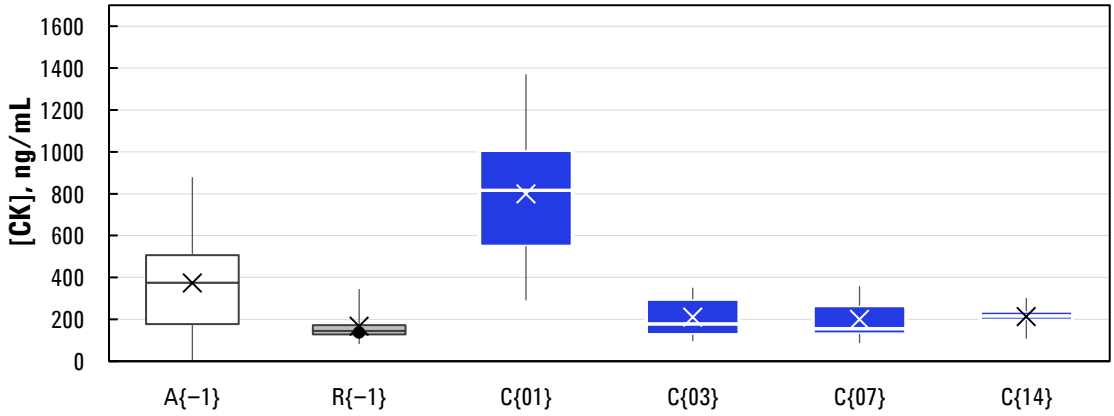

Fig. 4-20. The plasma concentration of creatine kinase [CK] in rats, with quartile distribution (average as 'X'), of the [C] positive control groups (C{01}, C{03}, C{07} and C{14}) during a 14-d passive recovery after eccentric-exercise induced skeletal muscle damage. The C{01} with 800 (SD:400) ng CK/mL is significantly from the rest of the (p≤0.027), and the relative-negative control, R{−1} (p≤0.011), sampled prior to the muscle damage. The R{−1}=170(±80) ng CK/mL, has been treated with outlier analysis showing its altered average as 'black circle' at R{−1}'=140(±30) ng/mL. Analysis with: 1-way ANOVA with Turkey's test (p<0.05).

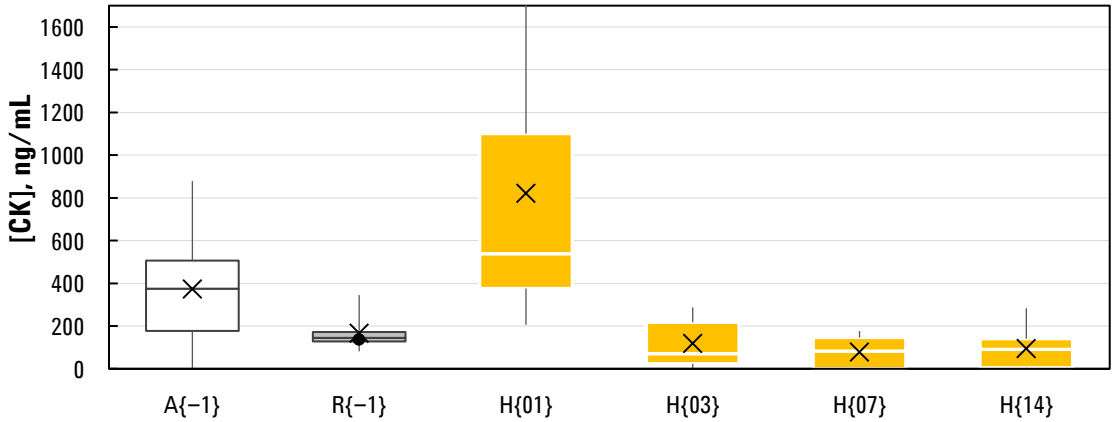

Fig. 4-21. The plasma concentration of creatine kinase [CK] in rats, with quartile distribution (average as 'X'), of the [H] hypoxia groups (H{01}, H{03}, H{07} and H{14}) during a 14-d recovery, with intermittent hypoxia, after eccentric-exercise induced skeletal muscle damage. The H{01} with 800 (SD:700) ng CK/mL is significantly from the rest of the (p≤0.003), and the relative-negative control, R{−1} (p≤0.007), sampled prior to the muscle damage. The R{−1}=170(±80) ng CK/mL, has been treated with outlier analysis showing its altered average as 'black circle' at R{−1}'=140(±30) ng/mL. Analysis with: 1-way ANOVA with Turkey's test (p<0.05).

The hypoxia group, [H]-groups Fig. 4-21, shows similarity to the [C]-groups; perhaps, slightly more exaggerated profile. From the basal range on Day −1, the concentration reaches its peak on Day 1 (H{01}=800(±700) ng Mb/mL) and is the only significantly different subgroup from the rest in the [H]-group, with overall p≤0.003, and the R{−1} (p=0.007). After Day 1 the concentration drops down to the basal range, and perhaps a bit lower, and stays there at about 100 ng CK/mL.

The CK plasma concentration pattern within the [E]-groups (Fig. 4-22) is markedly different from the rest. Still, it does not have any significant differences between any of the subgroup. From the basal level on Day −1, the concentration suddenly rises on Day 1 (E{01}=500(±400 ng/mL) and has continued to rise on Day 3 (at E{03}=700(±500) ng/mL). From Day 7 to Day 14 it seems to be gradually decreasing ending at 300(±200) ng/mL.

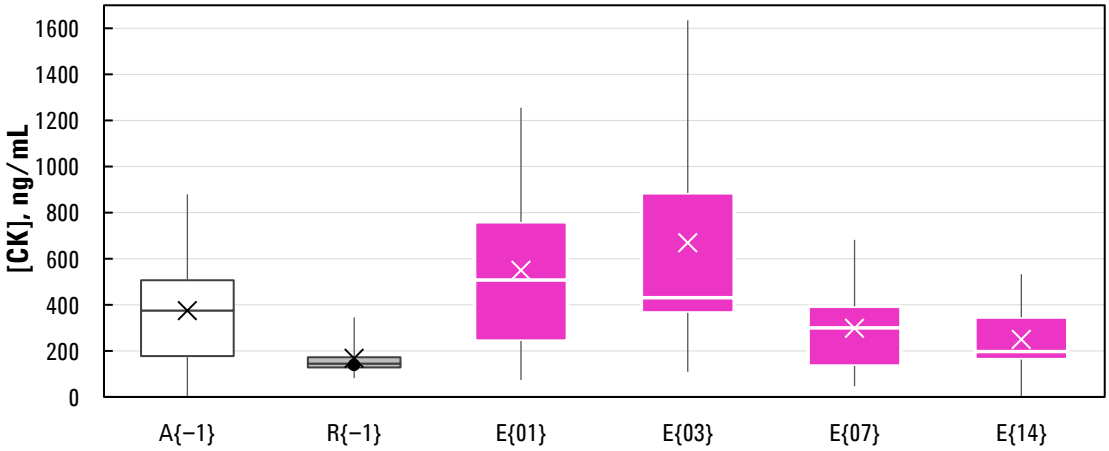

Fig. 4-22. The plasma concentration of creatine kinase [CK] in rats, with quartile distribution (average as 'X'), of the [E] hypoxia+exercise groups (E{01}, E{03}, E{07} and E{14}) during a 14-d recovery, with intermittent hypoxia and exercise, after eccentric-exercise induced skeletal muscle damage. The concentration is the highest at E{01}=500(±400) ng/mL and E{03}=700(±500) ng/mL. However, no groups are significantly different from one another. The R{−1}=170(±80) ng CK/mL, sampled prior to the muscle damage induction, has been treated with outlier analysis showing its altered average as 'black circle' at R{−1}'=140(±30) ng/mL. Analysis with: 1-way ANOVA with Turkey's test (p<0.05).

The Inter-Experimental Group Comparison

The overall comparison of the CK concentration in plasma (Fig. 4-23) demonstrates, first of all, very similar patterns between the [C] and the [H] groups. Both C{01} and H{01} are significantly different higher than all the other subgroups within the [C] and the [H] groups. However, these peaks, along with E{01} and E{03} are not significantly different from each other. E{03}, which represents the peak of the [E]-group, seems to be significantly different from the H{07} and H{14}, but not from its own corresponding E[07} and E{14}, nor the C{07} and C{14}. This suggests that the pattern of the [E]-group, generally, has a higher concentration than [C] and [H] groups (on the Day 7 and 14). Whilst

C{07} and C{14} are somewhere in the middle around the basal range of R{−1}, the [H]-group drops the lowest concentration of them all, after its peak on Day 1.

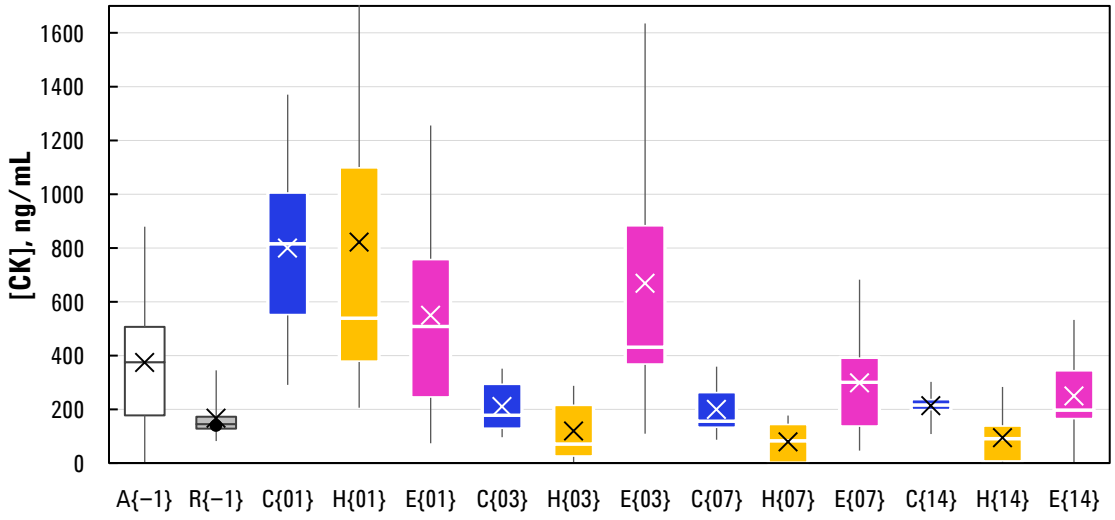

Fig. 4-23. The plasma concentration of creatine kinase [CK] in rats, with quartile distribution (average as 'X'), with the attention on inter-experimental group comparison of the [C] control, [H] hypoxia and [E] hypoxia+exercise, on the four sampled recovery days {01, 03, 07 and 14} after two-eccentric exercise sessions. C{01} and H{01} are significantly different from each other's corresponding subgroups ($p \leq 0.004$ and $p \leq 0.017$, respectively). E{03} is significantly different from H{07} and H{14} ($p \leq 0.034$), and H{01} in comparison with E{14} ($p = 0.034$). Analysis with: 1-way ANOVA with Turkey's test ($p < 0.05$), includes A15-outlier adjustment on group R{−1}.

4.3.3 Outliers and the Plasma Evaluation

Table 4-6 shows the intra-distribution, in percentage, of the plasma samples with the non-outliers and pushed outliers, with reference to the haemolytic evaluation of each plasma. The data lot from the N_{Rat}=98 essentially did not have any problems concerning outlier, and only two were detected with the Grubb's method. Both plasma samples had been evaluated as '+++' (Order no. 8 in the table) and, therefore, no particular reason to link the level of haemolysis to the outliers. However, the RSD for each subgroup in the plasma analysis was generally rather high. The A15 estimation was run z10-cycles for all subgroups (not just the ones with the Grubb's-outliers), to determine the most likely outliers, and of them, to see which would be determined as an outlier with quartile calculations of all the new A15-adjusted groups.

Table 4-6. The intra-distribution of Mb and CK plasma markers non-outliers, IQR-outliers and A15-outliers throughout the haemolytic order of FEH·lab's plasma evaluation core.

Order	Code	non outliers	A15-outliers	IQR-outliers *
1	-	2%		
2	(-)	8%	7%	
3	(+)	8%	3%	
4	+	21%	13%	
5	(++)	14%	20%	33%
6	++	19%	23%	17%
7	(+++)	17%	10%	17%
8	+++	8%	13%	17%
9	(++++)	3%	3%	
10	H		7%	17%
	Total:	*100%*	*100%*	*100%*

* IQR-outliers are simultaneously A15-outliers.

The overview, given in the Table 4-6, demonstrates that in the three criteria, the majority of the plasma had the appearance order from No. 4 to No. 7. Only the samples rated with the highest haemolytic appearance (red/dark red, Order no. 10) only appears in the plasma of the 'pushed' outliers. Comparing the concentration values of the plasma of Order No. 10, it appeared they collectively were with [Mg]<85 ng/mL and [CK]<360 ng/mL. Thus, the haemolytic appearance does not predict an outlier via the ELISA assays in question.

4.4 The Differential Gene Expression

As previously explained (Chapter 3.5.1), the subject count for the differential expression analysis reflects n=3 per subgroup (N_{Rat}=42), i.e. chosen from the existing n=7 per subgroups. The choice was based on fulfilling the assay criteria regarding the required minimum sample quantity, which coincidently ruled many of the rats out by default, as the dissected m. soleus was generally quite small.

4.4.1 The RNA Extracted Samples and Global Overview of the Expression

The resulting RNA extract from each sample was sent to the commercial analyser who checked each sample for quantity and quality (i.e. contamination). All samples passed with the quality grade Class 1 for integrity values, volume and concentration for the DNA microanalysis; with the exception of two samples that were replaced with other Class 1-graded sample to complete the subject count in each corresponding subgroup. The sample assessment can be found in Appendix D.3, p. 199.

Table 4-7 demonstrates the overall count of the significantly upregulated and downregulated genes between any two subgroups. The gene count is limited to the statistical correction of false rate discovery with reference to the selected 742 relevant genes (Appendix D.2). Of any two compared groups, one is the objective and the other is the reference group (the latter one in table Table 4-7: vs 'Group'), meaning that any value reflects a difference, present in the objective group in comparison with the reference group. Overall, the most numerous differential expression take place on Day 1, after the muscle damage induction, with only minor significant differences throughout the recovery period, until day 14.

Based on the selected gene pathways to reflect the profiles of each experimental subgroup, the following results are presented in four parts according to: (**1**) the Skeletal Muscle (Myogenesis and Myopathy) pathway, (**2**) the Hypoxia Signalling pathway, (**3**) the VEGF pathway, and (**4**) the Wound Healing pathway. Although there are some pattern parallels between the genes within the same pathway, they can show different expression profiles when comparing all the subgroups. In theory, if a gene would be differentially expressed in all possible comparisons of the groups, there would be 91 of them to interpret. Multiplying that by the number of genes in a pathway, and then repeat for the other pathways, make the overall picture extremely intricate. Although these 91 comparisons would not realistically all demonstrate differential gene expression, there still are between 1 and 45 for the significantly expressed genes. For this reason, when looking at the upregulation and downregulation profiles of each gene, only the numerical results of the pathway

line with the highest count of significantly expressed genes in most subgroup comparison will be presented here, along with some standout genes which show a significant expression throughout the recovery period. The expression profiles of significant genes within all the pathway lines (both before and after the false rate discovery correction) can be found in Appendix D.4 (p. 201).

Table 4-7. The number genes in m. soleus with significant up- and downregulation between the all the subgroups (n=3 each) in the experiment.

Reference		Subgroups			
***vs* A{−1}:**		**R{−1}**			
	Up	0			
	Down	0			
	Total	**0**			
		C{01}	**C{03}**	**C{07}**	**C{14}**
	Up	30	0	0	0
	Down	35	2	0	0
	Total	**65**	**2**	**0**	**0**
		H{01}	**H{03}**	**H{07}**	**H{14}**
	Up	70	2	0	0
	Down	63	2	0	0
	Total	**133**	**4**	**0**	**0**
		E{01}	**E{03}**	**E{07}**	**E{14}**
	Up	55	10	1	0
	Down	37	3	2	0
	Total	**92**	**13**	**3**	**0**
***vs* R{−1}:**		**C{01}**	**C{03}**	**C{07}**	**C{14}**
	Up	11	0	0	3
	Down	30	0	1	0
	Total	**41**	**0**	**1**	**3**
		H{01}	**H{03}**	**H{07}**	**H{14}**
	Up	32	1	1	1
	Down	23	2	2	0
	Total	**55**	**3**	**3**	**1**
		E{01}	**E{03}**	**E{07}**	**E{14}**
	Up	38	0	4	1
	Down	43	0	3	0
	Total	**81**	**0**	**7**	**1**

Reference		Subgroups			
[C]:		**C{03} vs C{01}**	**C{07} vs C{03}**	**C{14} vs C{07}**	
	Up	22	0	0	
	Down	6	0	0	
	Total	**28**	**0**	**0**	
		H{01} vs C{01}	**H{03} vs C{03}**	**H{07} vs C{07}**	**H{14} vs C{14}**
	Up	0	0	0	0
	Down	0	0	0	0
	Total	**0**	**0**	**0**	**0**
		E{01} vs C{01}	**E{03} vs C{03}**	**E{07} vs C{07}**	**E{14} vs C{14}**
	Up	19	0	1	0
	Down	5	0	0	0
	Total	**24**	**0**	**1**	**0**
[H]:		**H{03} vs H{01}**	**H{07} vs H{03}**	**H{14} vs H{07}**	
	Up	21	0	0	
	Down	13	0	0	
	Total	**34**	**0**	**0**	
		E{01} vs H{01}	**E{03} vs H{03}**	**E{07} vs H{07}**	**E{14} vs H{14}**
	Up	0	0	1	0
	Down	0	0	0	0
	Total	**0**	**0**	**1**	**0**
[E]:		**E{03} vs E{01}**	**E{07} vs E{03}**	**E{14} vs E{07}**	
	Up	11	0	0	
	Down	13	0	0	
	Total	**24**	**0**	**0**	

Information provided by Bioarray S.L. (Alicante, Spain).

4.4.2 The Skeletal Muscle (Myogenesis and Myopathy) Pathway

Table 4-8 shows the pathway lines within the Skeletal Muscle pathway, listed with all the genes that compose them along with an absolute gene count (N_{gene}) and a relative count (N_{gene}%) with reference to the 84 different genes in the pathway. Note that some genes may be repeated between the different lines, which does not affect the overall count. The genes (or the gene symbols) in boldface letters are significantly expressed ($p \leq 0.05$), with an ordinary t-test, in at least

one of the subgroup comparisons, and are accompanied with their relative gene count (N_p%) referenced to the 84 different genes of the pathway. Genes in boldface letters marked with an asterisk are, furthermore, significantly expressed after the false discovery rate corrections (p(adj)≤0.05), and are accompanied with the relative gene count ($N_{p(adj)}$%) referenced to the 84 genes in the pathway. The genes in lightface letters do not demonstrate any significant differential expressions.

Table 4-8. The Genes of the Skeletal Muscle (Myogenesis and Myopathy) Pathway.

Line	Genes (Symbols)	N_{gene}	N_{gene}%	N_p%	$N_{p(adj)}$%
Skeletal Muscle Contractility, Dystrophin-Glycoprotein Complex:					
	Capn3*, Emd*, Lmna*, Cav3*, Dmd*, Dysf*, Dag1, Camk2g, Mapk1, Sgca.	10	12%	10%	7%
Skeletal Muscle Contractility, Titin Complex:					
	Actn3*, Capn3*, Lmna*, Myot*, Cryab*, Tnnt3*, Tnni2*, Trim63*, Acta1, Des, Ttn, Myh1, Myh2, Mapk1, Mstn, Neb, Sgca, Tnnt1.	18	21%	15%	10%
Skeletal Muscle Contractility, Energy Metabolism:					
	Hk2*, Slc2a4*, Cs*, Pdk4.	4	5%	5%	4%
Skeletal Muscle Contractility, Fast-Twitch Fibres:					
	Atp2a1*, Tnnt3*, Tnni2*, Myh1, Myh2.	5	6%	6%	4%
Skeletal Muscle Contractility, Slow-Twitch Fibres:					
	Mb, Myh1, Tnnc1, Tnnt1.	4	5%	4%	0%
Skeletal Muscle Contractility, Other:					
	Rps6kb1*, Dmpk, Ikbkb.	3	4%	1%	1%
Skeletal Myogenesis:					
	Myod1*, Mef2c*, Hdac5*, Myog*, Adrb2*, Dmd*, Rps6kb1*, Agrn*, Igfbp5*, Cast*, Utrn*, Cav1*, Bmp4, Capn2, Acta1, Myf5, Igfbp3, Igf1, Mbnl1, Myf6, Ppp3ca, Bcl2, Ctnnb1, Mstn, Musk, Myog, Pax3, Rhoa.	28	33%	25%	14%
Skeletal Muscle Hypertrophy:					
	Myod1*, Adrb2*, Acvr2b*, Rps6kb1*, Igfbp5*, Acta1, Igf1, Myf6, Mstn.	9	11%	10%	6%
Skeletal Muscle Autocrine Signalling:					
	Il6*, Tgfb1*, Igf2*, Adipoq, Fgf2, Igf1, Lep, Mstn.	8	10%	7%	4%
Diabetes/Metabolic Syndrome:					
	Ppargc1a*, Prkaa1*, Slc2a4*, Prkab2, Ppargc1b, Adipoq, Pparg, Lep, Prkag1, Prkag3.	10	12%	8%	4%
Skeletal Muscle Wasting/Atrophy, Autophagy:					
	Fbxo32*, Casp3*, Nos2*, Rps6kb1*, Ppargc1a*, Trim63*, Foxo3, Capn2, Ppargc1b, Mstn.	10	12%	11%	7%
Skeletal Muscle Wasting/Atrophy, Dystrophy:					
	Fbxo32*, Akt2*, Il1b*, Trim63*, Mapk8*, Utrn*, Mapk14, Tnf, Akt1, Mapk3, Nfkb1, Mapk1, Mmp9.	13	15%	13%	7%

The suggested 84 different genes for the pathway by Sabiosciences (2015). Significantly expressed genes (p≤0.05) are in boldface letters. Genes marked with an asterisk are significant (p(adj)≤0.05) with a false discovery rate-corrected p-value.

Table 4-9 shows the distribution of the maximum significant relative count, both with and without the false discovery rate correction, for the genes in the subgroups within all the pathway lines. The relative count demonstrates the greatest subgroup-coverage in three pathway lines: Contractility Dystrophin-Glycoprotein Complex, Contractility Titin Complex, and Myogenesis. However, the focus is not on the highest percentage in the table *per se*, but how close these percentages are to their corresponding pathway line percentage given in Table 4-8; and if the percentage is

maintained high throughout the subgroup-coverage in the pathway line. With reference to $N_{p(adj)}$%, the Contractility Dystrophin-Glycoprotein Complex pathway line should be as close to 7% (as per Table 4-8) and is here seen with a maximum of 6.0% (i.e. 80% of the 7.0%) in three of the subgroups. The other subgroups show somewhat similar percentage. The Contractility Titin Complex pathway line should be close to $N_{p(adj)}$%=10%, and is here with a maximum of 4.8% (i.e. 50% of the 10%) in only one subgroup; still, the percentage of others are following close behind. The Myogenesis pathway line should be as close to $N_{p(adj)}$%=14%, and is here seen with a maximum of 6.0% (i.e. 40% of the 14%) in three of the subgroups, and the other subgroups follow somewhat closely. Therefore, of these three pathway lines, the Contractility Dystrophin-Glycoprotein Complex pathway line has the greatest coverage.

Table 4-9. The Overall Profile Coverage of the Skeletal Muscle (Myogenesis and Myopathy) Pathway Based on the Maximum Relative Count of Significantly Expressed Genes.

Line	Day −1	Day 1			Day 3			Day 7			Day 14		
	R{−1}	C{01}	H{01}	E{01}	C{03}	H{03}	E{03}	C{07}	H{07}	E{07}	C{14}	H{14}	E{14}
Skeletal Muscle Contractility: Dystrophin−Glycoprotein Complex.													
Np%		6.0%	7.1%	7.1%	2.4%	6.0%	2.4%	1.2%	6.0%	7.1%	2.4%	7.1%	7.1%
Np(adj)%		3.6%	6.0%	4.8%	1.2%				6.0%	2.4%		6.0%	3.6%
Skeletal Muscle Contractility: Titin Complex.													
N_p%	2.4%	8.3%	7.1%	6.0%	8.3%	7.1%	3.6%	2.4%	7.1%	4.8%	3.6%	4.8%	4.8%
$N_{p(adj)}$%		4.8%	3.6%	3.6%	3.6%	1.2%			2.4%	2.4%		3.6%	2.4%
Skeletal Muscle Contractility: Energy Metabolism.													
N_p%		2.4%	1.2%	2.4%	2.4%	1.2%	1.2%	1.2%	2.4%	1.2%		2.4%	2.4%
$N_{p(adj)}$%				1.2%	1.2%				1.2%	1.2%			2.4%
Skeletal Muscle Contractility: Fast−Twitch Fibres.													
N_p%		3.6%	2.4%	4.8%	4.8%	2.4%	1.2%		1.2%		1.2%	4.8%	2.4%
$N_{p(adj)}$%		1.2%		1.2%	3.6%	1.2%							
Skeletal Muscle Contractility: Slow−Twitch Fibres.													
N_p%		1.2%	4.8%			3.6%			6.0%		3.6%	3.6%	3.6%
$N_{p(adj)}$%													
Skeletal Muscle Contractility: Other.													
N_p%		1.2%	1.2%	1.2%			1.2%		1.2%			1.2%	1.2%
$N_{p(adj)}$%			1.2%										
Skeletal Myogenesis.													
N_p%	2.4%	7.1%	13.1%	9.5%	3.6%	8.3%	10.7%	4.8%	11.9%	8.3%	3.6%	11.9%	10.7%
$N_{p(adj)}$%		1.2%	6.0%	3.6%	1.2%	3.6%	1.2%		4.8%	6.0%		4.8%	6.0%
Skeletal Muscle Hypertorphy.													
N_p%	1.2%	3.6%	4.8%	4.8%		2.4%	3.6%		6.0%	4.8%		7.1%	6.0%
$N_{p(adj)}$%			2.4%	1.2%					1.2%	2.4%		3.6%	3.6%
Skeletal Muscle Autocrine Signalling.													
N_p%	1.2%	1.2%	2.4%	3.6%	1.2%	2.4%	2.4%	1.2%	2.4%	2.4%	1.2%	2.4%	2.4%
$N_{p(adj)}$%		1.2%	1.2%	1.2%					2.4%	2.4%		1.2%	1.2%
Diabetes/Metabolic Syndrome.													
N_p%	2.4%	2.4%	2.4%	3.6%	2.4%	3.6%	3.6%	1.2%	1.2%	1.2%		2.4%	2.4%
$N_{p(adj)}$%			1.2%	1.2%	1.2%		1.2%			1.2%			
Skeletal Muscle Wasting/Atrophy: Autophagy.													
N_p%	2.4%	6.0%	4.8%	4.8%	2.4%	2.4%	3.6%	2.4%	6.0%	4.8%	2.4%	3.6%	6.0%
$N_{p(adj)}$%		1.2%	2.4%	1.2%	1.2%	1.2%			1.2%	3.6%	1.2%	1.2%	1.2%
Skeletal Muscle Wasting/Atrophy: Dystrophy.													
N_p%	2.4%	8.3%	4.8%	6.0%	3.6%	3.6%	4.8%	2.4%	4.8%	4.8%	1.2%	1.2%	2.4%
$N_{p(adj)}$%		1.2%	2.4%	1.2%	1.2%	1.2%			2.4%	2.4%	1.2%	1.2%	2.4%

N_p%, relative count of significantly expressed genes ($p \leq 0.05$) with ordinary t-test.
$N_{p(adj)}$%, relative count of significantly expressed genes ($p(adj) \leq 0.05$) with an adjusted p-value for false rate discovery.

The Skeletal Muscle Contractile - Dystrophin-Glycoprotein Complex Profile.

Table 4-10 demonstrates the profile of significant differential expression that corresponds to the Skeletal Muscle Contractile Dystrophin-Glycoprotein Complex pathway line. For a given gene the average expression, for each objective vs reference group, is displayed in a logarithmic ratio, i.e. fold changes on a log_2-scale (log_2(FC). The positive fold changes represent upregulated differential expressions and are written in a white font on a dark background, to distinguish them from the negative fold changes that represent downregulated differential expressions. The fold changes marked with an asterisk and written with boldface letters are significant after the false discovery rate correction, whilst the others are only significant with the t-test.

Table 4-10. The Skeletal Muscle Contractility – Dystrophin-Glycoprotein Complex Gene Profile of the Significant Differential Fold Changes (log_2(FC)).

Timing	*Reference*	*Objective*	Gene (Symbol)							
			Capn3	Emd	Lmna	Cav3	Dmd	Dysf	Dag1	Camk2g
Day −1	4{−1}	R{−1}								
Day 1	4{−1}	C{01}	**−0.59***	*0.28*	**0.57***	*−0.23*		**0.49***		
	R{−1}		**−0.52***	*0.24*	**0.48***			*0.30*		
	4{−1}	H{01}	**−0.56***	**0.36***	**0.72***	**−0.41***	*−0.39*	**0.50***		
	R{−1}		**−0.49***	**0.31***	**0.64***	*−0.29*	*−0.44*	*0.31*		
	4{−1}	E{01}	**−0.64***	**0.32***	**0.59***	**−0.39***		*0.41*	*−0.26*	
	R{−1}		**−0.57***	*0.27*	**0.50***	*−0.26*			*−0.24*	
	C{01}									*−0.61*
Day 3	4{−1}	C{03}			*0.48*			*0.48*		
	R{−1}				*0.39*					
	C{01}		**0.52***							
	4{−1}	H{03}			*0.36*			*0.33*		
	H{01}		*0.44*	*−0.29*	*−0.36*	*0.30*	*0.53*			
	4{−1}	E{03}			*0.49*			*0.33*		
	R{−1}				*0.41*					
	E{01}		*0.39*			*0.28*				
Day 7	*C{03}*	C{07}			*−0.28*					
	4{−1}	H{07}					*0.44*			
	R{−1}						*0.39*			
	H{01}		**0.70***	**−0.42***	**−0.57***	**0.36***	**0.84***			
	C{07}						*0.38*			
	E{01}	E{07}	**0.61***	*−0.27*	**−0.40***	*0.27*		*−0.38*		*0.46*
	E{03}				*−0.30*			*−0.29*		
	H{07}						*−0.37*			
Day 14	*R{−1}*	C{14}	*0.33*							*0.48*
	4{−1}	H{14}							*−0.24*	
	R{−1}		*0.34*						*−0.23*	
	H{01}		**0.84***	**−0.30***	**−0.52***	**0.36***	**0.71***	*−0.30*		
	H{03}		*0.39*							
	E{01}	E{14}	**0.62***	**−0.35***	**−0.44***	*0.21*	*0.37*	*−0.39*		
	E{03}				*−0.34*			*−0.30*		

Fold change values marked with an asterisk and in boldface letters are significant ($p \leq 0.05$) with an adjusted p-value (false discovery rate corrected). Positive fold change values are in white letters on dark background. Genes within this pathway line with no significant differential expression are: Mapk1, Sgca.

None of the genes in the pathway line demonstrate significant differential expressions between the R{−1} and the A{−1} subgroups on Day −1, and, therefore, jointly situate the reference level. However, the general physiological reference for the three groups, the [C], [H] and [E], is the R{−1} subgroup. *Capn3* is downregulated on Day 1 in all the three groups, still, without any significant difference between them. The downregulation is then returned to the reference level on Day 3, especially for the [C]-group, and then more pronouncedly from Day 7 for the [H] and the [E]-groups. There is even slight evidence of upregulation in the [H]-group on Day 14. Contrary to *Capn3, Emd* shows an upregulation in all three groups on Day 1, although slightly more pronounced in the [H]-group. The [C]-group shows an indication of being immediately returned to reference level on Day 3. In the [H] and [E]-groups the upregulation is returned to the reference level on Day 14, sooner for the [H]-group, from Day 3/7, from Day 7/14 for the [E]-group. The exact measurable day depends on whether which level of significance is taken into account. *Lmna* shows an upregulation in all the groups on Day 1, that is gradually returned to the reference levels on Day 7 for the [C] and [H]-groups, whilst the gradual change within the [E]-group is much slower, especially until Day 3. *Cav3* is downregulated on Day 1, with the more significant change in the [H] and [E]-groups, that is returned on Day 3. Moreover, on Day 1, the downregulation with reference to A{−1} and R{−1}, suggests that Cav3 might be slightly downregulated in the R{−1} compared to A{−1}, still, not significantly. *Dmd* shows the most marked response on Day 1 in the [H]-group with a small downregulated expression, which seems to be returned on Day 3 but reversed to an upregulation on Day 7 and thereafter. The [E]-group seems to be shadowing this pattern of the [H] group, as its only significant expression, throughout, is present on Day 14 with a small upregulation. *Dysf* shows an upregulation on Day 1 in all the groups; that seems prolonged until Day 3, and furthermore, more emphasises in reference to the A{−1}-group. The [E]-group indicates to show a slightly more notable return of this upregulation from Day 7 to Day 14. The semi one-time significant differential expressions of *Dag1* and *Camk2g* are too isolated to be indicative of any trend and do, furthermore, only show significant expression according to the t-test. *Mapk1* and *Sgca* do not show any significant differential expressions.

The Skeletal Muscle Contractility — The Titin Complex Profile; the Energy Metabolism Profile; the Fast-Twitch Fibres Profile; the Slow-Twitch Fibres Profile; and Other Related Genes

The tables of differential expression of the following five profiles can be found in Appendix D.4.1: The Titin Complex Profile (Table ApxD - 3); the Energy Metabolism Profile (Table ApxD - 4); the Fast-Twitch Fibres Profile (Table ApxD - 5); the Slow-Twitch Fibres Profile (Table ApxD - 6); and

Other Related Genes (Table ApxD - 7). Between these profiles, the most significantly expressed genes, apart from *Capn3* and *Lmna*, already described above, are *Myot*, *Hk2* and *Atp2a1*. None is expressed differentially between the R{−1} and A{−1}. *Myot* is downregulated in all groups on Day 1, which is returned to reference level on Day 3. The [H]-group might be slightly less downregulated, although, not significantly. *Hk2* is only responsive in the [E]-group on Day 1, reflected in an upregulation which is returned from Day 7. Group [C] and [H] are also responsive (the [C]-group less than the [H]-group) with a significant downregulation on Day 7. The difference in the downregulation between all the groups on Day 7 suggest a slight more reaction in the [H]-group. *Atp2a1* is downregulated in the [C] and [H]-groups on Day 1, which is then returned on Day 3. On the contrary, the [E]-group is upregulated on Day 1 which is gradually returned thereafter.

The Skeletal Muscle — The Myogenesis Profile; and the Hypertrophy Profile

The tables of differential expression of the following two profiles can be found in Appendix D.4.1: The Myogenesis Profile (Table ApxD - 8); and the Hypertrophy Profile (Table ApxD - 9). Between these profiles, the most significantly expressed genes are *Myod1*, *Mef2c* and *Myog*. None is expressed differentially between the R{−1} and A{−1}. *Myod1* is upregulated in all groups on Day 1, which is gradually returned to reference level on Day 7. The [C]-group is responsive to a lesser extent, and there is an indication of the [E]-group being more responsive. *Mef2c* is downregulated in all groups on Day 1 and immediately returned to reference level on Day 3, still, without any significant differences between the groups. *Myog* is upregulated in the [H] and [E]-groups on Day 1 and gradually returned to reference level on Day 7, with no distinction between the two groups. However, the [C]-group does not show any significant expression.

The Skeletal Muscle — The Autocrine Signalling Profile; and the Diabetes/Metabolic Syndrome Profile

The tables of differential expression of the following two profiles can be found in Appendix D.4.1: The Autocrine Signalling Profile (Table ApxD - 10); and the Diabetes/Metabolic Syndrome Profile (Table ApxD - 11). Between these profiles, the most significantly expressed genes are *Il6*, *Tgfb1* and *Ppargc1a*. None is expressed differently between the R{−1} and A{−1}. *Il6* is upregulated in the [E]-group on Day 1 and immediately returned to reference level on Day 3. However, the [C] and [H]-groups do not show any significant differential expression. *Tgfb1* is the most responsive gene in the [H]-group, with an upregulation on Day 1 which gradually returns to reference level on Day 7. Both the [C] and [E]-groups are upregulated to a slightly lesser extent on Day 1 (to even lesser extent in the [E]-group), and maintained upregulated until Day 3. Thereafter the expression returns to the reference level.

The Skeletal Muscle Wasting/Atrophy — The Autophagy Profile; and the Dystrophy Profile

The tables of differential expression of the following two profiles can be found in Appendix D.4.1: The Autophagy Profile (Table ApxD - 12); and the Dystrophy Profile (Table ApxD - 13). Between these profiles, the most significantly expressed genes are *Fbxo32*, *Casp3*, *Akt2* and *Trim63*. *Fbxo32* is downregulated on Day −1 in the R{−1} in comparison with A{−1}. On Day 1 it then shows an upregulation in the [C] and [H]-groups, but to slightly more extent in the [C]-group. The upregulation is maintained in both groups until Day 14, although it slightly lags in the [C]-group in between Day 3 and Day 7, but rises up again on Day 14. The [E]-group does not show any significant differential expression of *Fbxo32*. *Casp3* is not expressed differentially between R{−1} and A{−1}. On Day 1 the gene is upregulated in all three groups and maintained upregulated on Day 3 in the [H]-group. After upregulation in the [H] and [E], the expression immediately returns to the reference level on Day 7. The [C]-group shows less gradual return. *Akt2* is not expressed differentially between R{−1} and A{−1}. On Day 1 the gene is downregulated in all three groups and maintained downregulated until Day 7 in the [E]-group. The [C]-group immediately returns to reference level on Day 3, whilst the [H]-group does so gradually until Day 14. *Trim63* is downregulated on Day −1 in the R{−1} and are also downregulated in the [C] and [H]-groups on Day 1. The [H]-group then immediately returns to reference level on Day 3, whilst the [C]-group has a slightly more planar return. The [E]-group, on the other hand, immediately returns to reference level on Day 1 and maintains it until Day 14.

4.4.3 The Hypoxia Signalling Pathway

Table 4-11 shows the pathway lines within the Hypoxia Signalling pathway, listed with all the genes that compose them along with an absolute gene count (N_{gene}) and a relative count (N_{gene}%) referenced to the 84 different genes of the pathway. As for the other pathways, some genes may be repeated between the different lines, without affecting the overall count. The genes in boldface letters have significantly expressed ($p \leq 0.05$), with an ordinary t-test, in at least one of the subgroup comparisons, and are accompanied with their relative gene (N_p%) referenced to the 84 different genes of the pathway. Genes in boldface letters marked with an asterisk are, furthermore, significantly expressed after the false discovery rate corrections ($p(adj) \leq 0.05$), and are accompanied with the relative gene count ($N_{p(adj)}$%) referenced to the 84 genes in the pathway. The genes in lightface letters do not demonstrate any significant differential expressions.

Table 4-11. The Genes of the Hypoxia Signalling Pathway.

Line	Genes (Symbols)	N_{gene}	N_{gene}%	N_p%	$N_{p(adj)}$%
HIF1 & Co-Transcription Factors:					
	Arnt*, Per1, Hif1a, Cops5, Hif3a, Hnf4a.	6	7%	6%	1%
Other HIF1 Interactors:					
	Egln3*, P4hb*, Tp53*, Apex1*, P4ha1, Nfkb1, Cdkn2a, Egln1.	8	10%	7%	5%
Angiogenesis:					
	Hmox1*, Btg1*, Adora2b*, Anxa2*, Plau*, Serpine1*, Lox*, Pgf*, Vegfa*, Jmjd6, Angptl4, F3, Gpi, Egr1, Edn1, Epo, Mmp9.	17	20%	15%	11%
Coagulation:					
	Anxa2*, Plau*, Serpine1*, Aldoa*, F10, F3, Slc16a.	7	8%	7%	5%
DNA Damage Signalling & Repair:					
	Mif*, Ndrg1, Ruvbl2, LOC367198.	4	5%	4%	1%
Metabolism:					
	Pdk1*, Pfkl*, Ero1l*, Hk2*, Pgam1*, Slc2a1*, Aldoa*, Ldha*, Pkm*, Ddit4*, Pgm2*, Pfkp, Gpi, Gys1, Tpi1, Eno1, Pfkfb3, Pfkfb4, Pgk1, Slc2a3.	20	24%	18%	13%
Regulation of Apoptosis:					
	Bnip3*, Btg1*, Pim1*, Mif*, Ddit4*, Ier3, Bnip3l, Adm, Nos3.	9	11%	6%	11%
Regulation of Cell Proliferation:					
	Btg1*, Pim1*, Mxi1*, Ccng2*, Mif*, Pgf*, Odc1, Igfbp3, Met, Adm, Nampt, Nos3, Blm, Egr1, Txnip.	15	18%	14%	7%
Transcription Factors:					
	Usf2*, Bhlhe40, Fos, Rbpjl.	4	5%	4%	1%
Transporters, Channels & Receptors:					
	Tfrc*, Slc16a3*, Slc2a1*, Vdac1, Slc2a3.	5	6%	5%	4%
Other Responsive Genes:					
	Lgals3*, Ctsa*, Ankrd37*, Car9, Dnajc5, Eif4ebp1, Map3k1.	7	8%	8%	4%

The suggested 84 different genes for the pathway by Sabiosciences (2015). Significantly expressed genes ($p \leq 0.05$) are in boldface letters. Genes marked with an asterisk are significant ($p(adj) \leq 0.05$) with a false discovery rate-corrected p-value.

Table 4-11 shows the distribution of the maximum significant relative count, both with and without the false discovery rate correction, for the genes in the subgroups within all the pathway lines. The relative count demonstrates the greatest subgroup-coverage in three pathway lines; Angiogenesis, Metabolism, and Regulation of Apoptosis. However, the focus is not on the highest percentage in the table *per se*, but how close these percentages are to their corresponding pathway line percentage given in Table 4-12, and if the percentage is maintained high throughout the subgroup-coverage in the pathway line.

With reference to $N_{p(adj)}$%, the Angiogenesis pathway line should be as close to 11% (as per Table 4-12) and is here seen with a maximum of 8.3% (i.e. 78% of the 11%) in three of the subgroups. The other subgroups show somewhat similar percentage. The Metabolism pathway line should be close to $N_{p(adj)}$%=13%, and is here with a maximum of 4.8% (i.e. 36% of the 13%) in only one subgroup; still, the percentage of others are following close behind. The Regulation of Apoptosis pathway line should be as close to $N_{p(adj)}$%=11%, and is here seen with a maximum of 4.8% (i.e. 44% of the 11%) in three of the subgroups, and the other subgroups follow somewhat closely. Therefore, of these three pathway lines, the Angiogenesis pathway line has the greatest.

Table 4-12. The Overall Profile Coverage of the Hypoxia Signalling Pathway Based on the Maximum Relative Count of Significantly Expressed Genes.

Line	Day −1	Day 1			Day 3			Day 7			Day 14		
	R{−1}	C{01}	H{01}	E{01}	C{03}	H{03}	E{03}	C{07}	H{07}	E{07}	C{14}	H{14}	E{14}
HIF1 & Co−Transcription Factors.													
N_p%	1.2%	4.8%	1.2%	2.4%	2.4%	1.2%	1.2%	2.4%	2.4%	1.2%	2.4%	2.4%	1.2%
$N_{p(adj)}$%				1.2%									
Other HIF1 Interactors.													
N_p%		3.6%	4.8%	2.4%	2.4%	3.6%	2.4%	1.2%	3.6%	2.4%	2.4%	3.6%	3.6%
$N_{p(adj)}$%		1.2%	3.6%	1.2%	1.2%	2.4%			2.4%			2.4%	1.2%
Angiogenesis.													
N_p%		3.6%	9.5%	9.5%	3.6%	4.8%	7.1%	2.4%	8.3%	10.7%	1.2%	9.5%	9.5%
$N_{p(adj)}$%			7.1%	8.3%		1.2%	3.6%		4.8%	4.8%		8.3%	8.3%
Coagulation.													
N_p%		3.6%	4.8%	3.6%	2.4%	3.6%	3.6%	1.2%	3.6%	3.6%	1.2%	3.6%	3.6%
$N_{p(adj)}$%			3.6%	3.6%		2.4%	1.2%		2.4%	1.2%		3.6%	2.4%
DNA Damage Signalling & Repair.													
N_p%		1.2%		1.2%			1.2%		1.2%	2.4%		1.2%	1.2%
$N_{p(adj)}$%				1.2%									
Metabolism.													
N_p%		8.3%	4.8%	6.0%	9.5%	6.0%	6.0%	2.4%	7.1%	4.8%	2.4%	6.0%	7.1%
$N_{p(adj)}$%		2.4%	3.6%	3.6%	2.4%	2.4%	2.4%		4.8%	2.4%		2.4%	4.8%
Regulation of Apoptosis.													
N_p%		6.0%	4.8%	6.0%	3.6%	4.8%	6.0%		3.6%	6.0%	1.2%	3.6%	3.6%
$N_{p(adj)}$%		2.4%	3.6%	4.8%	1.2%	2.4%	2.4%		3.6%	3.6%		3.6%	3.6%
Regulation of Cell Proliferation.													
N_p%		6.0%	4.8%	7.1%	1.2%	3.6%	6.0%		3.6%	7.1%	1.2%	4.8%	7.1%
$N_{p(adj)}$%		1.2%	3.6%	3.6%		1.2%	1.2%		2.4%	2.4%		2.4%	6.0%
Transcription Factors.													
N_p%				1.2%	1.2%				1.2%	2.4%		1.2%	1.2%
$N_{p(adj)}$%										1.2%			
Transporters, Channels & Receptors.													
N_p%		2.4%	2.4%	3.6%	3.6%	2.4%	1.2%	2.4%	3.6%	2.4%	2.4%	3.6%	3.6%
$N_{p(adj)}$%			1.2%	1.2%		2.4%			2.4%	2.4%			2.4%
Other Responsive Genes.													
N_p%		4.8%	4.8%	2.4%	2.4%	4.8%	2.4%	1.2%	3.6%	2.4%		3.6%	3.6%
$N_{p(adj)}$%		3.6%	2.4%	1.2%			1.2%		2.4%	1.2%		2.4%	1.2%

N_p%, relative count of significantly expressed genes ($p \leq 0.05$) with ordinary t-test.
$N_{p(adj)}$%, relative count of significantly expressed genes ($p(adj) \leq 0.05$) with an adjusted p-value for false rate discovery.

The Hypoxia Signalling Angiogenesis Profile

Table 4-13 demonstrates the profile of significant differential expression that corresponds to the Hypoxia Signalling Angiogenesis pathway line. For a given gene the average expression, for each objective vs reference group, is displayed in fold changes on a log_2-scale (log_2(FC). The positive fold changes represent upregulated differential expressions and are written in a white font on a dark background, to distinguish them from the negative fold changes that represent downregulated differential expressions. The fold changes marked with an asterisk and written with boldface letters are significant after the false discovery rate correction, whilst the others are only significant with the t-test.

Table 4-13. The Hypoxia Signalling Angiogenesis Gene Profile of Significant Differential Fold Changes (log_2(FC)).

Timing	Reference	Objective	Gene (Symbol)												
			Hmox1	Btg1	Adora2b	Anxa2	Plau	Serpine1	Lox	Pgf	Vegfa	Jmjd6	Angptl4	F3	Gpi
Day −1	A{−1}	R{−1}													
Day 1	A{−1}	C{01}					*0.69*	*1.21*	*1.29*			*−0.38*			
	R{−1}							*1.16*							
	A{−1}	H{01}	*1.26*	**0.57***	*0.52*	**1.33***	**1.05***	**1.99***	**2.03***		**−1.11***				
	R{−1}		*1.23*	**0.46***		*0.99*	*0.73*	**1.94***	**1.46***		*−0.62*				
	C{01}			*0.35*											
	A{−1}	E{01}	**1.96***	**0.89***	**0.72***	**1.09***	**1.29***	**2.24***	**1.90***		*−0.62*				
	R{−1}		**1.93***	**0.79***	*0.50*	*0.76*	**0.97***	**2.20***	*1.34*	*0.74*					
	C{01}		**1.59***	**0.68***			*0.60*	*1.03*		*0.59*			*2.92*		
	H{01}			*0.32*						*0.56*					
Day 3	A{−1}	C{03}				*0.87*		*0.97*	*1.94*						
	R{−1}							*0.92*	*1.38*						
	A{−1}	H{03}				*0.83*	*0.56*		*1.77*		*−1.02*				
	R{−1}								*1.20*			*−0.33*			
	H{01}		*−0.98*	*−0.30*	*−0.45*			**−1.51***							
	A{−1}	E{03}				*0.82*	*0.56*	**1.85***	*1.59*		*−0.98*				
	R{−1}							*1.80*	*1.02*						
	E{01}		**−1.51***	**−0.80***	**−0.72***		*−0.72*			*−0.73*			*−2.49*		
	H{03}							*1.37*							
Day 7	C{03}	C{07}						*−0.97*	*−1.04*						
	A{−1}	H{07}								*−0.63*		*−0.36*			
	R{−1}											*−0.43*			
	H{01}		**−1.38***	**−0.69***	*−0.53*	**−1.32***	*−0.66*	**−1.59***	*−1.17*						
	H{03}			*−0.39*		*−0.81*									
	A{−1}	E{07}					*0.57*	*1.14*							
	R{−1}							*1.09*							
	E{01}		**−1.82***	**−1.07***	**−0.66***	**−1.12***	*−0.71*	*−1.10*	*−1.21*	*−0.73*			*−2.84*		
	E{03}					*−0.84*					*0.91*				
	C{07}							*1.14*							
Day 14	R{−1}	C{14}												*−0.74*	
	H{01}	H{14}	**−1.39***	**−0.69***	**−0.62***	**−1.22***	**−0.81***	**−1.44***	**−1.46***		*0.68*				
	H{03}			*−0.39*		*−0.72*			*−1.20*		*0.59*				
	H{07}									*0.55*					
	A{−1}	E{14}						*1.02*							*−0.29*
	R{−1}							*0.97*							
	E{01}		**−1.84***	**−1.01***	**−0.79***	**−1.27***	**−0.94***	*−1.22*	**−1.84***	**−0.77***					
	E{03}					*−1.00*			*−1.52*		*0.62*				

Fold change values marked with an asterisk and in boldface letters are significant ($p \leq 0.05$) with an adjusted p-value (false discovery rate corrected). Positive fold change values are in white letters on dark background. Genes within this pathway line with no significant differential expression are: Egr1, Edn1, Epo, Mmp9.

None of the genes in the pathway line demonstrate significant differential expressions between the R{−1} and the A{−1} subgroups on Day −1, and, therefore, jointly situate the reference level. Hmox1, Btg1 and Adora2b all show similar profiles of upregulation on Day 1, which has returned to reference level on Day 7, in the [H] and [E]-groups. The return is perhaps indicated to be slightly faster in the [E]-group. However, the [C]-group does not show any significant reaction on any of the days. *Anxa2* is similar to *Hmox1*, *Btg1* and *Adora2b* regarding being only significantly reactive in the [H] and [E] groups and not in the [C]-group, demonstrating an upregulation on Day 1 that has returned bac to the reference levels on Day 7. However, the upregulation is still detectable on Day 3. Furthermore, the overall expression levels do indicate that the gene is slightly upregulated in R{−1} in comparison with A{−1}, still, not significantly. *Plau* shows a similar pattern to *Anx2*, commencing with an upregulation on Day 1 for the [H] and [E]-groups, still, also seems to be

slightly upregulated in C{01} which is then immediately returned. The upregulation is gradually returned to reference levels on Day 14, from being with somewhat more emphasised upregulation at the start. *Serpine1* is upregulated in all three groups on Day 1 and is prolonged until Day 3 for the [C]-group and until Day 14 for the [E]-group, although both seem to decrease gradually. The [H]-group, which is upregulated to a similar level of [E]-group, shows a little bit steeper decrease in the upregulation on Day 3 (in comparison with the [C]-group) but is maintained at that level throughout, until Day 14. *Lox* is also upregulated in all the groups on Day 1, which is slightly prolonged until Day 3, and thereafter returned to reference level on Day 14 in the [E]-group, whilst the [H]-group is slightly lagging. The [C]-group, however, shows an indication of gradually increasing the upregulation until Day 3 but has dropped on Day 7. *Pgf* is mostly reactive in the [E]-group, demonstrating an upregulation on Day 1 that is returned on Day 3. *Vegfa* is mostly reactive in the [H] and [E] groups, showing an upregulation on Day 1, perhaps more pronounced in the [H]-group, but gradually returns until Day 14. Whilst *Angptl4* seems to be upregulated only in the [E]-group, which is returned on Day 3; *Jmjd6, F3* and *Gpi* show too sporadic significant expressions to make them logical. *Egr1*, *Edn1*, *Epo* and *Mmp9* do not show significant differential expression.

The Hypoxia Signalling — The HIF1 & Co-Transcription Factors Profile; and the Profile of Other HIF1 Interactors

The tables of differential expression of the following two profiles can be found in Appendix D.4.2: The HIF1 & Co-Transcription Factors Profile (Table ApxD - 15); and the Profile of Other HIF1 Interactors (Table ApxD - 16). Between these profiles, the most significantly expressed genes are *Egln3* and *Tp53*. Neither is expressed differentially between the R{−1} and A{−1}. *Egln3* is downregulated on Day 1 in all three groups, but to a lesser extent in the [E]-group. On Day 3 all three groups have immediately returned expression back to the reference level. *Tp53* is upregulated in group [H] on Day 1, but immediately returns to reference level on Day 3. However, the [C] and [E]-groups do not show any significant differential expression for this gene.

The Hypoxia Signalling — The Coagulation Profile; the DNA Damage Signalling & Repair Profile; and the Metabolism Profile

The tables of differential expression of the following three profiles can be found in Appendix D.4.2: The Coagulation Profile (Table ApxD - 17); the DNA Damage Signalling & Repair Profile (Table ApxD - 18); and the Metabolism Profile (Table ApxD - 19). Between these profiles, the most significantly expressed gene is *Pdk1*, which is, furthermore, not expressed differentially between the R{−1} and A{−1}. *Pdk1* is downregulated in all three groups on Day 1, with a hint of gradual difference from less downregulated [C]-group to the more downregulated [E]-group (with the [H]-

group in between). The expression is gradually returned in the [H] and [E]-groups on Day 14 and Day 7 respectively, whilst the [C]-groups does so on Day 7.

The Hypoxia Signalling — The Regulation of Apoptosis Profile; and the Regulation of Cell Proliferation Profile

The tables of differential expression of the following two profiles can be found in Appendix D.4.2: The Regulation of Apoptosis Profile (Table ApxD - 20); and the Regulation of Cell Proliferation Profile (Table ApxD - 21). Between these profiles, the most significantly expressed genes are *Bnip3* and *Pim1*. Neither is expressed differentially between the R{−1} and A{−1}. *Bnip3* is downregulated in all three groups on Day 1, with the [E] group to a somewhat lesser extent. Whilst the expression in the [C] and [H]-groups returns in relatively planar manner, the expression in the [E]-group do so until Day 14, but with a more pronounced gradient. *Pim1* is upregulated in all three groups on Day 1, with the [C]-group to a lesser extent, whilst no difference can be seen between the [H] and [E]-groups. The [H] and [E]-groups, thereafter, show a gradual return to the reference level until Day 14.

The Hypoxia Signalling — The Transcription Factors Profile; the Transporters, Channels & Receptors Profile; and the Profile of Other Responsive Genes

The tables of differential expression of the following three profiles can be found in Appendix D.4.2: The Transcription Factors Profile (Table ApxD - 22); the Transporters, Channels & Receptors Profile (Table ApxD - 23); and the Profile of Other Responsive Genes (Table ApxD - 24). Between these profiles, the most significantly expressed genes are *Tfrc* and *Lgals3*. Neither is expressed differentially between the R{−1} and A{−1}. *Tfrc* seems to react slowly, without any significant differential expression on Day 1, but then downregulated on Day 3, mostly emphasises in the [H]-group. This downregulation is then maintained from Day 3 until Day 14. *Lgals3* is upregulated in all three groups on Day 1, ranking with the higher upregulation in the [H]-group, followed by the [C]-group, then the [E]-group (although the difference between them is not significant). The overall expression is then gradually returning to reference level on Day 14.

4.4.4 The VEGF Pathway

Table 4-14 shows the pathway lines within the VEGF pathway, listed with all the genes that compose them along with an absolute gene count (N_{gene}) and a relative count (N_{gene}%) with reference to the 84 different genes in the pathway. genes may be repeated between the different lines, which does not affect the overall count. The genes (or the gene symbols) in boldface letters are significantly expressed ($p \leq 0.05$), with an ordinary t-test, in at least one of the subgroup

comparisons, and are accompanied with their relative gene count (N_p%) referenced to the 84 different genes of the pathway. Genes in boldface letters marked with an asterisk are, furthermore, significantly expressed after the false discovery rate corrections (p(adj)≤0.05), and are accompanied with the relative gene count ($N_{p(adj)}$%) referenced to the 84 genes in the pathway. The genes in lightface letters do not demonstrate any significant differential expressions.

Table 4-14. The Genes of the VEGF Pathway.

Line	Genes (Symbols)	N_{gene}	N_{gene}%	N_p%	$N_{p(adj)}$%
Growth Factors & Receptors:					
	Vegfc*, Kdr*, Flt1*, Pgf*, Vegfa*, Vegfb, Pdgfc, Figf, Nrp1, Flt4, Nrp2.	11	13%	11%	6%
Akt & PI-3-Kinase Signalling:					
	Pik3r1*, Pik3ca*, Akt2*, Pik3r3*, Pik3r2*, Akt3, Pik3r5, Akt1, Pik3cb, Pik3cd, Pik3cg.	11	13%	12%	6%
Small G-Protein Signalling:					
	Nras*, Raf1*, Rac1*, Rac2*, Shc2, Src, Hras, Kras.	8	10%	8%	5%
Heat Shock Proteins:					
	Hsp90aa1*, Hspb1*.	2	2%	2%	2%
MAP Kinase Signalling:					
	Map2k1*, Mapk11*, Mapk14, Mapkapk3, Mapk3, Map2k2, Mapk1, Mapk12, Mapk13, Mapkapk2.	10	12%	6%	2%
Nfat Signalling:					
	Nfatc2, Nfatc3, Nfatc4, Nfat5, RGD1560225.	5	6%	4%	0%
Phospholipase A2 & C:					
	Pla2g2d*, Pla2g2e*, Pla2g1b*, Pla2g6*, Pla2g12a*, Pla2g2a, Pla2g4a, Pla2g3, Pla2g5, Pla2g2f, Pla2g10, Pla2g12b, Pla2g4b, Plcg1, Plcg2.	15	18%	13%	6%
Protein Kinase C:					
	Prkca*, Prkcb, Prkcg.	3	4%	2%	1%
Protein Phosphatases:					
	Ppp3cc, Ppp3r1, Ppp3cb, Ppp3ca, Ppp3r2.	5	6%	6%	0%
Transcription Factors:					
	Arnt*, Nfatc2, Nfatc4, Hif1a, Nfatc3, Nfat5, RGD1560225.	7	8%	6%	1%
Apoptosis & Cell Cycle:					
	Bad*, Casp9, Cdc42.	3	4%	2%	1%
Cell Motility, Migration & Morphology:					
	Ptk2*, Pxn.	2	2%	2%	1%
Others:					
	Grb2*, Sh2d2a*, Cav1*, Sphk2, Nos3, Ptgs2, Sphk1.	7	8%	7%	4%

The suggested 84 different genes for the pathway by Sabiosciences (2015). Significantly expressed genes (p≤0.05) are in boldface letters. Genes marked with an asterisk are significant (p(adj)≤0.05) with a false discovery rate-corrected p-value.

Table 4-15 shows the distribution of the maximum significant relative count, both with and without the false discovery rate correction, for the genes in the subgroups within all the pathway lines. The relative count demonstrates the greatest subgroup-coverage in two pathway lines: Small G-Protein Signalling and Akt & PI-3-Kinase Signalling. However, the focus is not on the highest percentage in the table *per se*, but how close these percentages are to their corresponding pathway line percentage given in Table 4-14 and if the percentage is maintained high throughout the subgroup-coverage in the pathway line. Concerning $N_{p(adj)}$%, the Small G-Protein Signalling pathway line

should be close to 4.8% (5% as per Table 4-14) and is here seen with a maximum of 4.8% (i.e. 100% of the 5%-reference) in one of the subgroups. The other subgroups show similar percentage. The Akt & PI-3-Kinase Signalling pathway line should be close to $N_{p(adj)}$%=6%, and is here seen with a maximum of 3.6% (i.e. 60% of the 6%) in two subgroups, and the other subgroups follow somewhat closely. Therefore, of these two pathway lines, the Small G-Protein Signalling pathway line has the greatest coverage.

Table 4-15. The Overall Profile Coverage of the VEGF Pathway Based on the Maximum Relative Count of Significantly Expressed Genes.

Line	Day −1	Day 1			Day 3			Day 7			Day 14		
	R{−1}	C{01}	H{01}	E{01}	C{03}	H{03}	E{03}	C{07}	H{07}	E{07}	C{14}	H{14}	E{14}
Growth Factors & Receptors.													
N_p%	1.2%	3.6%	3.6%	2.4%	4.8%	4.8%		4.8%	3.6%	1.2%	4.8%	2.4%	
$N_{p(adj)}$%		2.4%	1.2%						1.2%		2.4%	2.4%	
Akt & PI−3−Kinase Signaling.													
N_p%	4.8%	2.4%	6.0%	3.6%	2.4%	2.4%		6.0%	2.4%	1.2%	6.0%	1.2%	
$N_{p(adj)}$%	2.4%	2.4%	2.4%	3.6%		1.2%		3.6%	1.2%		1.2%	1.2%	
Small G−Protein Signalling.													
N_p%	2.4%	6.0%	4.8%	4.8%	2.4%	2.4%	1.2%	4.8%	3.6%		4.8%	4.8%	
$N_{p(adj)}$%	1.2%	3.6%	3.6%	1.2%				4.8%	3.6%		3.6%	3.6%	
Heat Shock Proteins.													
N_p%		1.2%	2.4%		1.2%	2.4%	1.2%	2.4%	2.4%		2.4%	2.4%	
$N_{p(adj)}$%		1.2%	1.2%					2.4%	1.2%		2.4%	1.2%	
MAP Kinase Signalling.													
N_p%	2.4%	2.4%	1.2%	2.4%	2.4%	2.4%	1.2%	2.4%	2.4%		2.4%	1.2%	
$N_{p(adj)}$%	1.2%	2.4%	1.2%	1.2%		1.2%		1.2%			1.2%		
Nfat Signalling.													
N_p%	1.2%	1.2%	1.2%	1.2%	1.2%	1.2%		1.2%				2.4%	
$N_{p(adj)}$%													
Phosholipase A2 & C.													
N_p% 1.2%	3.6%	6.0%	7.1%	6.0%	4.8%	3.6%	1.2%	6.0%	4.8%	2.4%	7.1%	4.8%	
$N_{p(adj)}$%	2.4%	2.4%	2.4%		1.2%	1.2%		1.2%	2.4%				
Protein Kinase C.													
N_p%	2.4%	2.4%	2.4%	1.2%	1.2%	1.2%	1.2%	2.4%	1.2%	1.2%	1.2%	2.4%	
$N_{p(adj)}$%	1.2%	1.2%	1.2%					1.2%					
Protein Phosphatases.													
N_p%	1.2%	2.4%	1.2%	1.2%	1.2%			1.2%	1.2%				
$N_{p(adj)}$%													
Transcription Factors.													
N_p%	3.6%	1.2%	3.6%	1.2%	1.2%	1.2%	1.2%	2.4%	1.2%	1.2%	1.2%	2.4%	
$N_{p(adj)}$%			1.2%										
Apoptosis & Cell Cycle.													
N_p%	2.4%	2.4%	1.2%	1.2%	1.2%		1.2%	1.2%		1.2%	1.2%	1.2%	
$N_{p(adj)}$%		1.2%											
Cell Motility, Migration, & Morphology.													
N_p%	1.2%	1.2%	1.2%		1.2%						1.2%		
$N_{p(adj)}$%		1.2%	1.2%								1.2%		
Others.													
N_p%	2.4%	3.6%	2.4%	1.2%	2.4%	2.4%	1.2%	2.4%	2.4%	1.2%	2.4%	2.4%	
$N_{p(adj)}$%	1.2%	2.4%						1.2%	1.2%		1.2%	1.2%	

N_p%, relative count of significantly expressed genes ($p \leq 0.05$) with ordinary t-test.
$N_{p(adj)}$%, relative count of significantly expressed genes ($p(adj) \leq 0.05$) with an adjusted p-value for false rate discovery.

The VEGF Small G-Protein Signalling Profile

Table 4-16 demonstrates the profile of significant differential expression that corresponds to the VEGF Small G-Protein Signalling pathway line. For a given gene the average expression, for each objective vs reference group, is displayed in fold changes on a log_2-scale (log_2(FC). The positive fold changes represent upregulated differential expressions and are written in a white font on a dark background, to distinguish them from the negative fold changes that represent downregulated differential expressions. The fold changes marked with an asterisk and written with boldface letters are significant after the false discovery rate correction, whilst the others are only significant with the t-test.

Table 4-16. The VEGF Small G-Protein Signalling Gene Profile of Significant Differential Fold Changes (log_2(FC)).

Timing	Reference	Objective	Gene (Symbol)						
			Nras	Raf1	Rac1	Rac2	Shc2	Src	Hras
Day −1	A{−1}	R{−1}							
Day 1	A{−1}	C{01}	*0.40*	**−0.52***					
	R{−1}			**−0.6***					
	A{−1}	H{01}	**0.53***	*−0.39*	**0.43***	**1.14***	*0.33*		
	R{−1}		*0.36*	**−0.47***	*0.37*	*0.92*	*0.29*		
	A{−1}	E{01}	**0.53***	**−0.51***	*0.28*	**1.16***			
	R{−1}		*0.37*	**−0.6***		*0.94*			
Day 3	A{−1}	C{03}	*0.44*		*0.29*		*0.41*	*0.37*	
	R{−1}						*0.38*	*0.27*	
	C{01}			**0.45***			*0.33*		
	A{−1}	H{03}					*0.38*		*−0.51*
	R{−1}						*0.35*		*−0.38*
	H{01}			*0.32*					
	E{01}	E{03}		*0.34*		*−0.82*			
Day 7	A{−1}	C{07}						*0.24*	
	H{01}	H{07}	**−0.64***	**0.42***	**−0.40***	**−1.08***			
	H{03}		*−0.38*						
	E{01}	E{07}	**−0.67***	**0.44***		**−1.27***			
	E{03}		*−0.46*						
Day 14	A{−1}	H{14}					*0.30*		
	R{−1}						*0.26*		
	C{14}						*0.29*		
	H{01}		**−0.53***	**0.46***	*−0.31*	**−1.22***			
	R{−1}		*−0.36*						
	E{01}	E{14}	**−0.74***	**0.39***	*−0.31*	**−1.28***			
	E{03}		*−0.52*						

Fold change values marked with an asterisk and in boldface letters are significant ($p \leq 0.05$) with an adjusted p-value (false discovery rate corrected). Positive fold change values are in white letters on dark background. Genes within this pathway line with no significant differential expression are: Kras.

None of the genes in the pathway line demonstrates significant differential expressions between the R{−1} and the A{−1} subgroups on Day −1, and, therefore, jointly situate the reference level. *Nras* shows an upregulation in all of the three groups on Day 1, with expression values that simultaneously suggest that the gene is non-significantly upregulated in R{−1} in comparison with

A{−1}. With, apparently, more emphasised upregulation in the [H] and [E]-groups, the expression is gradually returned to reference level on Day 7. *Raf1* seems to be expressed fairly evenly between all the three groups on Day 1 with a downregulation. The expression is then returned to reference levels from Day 3 onwards, perhaps more quickly in the [C]-group. *Rac1* is overall more expressed in the [H]-group, with an upregulation on Day 1 which has gradually returned on Day 7. *Rac2*, is overall expressed in the [H] and [E]-groups, with a similar profile as *Rac1*, upregulated on Day 1, which has returned on Day 7 back to the reference level. *Shc2* demonstrated no differential expression for the [E]-group but is upregulated for the [H]-group from Day 1 to Day 14. The [C]-group seems to shadow the pattern for the [H]-group, with only significant upregulation on Day 3. Although with fairly sparse significant data, *Src*, seem to be gradually upregulated until Day 3 which thereafter gradually return, only in the [C]-group. *Hras* is only expressed with a significant downregulation in H{03}, but without any significance in any of the rest of the comparisons. *Kras* does not show any significant differential expression.

The VEGF — The Growth Factors & Receptors Profile; and the Akt & PI-3-Kinase Signalling Profile

The tables of differential expression of the following two profiles can be found in Appendix D.4.3: The Growth Factors & Receptors Profile (Table ApxD - 26); and the Akt & PI-3-Kinase Signalling Profile (Table ApxD - 27). Between these profiles, the most significantly expressed genes are *Vegfc* and *Kdr*. Neither is expressed differentially between the R{−1} and A{−1}. *Vegfc* is only responsive in the [H] and [E]-groups, showing a downregulation on Day 1, to a slightly more extent in the [E]-group (although not significantly). Both groups demonstrate less downregulation on Day 3, which then takes a dip on Day 7, but rises again on Day 14, with the expression at reference level in the [H]-group. *Kdr* is downregulated in all three groups on Day 1, with a more notable expression in the [H]-group. The groups are similarly downregulated still on Day 3, but thereafter gradually return to the reference level (again, more pronounced in the expression in the [H]-group).

The VEGF — The Heat Shock Proteins Profile; the MAP Kinase Signalling Profile; and, the Nfat Signalling Profile

The tables of differential expression of the following three profiles can be found in Appendix D.4.3: The Heat Shock Proteins Profile (Table ApxD - 28); the MAP Kinase Signalling Profile (Table ApxD - 29); and, the Nfat Signalling Profile (Table ApxD - 30). Between these profiles, the most significantly expressed genes are *Hspb1* and *Mapk2k1*. Neither is expressed differentially between the R{−1} and A{−1}. *Hspb1* is only significantly responsive in the [H] and [E]-groups, showing upregulation on Day 1. The [H]-group gradually returns from Day 3 until Day 14. The [E]-group is maintained upregulated on Day 3, but takes a sudden dip to reference level on Day 7 and then becomes downregulated on Day 14. *Map2k1* is mostly responsive in the [H]-group, with an upregulation on

Day 1 which gradually returned to its reference level on Day 7 and stays that way until Day 14. The [E]-group indicates that it is shadowing the profile of the [H]-group, but to a much lower extent.

The VEGF — The Phospholipase A2 & C Profile; the Protein Kinase C Profile; and the Protein Phosphatases Profile

The tables of differential expression of the following three profiles can be found in Appendix D.4.3: The Phospholipase A2 & C Profile (Table ApxD - 31); the Protein Kinase C Profile (Table ApxD - 32); and the Protein Phosphatases Profile (Table ApxD - 33). Between these profiles, the most significantly expressed gene is *Pla2g2d*, which is upregulated in R{−1} in comparison with A{−1}, on Day −1, and even more so in all the groups on Day 1. Whilst the [C] and [H]-groups maintain the upregulation until Day 14, with a non-significant decrease, after Day 3, the [E]-group takes a dip until Day 14, towards its reference level.

The VEGF — The Transcription Factors Profile; the Apoptosis & Cell Cycle Profile; the Cell Motility, Migration & Morphology Profile; and the Profile of Other Related Genes

The tables of differential expression of the following four profiles can be found in Appendix D.4.3: The Transcription Factors Profile (Table ApxD - 34); the Apoptosis & Cell Cycle Profile (Table ApxD - 35); the Cell Motility, Migration & Morphology Profile (Table ApxD - 36); and the Profile of Other Related Genes (Table ApxD - 37). Between these profiles, the most significantly expressed gene is *Ptk2* and is not expressed differentially between the R{−1} and A{−1}. *Ptk2* is mostly responsive in the [H]-group where it is downregulated on Day 1 and gradually returns to its reference level on Day 14. However, the [E]-group is also downregulated on Day 1 but indicates a more planar return to reference level thereafter.

4.4.5 The Wound Healing Pathway

Table 4-17 shows the pathway lines within the Wound Healing pathway, listed with all the genes that compose them along with an absolute gene count (N_{gene}) and a relative count (N_{gene}%) referencing the 84 different genes in the pathway. Note that some genes may be repeated between the different lines, which does not affect the overall count. The genes (or the gene symbols) in boldface letters are significantly expressed ($p \leq 0.05$), with an ordinary t-test, in at least one of the subgroup comparisons, and are accompanied with their relative gene count (N_p%) referenced to the 84 different genes of the pathway. Genes in boldface letters marked with an asterisk are, furthermore, significantly expressed after the false discovery rate corrections ($p(adj) \leq 0.05$), and are accompanied with the relative gene count ($N_{p(adj)}$%) referenced to the 84 genes in the pathway. The genes in lightface letters do not demonstrate any significant differential expressions.

Table 4-17. The Genes of the Wound Healing Pathway.

Line	Genes (Symbols)	N_{gene}	N_{gene}%	N_p%	$N_{p(adj)}$%
Extracellular Matrix & Cell Adhesion, ECM Components:					
	Col14a1*, Col4a1*, Col1a2, Col5a2, Col5a1, Col3a1, Col1a1, Col5a3, Col4a3,	10	12%	12%	2%
Extracellular Matrix & Cell Adhesion, Remodelling Enzymes:					
	Plaur*, Ctsl1*, F13a1*, Plau*, Mmp7*, Fga, Ctsk, Mmp2, Ctsg, F3, Plg, Mmp1, Mmp9, Plat, Serpine1, Timp1.	16	19%	13%	6%
Extracellular Matrix & Cell Adhesion, Cellular Adhesion:					
	Itga1*, Itgb1*, Itga6*, Cdh1, Itga5, Itgb5, Itga4, Itgb3, Itga2, Itga3, Itgav,	12	14%	10%	4%
Extracellular Matrix & Cell Adhesion, Cytoskeleton:					
	Rac1*, Actc1, Tagln, Acta2, Rhoa.	5	6%	4%	1%
Inflammatory Cytokines & Chemokines:					
	Ccl7*, Ccl12*, Il6*, Il1b*, Cxcl3*, Il10, Cxcl1, Ifng, Il4, Cd40lg, Cxcl11, Cxcl5,	13	15%	11%	6%
Growth Factors:					
	Pdgfa*, Csf3*, Hbegf*, Mif*, Fgf7, Hgf, Angpt1, Fgf2, Fgf10, Ctgf, Igf1, Csf2, Egf, Tgfa, Tgfb1, Tnf, Vegfa.	17	20%	13%	5%
Signal Transduction, TGF:					
	Tgfb1*, Stat3*, Tgfbr3.	3	4%	2%	2%
Signal Transduction, WNT:					
	Wnt5a*, Wisp1, Ctnnb1.	3	4%	2%	1%
Signal Transduction, Phosphorylation:					
	Pten, Mapk3, Mapk1.	3	4%	2%	0%
Signal Transduction, Receptors:					
	Il6st, Egfr.	2	2%	1%	0%
Signal Transduction, Other:					
	Ptgs2.	1	1%	0%	0%

The suggested 84 different genes for the pathway by Sabiosciences (2015). Significantly expressed genes ($p \leq 0.05$) are in boldface letters. Genes marked with an asterisk are significant ($p(adj) \leq 0.05$) with a false discovery rate-corrected p-value.

Table 4-17 shows the distribution of the maximum significant relative count, both with and without the false discovery rate correction, for the genes in the subgroups within all the pathway lines. The relative count demonstrates the greatest subgroup-coverage in two pathway lines: Remodelling Enzymes and Inflammatory Cytokines & Chemokines. However, the focus is not on the highest percentage in the table *per se*, but how close these percentages are to their corresponding pathway line percentage given in Table 4-18, and if the percentage is maintained high throughout the subgroup-coverage in the pathway line. Concerning the $N_{p(adj)}$%, the Remodelling Enzymes pathway line should be as close to 6% (as per Table 4-18) and is here seen with a maximum of 4.8% (i.e. 80% of the 6%) in three of the subgroups. The other subgroups show somewhat similar percentage. The Inflammatory Cytokines & Chemokines pathway line should also be close to $N_{p(adj)}$%=6%, and is also seen with a maximum of 4.8% in three of the subgroups. However, the percentage of the subgroups are less close to the reference $N_{p(adj)}$%. Therefore, of these two pathway lines, the Remodelling Enzymes pathway line has the greatest coverage.

Table 4-18. The Overall Profile Coverage of the Wound Healing Pathway Based on the Maximum Relative Count of Significantly Expressed Genes.

Line	Day −1	Day 1			Day 3			Day 7			Day 14		
	R{−1}	C{01}	H{01}	E{01}	C{03}	H{03}	E{03}	C{07}	H{07}	E{07}	C{14}	H{14}	E{14}
Extracellular Matrix & Cell Adhesion: ECM Components.													
N_p%	1.2%	1.2%	1.2%		7.1%	7.1%	6.0%	3.6%	1.2%	4.8%	3.6%	4.8%	8.3%
$N_{p(adj)}$%						1.2%				1.2%		1.2%	1.2%
Extracellular Matrix & Cell Adhesion: Remodelling Enzymes.													
N_p%	2.4%	2.4%	4.8%	6.0%	1.2%	4.8%	3.6%	2.4%	4.8%	6.0%	2.4%	4.8%	6.0%
$N_{p(adj)}$%		1.2%	4.8%	3.6%		1.2%		1.2%	3.6%	2.4%		4.8%	4.8%
Extracellular Matrix & Cell Adhesion: Cellular Adhesion.													
N_p%	1.2%	3.6%	6.0%	6.0%	3.6%	7.1%	6.0%	2.4%	2.4%	2.4%	1.2%	3.6%	2.4%
$N_{p(adj)}$%		1.2%	3.6%	1.2%								1.2%	
Extracellular Matrix & Cell Adhesion: Cytoskeleton.													
N_p%	2.4%	1.2%	2.4%	1.2%	3.6%	2.4%	1.2%		1.2%	1.2%	1.2%	2.4%	1.2%
$N_{p(adj)}$%			1.2%						1.2%				
Inflammatory Cytokines & Chemokines.													
N_p%			2.4%	7.1%		1.2%	6.0%	1.2%	4.8%	8.3%		2.4%	8.3%
$N_{p(adj)}$%			1.2%	4.8%		1.2%	2.4%		2.4%	4.8%		2.4%	4.8%
Growth Factors.													
N_p%		6.0%	4.8%	3.6%	2.4%	1.2%	2.4%	2.4%	3.6%	3.6%	2.4%	2.4%	7.1%
$N_{p(adj)}$%		1.2%		2.4%			1.2%			1.2%		1.2%	2.4%
Signal Transduction: TGF.													
N_p%		1.2%	2.4%	2.4%	1.2%	1.2%	1.2%		2.4%	1.2%		2.4%	2.4%
$N_{p(adj)}$%		1.2%	1.2%	1.2%					1.2%			1.2%	1.2%
Signal Transduction: WNT.													
N_p%			1.2%	1.2%	1.2%	1.2%	1.2%		1.2%		1.2%	1.2%	
$N_{p(adj)}$%			1.2%										
Signal Transduction: Phosphorylation.													
N_p%					1.2%				1.2%		1.2%		1.2%
$N_{p(adj)}$%													
Signal Transduction: Receptors.													
N_p%									1.2%				
$N_{p(adj)}$%													

N_p%, relative count of significantly expressed genes ($p \leq 0.05$) with ordinary t-test.
$N_{p(adj)}$%, relative count of significantly expressed genes ($p(adj) \leq 0.05$) with an adjusted p-value for false rate discovery.

The Wound Healing ECM & Cell Adhesion – Remodelling Enzymes Profile

Table 4-19 demonstrates the profile of significant differential expression that corresponds to the Wound Healing ECM & Cell Adhesion – Remodelling Enzymes pathway line. For a given gene the average expression, for each objective vs reference group, is displayed in fold changes on a $\log_2$-scale ($\log_2$(FC). The positive fold changes represent upregulated differential expressions and are written in a white font on a dark background, to distinguish them from the negative fold changes that represent downregulated differential expressions. The fold changes marked with an asterisk and written with boldface letters are significant after the false discovery rate correction, whilst the others are only significant with the t-test.

Table 4-19. The Wound Healing ECM & Cell Adhesion – Remodelling Enzymes Gene Profile of Significant Differential Fold Changes (log_2(FC)).

Timing	Reference	Objective	Gene (Symbol)										
			Plaur	Ctsl1	F13a1	Plau	Mmp7	Fga	Ctsk	Mmp2	Ctsg	F3	Plg
Day −1	A{−1}	R{−1}			*1.08*		*0.92*						
Day 1	A{−1}	C{01}			**1.49***	*0.69*							
	R{−1}						**−0.84***						
	A{−1}	H{01}	**0.96***	**0.90***	**1.81***	**1.05***							
	R{−1}		**0.90***	*0.60*		*0.73*	**−0.76***						
	C{01}		*0.51*	*0.54*									
	A{−1}	E{01}	**1.38***	*0.75*	**1.54***	**1.29***		*0.45*					
	R{−1}		**1.33***			**0.97***	**−0.79***	*0.48*					
	C{01}		**0.93***			*0.60*		*0.54*					
	H{01}							*0.55*					
Day 3	A{−1}	C{03}			*1.07*								
	R{−1}						*−1.05*						
	A{−1}	H{03}			*1.50*	*0.56*			*0.76*	*0.87*			
	R{−1}						**−1.06***						
	H{01}		*−0.70*	*−0.50*					*0.67*				
	A{−1}	E{03}	*0.71*		*1.44*	*0.56*							
	R{−1}		*0.66*				*−0.57*						
	C{03}						*0.48*						
	H{03}						*0.48*						
	E{01}		*−0.66*			*−0.72*		*−0.39*					
Day 7	A{−1}	C{07}							*0.80*	*0.83*			
	R{−1}						**−1.07***						
	C{03}												
	R{−1}	H{07}					*−0.84*						
	H{01}		**−1.12***	**−0.98***	**−1.42***	*−0.66*							
	H{03}				*−1.11*								
	A{−1}	E{07}				*0.57*							
	R{−1}						*−0.78*						
	C{07}												
	E{01}		**−1.14***	**−0.88***	*−1.12*	*−0.71*		*−0.41*					
	E{03}				*−1.02*								
Day 14	A{−1}	C{14}					*0.58*						
	R{−1}											*−0.74*	
	C{07}						*0.73*		*−0.83*				
	R{−1}	H{14}					*−0.48*						
	C{14}										*−0.25*		
	H{01}		**−0.88***	**−0.96***	**−1.20***	**−0.81***							
	H{03}				*−0.89*		*0.57*						
	A{−1}	E{14}						*0.51*					
	R{−1}			*−0.58*			*−0.59*	*0.54*					
	C{14}							*0.54*					
	H{14}							*0.55*					*−0.63*
	E{01}		**−1.27***	**−1.04***	**−1.30***	**−0.94***							
	E{03}		*−0.60*	*−0.58*	*−1.21*			*0.45*	*−0.64*				
	E{07}							*0.47*					

Fold change values marked with an asterisk and in boldface letters are significant ($p \leq 0.05$) with an adjusted p-value (false discovery rate corrected). Positive fold change values are in white letters on dark background. Genes within this pathway line with no significant differential expression are: Mmp1, Mmp9, Plat, Serpine1, Timp1.

In general, none of the genes in the pathway line (except for F13a1 and Mmp7) demonstrate significant differential expressions between the R{−1} and the A{−1} subgroups on Day −1, and, therefore, jointly situate the reference level. *Plaur* is only reactive in the [H] and [E]-groups, with a prolonged upregulation between Day 1 and Day 3 in the [E]-group which has returned on Day 7. The [H]-group, however, does only show the upregulation on Day 1 before being returned on Day 3. *Ctsl1* shows a similar response as *Plaur*, with an upregulation on Day 1 in the [H] and [E]-groups which gradually returns to the reference levels thereafter. Plau, is again, similar to Plaur, with

an upregulation on Day 1 on all three groups, that is slowly returning to the reference level on Day 14 in the [E]-group, and perhaps a little bit sooner for the [H]-group. Both *F13a1* and *Mmp7* are upregulated in R{−1} in comparison with A{−1}, which slightly alters the perspective as to whether the significant expression is up or downregulated. The *F13a1* does show an upregulated expression peak on Day 1 in all the groups, with the most emphasis on the [H]-group. On Day 3 the expression has overall slightly reduced, and from Day 7 and onwards, back to the reference level of A{−1}; with a slightly steeper change in the [H]-group in comparison with the [E]-group, and possibly with the most planar change in the [C]-group. In *Mmp7* the upregulation on Day −1 seems to have returned close to the reference level of A{−1} on Day 1 in all the groups. This return seems to be maintained throughout until Day 14, where there is a hint for a slight upregulation again, in both the [C] and [H]-groups. Meanwhile, the return in the [E]-group is more planar throughout and on Day 14 as well. *Fga* only demonstrates differential expression for the [E]-group, with an upregulation on Day 1, which is partially reduced on Day 3 and Day 7 but continued to be maintained upregulated on Day 14. *Ctsk*, *Mmp2*, *Ctsg*, *F3* and *Plg* show too sparse differential expression between the groups for any trend description, although *Ctsk* and *Mmp2* seem to be more reactive in the [H] on Day 3. *Mmp1*, *Mmp9*, *Plat*, *Serpine1* and *Timp1* do not show any significant differential expression.

The Wound Healing ECM & Cell Adhesion — The ECM Components Profile; the Cellular Adhesion Profile; and the Cytoskeleton Profile

The tables of differential expression of the following three profiles can be found in Appendix D.4.4: The ECM Components Profile (Table ApxD - 39); the Cellular Adhesion Profile (Table ApxD - 40); and the Cytoskeleton Profile (Table ApxD - 41). Between these profiles, the most significantly expressed genes, apart from *Rac1* described in the VEGF Pathway, are *Col4a1* and *Itga1*. Neither is expressed differentially between the R{−1} and A{−1}. *Col4a1* is most responsive on Day 7 and Day 14, with downregulation in the [H] and [E]-groups, although, to a slightly less extent in the [H]-group. *Itga1*, however, is mostly responsive in the [H]-group with a downregulation on Day 1 which is return fairly immediately, or on Day 3.

The Wound Healing — The Inflammatory Cytokines & Chemokines Profile; and the Growth Factors Profile

The tables of differential expression of the following two profiles can be found in Appendix D.4.4: The Inflammatory Cytokines & Chemokines Profile (Table ApxD - 42); and the Growth Factors Profile (Table ApxD - 43). Between these profiles, the most significantly expressed genes, apart from *Il6* described in the Skeletal Muscle Pathway, are *Ccl7*, *Ccl12*, *Il1b* and *Pdgfa*. None is expressed differentially between the R{−1} and A{−1}. *Ccl7* is quite strongly affected on Day 1 in both the [H] and [E] groups (slightly more so in the [E]-group), demonstrated with an upregulation, which is though returned on Day 3. *Ccl12*, shows a similar pattern, although, overall slightly expressed and

also to a lesser degree in the [H]-group. *Il1b* is only responsive in the [E]-group, with an upregulation on Day 1 which gradually returns to its reference level on Day 14. *Pdgfa* is very similar to *Il1b* regarding the effect within the [E]-group, with the addition of being slightly downregulated on Day 1 in the control group that is thereafter returned.

The Wound Healing Signal Transduction — The TGF Profile; the WNT Profile; the Phosphorylation Profile; and the Receptor Profile

The tables of differential expression of the following five profiles can be found in Appendix D.4.4: The TGF Profile (Table ApxD - 44); the WNT Profile (Table ApxD - 45); the Phosphorylation Profile (Table ApxD - 46); and the Receptor Profile (Table ApxD - 47). Between these profiles, the most significantly expressed gene, apart from *Tgfb1* described in the Skeletal Muscle Pathway, is *Stat3*. *Stat3* does not show any significant differential expression between R{−1} and A{−1}, but is significantly upregulated in the [E]-group on Day 1, but is gradually returned to its reference level until Day 14. The [H]-group shadows the same profile, but not to the same extent.

5 Discussion

5.1 Overture

With a quick glimpse of the results, two important things that are difficult to justify as being successfully concluded as set out in our experimental objectives. (**i**) Inducing muscle damage in the trained rats, as the experimental critical point, was not as impactful as we hoped. Therefore, any trend analysis throughout the recovery period is mostly based on non-significantly different results. (**ii**) Any measurement, reflecting the low level of muscle damage, is not reinforced by the fact that the evolution throughout the recovery period is not based on continuous measurements of the same subjects. Therefore, the variability within and between subgroups potentially does not follow a specific trend by its own.

However, in favour of the results, the subgroups are not represented by extreme variability and therefore, both the experimental execution as a whole and its impact on the subjects, in general, is reflective of being uniform. The timespan of the complete experimental execution itself and any potential changes related to that, could have easily played a bigger role in the uncertainty of the results.

5.2 AEY

It goes without saying that it is easy to design a scoring system that is only based on good runners, with results reflecting just that, that they are indeed good runners! The main objective of the development of the AEY scoring system, however, was to provide a way to assess different levels of performances of the rats when running on the treadmill. The fact that in the majority of published work, problems with training the rats are not mentioned, is somewhat understandable as the majority of rats trained run relatively well, or at the very least, can be trained to do so over time. Still, the relativeness of being a 'good runner' can be categorised.

From our experience, we could see that some rats seem to have no issues with running; as if they could do with increased speed for the running to become troublesome. Other rats, appeared to put such focus on not receiving an electric shock from the metal grid that the contrary occurred; they ended up touching the metal grid continuously and, overall, took them a relatively long time to become continuous runners. The question is, therefore, at the end of a training period where both of these types of rats would be running continuously, 'are these rats equal in physiological terms?' Hence, the next fundamental question is whether the score itself can quantitatively differentiate between these types of rats in a way that correlates to the qualitative difference observed when they are monitored during their training.

5.2.1 Are the Averages Useful?

Whilst the elements within the A-criteria have been quantified by their impact on the theoretical best style of running (mark-A), the fairly simple underlying mathematical design is not constructed in a way that, e.g. an average score from a training session, could be directly back traced to the most dominant style/mark registered. For that sort of evaluation, one would need to look at the actual registry and use different statistical tools. Thus, all the accumulative average calculations render the back tracing-style estimation improbable. Furthermore, between certain A-styles, it is difficult to establish which of them a rat is putting more effort into running as opposed to putting effort into doing anything else. Therefore, the applied score value (α) was intentionally made to be the same in some cases. In this way, one needs to look at the marks in the registry sheet for the A-score, the α score value, and the calculated scores, as three somewhat-independent parameters. The E-criteria focuses exclusively on the positioning of the tail as a sign of tiredness. Therefore, the marks of the E-criteria are more descriptive and correlate better with the actual score value (ε) they give, in contrast with the α. The assessment for the Y-criteria is different altogether. It serves more as a quality control index for the data output from the treadmill monitoring apparatus. Although the digital data output for the electric shocks is not shown here, in the work of Tekin, Dursun and Ficicilar (2008),the authors have mentioned how the shock count seems to 'more or less' represent a good or a bad runner. However, the unknown portion of this 'more-or-less-notion' is probably reflected in the Y-score.

We repeatedly noted that the rats caught up differently with the running for the first few training sessions, as expected. We can see this progression reflected in the greatest deviation in the A-score on Week 1 and decreasing until Week 4. Simultaneously, the E-score demonstrates increasing deviation from Week 1 to Week 4. This might seem contradictory. Still, let us bear in mind that concerning the treadmill speed, the session count and duration, the hypothetical power output increases over the weeks, and moreover, could also be considered as accumulating. We like to think that although the rats respond very differently to the running at the beginning, the sessions, per se, are more difficult in Week 4.

The exercise sessions at Day 0 are very different from the four weeks prior, being downhill running-to-exhaustion protocol. During this protocol, more A-style variety takes place (registry data not shown) reflected in a lower average A-score and with greater underlying variation, just as in the E-score. On the contrary, in the weeks that follow (Week 5 - Week 6), the exercise protocol is designed to be easier where both A- and E-score improving; the A-score with greater deviation. The overall lower Y-score does not necessarily have anything to do with the overall changed protocol structure,

apart from the fact that it is likely that as the duration of each session at Day 0 was considerably longer, the frequency of artefacts could have been greater.

5.2.2 Are the Averages Useful?

It is likely that motor control memory plays a role in the success of a good A-score. Thus, frequent similar session might improve it, whilst less frequent or different sessions do not. Perhaps the training time related to circadian and internal biorhythms also plays a considerable part (Boersma *et al.*, 2012). Comparing the morning and afternoon sessions throughout the weeks, there is not a very noticeable difference in the A-score. Possibly, it has somewhat improved on an individual level in the afternoon, which was the general feeling through the training from the experimenters' point of view. On the contrary, as the resting period before the afternoon session is short, the E-score (representing tiredness) decreases in the afternoon sessions. However, one should not numerically compare the scale of the separate changes that occur between these two scores (A and E scores).

Furthermore, as the hair on the rat's tail is considered 'preventing' it from receiving an electric shock, we cannot exclude that some rats realised that whilst others reacted with a squeak even before actually touching the grid. In the former case, the E-score is not reliable. However, the general observation, before the systematic qualitative assessment took place, was that the tail was held up in the beginning, and was lagging at the end of sessions or when a rat seemed to be very tired after that session. As a semi-disclaimer with the Y-score interpretation; It is true that, when stressed, rats deposit more faeces and urine which could lead to a lower Y-score (via apparatus artefacts). One could then logically assume that after a long period of training, the stress factor is markedly less prominent and represented in a potentially higher Y-score in comparison with the commencing score. However, in our experience, this is not a reliable correlation.

As many physiological parameters, the variables represented in AEY score are likely not to be identical in a repeated measurement for the same individual. However, we do believe that the number of rats that have been observed plays in favour of the score's reliability. One could argue that even so, the scores, presented in this dissertation, are generally fairly high, thus, what type of distinction between the rats can we truly make? We cannot dispute the fact that the mark values could have been distributed differently between the defined styles, resulting in a different representative average score. However, we do underpin the fact that here we are representing the average scores. Presumably, a lot can happen over six weeks and perhaps a weekly-average representation is not necessarily the best choice. Still, with these weekly averages, we are able to observe tendencies in the results. In the experimental setup followed for this evaluation, we

consider that deviation in the scores represented on a weekly basis are indicating enough to lead us to the potential outlier rats for a more profound analysis.

The negative aspect of the proposed score is that the qualitative assessment is far from being automatic, although it gets easier with practice. There are many calculations involved, albeit simple, and setting them up in software like MS Excel or Matlab is one way to work automatically through them. The main benefits, besides the pinpointing of potential outliers, are that the method provides a systematic way to compare rats and different studies. Still, the assessment leading up to an individual AEY-score will always be subject to some bias. Similar to Borg's scale for rating perceived exertion, the next step in developing the AEY score would be to correlate it with VO_2 measurements (Borg, 2001; Borg and Kaijser, 2006) and perhaps that would either fortify our style-score correlation or shed some new light on the running performance score measurements. Perhaps it is difficult and unrealistic to get a $\%VO_2(max)$ correlation with specific running styles, but maybe it could correlate to either or both of our 0-1 scale in the A- and the E-score.

5.3 Plasma

5.3.1 Muscle Damage Protocol

At this stage it was difficult to use the concentration values specifically to determine how effective the 1 session per day (1 Sess/d) protocol was, especially as no reference samples from prior to the critical point were available. However, the relative-relationship between the other samples gave a sufficient clue to estimate the effectiveness of the protocol. Although, both TnI and Mb ELISAs gave some indication of descending concentration from Day 1 and onwards, the standard deviation is too great for each day. Therefore, despite the absence of a reference sample, the solution was simple — The objective of the muscle damage protocol needed to be much more pronounced, giving a potentially descending concentration profile a clearer image as different concentration profiles would also need to distinguish different experimental group later on. However, there is a roof to making these changes. It is difficult to go beyond the point of exhaustion (if rats demonstrated no visible signs of muscle damage) in the 1 Sess/d-protocol is difficult. The velocity during the protocol could not be increased too much, as it would not be favourable to potentially exhaust the rats before inducing the muscle damage. Furthermore, any alteration needed to result in a humane treatment. The resulting procedure to induce muscle damage was therefore running the same protocol twice during the day with a minimum of 4 h between the end of the former session and the beginning of the latter session. In this way the good runners that would not have any muscle damage in the former session and endure longer in it, would have 4-h rest and

hopefully have the muscle damage induced in the latter. Meanwhile the worse runners that would have induced muscle damage form the former session (and removed quickly from the treadmill) would have a little more rest between sessions and not likely to endure for long in the latter session and then quickly ending that one as well. This clearly meant that it was not likely that the level of the muscle damage would be equal for all the rats; still, the aim was to at least try to ensure muscle damage and hopefully with a generally pronounced effects. Still, with practically no more anymore ethical room to change the procedure anymore, the muscle damage protocol was now considered established.

5.3.2 Plasma marker ELISAs

As mentioned, each ELISA (Mb and TnI) had been run twice with similar results for the calibration curves. The TnI-calibration curve is simple not acceptable with that high RSD values. There could be potentially many factors that contribute to the outcome; imprecise pipetting between well-replicas, imprecise pipetting during the dilution of the calibration standard; inconsistent reagents used in the assay; instrumental error in the absorbance reading; the well plate coating was inconsistent; the nature/size of the marker; etc. However, the factors that can be controlled in the laboratory have more to do with the pipetting or instrumental maintenance. Still, it would be logical for any of these inconsistencies to be reflected in the myoglobin ELISA as well, and not in the troponin-I ELISA, two times.

Therefore, as this was also at the point of altering the muscle damage protocol to the point of not being able to force any more changes there, it was decided to not take any more chances with the troponin-I ELISA and replace it with creatine kinase (CK-MM) biomarker ELISA, accompanying the myoglobin ELISA; Crossing the fingers the calibration curves would be reliable from this point on.

The TnI-calibration curve, clearly, reduces the validity given to the TnI quantification to estimate the muscle damage protocol. However, greater deviation in those samples only under backup the decision made about the protocol.

Moreover, the analysis of the calibration curve, led to other procedural changes. To avoid any potential inaccuracy due to low quality pipetting practice, a pipetting precision test was set up to train every agent working with the ELISAS, and a secondary procedure to analyse every calibration curve and re-run samples that did not fit into the most reliable parts of the curve, if possible.

5.3.3 The Negative Controls

The relative expectancy between the two controls, the absolute negative A{−1} and the relative negative R{−1}, would be somewhat as the following, both for myoglobin myoglobin and creatine kinase — Given that the sedentary rats A{−1} were not exposed to any type of controlled exercise, the concentration of the plasma markers should be really low. Meanwhile, the trained rats R{−1} did go through regular training for 4 weeks, still the objective of that training was not to cause induced muscle damage, therefore ideally the plasma marker concentration would be similar to the control group, or, given that the training could have caused some damage (although hopefully none) it would be logical that the plasma markers concentration would be somewhat higher than for A{−1}. Simultaneously, the notion that CK plasma markers have been detected after exercise in other studies (Kanda *et al.*, 2013, 2014), it would not be surprising that R{−1} would have higher plasma marker concentration than A{−1}. Furthermore, as the rats are still growing at this stage, the cellular turnover might be the reason for any basal concentration in A{−1}. The CK in plasma has been suspected to be due to this turnover process if the concentration is not related to exercise or injury (Sayers and Clarkson, 2003).

Although the results demonstrate no significant difference between A{−1} and R{−1}, we can say that the regular cellular turnover or other related basal processes are likely to contribute to the plasma marker concentration (given that the concentrations are not 0). Furthermore the training (prior to the planned induction of the muscle damage) is not causing any muscle damage (at least not detectable via the plasma markers). However, it is difficult to ignore the visible difference between the A{−1} and R{−1} in the box plots (reminding that the box plot the entire data range in the group with the whiskers). The CK-MM concentration, especially, does not suggest equal subgroups (another reminder: the N is equal in all subgroups). A part from the average concentration being much lower (A{−1}=400(±200) ng/mL, R{−1}=170(±80) ng/mL), the rats in A{−1} seem much more heterogeneous than the rats in R{−1} if taking note of the variability. This goes against our speculations, as we would, furthermore, logically assume that the R{−1} should have greater variability in the concentration in comparison with A{−1} as all rats might not potentially respond to the exercise in a similar way. So what can this be? Is it possible that the implication of 'unnatural and regular' exercise is somewhat restricting the natural variability? Let us remind ourselves that there is no significant difference between the two subgroups though; still, before pondering about this anymore, let us check the rest of the data.

5.3.4 Muscle damage and Recovery

It is clear, by looking on Day 1 for all group, the latest version of the muscle damage protocol is better than the one used in the developmental phase, even if the data set is small there. However, without analysing the subsequent days to the finest detail, the majority of the subgroups have concentration values back at the level of the negative controls; which in theory would mean 'everything back to normal'. Still, how effective is the induction of muscle damage, in the end? Should the protocol have been more harsh?

We consider that we were at the ethical limits in terms of protocol design for inducing muscle damage. Perhaps, the velocity settings could have been a little higher or the declination even steeper. However, the duration which depended on each rat (until either exhaustion or visible signs of muscle damage), and the rats could not have been forced more than that without discarding their welfare. What about the training prior to the muscle damage?

It is possible that untrained rats (although the first few minutes, or more, of the protocol would have gone into 'making' the rats run in the first place) that they would induce muscle damage even quicker and perhaps more severe, given that they would not have a proper hang on how to manoeuvre themselves on the treadmill. Still, that option would not have been representative for the project's premises of muscle damage in trained rats. Then what about the training itself? With the logic displayed by the plasma marker data, sedentary and trained rat groups (A{−1} vs R{−1}) are not significantly distinct. Therefore, reducing the training to make a higher jump to muscle damage plasma marker concentration, probably would not have demonstrated any more noticeable difference (Ahmadi, Sinclair and Davis, 2008).

Increasing the training, in order to make a difference between A{−1} and R{−1} greater, relying on the fact that the plasma marker concentrations in R{−1} would be a little higher due to exercise or even small injury, would possibly only make the goal of inducing muscle damage even harder. Although, not being the aim of the project either, the muscle damage protocol could have been carried out 2 per day and on more than one day. This would probably not make the recovery pattern practically drop to the baseline on Day 3. Still, interpreting that data would be more complex as the injury period would have over night hours of (partial) recovery; and the data would essentially represent recovery of reinjured partially-recovered tissue. Thus, the at least carrying out the induction only during one day, provides more fundamental ideas.

5.4 Differential Gene Expression

The coverage of significantly expressed gene expression only identifies the best pathway or profile line fit, and was used here to systematic choosing. However, looking at the coverage in this way does not reduce the validity of the genes that form the other pathway lines, but reflects the strongest profile.

5.4.1 The Skeletal Muscle Pathway

Capn3 is a Ca^{2+}-dependent protease that plays a role in the regulation of sarcomeric turnover (Stuelsatz *et al.*, 2010). Its downregulation on Day 1 in all three groups, [C], [H] and [E]-groups, might be an indication of the impact of damaged tissue. Whereas on Day 3 and until Day 14, the gene ends up being upregulated in both the [H] and [E]-groups as part of the regenerating tissue — and even slightly more so in the [H]-group. The return from the downregulation in the [C]-group demonstrates the slowest rate to the reference level. *Emd* expresses structural protein for the cytoskeleton (Tilgner *et al.*, 2009), and irrespective of which group, all of them get upregulated on Day 1 to a fairly equal level. The upregulation is then gradually returned until Day 14 in the [H] and the [E]-groups, whilst the return in the [C]-group falls within non-significant changes, and therefore slower. The profile is therefore in favour of either the conditions of the [H] or the [E]-group, as no significant difference between them is detectable. *Lmna* expresses proteins that play a role in nuclear and chromatin stability (Boschmann *et al.*, 2010), which seems to mirror an immediate reaction on Day 1 with an upregulation in all the groups, which is still quite strong on Day 3. The strongest upregulation takes place in the [H]-group. Thereafter, the [H] and [E]-groups show an immediate return of the expression on Day 7 and Day 14, whilst the return in the [C]-groups is quite milder. Dmd encodes dystrophin which anchors the skeletal muscles cytoskeleton to the extracellular matrix (Taylor *et al.*, 2010). Although it shows the most downregulation on Day 1 in the [H]-group, it is also within that group where it is upregulated significantly on Day 7 and Day 14, indicating a long-term effect of hypoxia in relation to the muscle damage.

Myot encodes myotitin, which stabilises the contractile filament when 'working' (Claeys *et al.*, 2009). The downregulation on Day 1, might be representative of a tissue damage that needs to be addressed by degrading the corresponding injured cells, and therefore, the process of *Myot* is slowed down. Still, as only being evident on Day 1, it might be indicative of a mild muscle damage. *Hk2* encodes hexokinase which converts glucose into glucose-6-phosphate (Ahn *et al.*, 2009) destined for utilisation and it is, therefore, reasonable that the only significant upregulation on Day 1 appears in the [E]-group. However, as it does not continue to be differentially upregulated,

it is possible that the first rehabilitation session is having some 'shock' effect. *Atp2a1* expresses the pumps that reduce the intracellular level of Ca^{2+} in muscle cells, by pumping the calcium into sarcoplasmic reticulum (Kimura *et al.*, 2005). As the [C] and [H]-groups are sedentary after the heavy exercise induction of muscle damage, we could assume that as a response and perhaps a precaution or preparation for potentially similar situation to follow, the *Atp2a1* is downregulated but then the downregulation is reduced over the following days. Similarly, the [E]-group might have shown the same profile if a light exercise was not a part of their new regime after the muscle damage, and as a response to the hypoxia+exercise, *Atp2a1* is upregulated, with a more gradual return over the recovery period, perhaps mirroring the mild level of exercise.

Myod1 is a transcription promoter that plays a role in the differentiation of myoblasts (Yang *et al.*, 2009). All of the groups do demonstrate upregulation on Day 1, which indicates muscle tissue repair. As the [H] and [E]-groups show a little higher degree of response, it is likely that the hypoxia favours the condition. Furthermore, the indication of the [E]-group, showing even stronger upregulation response (although not significantly), might mirror a more hypoxic environment, proposed by the addition exercise. *Mef2c* is a transcription promoter that plays a role in maintaining the state of differentiated muscle cells (McDermott *et al.*, 1993). If the tissue has suffered damage, the regeneration process needs to ignore the effect of this promoter and is therefore downregulated as a response. However, since the upregulation is only visible on Day 1, the expression indicates a mild level of tissue damage. Moreover, with no significant difference between the three groups, it is somewhat telling for an equal level of muscle damage. *Myog* is a transcription promoter that plays roles in differentiating the myoblasts (Li *et al.*, 2009), similar to *Myod1*. As the [H] and [E]-groups are only responsive with an upregulation, in comparison with the [C]-group, that does not show any significant differential expression, it seems that the role of hypoxia boosts the expression of this gene. The addition of exercise to hypoxia does not have any further effect on the expression.

Il6 expresses a cytokine as part of an acute response to an inflammation (Novakova *et al.*, 2010). As the [E]-group does only demonstrate significant differential expression, in comparison with the other groups, and from Day 1, it is likely that the addition of exercise to the regime is slightly counteractive and causes more inflammation in the wounded tissue. *Tgf1* expresses cytokines that regulate proliferation, differentiation and migration of leukocytes as a response to a damaged area (Hussein *et al.*, 2010). Given the [H]-group demonstrates the most responsive differential expression on Day 1, it is likely that the hypoxic environment acts as a promoter. However, since the [E]-group also undergoes hypoxia, perhaps, a slightly wounding effect of the exercise itself reduces the effect of hypoxia as a promoter. *Ppargc1a* partakes in regulating the mitochondrial gene expression

which in turn determines the muscle fibre type (Little *et al.*, 2010). It is, therefore, reasonable that the [E]-group, being the only group carrying out exercise during the recovery period, demonstrates a responsive differential expression, whilst the sedentary groups, [C] and [H], do not.

Fbxo32 is generally upregulated in muscle atrophy as a response to protein loss (Csibi *et al.*, 2009). The gene is downregulated on Day −1 after the preconditioning period, indicating growing or strengthening muscle system. As a response to muscle damage, the gene is upregulated, in the [C] and [H] groups on Day 1, which is maintained. However, the [E]-group, not showing any significant differential expression, might show a favourable counteracting effect, due to the addition of light exercise to hypoxia. *Casp3* plays an active role in apoptosis (González *et al.*, 2010), and is upregulated in all three groups on Day 1. The continuing upregulation on Day 3 in the [H]-group might suggest a stronger response for a repair, in relation to hypoxia. *Akt2* expression in myoblasts, forms part of their differentiation as part of regeneration, but has also been shown to cause cell death in its absence (Rotwein and Wilson, 2009). As the gene is downregulated on Day 1, it is possible that is mirrors the reaction of terminating damaged cells, and do so more efficiently with hypoxia which has a gradual return of the downregulation until Day 14, and with the addition of exercise to hypoxia, even further. *Trim63*, showing a downregulation in R{−1} in comparison with A{−1} seems to have its logic to those genes that are upregulated parallel to protein loss (Centner *et al.*, 2001; Csibi *et al.*, 2009) in relation to degradation related to damaged fibres. Although this indicates the exercise difference between the R{−1} and A{−1} groups is in favour of the exercise; it does not explain the downregulation per se. Assuming we accept that small direct injuries are part of a 'healthy' exercise training, the upregulation of the genes can be easily triggered, but are still designated for the degradation of a 'seriously' damaged fibre. The downregulation of these genes could then be part of a secondary protective mechanism to reduce the interactive effects of the proteins they encode. The consequence of this secondary protective mechanism could be reinforced by the slow increase in upregulation from Day 1 to Day 14. The downregulation on Day −1 is somewhat levelled out on Day 1, which could mean that the effect of the injury protocol is generally fairly subtle and not injurious enough (or at least relative to this exercise protection). However, as the gene gets more upregulated with throughout [E]-group, but not in [H]-group, it is likely that injury was induced and is now provoked by the application of exercise.

5.4.2 The Hypoxia Signalling Pathway

Hmox1 encodes an enzyme that catalyses the degradation of haem in erythrocytes and also signals cells for apoptosis (Biburger *et al.*, 2010). It is only significantly responsive in the [H] and [E]-groups and more so in the [E]-group, showing an upregulation on Day 1; which is in line with the

occurrence of tissue damage. However, this upregulation as markedly reduced on Day 3, and back to reference level on Day 7, underpinning a mild and manageable tissue damage. *Btg1* plays an important role in the process of angiogenesis, promoting it with being expressed (Iwai *et al.*, 2004). It shows a parallel profile to *Hmox1*, emphasising a mild tissue damage, and the augmented [E]-group seems to benefit from the occurrence of exercise in addition to hypoxia. *Adora2b* is expressed as part of tissue protection against hypoxia (Yang *et al.*, 2009), and only significantly responsive in the [H] and [E]-group, with an upregulation on Day 1, but to fairly similar levels; and is thereafter returned. Curiously, it does not respond to the actual hypoxia sessions, indicating that the tissular hypoxia is not necessarily determined by the hypoxia on a systemic level (given that it effective enough there as well). Furthermore, it also suggests that any additional hypoxia pretended to be caused by the addition of exercise to hypoxia in the [E]-group, is not effective in that way, but is so in the muscle damage protocol, where the rats run to exhaustion. The only thing that reduces that credibility, at least with the measurements presented here, is the lack of differential expression in the [C]-group on Day 1; however, as the expression levels of this gene seem fairly low in general, it is likely that non-significant upregulation took place. *Anxa2* plays a part in angiogenesis (Aitkenhead *et al.*, 2002) and is only responsive in the [H] and [E]-groups (slightly more in the [H]-group) and is upregulated on Day 1, with a slow return on Day 3. However, on Day 7 it has returned completely. It does slightly suggest some accumulative hypoxic effect on between Day 1 and Day 3, but no effect that is longer term than that. The expression of *Plau* reflects proteolysis as part of extracellular matrix degradation (Luikart *et al.*, 2002) making the manifestation of angiogenesis more probable. It is upregulated on Day 1 in the [H]-group, but even slightly more in the [E]-group, indicating the influence of hypoxia in general to the remodelling of the tissue. *Serpine* is involved in the regulation of fibrinolysis (Heit *et al.*, 2013), and its upregulation in all groups is indicative of the effect of tissue damage. Interestingly, the [H]-group returns its upregulation back on Day 3, whilst the [E]-group continues to upregulate (although slightly reduced) until Day 14. Meanwhile, the profile of the [C]-group is somewhere in the middle of the other two. This does indicate an effect of the hypoxia to inhibit fibrinolysis, but the effect of the additional exercise to forego the inhibition.

In normoxia, *Egln3* expresses a cellular oxygen sensor that catalyses the formation of hydroxyproline in the HIF alpha proteins as part of their degradation (Cioffi *et al.*, 2003). Between all the groups on Day 1, the gene seems downregulated the most in the [C]-group, whilst it is less downregulated in the [H]-group, and then even less in the [E]-group. This could support the role hypoxic-dependant pathways in repairing tissues. If so, the downregulation in the [C]-group averts degrading the HIF-alpha protein, which also would have happened in hypoxia. Therefore, in the

[H]-group, downregulating *Egln3* is less important. The addition exercise then seems to temporarily increase the level of hypoxia even further, and again, the downregulation of *Egln3* is even less important. However, the results suggest a short-term and long-term effect. Short-term, where hypoxia and exercise are more effective in promoting hypoxic-dependant pathways (given the level of tissue damage) and long-term, where the hypoxia alone seems more effective regarding promoting the pathway in comparison with hypoxia+exercise. *Tp53* is a transcription factor that takes part in regulating cell cycle arrest, apoptosis and DNA repair (Matlashewski *et al.*, 1984). It is mostly responsive in the [H]-group, with an upregulation on Day 1, emphasising the immediate effect of hypoxia alone to a damaged tissue, in comparison with the hypoxia+exercise.

Pdk1 regulates metabolite flux and downregulates aerobic respiration as a response to hypoxia and oxidative stress (Kim *et al.*, 2007). As all the groups react with downregulating the gene on Day 1, which is returned thereafter, oxidative stress as a consequence of the exercise-induction of tissue damage, is possibly the greatest factor here. On that note, the [E]-group seems to push the downregulation a slightly further than the [H]-group, which does suggest hypoxia+exercise to be more effective on that specific front, whilst the [C]-group show the least responsive downregulation between the three. *Bnip3* takes part in promoting the induction of cell death pathway (Ghavami *et al.*, 2009), and is downregulated in all groups on Day 1 as a short-term effect. There is little difference between the [C] and [H]-groups (although the [H]-group has the gene slightly less downregulated). However, the [E]-group is demonstrating a markedly less downregulation in comparison with the other two. The different downregulation in the [E]-group hints either to the rats of that group having less tissue damage; or the addition of exercise to hypoxia promoting less need of the induction of the cell death pathway. Still, the data does not suggest exercise causing more tissue damage, unless the effect of hypoxia was that stronger (in comparison with the [H]-group) that it counteracted any damage in relation to exercise, and even more. *Pim1* encodes for kinases the regulate control cell growth, differentiation and apoptosis by inhibition to protect the cell (Borillo *et al.*, 2010). With the gene being upregulated in all groups on Day 1, especially the [C]-group although significantly lower than in the [H] and [E]-groups, suggest a protective element caused by the preconditioning training until Day −1 in the first place, and at least hypoxia promoting the upregulation even further. Whilst this immediate reaction gradually gets reduced throughout the recovery period, the duration of the expression is a little bit stronger, which in turn, favours the addition of exercise having a protective element to it.

Tfrc encodes a receptor for cellular iron uptake that mediates endocytosis which leads to the positive regulation of the T-cells (Buchegger *et al.*, 1996) and the B-cells. However, whilst not being expressed differentially on Day 1 in any of the group, and thereafter being downregulated (the

gene being mostly responsive in the [H]-group), does indicate a contradictory result, given that upregulation would be expected. The potential way for the function of the gene being true and reflecting the experimental groups in question, excluding the fact of the data being reversed or gene function being wrong, might consider a suppression of this route of activating T- and B-cells as it might negatively influence another favourable pathway for tissue repair. However, that possibility is not backed up by any scientific finding. *Lgals3* plays a role in e.g. regulating apoptosis and T-cell regulation (Kariya *et al.*, 2010) and is upregulated in all groups on Day 1, underpinning the existing of tissue damage repair. Interestingly, the [H]-group has the highest upregulation (of the three groups, markedly) and is kept on upregulated (although decreasing) until Day 14. Whilst the [E]-group demonstrates a significant upregulation (higher than in the [C]-group) it rate of returning to the reference levels are fairly slow, which in this case, does not favour the addition of exercise during the recovery.

5.4.3 The VEGF Pathway

Nras encodes Ras-protein that part takes in the role of migrating leukocytes (Davidsson *et al.*, 2010) which fit with its upregulation on Day 1 in all the groups as a response to tissue damage. The application of hypoxia, in general, seems to upregulate this gene even further. *Raf1* is activated by GTP-bound *Ras* protein but has hindering effect onto cell proliferation and differentiation (Zang, Hayne and Luo, 2002), which explains the downregulation on Day 1; however, without any hypoxia or hypoxia+exercise applications, the downregulation is reduced more quickly in comparison with the rest. *Rac* encodes proteins involved in cell growth, cytoskeletal reorganisation and the activation of protein kinases (Frasa *et al.*, 2010); conditions that aid in the repair of damaged tissue. Between the groups, *Rac* is expressed overall more in the [H]-group with an upregulation, underpinning the hypoxic boost to the system. *Rac2* regulates various processes, such as phagocytosis (Kwofie and Skowronski, 2008), which might also be a favourable function in the situation of damaged tissue, most likely provoked by hypoxia, according to the results. *Shc2* encodes a signalling adapter necessary to organise the signalling pathway in neurons (Teodorczyk *et al.*, 2015), but can aid in the regeneration of tissue damage, and demonstrates the strongest expression in the [H]-group, but also more pronouncedly until Day 3, but drops thereafter.

Both *Vegfc* and *Kdr* (encoding a receptor protein) promote angiogenesis and endothelial growth (Terman *et al.*, 1992; Joukov *et al.*, 1996). After the induction of muscle damage, *Vegfc* and *Kdr* are generally downregulated, with the most hint of upregulation not until Day 14. It is slightly possible that *Vegfc*, for example, affects the permeability of the blood vessels, which might justify its downregulation. *Hspb1* is involved in stress resistance and actin organisation (Evans, Britton and

Zachary, 2008), and *Mapk2k1* encodes a protein that binds ligands and cytokines (Si and Liu, 2009). Both are most responsive on Day 1 in the [H] and [E]-groups, regarding *Hspb1* and in the [H]-group mostly, regarding *Mapk2k1*. Both data underpin the level of hypoxia alone, with reference to *Kdr*; whilst *Hspb1* is likely to be jointly affected by the conditions of the [H] and [E]-group. *Pla2g2d* encodes a secreted enzyme that is involved with an inflammation and an immune response (Lambeau and Gelb, 2008). The fact that the gene demonstrates upregulation in the R{−1} indicates that there might have been some small tares before the induction of skeletal muscle injury. It explains the upregulation thereafter in the [C] and [H]-groups if injury-induction was successful. However, the mild exercise seems to reduce this expression effect. *Ptk2* partakes in regulating of cell migration (Lee *et al.*, 2010), which is promoted via its downregulation. The [H]-group seems to be the most responsive, due to the hypoxia, and the gene is downregulated on Day 1, just after the muscle damage. The [E]-group however, does not show the same drop, i.e. downregulation as in the [H]-group, but is generally more downregulated overall the period, suggesting the compensating effect of exercise on top of the hypoxia; and potentially more long-term reactions.

The overall effect within the VEGF pathway is the general favourable dominance of intermittent hypoxia alone. From this pathway aspect, the addition of exercise after hypoxia, is more deconstructive in general, at the start; but does seem to be more favourable as a long term application.

5.4.4 The Wound Healing Pathway

The expression of *Plau* and Plau-protein receptor, *Plaur*, reflect proteolysis as part of extracellular matrix degradation (Luikart *et al.*, 2002). The process that seems to be enhanced with an upregulation on Day 1 in the [H]-group, but even slightly more in the [E]-group, indicating the influence of hypoxia to the remodelling of the tissue. This sign of degradation is, furthermore, supported by the upregulation of *Ctsl1*, encoding for a lysosomal proteinase (Lankelma *et al.*, 2010), in the both the [H] and [E]-groups, on Day 1. Although, the upregulation is with more emphasises in the [H]-groups, suggesting the favourable effects of hypoxia as well. *Mmp7* which is involved in tissue remodelling and promotes angiogenesis (Ito *et al.*, 2009), however, does give the [E]-group a more negative image. The preconditioning exercise prior to the induction of muscle damage, does seem to upregulate the gene, whilst the damage reduces it in all three groups and maintains it that way, but to slightly less extent in the [E]-group, suggesting the beneficial effects of adding light exercise to the hypoxia session. Both *F13a1* and *Fga* partake in the process of coagulation following vascular injury (Carty *et al.*, 2010; Ivaskevicius *et al.*, 2010). However, their upregulation on Day 1 (and Day 3 *F13a1*), with some emphasis on the [E]-group, does suggest a negative effect of

the application of exercise to hypoxia, and maybe some type of re-rupturing, especially given that *Fga* is upregulated on Day 14 as well.

Col14a1 and *Itga1* express collagen and collagen binding receptor, which enhance the extracellular matrix and inhibit angiogenesis (Nyberg *et al.*, 2008). The immediate downregulation of *Itga1* on Day 1 in the [H]-group suggest the favourable effects of hypoxia, whilst the addition of exercise, in this case, might be inflammation reducing. The late downregulation of *Col4a1* at Day 7 and Day 14, indicate a long-term of the effect of both the hypoxia alone and with light exercise, at least to the extent of making ways for angiogenesis. *Ccl7* and *Ccl12* express chemokines which secreted to attract macrophages during inflammation (Lee *et al.*, 2009), and their brief upregulation on Day 1, both in the [H] and [E]-group, suggest an initial response to induction of muscle damage. However, the response is short lived as on Day 3 the genes have their expression returned. As the difference between the two groups is very little and not significant, although stronger in the [E]-group, the addition of exercise is not evident to be any more favourable in comparison with hypoxia which these data suggest. However, as *Il1b*, which encodes for a cytokine (Bensi *et al.*, 1987) is only responsive in the [E]-group, with an upregulation on Day 1 and thereafter returns to reference levels, there might be some hypoxia+exercise related effect. The question is if it is increasing the inflammation, and therefore upregulated, or since it would be likely to continue to do so throughout the recovery period, the expression of *Il1b* might be a slight sign of favourable effect from the addition of exercise with hypoxia. The Day 1-upregulation of *Stat3* as being a signal transducer for interleukins (Ito *et al.*, 2010), might suggest a mild push by the condition of hypoxia as a response to a mild muscle damage, which is then further augmented by the addition of light exercise. Given that the upregulation is thereafter gradually returned, furthermore, emphasises the mild level of tissue damage. The fact that the genes are not expressed differently between the R{−1} and the A{−1}-groups, underlines that the preconditioning training was not causing any damage either, prior to the planned induction of skeletal muscle damage.

The overall effect within the Wound healing pathway does suggest a favourable condition for the application of intermittent hypoxia, albeit mild. However, in general, the addition of exercise does not seem to readily help the inflammation and in might cause some type of re-rupturing.

5.5 Adding the Secondary Measurements

5.5.1 The Changes in the Body Weight

The rat's body weight could have been affected in many ways throughout the experimental procedure. Irrespective of any intentional physiological applications, stress related to running on the treadmill, in general, could always be the most uncontrollable factor reflected in a considerable body weight variability (Radahmadi *et al.*, 2013). On top of that, the physiological applications could alter the body weight even further. Rats could become leaner with some weeks of exercise (Brown *et al.*, 2007), and there is reported evidence of body weight loss in relation to hypoxia exposure as an indication of ineffective acclimatisation (Leal *et al.*, 1995).

Although the rats were not specifically checked for stress markers, other than their appearance, the overall body weight log (and the tracking of each rat in real time; data not shown here) does not indicate any unusual weight loss or weight gain. In fact, the regression in the body weight gain, from Week 1 to Week 6, shows that small variability that it is not until the very end of the recovery period some difference is noticeable; the [C]-group (sedentary trained rats) and the [E]-group (light exercise and hypoxia) show some significant difference (with the [H]-group non-significantly situated in between the two). From this weight perspective, the 98 rats used in the experiment demonstrate a fairly uniform group, with (at the very least) mild hypoxia sessions, and the light exercise during the recovery period was not strenuous. It is even more possible that the weight loss in the [E]-group is because of an exercise regimen stretching from Week 1 to Week 6, rather than just a product of the last two weeks.

5.5.2 The Changes in the Weight Ratios and in the Fulton Index

With a continuous exposure to environmental hypoxia, the heart rate increases and the stroke volume starts to decrease, as an adaptive process, mainly due to the volume reduction of the left ventricle of the heart (Siebenmann and Lundby, 2015), but also in the right ventricle. Still, there is some evidence suggesting that chronic hypoxia exposure leads to right ventricle hypertrophy (McGuire and Bradford, 1999). Moreover, rapid exposure to high altitudes has been observed to cause the development of pulmonary oedema (West, 2004). However, the effects on cardiopulmonary parameters are still not well understood, although hypoxia exposure is common nowadays, e.g. altitude work shifts and in sports medicine.

In the experiment presented here, the focus is rather on a programme of intermittent hypoxia exposure accompanied with a low-intensity exercise and the physiological adaptations. The lung weight fraction in the hypoxic rats (the [H]-group) increased significantly at the same time the right ventricular weight decreased, suggesting a higher perfusion (or subclinical pulmonary oedema). The addition of exercise to hypoxia (the [E]-group) does not seem to for the [H]- group. However, this change in the weight is not evident for [E]-group. Our data support previous findings that hypoxia reduces both left and right ventricular volume (Naeije, 2010), reflected in the changed heart mass for the [H] group (Suarez, Alexander and Houston, 1987). However, we noted that the reduction of these two compartments seem to happen on distinct rates, faster for the right ventricle than the left.

We also observed that the continuance of intermittent exposure strengthens the right ventricle on the expense of the left one, reflected in an increase (after the initial decrease) in the right ventricle's weight which remained that way throughout the rest of the sampling period. The addition of low intensity exercise seems to be sufficient enough to counteract the changes in rats solely exposed to hypoxia. This was reflected in an unchanged Fulton index as there was because of no regression of the left ventricle's muscle mass. It is therefore likely that the supplementary light aerobic exercise with intermittent altitude exposure could be beneficial for trained individuals in terms of minor physiological alterations on the cardiopulmonary system. However, the level and the nature of microstructural and functional alteration would need much support and refining than the gatherings from the result presented in this dissertation.

5.6 Coda

Upon drawing the results together, what sticks out is that despite the rigorous methodology and traceability, when at least to a good part can verify the validity of the result, despite what they convey, is that the key ingredient, the experimental critical point, perhaps was not effective to gain proper insight. However, that does not suggest that the model for this experimental setup is completely useless. There are indicators of muscle damage, although being week, in the majority of the results, however, they can only cover up to Day 1, Day 3 the most. Simultaneously, it raises the question of how easy the experimental version of recreational model is in reality, as it is difficult to define that group, to begin with. Still, as the rats were running to their exhaustion, and it is fairly clear that it was to exhaustion rather than stopping because of muscle damage per se, the rats would not have been pushed any further because of ethical reason. Therefore, even if the rat could, and perhaps would sustain more drastic protocol to induce the damage, than another application of measuring the rats wellbeing would be necessary.

6 Conclusions

The intention of this thesis was to investigate the effects of intermittent hypobaric hypoxia, alone or followed by a light exercise in normoxia, on the recovery of skeletal muscle damage induced with eccentric exercise-running on a treadmill, in trained laboratory rats; using plasma markers and differential gene expression of m. soleus for the evaluation, in conjunction with a running performance score and simple weight ratios to assess the level of homogeneity of the rat subject groups.

The Weight Measurements

(**1**) The overall rat body weight with low variability monitored throughout the relatively long preconditioning, indicate a sufficiently uniform pool of rats prior to the point of their allocation to different subgroups.

(**2**) The gradual body weight changes with low variability throughout the muscle damage recovery period indicate a uniform group of rats, irrespective of being: sedentary, enduring intermittent hypoxia sessions alone or followed by light exercise, until at the end of the 14-day recovery; demonstrating the use of sustainable hypoxia sessions, and a light exercise schedule appropriate for a recovery.

(**3**) The lung weight fraction indicates a further induction of hypoxia on a systemic level with the addition of light exercise, immediately following a hypoxia session, when the sessions are not discontinued, hinting the possible effect of exercise being gradually more stable.

(**4**) The cardiac weight fractions in conjunction with the Fulton index are indicative of a mild longer-term effect of the intermittent hypoxia sessions affecting parts of the heart on a different rate. — Still, can be counteracted with a light addition of exercise.

The AEY Running Performance Score

(**5**) The three-criteria qualitative running-style evaluation is sufficiently detailed to distinguish between rats that are running relatively differently, reflected in the score values; addressing the participation of running, an indication of gradual tiredness and the validity of objective monitoring via a treadmill apparatus.

(**6**) The AEY score reflected on an acceptably equal training progress between the rats, suitable to consider them as the equivalent of recreational athletes, and a certain level of uniformity during the exercise session designed to induce muscle damage; although, simultaneously, suggesting a relatively low level of difficulty considering their training.

The Plasma Markers

(**7**) The plasma markers are indicative of the existence of muscle damage, just after the induction, still, suggest a low impact of the damage induction itself.

(**8**) The application of intermittent hypoxia alone does not alter the recovery profile in comparison with passive recovery. However, the impact of the muscle damage seems sufficient to reflect on an altered profile in both cases, in comparison with the variability of the reference-sedentary rats.

(**9**) The addition of exercise following intermittent hypoxia sessions shows a different recovery profile, which slightly reduces and distributes the immediate impact of the muscle damage, however, indicates a slower recovery.

The Differential Gene Expression of m. Soleus

(**10**) The four pathways examined for m. soleus, indicate that the major effect took place one day after the induction of skeletal muscle damage, suggesting a low level of injury, probably due to the induction method of downhill running. However, the factor of exercise, in general, seems to affect the expression in relative negative controls more emphasised way.

(**11**) Both the skeletal muscle pathway and the VEGF pathway demonstrated genes, which in general reflected damaged muscle tissue, regarding the expression of proteins that are structurally relevant to skeletal muscle tissue and angiogenesis. However, these trends were more evident in the group that carried out light exercise after a hypoxia exposure and even the trained reference group; suggesting a strong impact of exercise in the experimental process.

(**12**) The analysis of both the hypoxia signalling pathway and the wound healing pathway, showed responses in genes expressing proteins partaking in inflammatory processes, still not to hypoxia specifically, thus suggesting that the level of atmospheric hypoxia was not a limiting factor at the muscle cellular level, probably due to the low energy muscle requirements by the activity depression manifested by the rats during the simulated altitude exposure.

Global points

(**13**) The overall effects of the intermittent hypoxia sessions only suggest a mild implication, and although relatively 'stronger' effects detectable with the addition of light exercise, the recovery suggest pattern seem to be sensitive to breaks and need a higher frequency of sessions on a week-to-week basis. Although, seeming to have brought benefits to the table, the addition of exercise simultaneously provokes some other processes.

(**14**) Preconditioning the rats with training indicates a level of resistance to experiencing exercise-induced skeletal muscle damage, based on the performance evaluation, the overall low level of markers in plasma, and relatively low differential gene expression. However, the design of the exercise induction with trained rats on a treadmill, does demonstrate a limitation of the experimental model, regarding developing it to be more impactful on the trained rats, for ethical reasons.

References

Agilent Technologies, A. (2010) *Two-color microarray-based gene expression analysis: Low input quick Amp labeling*. Version 6., *Agilent Technologies User Manual*. Version 6. Santa Clara, USA: Agilent Technologies. Available at: http://www.agilent.com/en-us/library/literature.

Ahmadi, S., Sinclair, P. J. and Davis, G. M. (2008) 'Muscle oxygenation after downhill walking-induced muscle damage', *Clinical Physiology and Functional Imaging*, 28(1), pp. 55–63. doi: 10.1111/j.1475-097X.2007.00777.x.

Ahn, K. J., Kim, J., Yun, M., Park, J. H. and Lee, J. D. (2009) 'Enzymatic properties of the N- and C-terminal halves of human hexokinase II', *BMB Reports*, 42(6), pp. 350–355. Available at: http://210.101.116.28/W_files/ksi3/02617221_pv.pdf.

Aitkenhead, M., Wang, S.-J., Nakatsu, M. N., Mestas, J., Heard, C. and Hughes, C. C. W. (2002) 'Identification of endothelial cell genes expressed in an in vitro model of angiogenesis: Induction of ESM-1, (beta)ig-h3, and NrCAM.', *Microvascular Research*, 63(2), pp. 159–171. doi: 10.1006/mvre.2001.2380.

Allen, D. G. (2001) 'Eccentric muscle damage: Mechanisms of early reduction of force', *Acta Physiologica Scandinavica*, 171(3), pp. 311–319. doi: 10.1046/j.1365-201X.2001.00833.x.

Armstrong, R. B., Ogilvie, R. W. and Schwane, J. A. (1983) 'Eccentric exercise-induced injury to rat skeletal muscle', *Journal of Applied Physiology - Respiratory Environmental and Exercise Physiology*, 54(1), pp. 80–93. Available at: http://search.ebscohost.com.ezproxy.liv.ac.uk/login.aspx?direct=true&db=edselc&AN=edselc.2-52.0-0020567591&site=eds-live&scope=site.

Aydin, S. (2015) 'A short history, principles, and types of ELISA, and our laboratory experience with peptide/protein analyses using ELISA', *Peptides*. Elsevier Inc., 72, pp. 4–15. doi: 10.1016/j.peptides.2015.04.012.

Bassett, D. R. and Howley, E. T. (2000) 'Limiting factors for maximum oxygen uptake and determinants of endurance performance', *Medicine and Science in Sports and Exercise*, 32(1), pp. 70–84. doi: 10.1097/00005768-200001000-00012.

Beidleman, B. A., Muza, S. R., Fulco, C. S., Cymerman, A., Ditzler, D., Stulz, D., Staab, J. E., Skrinar, G. S., Lewis, S. F. and Sawka, M. N. (2004) 'Intermittent altitude exposures reduce acute mountain sickness at 4300 m', *Clinical Science*, 106(3), pp. 321–328. doi: 10.1097/00005768-200305001-00896.

Bensi, G., Raugei, G., Palla, E., Carinci, V., Buonamassa, D. T. and Melli, M. (1987) 'Human interleukin-1 betargene', *Gene*, 52(1), pp. 95–101. doi: 10.1016/0378-1119(87)90398-2.

Biburger, M., Theiner, G., Schädle, M., Schuler, G. and Tiegs, G. (2010) 'Pivotal Advance: Heme oxygenase 1 expression by human CD4+ T cells is not sufficient for their development of immunoregulatory capacity', *Journal of Leukocyte Biology*, 87(2), pp. 193–202. doi: 10.1189/jlb.0508280.

Boersma, G. J., Barf, R. P., Benthem, L., Dijk, G. Van and Scheurink, A. J. W. (2012) 'Forced and voluntary exercise counteract insulin resistance in rats: The role of coping style', *Hormones and Behavior*. Elsevier Inc., 62(1), pp. 93–98. doi: 10.1016/j.yhbeh.2012.05.006.

Borg, E. (2001) 'A comparison between two rating scales for perceived exertion', pp. 4–9. Available at: http://uni-leipzig.de/~isp/isp/conferences/fd01_files/generalinfo/PDFs/EBorg.pdf.

Borg, E. and Kaijser, L. (2006) 'A comparison between three rating scales for perceived exertion and two different work tests', *Scandinavian Journal of Medicine and Science in Sports*, 16(1), pp. 57–69. doi: 10.1111/j.1600-0838.2005.00448.x.

Borillo, G. A., Mason, M., Quijada, P., Völkers, M., Cottage, C., McGregor, M., Din, S., Fischer, K., Gude, N., Avitabile, D., Barlow, S., Alvarez, R., Truffa, S., Whittaker, R., Glassy, M. S., Gustafsson, A. B., Miyamoto, S., Glembotski, C. C., Gottlieb, R. A., Brown, J. H. and Sussman, M. A. (2010) 'Pim-1 kinase protects mitochondrial integrity in cardiomyocytes', *Circulation Research*, 106(7), pp. 1265–1274. doi: 10.1161/CIRCRESAHA.109.212035.

Boschmann, M., Engeli, S., Moro, C., Luedtke, A., Adams, F., Gorzelniak, K., Rahn, G., Mähler, A., Dobberstein, K., Krüger, A., Schmidt, S., Spuler, S., Luft, F. C., Smith, S. R., Schmidt, H. H.-J. and Jordan, J. (2010) 'LMNA mutations,

skeletal muscle lipid metabolism, and insulin resistance', *Journal of Clinical Endocrinology and Metabolism*, 95(4), pp. 1634–1643. doi: 10.1210/jc.2009-1293.

Bottinelli, R., Canepari, M., Reggiani, C. and Stienen, G. J. M. (1994) 'Myofibrillar ATPase activity during isometric contraction and isomyosin composition in rat single skinned muscle fibres', *The Journal of Physiology*, 481(3), pp. 663–675. doi: 10.1113/jphysiol.1994.sp020472.

Brancaccio, P., Lippi, G. and Maffulli, N. (2010) 'Biochemical markers of muscular damage', *Clinical Chemistry and Laboratory Medicine*, 48(6), pp. 757–767. doi: 10.1515/CCLM.2010.179.

Brotto, M. A., Biesiadecki, B. J., Brotto, L. S., Nosek, T. M. and Jin, J.-P. (2006) 'Coupled expression of troponin T and troponin I isoforms in single skeletal muscle fibers correlates with contractility', *American Journal of Physiology - Cell Physiology*, 290(2), pp. C567–C576. doi: 10.1152/ajpcell.00422.2005.

Brown, D. a, Johnson, M. S., Armstrong, C. J., Lynch, J. M., Caruso, N. M., Ehlers, L. B., Fleshner, M., Spencer, R. L. and Moore, R. L. (2007) 'Short-term treadmill running in the rat: what kind of stressor is it?', *Journal of Applied Physiology*, 103(6), pp. 1979–1985. doi: 10.1152/japplphysiol.00706.2007.

Brown, L. M. and Hill, L. (1991) 'Some observations on variations in filament overlap in tetanized muscle fibres and fibres stretched during a tetanus, detected in the electron microscope after rapid fixation', *Journal of Muscle Research and Cell Motility*, 12(2), pp. 171–182. doi: 10.1007/BF01774036.

Buchegger, F., Trowbridge, I. S., Liu, L.-F. S., White, S. and Collawn, J. F. (1996) 'Functional analysis of human/chicken transferring receptor chimeras indicates that the carboxy-terminal region is important for ligand binding', *European Journal of Biochemistry*, 235, pp. 9–17.

Bunn, H. F. and Poyton, R. O. (1996) 'Oxygen sensing and molecular adaptation to hypoxia', *Physiological Reviews*, 76(3), pp. 839–885. Available at: http://physrev.physiology.org.liverpool.idm.oclc.org/content/76/3/839.full.pdf+html.

Capitanio, M., Canepari, M., Cacciafesta, P., Lombardi, V., Cicchi, R., Maffei, M., Pavone, F. S. and Bottinelli, R. (2006) 'Two independent mechanical events in the interaction cycle of skeletal muscle myosin with actin', *Proceedings of the National Academy of Sciences of the United States of America*, 103(1), pp. 87–92. doi: 10.1073/pnas.0506830102.

Carlson, B. M. and Faulkner, J. (1983) 'The regeneration of skeletal muscle fibers following injury: A review', *Medicine & Science in Sports & Exercise*, 15(3), pp. 187–198.

Carty, C. L., Heagerty, P., Heckbert, S. R., Jarvik, G. P., Lange, L. A., Cushman, M., Tracy, R. P. and Reiner, A. P. (2010) 'Interaction between fibrinogen and IL-6 genetic variants and associations with cardiovascular disease risk in the cardiovascular health study', *Annals of Human Genetics*, 74(1), pp. 1–10. doi: 10.1111/j.1469-1809.2009.00551.x.

Centner, T., Yano, J., Kimura, E., McElhinny, A. S., Pelin, K., Witt, C. C., Bang, M. L., Trombitas, K., Granzier, H., Gregorio, C. C., Sorimachi, H. and Labeit, S. (2001) 'Identification of muscle specific ring finger proteins as potential regulators of the titin kinase domain', *Journal of Molecular Biology*, 306(4), pp. 717–726. doi: 10.1006/jmbi.2001.4448.

Champy, M. F., Selloum, M., Piard, L., Zeitler, V., Caradec, C., Chambon, P. and Auwerx, J. (2004) 'Mouse functional genomics requires standardization of mouse handling and housing conditions', *Mammalian Genome*, 15(10), pp. 768–783. doi: 10.1007/s00335-004-2393-1.

Chargé, S. B. P. and Rudnicki, M. A. (2004) 'Cellular and molecular regulation of muscle regeneration', *Physiological Reviews*, 84(1), pp. 209–238. doi: 10.1152/physrev.00019.2003.

Chi, J.-T., Wang, Z., Nuyten, D. S. A., Rodriguez, E. H., Schaner, M. E., Salim, A., Wang, Y., Kristensen, G. B., Helland, Å., Børresen-Dale, A.-L., Giaccia, A., Longaker, M. T., Hastie, T., Yang, G. P., Van de Vijver, M. J. and Brown, P. O. (2006) 'Gene expression programs in response to hypoxia: Cell type specificity and prognostic significance in human cancers', *PLoS Medicine*, 3(3), pp. 47–61. doi: 10.1371/journal.pmed.0030047.

Cioffi, C. L., Liu, X. Q., Kosinski, P. A., Garay, M. and Bowen, B. R. (2003) 'Differential regulation of HIF-1α prolyl-4-hydroxylase genes by hypoxia in human cardiovascular cells', *Biochemical and Biophysical Research Communications*,

303(3), pp. 947–953. doi: 10.1016/S0006-291X(03)00453-4.

Claeys, K. G., van der Ven, P. F. M., Behin, A., Stojkovic, T., Eymard, B., Dubourg, O., Laforêt, P., Faulkner, G., Richard, P., Vicart, P., Romero, N. B., Stoltenburg, G., Udd, B., Fardeau, M., Voit, T. and Fürst, D. O. (2009) 'Differential involvement of sarcomeric proteins in myofibrillar myopathies: A morphological and immunohistochemical study', *Acta Neuropathologica*, 117(3), pp. 293–307. doi: 10.1007/s00401-008-0479-7.

Conkin, J. and Wessel, J. H. (2008) 'Critique of the equivalent air altitude model', *Aviation Space and Environmental Medicine*, 79(10), pp. 975–982. doi: 10.3357/ASEM.2331.2008.

Conover, G. M., Henderson, S. N. and Gregorio, C. C. (2009) 'A myopathy-linked desmin mutation perturbs striated muscle actin filament architecture', *Molecular Biology of the Cell*, 20(3), pp. 834–845. doi: 10.1091/mbc.E08-07-0753.

Coppel, J., Hennis, P., Gilbert-Kawai, E. and Grocott, M. P. W. (2015) 'The physiological effects of hypobaric hypoxia versus normobaric hypoxia: A systematic review of crossover trials', *Extreme Physiology and Medicine*, 4(2), pp. 2–21. doi: 10.1186/s13728-014-0021-6.

Coyle, E. F. (2000) 'Physical activity as a metabolic stressor', *American Journal of Clinical Nutrition*, 72(2 Suppl), p. 512S–520S. Available at: http://ajcn.nutrition.org.liverpool.idm.oclc.org/content/72/2/512s.full.pdf+html.

Csibi, A., Leibovitch, M. P., Cornille, K., Tintignac, L. A. and Leibovitch, S. A. (2009) 'MAFbx/Atrogin-1 controls the activity of the initiation factor eIF3-fin skeletal muscle atrophy by targeting multiple C-terminal lysines', *Journal of Biological Chemistry*, 284(7), pp. 4413–4421. doi: 10.1074/jbc.M807641200.

Davidsson, J., Paulsson, K., Lindgren, D., Lilljebjörn, H., Chaplin, T., Forestier, E., Andersen, M. K., Nordgren, A., Rosenquist, R., Fioretos, T., Young, B. D. and Johansson, B. (2010) 'Relapsed childhood high hyperdiploid acute lymphoblastic leukemia: presence of preleukemic ancestral clones and the secondary nature of microdeletions and RTK-RAS mutations', *Leukemia*, 24(5), pp. 924–31. doi: 10.1038/leu.2010.39.

Davies, C. T. M. and White, M. J. (1981) 'Muscle weakness following eccentric work in man', *Pflügers Archiv European Journal of Physiology*, 392(2), pp. 168–171. doi: 10.1007/BF00581267.

Directive (no date) *of the european parliament and of the council of 22 september 2010 on the protection of animals used for sentific purposes*, *Official Journal of the European Union*. Available at: http://eur-lex.europa.eu/legal-content/EN/TXT/?uri=celex:32010L0063.

Donovan, C. M. and Faulkner, J. A. (1987) 'Plasticity of skeletal muscle: Regenerating fibers adapt more rapidly than surviving fibers', *Journal of Applied Physiology*, 62(6), pp. 2507–2511. Available at: http://jap.physiology.org/content/62/6/2507.full.pdf+html.

Eder, M., Schlattner, U., Becker, A., Wallimann, T., Kabsch, W. and Fritz-Wolf, K. (1999) 'Crystal structure of brain-type creatine kinase at 1.41 A resolution', *Protein Science*, 8(11), pp. 2258–2269. doi: 10.1110/ps.8.11.2258.

Ellison, S. L. R., Barwick, V. J. and Farrant, T. J. D. (2009) *Practical statistics for the analytical scientist*. 2nd edn. Cambridge, UK: RSC Publishing.

Essig, D. A. (1996) 'Contractile activity-induced mitochondrial biogenesis in skeletal muscle', *Exercise and Sport Sciences Reviews*, 24(1), pp. 289–319.

Esteva, S., Panisello, P., Torrella, J. R., Pagès, T. and Viscor, G. (2009) 'Enzyme activity and myoglobin concentration in rat myocardium and skeletal muscles after passive intermittent simulated altitude exposure', *Journal of Sports Sciences*, 27(6), pp. 633–640. Available at: http://eds.b.ebscohost.com.ezproxy.liv.ac.uk/eds/pdfviewer/pdfviewer?sid=aea2fe3c-b322-4911-9938-584dcfdb6837@sessionmgr114&vid=4&hid=119.

Evans, I. M., Britton, G. and Zachary, I. C. (2008) 'Vascular endothelial growth factor induces heat shock protein (HSP) 27 serine 82 phosphorylation and endothelial tubulogenesis via protein kinase D and independent of p38 kinase', *Cellular Signalling*, 20(7), pp. 1375–1384. doi: 10.1016/j.cellsig.2008.03.002.

Faiss, R., Pialoux, V., Sartori, C., Faes, C., Dériaz, O. and Millet, G. P. (2013) 'Ventilation, oxidative stress, and nitric oxide in hypobaric versus normobaric hypoxia', *Medicine and Science in Sports and Exercise*, 45(2), pp. 253–260. doi: 10.1249/MSS.0b013e31826d5aa2.

Farah, C. S. and Reinach, F. C. (1995) 'The troponin complex and regulation of muscle contraction', *FASEB Journal*, 9(9), pp. 755–767. doi: 10.1096/fj.02-0402fje.

Franzini-Armstrong, C. and Jorgensen, A. O. (1994) 'Structure and development of E-C coupling units in skeletal muscle', *Annual Review of Physiology*, 56, pp. 509–534. doi: 10.1146/annurev.phl.56.030194.002453.

Frasa, M. A. M., Maximiano, F. C., Smolarczyk, K., Francis, R. E., Betson, M. E., Lozano, E., Goldenring, J., Seabra, M. C., Rak, A., Ahmadian, M. R. and Braga, V. M. M. (2010) 'Armus is a Rac1 effector that inactivates Rab7 and regulates E-Cadherin degradation', *Current Biology*. Elsevier Ltd, 20(3), pp. 198–208. doi: 10.1016/j.cub.2009.12.053.

Fraser, J., Vieira de Mello, L., Ward, D., Rees, H. H., Williams, D. R., Fang, Y., Brass, A., Gracey, A. Y. and Cossins, A. R. (2006) 'Hypoxia-inducible myoglobin expression in nonmuscle tissues', *Proceedings of the National Academy of Sciences of the United States of America*, 103(8), pp. 2977–2981. doi: 10.1073/pnas.0508270103.

Frauenfelder, H., McMahon, B. H., Austin, R. H., Chu, K. and Groves, J. T. (2001) 'The role of structure, energy landscape, dynamics, and allostery in the enzymatic function of myoglobin', *Proceedings of the National Academy of Sciences of the United States of America*, 98(5), pp. 2370–2374. doi: 10.1073/pnas.041614298.

Garber, C. E., Blissmer, B., Deschenes, M. R., Franklin, B. A., Lamonte, M. J., Lee, I.-M., Nieman, D. C. and Swain, D. P. (2011) 'Quantity and quality of exercise for developing and maintaining cardiorespiratory, musculoskeletal, and neuromotor fitness in apparently healthy adults: Guidance for prescribing exercise', *Medicine and Science in Sports and Exercise*, 43(7), pp. 1334–1359. doi: 10.1249/MSS.0b013e318213fefb.

Garry, D. J. and Mammen, P. P. A. (2007) 'Molecular insights into the functional role of myoglobin', *Hypoxia and the Circulation*, 618, pp. 181–193. doi: 10.1007/978-0-387-75434-5_14.

Gerald, M. C. (1978) 'Effects of (+)-amphetamine on the treadmill endurance performance of rats', *Neuropharmacology*, 17(9), pp. 703–704. doi: 10.1016/0028-3908(78)90083-7.

Ghavami, S., Eshragi, M., Ande, S. R., Chazin, W. J., Klonisch, T., Halayko, A. J., Mcneill, K. D., Hashemi, M., Kerkhoff, C. and Los, M. (2009) 'S100A8 / A9 induces autophagy and apoptosis via ROS- mediated cross-talk between mitochondria and lysosomes that involves BNIP3', *Nature*, 20, pp. 1–18. doi: 10.1038/cr.2009.xx.

González, D., Espino, J., Bejarano, I., López, J. J., Rodríguez, A. B. and Pariente, J. A. (2010) 'Caspase-3 and -9 are activated in human myeloid HL-60 cells by calcium signal', *Molecular and Cellular Biochemistry*, 333(1–2), pp. 151–157. doi: 10.1007/s11010-009-0215-1.

Gordon, A. M., Huxley, A. F. and Julian, F. J. (1966) 'The variation in isometric tension with sarcomere length in vertebrate muscle fibres', *The Journal of Physiology*, 184(1), pp. 170–192. doi: 10.1113/jphysiol.1966.sp007909.

Gordon, S. (2003) 'Alternative activation of macrophages', *Nature Reviews Immunology*, 3(1), pp. 23–35. doi: 10.1038/nri978.

Gosselin, L. E. (2000) 'Attenuation of force deficit after lengthening contractions in soleus muscle from trained rats', *Journal of Applied Physiology*, 88(4), pp. 1254–1258. Available at: http://www.ncbi.nlm.nih.gov/pubmed/10749815.

Griffiths, W. J. (1954) 'The occurrence of convulsion in rats in the absence of auditory stimulation', *Annual of Animal Psychology*, 4(1), pp. 1–6. doi: 10.2502/janip1944.4.1.

Griffiths, W. J. (1956) 'Diet selections of rats run to exhaustion on a treadmill', *Journal of Animal Behavior*, 49(4), pp. 334–335. Available at: http://eds.b.ebscohost.com.ezproxy.liv.ac.uk/eds/pdfviewer/pdfviewer?sid=51881455-0c4b-492b-92ae-7b15c7798b5d@sessionmgr115&vid=2&hid=121.

Grossman, S. H. (1983) 'Resonance energy transfer between the active sites of myocardial-type creatine kinase (isozyme MB)', *Biochemistry*, 22(23), pp. 5369–5375. doi: 10.1021/bi00292a018.

Grossman, S. H. (1990) 'Resonance energy transfer between the active sites of creatine kinase from rabbit brain', *Biochimica et Biophysica Acta*, 1040(2), pp. 276–280. doi: 10.1016/0167-4838(90)90087-V.

Grossman, S. H. and Mollo, E. (1979) 'Physical and serological comparison and hybridization of isozymes of creatine kinase from primates', *International Journal of Biochemistry*, 10(4), pp. 367–381. doi: 10.1016/0020-711X(79)90102-2.

Grover, R. F., Weil, J. V and Reeves, J. T. (1986) 'Cardiovascular adaptation to exercise at high altitude.', *Exercise and sport sciences reviews*, 14, pp. 269–302. Available at: http://ovidsp.tx.ovid.com.liverpool.idm.oclc.org/sp-3.22.1b/ovidweb.cgi?WebLinkFrameset=1&S=GFINFPHJGBDDIAILNCIKHDOBFOBEAA00&returnUrl=ovidweb.cgi?&Titles=S.sh.22%7c1%7c10&FORMAT=ovid&FIELDS=TITLES&S=GFINFPHJGBDDIAILNCIKHDOBFOBEAA00&.

Gussoni, M., Scorciapino, M. A., Vezzoli, A., Anedda, R., Greco, F., Ceccarelli, M. and Casu, M. (2011) 'Structural characterization of recombinant human myoglobin isoforms by 1H and 129Xe NMR and molecular dynamics simulations', *Biochimica et Biophysica Acta - Proteins and Proteomics*. Elsevier B.V., 1814(12), pp. 1919–1929. doi: 10.1016/j.bbapap.2011.06.014.

Häkkinen, K., Alen, M., Kraemer, W. J., Gorostiaga, E., Izquierdo, M., Rusko, H., Mikkola, J., Häkkinen, A., Valkeinen, H., Kaarakainen, E., Romu, S., Erola, V., Ahtiainen, J. and Paavolainen, L. (2003) 'Neuromuscular adaptations during concurrent strength and endurance training versus strength training', *European Journal of Applied Physiology*, 89(1), pp. 42–52. doi: 10.1007/s00421-002-0751-9.

Harrison, M. F., Anderson, P., Miller, A., O'Malley, K., Richert, M., Johnson, J. and Johnson, B. D. (2013) 'Physiological variables associated with the development of acute mountain sickness at the South Pole', *BMJ open*, 3(7), pp. 1–7. doi: 10.1136/bmjopen-2013-003064.

Hastings, K. E. M. (1997) 'Molecular evolution of the vertebrate troponin I gene family', *Cell Structure and Function*, 22(1), pp. 205–211. doi: 10.1247/csf.22.205.

Hawke, T. J. and Garry, D. J. (2001) 'Myogenic satellite cells: Physiology to molecular biology', *Journal of Applied Physiology*, 91(2), pp. 534–551. Available at: http://jap.physiology.org.liverpool.idm.oclc.org/content/91/2/534.full.pdf+html.

Hayashi, Y., Matsuda, R., Maitani, T., Imai, K., Nishimura, W., Ito, K. and Maeda, M. (2004) 'Precision, limit of detection and range of quantitation in competitive ELISA', *Analytical Chemistry*, 76(5), pp. 1295–1301. doi: 10.1021/ac0302859.

Heit, C., Jackson, B. C., McAndrews, M., Wright, M. W., Thompson, D. C., Silverman, G. a, Nebert, D. W. and Vasiliou, V. (2013) 'Update of the human and mouse SERPIN gene superfamily', *Human Genomics*, 7(22), pp. 1–14. doi: 10.1186/1479-7364-7-22.

Hibbert, D. B. (2007) 'Systematic errors in analytical measurement results', *Journal of Chromatography A*, 1158(1–2), pp. 25–32. doi: 10.1016/j.chroma.2007.03.021.

Hochachka, P. W. (1999) 'Two research paths for probing the roles of oxygen in metabolic regulation', *Brazilian Journal of Medical and Biological Research*, 32(6), pp. 661–672. doi: 10.1590/S0100-879X1999000600001.

Hochachka, P. W. (2000) 'Oxygen, homeostasis, and metabolic regulation', in Lahiri, S., Prabhakar, N. R., and Forster II, R. E. (eds) *Advances in Experimental Medicine and Biology*. London: Kluwer Academic/Plenum Publishers, pp. 311–336.

Hochachka, P. W. and Somero, G. N. (2002) '5. Human hypoxia tolerance', in *Biochemical adaptation: Mechanism and process in physiological evolution*. 1st edn. New York, United States of America: Oxford University Press, pp. 186–216.

Hoffmann, A., Gloe, T. and Pohl, U. (2001) 'Hypoxia-induced upregulation of eNOS gene expression is redox-sensitive: A comparison between hypoxia and inhibitors of cell metabolism', *Journal of Cellular Physiology*, 188(1), pp. 33–44. doi: 10.1002/jcp.1092.

Honig, C. R., Connett, R. J. and Gayeski, T. E. J. (1992) 'O2 transport and its interaction with meabolism; A systems view

of aerobic capacity', *Medicine and Science in Sports and Exercise*, 24(1). Available at: http://journals.lww.com/acsm-msse/pages/articleviewer.aspx?year=1992&issue=01000&article=00009&type=abstract.

Hurme, T. and Kalimo, H. (1992) 'Activation of myogenic precursor cells after muscle injury', *Medicine and Science in Sports and Exercise*, 24(2), pp. 197–205. Available at: http://journals.lww.com/acsm-msse/pages/articleviewer.aspx?year=1992&issue=02000&article=00007&type=abstract.

Hurme, T., Kalimo, H., Letho, M. and Järvinen, M. (1991) 'Healing of skeletal muscle injury: An ultrastructural and immunohistochemical study', *Medicine and Science in Sports and Exercise*, 23(7), pp. 801–810. Available at: http://journals.lww.com/acsm-msse/pages/articleviewer.aspx?year=1991&issue=07000&article=00006&type=abstract.

Hussein, A., Askar, E., Elsaeid, M. and Schaefer, F. (2010) 'Functional polymorphisms in transforming growth factor-beta-1 (TGFβ-1) and vascular endothelial growth factor (VEGF) genes modify risk of renal parenchymal scarring following childhood urinary tract infection', *Nephrology Dialysis Transplantation*, 25(3), pp. 779–785. doi: 10.1093/ndt/gfp532.

Huxley, A. F. and Niedergerke, R. (1954) 'Structural changes in muscle during contraction: Interference microscopy of living muscle fibres', *Nature*, 173(4412), pp. 971–973. doi: 10.1038/173971a0.

Huxley, A. F. and Simmons, R. M. (1971) 'Proposed mechanism of force generation in striated muscle', *Nature*, 233, pp. 533–538. doi: 10.1038/233533a0.

Huxley, A. F. and Taylor, R. E. (1958) 'Local ativation of striated muscle fibres', *Journal of Physiology*, 144(3), pp. 426–441. doi: 10.1113/jphysiol.1958.sp006111.

Huxley, H. E. (1953) 'Electron microscope studies of the organisation of the filaments in striated muscle', *Biochimica et Biophysica Acta*, 12(1–2), pp. 387–394. doi: 10.1016/0006-3002(53)90156-5.

Ingalls, C. P., Warren, G. L., Williams, J. H., Ward, C. W. and Armstrong, R. B. (1998) 'E-C coupling failure in mouse EDL muscle after in vivo eccentric contractions', *Journal of Applied Physiology*, 85(1), pp. 58–67. doi: 10.1097/00005768-199705001-01548.

Ito, S., Oyake, T., Murai, K. and Ishida, Y. (2010) 'Deguelin suppresses cell proliferation via the inhibition of survivin expression and STAT3 phosphorylation in HTLV-1-transformed T cells', *Leukemia Research*. Elsevier Ltd, 34(3), pp. 352–357. doi: 10.1016/j.leukres.2009.09.003.

Ito, T., Ishii, G., Saito, S., Yano, K., Hoshino, A., Suzuki, T. and Ochiai, A. (2009) 'Degradation of soluble VEGF receptor-1 by MMP-7 allows VEGF access to endothelial cells', *Blood2*, 113(10), pp. 2363–2369. doi: 10.1182/blood-2008-08-172742.

Ivaskevicius, V., Biswas, A., Bevans, C., Schroeder, V., Kohler, H. P., Rott, H., Halimeh, S., Petrides, P. E., Lenk, H., Krause, M., Miterski, B., Harbrecht, U. and Oldenburg (2010) 'Identification of eight novel coagulation factor XIII subunit A mutations: implied consequences for structure and function', *Haematologica*, 95(6), pp. 956–962. doi: 10.3324/haematol.2009.017210.

Iwai, K., Hirata, K. I., Ishida, T., Takeuchi, S., Hirase, T., Rikitake, Y., Kojima, Y., Inoue, N., Kawashima, S. and Yokoyama, M. (2004) 'An anti-proliferative gene BTG1 regulates angiogenesis in vitro', *Biochemical and Biophysical Research Communications*, 316(3), pp. 628–635. doi: 10.1016/j.bbrc.2004.02.095.

Järvinen, T. A. H., Järvinen, T. L. N., Kääriäinen, M., Kalimo, H. and Järvinen, M. (2005) 'Muscle injuries: Biology and treatment', *American Journal of Sports Medicine*, 33(5), pp. 745–764. doi: 10.1177/0363546505274714.

Jouett, N. P., Watenpaugh, D. E., Dunlap, M. E. and Smith, M. L. (2015) 'Interactive effects of hypoxia, hypercapnia and lung volume on sympathetic nerve activity in humans', *Experimental Physiology*, 100(9), pp. 1018–1029. doi: 10.1113/EP085092.

Joukov, V., Pajusola, K., Kaipainen, A., Chilov, D., Lahtinen, I., Kukk, E., Saksela, O., Kalkkinen, N. and Alitalo, K. (1996) 'A

novel vascular endothelial growth factor, VEGF-C, is a ligand for the Flt4 (VEGFR-3) and KDR (VEGFR-2) receptor tyrosine kinases', *The EMBO journal*, 15(2), pp. 290–298. Available at: http://www.pubmedcentral.nih.gov/articlerender.fcgi?artid=449944&tool=pmcentrez&rendertype=abstract.

Kääriäinen, M., Kääriäinen, J., Järvinen, T. L. N., Nissinen, L., Heino, J., Järvinen, M. and Kalimo, H. (2000) 'Integrin and dystrophin associated adhesion protein complexes during regeneration of shearing-type muscle injury', *Neuromuscular Disorders*, 10(2), pp. 121–132. doi: 10.1016/S0960-8966(99)00077-2.

Kääriäinen, M., Liljamo, T., Pelto-Huikko, M., Heino, J., Järvinen, M. and Kalimo, H. (2001) 'Regulation of α7 integrin by mechanical stress during skeletal muscle regeneration', *Neuromuscular Disorders*, 11(4), pp. 360–369. doi: 10.1016/S0960-8966(00)00193-0.

Kanda, K., Sugama, K., Hayashida, H., Sakuma, J., Kawakami, Y., Miura, S., Yoshioka, H., Mori, Y. and Suzuki, K. (2013) 'Eccentric exercise-induced delayed-onset muscle soreness and changes in markers of muscle damage and inflammation', *Exercise Immunology Review*, 19, pp. 72–85.

Kanda, K., Sugama, K., Sakuma, J., Kawakami, Y. and Suzuki, K. (2014) 'Evaluation of serum leaking enzymes and investigation into new biomarkers for exercise induced muscle damage', *Exercise Immunology Review*, 20, pp. 39–54.

Kannus, P., Parkkari, J., Jarvinen, T. L. N., Jarvinen, T. A. H. and Jarvinen, M. (2003) 'Basic science and clinical studies coincide: Active treatment approach is needed after a sports injury', *Scandinavian Journal of Medicine & Science in Sports*, 13(3), pp. 150–154. Available at: https://liverpool.idm.oclc.org/login?url=http://search.ebscohost.com/login.aspx?direct=true&db=s3h&AN=9885969&site=eds-live&scope=site.

Kariya, Y., Kawamura, C., Tabei, T. and Gu, J. (2010) 'Bisecting GlcNAc residues on laminin-332 down-regulate galectin-3-dependent keratinocyte motility', *Journal of Biological Chemistry*, 285(5), pp. 3330–3340. doi: 10.1074/jbc.M109.038836.

Karp, J. R. (2001) 'Muscle fiber types and training', *Strength and Conditioning Journal*, 23(5), pp. 21–26. Available at: https://liverpool.idm.oclc.org/login?url=http://search.ebscohost.com/login.aspx?direct=true&db=jlh&AN=106891896&site=eds-live&scope=site.

Kasperek, G. J. and Snider, R. D. (1985) 'The susceptibility to exercise-induced muscle damage increases as rats grow larger', *Experientia*, 41(5), pp. 616–617. doi: 10.1007/BF02007685.

Kasuga, N., Yamashita, S., Ogasawara, H., Suzuki, H., Tsuzimoto, H. and Ishihara, A. (1999) 'Various in running pattern and skeletal muscle adaptions in voluntary running rats at different load', *Japanese Journal of Physical Fitness and Sports Medicine*, 48, pp. 99–110.

Kim, J., Gao, P., Liu, Y.-C., Semenza, G. L. and Dang, C. V (2007) 'Hypoxia-inducible factor 1 and dysregulated c-Myc cooperatively induce vascular endothelial growth factor and metabolic switches hexokinase 2 and pyruvate dehydrogenase kinase 1', *Molecular and Cellular Biology*, 27(21), pp. 7381–793. doi: 10.1128/MCB.00440-07.

Kimura, T., Nakamori, M., Lueck, J. D., Pouliquin, P., Aoike, F., Fujimura, H., Dirksen, R. T., Takahashi, M. P., Dulhunty, A. F. and Sakoda, S. (2005) 'Altered mRNA splicing of the skeletal muscle ryanodine receptor and sarcoplasmic/endoplasmic reticulum Ca2+-ATPase in myotonic dystrophy type 1', *Human Molecular Genetics*, 14(15), pp. 2189–2200. doi: 10.1093/hmg/ddi223.

Komulainen, J., Kytola, J. and Vihko, V. (1994) 'Running-induced muscle injury and myocellular enzyme release in rats', *Journal of Applied Physiology*, 77(5), pp. 2299–2304. Available at: http://www.ncbi.nlm.nih.gov/pubmed/7868448.

Komulainen, J., Takala, T. E. S., Kuipers, H. and Hesselink, M. K. C. (1998) 'The disruption of myofibre structures in rat skeletal muscle after forced lengthening contractions', *Pflugers Archiv European Journal of Physiology*, 436(5), pp. 735–741. doi: 10.1007/s004240050696.

Kraemer, W. J., Fleck, S. J. and Evans, W. J. (1996) 'Strength and power training: Physiological mechanisms of adaptation', *Exercise and Sport Sciences Reviews*, 24(1), pp. 363–397. Available at:

http://www.ncbi.nlm.nih.gov/pubmed/8744256.

Kwofie, M. A. and Skowronski, J. (2008) 'Specific recognition of Rac2 and Cdc42 by DOCK2 and DOCK9 guanine nucleotide exchange factors', *Journal of Biological Chemistry*, 283(6), pp. 3088–3096. doi: 10.1074/jbc.M705170200.

Lambeau, G. and Gelb, M. H. (2008) 'Biochemistry and physiology of mammalian secreted phospholipases A2', *Annual Review of Biochemistry*, 77, pp. 495–520. doi: 10.1146/annurev.biochem.76.062405.154007.

Lambert, M. and Borresen, J. (2006) 'A theoretical basis of monitoring fatigue: A practical approach for coaches', *International Journal of Sports Science and Coaching*, 1(4), pp. 371–388. doi: 10.1260/174795406779367684.

Lankelma, J. M., Voorend, D. M., Barwari, T., Koetsveld, J., Van der Spek, A. H., De Porto, A. P. N. A., Van Rooijen, G. and Van Noorden, C. J. F. (2010) 'Cathepsin L, target in cancer treatment?', *Life Sciences*. Elsevier Inc., 86(7–8), pp. 225–233. doi: 10.1016/j.lfs.2009.11.016.

Leal, T. L., Alippi, R. M., Vargas, M., Leon-Velarde, F. and Bozzini, C. E. (1995) 'Body weight loss during acute hypoxia: Effects of increased convective oxygen transport or previous acclimation', *Acta Physiologica et Pharmacologica Latinoamericana*, 45(1), pp. 9–14. Available at: http://www.ncbi.nlm.nih.gov/entrez/query.fcgi?cmd=Retrieve&db=PubMed&dopt=Citation&list_uids=8580521.

Lee, K. S., Chung, J. H., Lee, K. H., Shin, M., Oh, B. H., Lee, S. H. and Hong, C. H. (2009) 'Plasma levels of monocyte chemotactic protein 3 and beta-nerve growth factor increase with amnestic mild cognitive impairment', *Cellular & Molecular Immunology*, 6(2), pp. 143–147. Available at: http://search.proquest.com.liverpool.idm.oclc.org/docview/1785751697/3FA05F0A632445C1PQ/10?accountid=12117.

Lee, S. H., Lee, Y. J., Song, C. H., Ahn, Y. K. and Han, H. J. (2010) 'Role of FAK phosphorylation in hypoxia-induced hMSCS migration: Involvement of VEGF as well as MAPKS and eNOS pathways', *American Journal of Physiology - Cell physiology*, 298(4), pp. C847–C856. doi: 10.1152/ajpcell.00418.2009.

Levin, A. and Wyman, J. (1927) 'The viscous elastic properties of muscle', *Proceedings of the Royal Society of London*, 101(709), pp. 218–243. doi: 10.1098/rspb.1927.0014.

Levitt, R. A. and Webb, W. B. (1965) 'Effect of infantile treadmill experience on body-weight and resistence to exhaustion in the rat', *Nature*, 208.

Li, D., Niu, Z., Yu, W., Qian, Y., Wang, Q., Li, Q., Yi, Z., Luo, J., Wu, X., Wang, Y., Schwartz, R. J. and Liu, M. (2009) 'SMYD1, the myogenic activator, is a direct target of serum response factor and myogenin', *Nucleic Acids Research*, 37(21), pp. 7059–7071. doi: 10.1093/nar/gkp773.

Lieber, R. L., Thornell, L.-E. and Fridén, J. (1996) 'Muscle cytoskeletal disruption occurs within the first 15 min of cyclic eccentric contraction', *Journal of Applied Physiology*, 80(1), pp. 278–284. Available at: http://jap.physiology.org/content/80/1/278.full.pdf+html.

Little, J. P., Safdar, A., Cermak, N., Tarnopolsky, M. A. and Gibala, M. J. (2010) 'Acute endurance exercise increases the nuclear abundance of PGC-1 in trained human skeletal muscle', *American Journal of Physiology - Regulatory, Integrative and Comparative Physiology*, 298(4), pp. R912–R917. doi: 10.1152/ajpregu.00409.2009.

Luikart, S., Masri, M., Wahl, D., Hinkel, T., Beck, J. M., Gyetko, M. R., Gupta, P. and Oegema, T. (2002) 'Urokinase is required for the formation of mactinin, an a -actinin fragment that promotes monocyte/macrophage maturation', *Biochimica et Biophysica Acta - Molecular Cell Research*, 1591(1–3), pp. 99–107. doi: 10.1016/S0167-4889(02)00255-0.

van Lunteren, E. and Moyer, M. (2003) 'Slowing of rat diaphragm action potential depolarization by endurance treadmill training', *Neuroscience Letters*, 339(3), pp. 175–178. doi: 10.1016/S0304-3940(03)00031-4.

Lyons, J. M., Schwimer, J. E., Anthony, C. T., Thomson, J. L., Cundiff, J. D., Casey, D. T., Maccini, C., Kucera, P., Wang, Y. Z., Boudreaux, J. P. and Woltering, E. A. (2010) 'The role of VEGF pathways in human physiologic and pathologic angiogenesis', *Journal of Surgical Research*. Elsevier Ltd, 159(1), pp. 517–527. doi: 10.1016/j.jss.2008.12.014.

Mathur, A. B., Collinsworth, A. M., Reichert, W. M., Kraus, W. E. and Truskey, G. A. (2001) 'Endothelial, cardiac muscle and skeletal muscle exhibit different viscous and elastic properties as determined by atomic force microscopy', *Journal of Biomechanics*, 34(12), pp. 1545–1553. doi: 10.1016/S0021-9290(01)00149-X.

Matlashewski, G., Lamb, P., Pim, D., Peacock, J., Crawford, L. and Benchimol, S. (1984) 'Isolation and characterization of a human p53 cDNA clone: expression of the human p53 gene', *The EMBO journal*, 3(13), pp. 3257–3262.

Mattson, J. P., Ross, C. R., Kilgore, J. L. and Musch, T. I. (2000) 'Induction of mitochondrial stress proteins following treadmill running', *Medicine and Science in Sports and Exercise*, 32(2), pp. 365–369. doi: 10.1097/00005768-200002000-00016.

Mayer, J., Vitale, J. J. and Mashayekh, M. B. (1954) 'Exercise, food intake and body weight in normal rats and genetically obese adult mice', *American Journal of Physiology*, 177(3), pp. 544–548.

McCully, K. K. and Faulkner, J. A. (1985) 'Injury to skeletal muscle fibers of mice following lengthening contractions', *Journal of Applied Physiology*, 59(1), pp. 119–126. Available at: http://jap.physiology.org/content/59/1/119.full.pdf+html.

McDermott, J. C., Cardoso, M. C., Yu, Y. T., Andres, V., Leifer, D., Krainc, D., Lipton, S. A. and Nadal-Ginard, B. (1993) 'hMEF2C gene encodes skeletal muscle- and brain-specific transcription factors', *Molecular and Cellular Biology*, 13(4), pp. 2564–2577. doi: 10.1128/MCB.13.4.2564.

McGuire, M. and Bradford, A. (1999) 'Chronic intermittent hypoxia increases haematocrit and causes right ventricular hypertrophy in the rat', *Respiration Physiology*, 117(1), pp. 53–58. doi: 10.1016/S0034-5687(99)00047-X.

Van der Meulen, J. H., Kuipers, H., Van der Wal, J. C. and Drukker, J. (1993) 'Quantitative and spatial aspects of degenerative changes in rat soleus muscle after exercise of different durations', *Journal of Anatomy*, 182(3), pp. 349–353. Available at: https://www-ncbi-nlm-nih-gov.liverpool.idm.oclc.org/pmc/articles/PMC1259807/pdf/janat00146-0045.pdf.

Millet, G. P., Roels, B., Schmitt, L., Woorons, X. and Richalet, J.-P. (2010) 'Combining hypoxic training methods for peak performance', *Sports Medicine*, 40(1), pp. 1–25. doi: 10.2165/11317920-000000000-00000.

Mitsui, T., Kawai, H., Naruo, T. and Saito, S. (1994) 'Ultrastructural localization of myoglobin mRNA in human skeletal muscle', *Histochemistry*, 101(2), pp. 99–104. doi: 10.1007/BF00269355.

Moraska, A., Deak, T., Spencer, R. L., Roth, D. and Fleshner, M. (2000) 'Treadmill running produces both positive and negative physiological adaptations in Sprague-Dawley rats', *American Journal of Physiology - Regulatory, Integrative and Comparative Physiology*, 279(4), pp. R1321–R1329. Available at: http://eds.b.ebscohost.com.ezproxy.liv.ac.uk/eds/SmartLink/OpenEjsSmartLink?sid=bbd0ba59-10d7-4333-9ac8-010e8fdf0058@sessionmgr113&vid=3.

Möbius-Winkler, S., Hilberg, T., Menzel, K., Golla, E., Burman, A., Schuler, G. and Adams, V. (2009) 'Time-dependent mobilization of circulating progenitor cells during strenuous exercise in healthy individuals', *Journal of Applied Physiology*, 107(6), pp. 1943–1950. doi: 10.1152/japplphysiol.00532.2009.

Naeije, R. (2010) 'Physiological adaptation of the cardiovascular system to high altitude', *Progress in Cardiovascular Diseases*. Erasme University Hospital, Brussels, Belgium. rnaeije@ulb.ac.be <rnaeije@ulb.ac.be>, 52(6), pp. 456–466. doi: 10.1016/j.pcad.2010.03.004.

Newham, D. J., Jones, D. A., Ghosh, G. and Aurora, P. (1988) 'Muscle fatigue and pain after eccentric contractions at long and short length', *Clinical Science*, 74(5), pp. 553–557. doi: 10.1042/cs0740553.

Newham, D. J., McPhail, G., Mills, K. R. and Edwards, R. H. T. (1983) 'Ultrastructural changes after concentric and eccentric contractions of human muscle', *Journal of the Neurological Sciences*, 61, pp. 109–122. doi: 10.1016/0022-510X(83)90058-8.

Novakova, Z., Hubackova, S., Kosar, M., Janderova-Rossmeislova, L., Dobrovolna, J., Vasicova, P., Vancurova, M., Horejsi, Z., Hozak, P., Bartek, J. and Hodny, Z. (2010) 'Cytokine expression and signaling in drug-induced cellular

senescence', *Oncogene*, 29(2), pp. 273–284. doi: 10.1038/onc.2009.318.

Nyberg, P., Xie, L., Sugimoto, H., Colorado, P., Sund, M., Holthaus, K., Sudhakar, A., Salo, T. and Kalluri, R. (2008) 'Characterization of the anti-angiogenic properties of arresten , an α1β1 integrin-dependent collagen-derived tumor suppressor', *Experimental Cell Research*. Elsevier Inc., 314(18), pp. 3292–3305. doi: 10.1016/j.yexcr.2008.08.011.

Ordway, G. A. and Garry, D. (2004) 'Myoglobin: An essential hemoprotein in striated muscle', *Journal of Experimental Biology*, 207(20), pp. 3441–3446. doi: 10.1242/jeb.01172.

Page, S. G. and Huxley, H. E. (1963) 'Filament lengths in striated muscle', *Journal of Cell Biology*, 19(2), pp. 369–390. doi: 10.1083/jcb.19.2.369.

Panisello, P., Torrella, J. R., Esteva, S., Pagès, T. and Viscor, G. (2008) 'Capillary supply, fibre types and fibre morphometry in rat tibialis anterior and diaphragm muscles after intermittent exposure to hypobaric hypoxia', *European Journal of Applied Physiology*, 103(2), pp. 203–213. doi: 10.1007/s00421-008-0691-0.

Panisello, P., Torrella, J. R., Pagès, T. and Viscor, G. (2007) 'Capillary supply and fiber morphometry in rat myocardium after intermittent exposure to hypobaric hypoxia', *High Altitude Medicine and Biology*, 8(4), pp. 322–330. doi: 10.1089/ham.2007.1030.

Parasuraman, S., Raveendran, R. and Kesavan, R. (2010) 'Blood sample collection in small laboratory animals', *Journal of Pharmacology and Pharmacotherapeutics*, 1(2), pp. 87–93. doi: 10.4103/0976-500X.72350.

Parizkova, J. and Stankova, L. (1964) 'Influence of physical activity on a treadmill on the metabolism of adipose tissue in rats', *British Journal of Nutrition*, 18, pp. 325–32.

Patel, T. J., Cuizon, D., Mathieu-Costello, O., Fridén, J. and Lieber, R. L. (1998) 'Increased oxidative capacity does not protect skeletal muscle fibers from eccentric contraction-induced injury', *American Journal of Physiology - Regulatory, Integrative and Comparative Physiology*, 274(5), pp. R1300–R1308. Available at: http://ajpregu.physiology.org.liverpool.idm.oclc.org/content/274/5/R1300.full-text.pdf+html.

Peeze, B. F., Kuipers, H., Heymans, J., Frederik, P. M., Slaaf, D. W., Tangelder, G. J. and Reneman, R. S. (1989) 'Exercise-induced focal skeletal muscle fiber degeneration and capillary morphology', *Journal of Applied Physiology*, 66(6), pp. 2857–2865. Available at: http://jap.physiology.org.liverpool.idm.oclc.org/content/jap/66/6/2857.full.pdf.

Perry, S. V (1998) 'Troponin T: Genetics, properties and function', *Journal of Muscle Research and Cell Motility*, 19(6), pp. 575–602. doi: 10.1023/A:1005397501968.

Pette, D. and Staron, R. S. (2000) 'Myosin isoforms, muscle fiber types, and transitions', *Microscopy Research and Technique*, 50(6), pp. 500–509. doi: 10.1002/1097-0029(20000915)50:6<500::AID-JEMT7>3.0.CO;2-7.

Pickering, L., Pang, H., Biemann, K., Munro, H. and Schimmel, P. (1985) 'Two tissue-specific isozymes of creatine kinase have closely matched amino acid sequences', *Proceedings of the national academy of sciences of the United States of America*, 82(8), pp. 2310–2314. doi: 10.1073/pnas.82.8.2310.

Proctor, C. H. (2008) 'A simple definition of detection limit', *Journal of Agricultural, Biological, and Environmental Statistics*, 13(1), pp. 99–120. doi: 10.1198/jabes.2009.0008.

Proske, U. and Allen, T. J. (2005) 'Damage to skeletal muscle from eccentric exercise', *Exercise and Sport Sciences Reviews*, 33(2), pp. 98–104. doi: 10.1097/00003677-200504000-00007.

Qiagen (2012) *Complete list of pathway-focused arrays*, *SABiosciences*. Available at: http://www.sabiosciences.com/ArrayList.php.

Radahmadi, M., Alaei, H., Sharifi, M.-R. and Hosseini, N. (2013) 'The effect of synchronized runningactivity with chronic stress on passive avoidance learning and body weight in rats', *International Journal of Preventive Medicine*, 4(4), pp. 430–437. Available at: http://www.pubmedcentral.nih.gov/articlerender.fcgi?artid=3685161&tool=pmcentrez&rendertype=abstract.

Raj, A. and Van Oudenaarden, A. (2008) 'Nature, nurture, or chance: Stochastic gene expression and its consequences', *Cell*, 135(2), pp. 216–226. doi: 10.1016/j.cell.2008.09.050.

Rayment, I., Holden, H. M., Whittaker, M., Yohn, C. B., Lorenz, M., Holmes, K. and Milligan, R. A. (1993) 'Structure of the actin-myosin complex and its implications for muscle contraction', *Science*, 261(5117), pp. 58–65. doi: 10.1126/science.8316858.

Reinach, F. C., Farah, C. S., Monteiro, P. B. and Malnic, B. (1997) 'Structural interactions responsible for the assembly of the troponin complex on the muscle thin filament', *Cell Structure and Function*, 22(1), pp. 219–223. doi: 10.1247/csf.22.219.

Richalet, J.-P. and Gore, C. J. (2008) 'Live and/or sleep high:train low, using normobaric hypoxia', *Scandinavian Journal of Medicine and Science in Sports*, 18(Suppl 1), pp. 29–37. doi: 10.1111/j.1600-0838.2008.00830.x.

Rivera-Brown, A. M. and Frontera, W. R. (2012) 'Principles of exercise physiology: Responses to acute exercise and long-term adaptations to training', *PM and R*. Elsevier Inc., 4(11), pp. 797–804. doi: 10.1016/j.pmrj.2012.10.007.

Ríos, E., Ma, J. and González, A. (1991) 'The mechanical hypothesis of excitation-contraction (EC) coupling in skeletal muscle', *Journal of Muscle Research and Cell Motility*, 12(2), pp. 127–135. doi: 10.1007/BF01774031.

Rossi-Fanelli, A. and Antonini, E. (1956) 'Heterogeneity of human myoglobin', *Archives of Biochemistry and Biophysics*, 65(2), pp. 587–590. doi: 10.1016/0003-9861(56)90223-5.

Rotwein, P. and Wilson, E. M. (2009) 'Distinct actions of Akt1 and Akt2 in skeletal muscle differentiation', *Journal of Cellular Physiology*, 219(2), pp. 503–511. doi: 10.1002/jcp.21692.

Sakakima, H., Yoshida, Y., Sakae, K. and Motimoto, N. (2004) 'Different frequency treadmill running in immobilization-induced muscle atrophy and ankle joint contracture of rats', *Scandinavian Journal of Medicine & Science in Sports*, 14, pp. 186–192. doi: 10.1111/j.1600-0838.2004.00382.x.

Saltin, B. (1985) 'Hemodynamic adaptations to exercise', *The American Journal of Cardiology*, 55(10), pp. D42–D47. doi: 10.1016/0002-9149(85)91054-9.

Sayers, S. P. and Clarkson, P. M. (2003) 'Short-term immobilization after eccentric exercise. Part II: Creatine kinase and myoglobin', *Medicine & Science in Sports & Exercise*, 35(5), pp. 762–768. doi: 10.1249/01.MSS.0000064933.43824.ED.

Schmidt-Nielsen, K. and Duke, J. B. (1997) '1. Respiration', in *Animal physiology: Adaptation and environment*. 5th edn. Cambridge, United Kingdom: Cambridge University Press, pp. 6–13.

Self, D. A., Mandella, J. G., Prinzo, O. V., Forster, E. M. and Shaffstall, R. M. (2011) 'Physiological equivalence of normobaric and hypobaric exposures of humans to 25,000 feet (7620 m)', *Aviation Space and Environmental Medicine*, 82(2), pp. 97–103. doi: 10.3357/ASEM.2908.2011.

Sembello, W. J. and Gladfelter, W. E. (1974) 'Effect of hypothalamic lesions on the treadmill performance of rats', *Physiology and Behavior*, 13(5), pp. 603–607.

Serebrovskaya, T. V, Nikolsky, I. S., Nikolska, V. V, Mallet, R. T. and Ishchuk, V. A. (2011) 'Intermittent hypoxia mobilizes hematopoietic progenitors and augments cellular and humoral elements of innate immunity in adult men', *High Altitude Medicine and Biology*, 12(3), pp. 243–252. doi: 10.1089/ham.2010.1086.

Si, H. and Liu, D. (2009) 'Isoflavone genistein protects human vascular endothelial cells against tumor necrosis factor-alpha-induced apoptosis through the p38beta mitogen-activated protein kinase', *Apoptosis*, 14(1), pp. 66–76. doi: 10.1007/s10495-008-0283-9.

Siebenmann, C. and Lundby, C. (2015) 'Regulation of cardiac output in hypoxia', *Scandinavian Journal of Medicine & Science in Sports*, 25(Suppl), pp. 53–59. doi: 10.1111/sms.12619.

Slater, H., Arendt-Nielsen, L., Wright, A. and Graven-Nielsen, T. (2005) 'Sensory and motor effects of experimental muscle pain in patients with lateral epicondylalgia and controls with delayed onset muscle soreness', *Pain*, 114(1–2),

pp. 118–130. doi: 10.1016/j.pain.2004.12.003.

Squibb, R. E., Collier, G. H. and Squibb, R. L. (1977) 'Effect of treadmill speeds and slopes on voluntary exercise in rats', *Journal of Nutrition*, 107(11), pp. 1981–1984. Available at: http://www.ncbi.nlm.nih.gov/pubmed/908955.

Stuelsatz, P., Pouzoulet, F., Lamarre, Y., Dargelos, E., Poussard, S., Leibovitch, S., Cottin, P. and Veschambre, P. (2010) 'Down-regulation of MyoD by calpain 3 promotes generation of reserve cells in C2C12 myoblasts', *Journal of Biological Chemistry*, 285(17), pp. 12670–12683. doi: 10.1074/jbc.M109.063966.

Suarez, J., Alexander, J. K. and Houston, C. S. (1987) 'Enhanced left ventricular systolic performance at high altitude during operation everest II', *American Journal of Cardiology*, 60(1), pp. 137–142. doi: 10.1016/0002-9149(87)91000-9.

Takekura, H., Fujinami, N., Nishizawa, T., Ogasawara, H. and Kasuga, N. (2001) 'Eccentric exercise-induced morphological changes in the membrane systems involved in excitation-contraction coupling in rat skeletal muscle', *Journal of Physiology*, 533(2), pp. 571–583. doi: 10.1111/j.1469-7793.2001.0571a.x.

Talbot, J. A. and Morgan, D. L. (1998) 'The effects of stretch parameters on eccentric exercise-induced damage to toad skeletal muscle', *Journal of Muscle Research and Cell Motility*, 19(3), pp. 237–245. doi: 10.1023/A:1005325032106.

Taylor, C. R., Caldwell, S. L. and Rowntree, V. J. (1972) 'Running up and down hills: Some consequences of size', *Science*, 178(4065), pp. 1096–1097. doi: 10.1126/science.178.4065.1096.

Taylor, P. J., Betts, G. A., Maroulis, S., Gilissen, C., Pedersen, R. L., Mowat, D. R., Johnston, H. M. and Buckley, M. F. (2010) 'Dystrophin gene mutation location and the risk of cognitive impairment in duchenne muscular dystrophy', *PLoS ONE*, 5(1), pp. 1–9. doi: 10.1371/journal.pone.0008803.

Tekin, D., Dursun, A. D. and Ficicilar, H. (2008) 'The body weight performance relationship of rats on treadmill running', *Journal of Exercise Physiology Online*, 11(6), pp. 44–55. Available at: http://eds.b.ebscohost.com.ezproxy.liv.ac.uk/eds/pdfviewer/pdfviewer?sid=c5182843-2b4e-4751-af98-399b939bc028%40sessionmgr198&vid=6&hid=121.

Teodorczyk, M., Kleber, S., Wollny, D., Sefrin, J. P., Aykut, B., Mateos, A., Herhaus, P., Hill, O., Gieffers, C., Sykora, J., Weichert, W., Eisen, C., Trumpp, A., Bergmann, F. and Welsch, T. (2015) 'CD95 promotes metastatic spread via Sck in pancreatic ductal adenocarcinoma', *Cell death and differentation*, 22, pp. 1192–1202. doi: 10.1038/cdd.2014.217.

Terman, B. I. I., Dougher-Vermazen, M., Carrion, M. E. E., Dimitrov, D., Armellino, D. C. C., Gospodarowicz, D., Böhlen, P. and Bohlen, P. (1992) 'Identification of the KDR tyrosine kinase as a receptor for vascular endothelial cell growth factor', *Biochemical and Biophysical Research Communications*, 187(3), pp. 1579–1586. doi: 10.1016/0006-291X(92)90483-2.

Tian, T. (2013) 'Chemical memory reactions induced bursting dynamics in gene expression', *PLoS ONE*, 8(1), pp. 1–10. doi: 10.1371/journal.pone.0052029.

Tiidus, P. M., Brown, L., Brant, A., Enns, D. L. and Bryden, P. J. (2008) 'Physiological, sensory, and functional measures in a model of wrist muscle injury and recovery', *Physiotherapy Canada*, 60(1), pp. 30–39. doi: 10.3138/physio/60/1/30.

Tiidus, P. M., Holden, D., Bombardier, E., Zajchowski, S., Enns, D. L. and Belcastro, A. (2001) 'Estrogen effect on post-exercise skeletal muscle neutrophil infiltration and calpain activity', *Canadian Journal of Physiology and Pharmacology*, 79(5), pp. 400–406. doi: 10.1139/y01-011.

Tilgner, K., Wojciechowicz, K., Jahoda, C., Hutchison, C. and Markiewicz, E. (2009) 'Dynamic complexes of A-type lamins and emerin influence adipogenic capacity of the cell via nucleocytoplasmic distribution of beta-catenin', *Journal of Cell Science*, 122(3), pp. 401–413. doi: 10.1242/jcs.026179.

Tsumiyama, W., Oki, S., Umei, N., Shimizu, M. E., Ono, T. and Otsuka, A. (2014) 'Evaluation of the lactate threshold during downhill running in rats', *Journal of Physical Therapy Science*, 26(1), pp. 125–126. doi: 10.1589/jpts.26.125.

Viscor, G., Javierre, C., Pagès, T., Ventura, J.-L., Ricart, A., Martin-Henao, G., Azqueta, C. and Segura, R. (2009) 'Combined intermittent hypoxia and surface muscle electrostimulation as a method to increase peripheral blood

progenitor cell concentration', *Journal of Translational Medicine*, 7, pp. 91–97. doi: 10.1186/1479-5876-7-91\r1479-5876-7-91.

Walliman, T., Turner, D. C. and Eppenberger, H. M. (1977) 'Localization of creatine kinase isoenzyme in myofibrils. I. Chicken skeletal muscle', *Journal of Cell Biology*, 75(2), pp. 297–317. doi: 10.1083/jcb.75.2.297.

Wallimann, T., Wyss, M., Brdiczka, D., Nicolay, K. and Eppenberger, H. M. (1992) 'Intracellular compartmentation, structure and function of creatine kinase isoenzymes in tissues with high and fluctuating energy demands: the "phosphocreatine circuit" for cellular energy homeostasis', *Biochemical Journal*, 281(Pt 1), pp. 21–40. doi: 10.1042/bj2810021.

Warren, G. L., Hayes, D. A., Lowe, D. A. and Armstrong, R. B. (1993) 'Mechanical factors in the initiation of eccentric contraction-induced injury in rat soleus muscle', *Journal of Physiology*, 464(1), pp. 457–475. doi: 10.1113/jphysiol.1993.sp019645.

Warren, G. L., Ingalls, C. P., Lowe, D. A. and Armstrong, R. B. (2001) 'Excitation-contraction uncoupling: Major role in contraction-induced muscle injury', *Exercise and Sport Sciences Reviews*, 29(2), pp. 82–87. doi: 10.1097/00003677-200104000-00008.

West, B. L., Babbittt, P. C., Mendez, B. and Baxter, J. D. (1984) 'Creatine kinase protein sequence encoded by a cDNA made from Torpedo californica electric organ mRNA', *Proceedings of the national academy of sciences of the United States of America*, 81(22), pp. 7007–7011. doi: 10.1073/pnas.81.22.7007.

West, J. B. (2004) 'The physiologic basis of high-altitude diseases', *Annals of Internal Medicine*, 141(10), pp. 789–800. Available at: https://liverpool.idm.oclc.org/login?url=http://search.ebscohost.com/login.aspx?direct=true&db=edswsc&AN=000225206900006&site=eds-live&scope=site.

West, J. B., Schoene, R. B. and Milledge, J. S. (2007) *High altitude medicine and physiology*. 4th edn. London, United Kingdom: Hodder Arnold, an imprint of Hodder Education and a member of the Hodder Headline Group.

Wiedow, O. and Meyer-Hoffert, U. (2005) 'Neutrophil serine proteases: potential key regulators of cell signalling during inflammation', *Journal of Internal Medicine*, 257(4), pp. 319–328. doi: 10.1111/j.1365-2796.2005.01476.x.

Wilber, R. L. (2001) 'Current trends in altitude training', *Sports Medicine*, 31(4), pp. 249–265. doi: 10.2165/00007256-200131040-00002.

Wilkinson, J. M. and Grand, R. J. A. (1978) 'Comparison of amino acid sequence of troponin I from different striated muscles', *Nature*, 271, pp. 31–35. doi: 10.1038/271031a0.

Wisløff, U., Helgerud, J., Kemi, O. J. and Ellingsen, Ø. (2001) 'Intensity-controlled treadmill running in rats: VO(2 max) and cardiac hypertrophy', *American Journal of Physiology - Heart and Circulatory Physiology*, 280(3), pp. H1301–H1310. doi: 0363-6135/01.

Wittenberg, J. B. (1970) 'Myoglobin-facilitated oxygen diffusion: Role of myoglobin in oxygen entry into muscle', *Physiological Reviews*, 50(4), pp. 559–636.

Yang, M., Ma, C., Liu, S., Shao, Q., Gao, W., Song, B., Sun, J., Xie, Q., Zhang, Y., Feng, A., Liu, Y., Hu, W. and Qu, X. (2009) 'HIF-dependent induction of adenosine receptor A2b skews human dendritic cells to a Th2-stimulating phenotype under hypoxia', *Immunology and Cell Biology*, 88(2), pp. 165–171. doi: 10.1038/icb.2009.77.

Yeung, E. W., Balnave, C. D., Ballard, H. J., Bourreau, J.-P. and Allen, D. G. (2002) 'Development of T-tubular vacuoles in eccentrically damaged mouse muscle fibres', *Journal of Physiology*, 540(2), pp. 581–592. doi: 10.1113/jphysiol.2001.013839.

Yoshimura, A., Toyoda, Y., Murakami, T., Yoshizato, H., Ando, Y. and Fujitsuka, N. (2005) 'Glycogen depletion in intrafusal fibres in rats during short-duration high-intensity treadmill running', *Acta Physiologica Scandinavica*, 185(1), pp. 41–50. doi: 10.1111/j.1365-201X.2005.01455.x.

Zang, M., Hayne, C. and Luo, Z. (2002) 'Interaction between active Pak1 and Raf-1 is necessary for phosphorylation and activation of Raf-1', *Journal of Biological Chemistry*, 277(6), pp. 4395–4405. doi: 10.1074/jbc.M110000200.

Appendices

Appendix A — Documents

Appendix A.1 The Ethical Approval for Using Experimental Animals

UNIVERSITAT DE BARCELONA

C.E.E.A
(Comitè Ètic d'Experimentació Animal)

Parc Científic de Barcelona
Baldiri i reixac 10-12
08028 Barcelona
Tel. 93.403.72.58
ceea@giga.sct.ub.es

2 9 GEN. 2010

39/10

INFORME DEL COMITÉ ÉTICO DE EXPERIMENTACIÓN ANIMAL

EL abajo firmante, Sr. Alvaro Gimeno Sandig, Secretario del Comité Ético de Experimentación Animal de la Universidad de Barcelona, **HACE CONSTAR:**

Que el Comité Ético de Experimentación Animal ha analizado la documentación correspondiente al proyecto de investigación **¿Puede la hipoxia intermitente contribuir a la reparación tisular?. ,** cuyo/a investigador/a principal es el/ la **Dr/a. Ginés Viscor Carraco.**

Este Comité entiende que dicha documentación se ajusta a las normas éticas esenciales y a la legislación vigente y, por tanto, ha acordado emitir un informe favorable al respecto.

Lo cual firma a los efectos oportunos.

UNIVERSITAT DE BARCELONA
Comitè Ètic d'Experimentació Animal

Barcelona, 29 de Enero del 2010

Fig. ApxA - 1. Scan of the ethical approval to use experimental animals for project in question which extends to all subprojects, including subproject DEP2010-22205-C02-01.

Appendix A.2 Janvier Lab's Research Model Sheet for Rat Subjects

RESEARCH MODELS

Rats | Mice | Other rodents

SPRAGUE DAWLEY® Rat

- **Strain name:** RjHan:SD
- **Type:** Outbred rat
- **Origin:** Zentralinstitut für Versuchstierzucht (Hannover) - 1982
- **Colour and related genotype:** Albino rat - *Tyr^c/Tyr^c*
- **Breeding:** Good breeder, strong maternal instinct

Description of our model

The strain was created by R. W. Dawley in 1925, from a hooded male hybrid of unknown origin and an albino female (probably Wistar), and was crossed with the female's progeny for 7 generations. The **SPRAGUE DAWLEY®** rat is an albino outbred rat with an elongated head and a tail that is longer than its body.

A fast growing rat, it is docile and easy to handle.

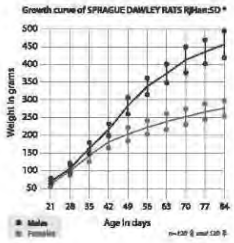

Hematological parameters* of 10-week old SPRAGUE DAWLEY® RjHan:SD rats

Parameters	Male	Female
Erythrocytes (10^6/l)	8.5 ± 0.4	8.7 ± 0.2
Hematocrit (l/l)	0.55 ± 0.02	0.55 ± 0.03
Hemoglobin (g/dl)	15.4 ± 0.5	15.7 ± 0.8
Mean corpuscular volume (fl)	65 ± 3	63 ± 1
Mean corpuscular rate (pg)	18.2 ± 0.7	18.0 ± 0.5
Hemoglobin concentration (g/dl)	28 ± 1	29 ± 1
Blood platelets (10^9/l)	761 ± 153	751 ± 210
Leukocytes (10^9/l)	11.5 ± 2.7	11.5 ± 2.7
Neutrophils (10^9/l)	1.56 ± 0.49	1.36 ± 0.37
Lymphocytes (10^9/l)	9.35 ± 2.15	9.62 ± 2.39
Eosinophils (10^9/l)	0.14 ± 0.03	0.15 ± 0.06
Monocytes (10^9/l)	0.31 ± 0.17	0.24 ± 0.10
Basophils (10^9/l)	0.11 ± 0.03	0.12 ± 0.03

Reproductive data*

Monogamous mating according Robertson System	
Litter size at birth	11.9
Weaning %	94.5
Productivity index	3
Sterility %	2
Gestation time	Between 20 and 23 days • D20: 1 % • D21: 16 % • D22: 77 % • D23: 6 %

Biochemical blood parameters* of 10-week old SPRAGUE DAWLEY® RjHan:SD rats

Parameters	Male	Female
Glucose (g/l)	1.6 ± 0.1	2.1 ± 0.2
Urea (g/l)	0.4 ± 0.1	0.6 ± 0.1
AST (ASAT) (UI/l)	160 ± 37	109 ± 17
ALT (ALAT) (UI/l)	71 ± 10	55 ± 16
Alkaline phosphatase (UI/l)	357 ± 60	92 ± 25
Cholesterolaemia (g/l)	0.9 ± 0.1	1.1 ± 0.1
Triglycerides (g/l)	1.5 ± 0.4	2.1 ± 0.5
Creatinine (mg/l)	6.1 ± 0.3	5.3 ± 0.8

* JANVIER LABS 2011 Data for an indicative basis

JANVIER LABS
Rodent research models & associated services

www.janvier-labs.com

Main application and research fields

- Experimental surgery
- General studies
- Metabolism, nutrition
- Neurology
- Oncology
- Pharmacology
- Physiology, ageing
- Teratology
- Toxicology

Our added value

- The « JANVIER LABS Genetic Policy », a specific programme, guarantees less than 1% inbreeding per generation.
- Animals with the SPF or SOPF standards.
- A gentling policy for docile and easy-to-handle animals.
- Optimal stability conditions of our models during shipments, thanks to our dedicated and internal transport service.
- A scientific support with a team of Veterinarians and PhD.

Our additional offer

Laboratory Services | Transgenic Services

The available scientific bibliography:

Research has been conducted, all over the world, from models bred in our laboratories.
Discover our updated bibliography of available studies on our Internet **website, heading: Customer Support.**

2013-06-ENG-RM-03

Appendix B — Operational Protocols

Appendix B.1 Rat Handling Protocol

Doc. Title:	**Rat Handling (Ref Db 3)**			Project:	DEP2010-22205-C02-01
Doc. No.:	QGR/101.065.005	Doc. Type:	Protocol	Sector:	333(41)
Doc. Version:	2.1	Revision Date:	2013.04.23	DEV-1:	G Viscor
Version Date:	2013.04.23	Revision by:	JG Rios	DEV-2:	JG Rios
Editor:	JG Rios	Next Revision:	2013.06.28	Page:	1 of 1

Procedure:
Parameters:

General Notes

A This protocol describes the defined process of handling the rats whilst within the FEH-lab's housing, with the goal of making a subsequent anaesthetic process for sampling less stressful for the rat.

B All sort of registration and observation must appear on this protocol's corresponding document no. QGR/101.066.010.

C The actions in this protocol should be carried out every working day, with the exception of the days of Ref Db 2 which by itself is enough handling.

Guide

Registering the rat's reaction in the following phases:

0

Calm:	Calm body position; Calm reaction to all sorts of manipulation; No stress.
Curious/Calm:	Exploring environment in a calm way; No stress.
Curious/fright:	Exploring environment in fright; Distracted because of stress.
Stressed:	Stressed body position; Reacts with stressful body reaction to manipulation; Urinates and disposes faeces.
Very Stressed:	Complains to every manipulation; Stressful body reactions; Urinates and disposes faeces; Nibbles on agent's skin.
Aggressive:	Complains with a force; Intents to bite; Reacts harshly.

Phase A – Getting the rat out of the cage.

1 Register which rat you will be opting for and register other principal data.
2 Put your hand in the cage and let the rat/rats smell your existence.
3 Calmly put your palm closer to the rat. Cradle the rat in your palm whilst lifting it out of the cage.
4 Register how the rat responds.

Phase B – Basic manipulation.

5 Place the rat on your forearm and see if you need to hold it back on its tail or not.
6 Pat or stroke the rat softly and communicate with the rat.
7 Cradle the rat in your palms and lift it towards your face
8 Register the overall rat's reaction.

Phase C – Second phase manipulation.

9 Put the rat's hind limbs in one palm and hold them down, and put the thumb and the index finger, of the other hand, around the torso below the fore limbs.
10 Stretch the torso vertically. Stroke its belly calmly if needed.
11 Register the overall rat's reaction.

Phase D – Pre-anaesthetic manipulation.

12 Repeat actions in note 9 and 10.
13 Make sure that the tail is hold down in with the "palm"-hand.
14 Put thumb and index finger above elbow on each forelimb and push them upwards and crosswise.
15 If possible (with a second person) calmly poke the rat on i.p. zone, to imitate an i.p. anaesthesia. Stroke its belly, talk calmly or blow gently onto its face if needed.
16 Register the overall rat's reaction.

Phase E – Putting the rat back to the cage.

17 Take the rat into your palm.
18 Communicate and stroke it calmly.
19 Put it into its cage.

□

Appendix B.2 Treadmill Preparation Stage Protocol

Doc. Title:	**Rat Preconditioning on a Treadmill**			Project:	DEP2010-22205-C02-01
Doc. No.:	QGR/**101.055.001**	Doc. Type:	**Protocol**	Sector:	333(41)
Doc. Version:	2.1	Revision Date:	2013.06.26	DEV-1:	Ginés Viscor
Version Date:	2013.06.26	Revision by:	J G Ríos	DEV-2:	J G Ríos
Editor:	J G Ríos	Next Revision:	2014.06.26	Page:	1 of 2
Procedure:	QGR/101.051.002				
Parameters:	d, day (d); a, acceleration (cm s^{-1} min^{-1}); t, time (min); u, velocity (cm s^{-1}); I, current (mA); T, temperature (°C)				

General Notes

A This protocol describes the process of: getting rats used to the environment of a treadmill; to comprehend necessity to run whilst the treadmill's belt moves; and, to run continuously at 45 cm s^{-1}.

B All sort of registrations and observations must appear on this protocol's corresponding document, no. QGR/101.056.001, a part from the reward registration which must appear on a dedicated document no. QGR/101.066.013.

C The protocol is set up for a training lot of maximum five rats on a 5-channel treadmill, but can be used for one rat on a 1-channel treadmill as well without any changes.

D The first 4 days of the programme include one session per day (called session A), and the rest of the days with two sessions per day, where the former one should be performed in the morning, session A, and the latter one in the afternoon, session B, with a minimum of 6 h rest between the end of session A and the beginning of session B.

E The exercise schedule should be followed precisely with changes in the current's intensity depending on 'the fitness level' of the worst performer in the training lot. The range of allowed intensity changes over the entire preconditioning process and of the initial intensity (I_i), should never be lower than I_{min} nor higher than I_{max} according to the schedule below. Furthermore, the intensity shouldn't either be lower than the last change in the intensity ($I_{u\,new}$) from the previous session ($I_{u\,prev}$).

F It is necessary to be familiar with the protocol of running style classification (QGR/101.055.010), actions to difficult training (QGR/101.055.052), actions to treadmill malfunction (QGR/101.055.053), and rewarding rats (QGR/101.065.007) to carry out an exercise session successfully.

Exercise Schedule

	phase 0		phase I			phase II			phase III		phase IV		summary				cubicle/channel				
Day	t_0	u_0	$(t_a)_1$	u_1	a_1	$(t_a)_2$	u_2	a_2	t_3	u_3	t_4	u_4	$t_{exerc.}$	t_{total}	I_{min}	I_{max}	Rat's position				
No.	min	cm s^{-1}	min	cm s^{-1}	cm s^{-1} min^{-1}	min	cm s^{-1}	cm s^{-1} min^{-1}	min	cm s^{-1}	min	cm s^{-1}	min	min	mA	mA	**1**	**2**	**3**	**4**	**5**
1A	10.0	0 (5)	0	0	0	0	0	0	0	0	0	0	0	10	0.2	0.6	i	ii	iii	iv	v
2A	10.0	0 (5)	0	0	0	0	0	0	0	0	0	0	0	10	0.2	0.6	v	i	ii	iii	iv
3A	3.5	0 (5)	5.0	10-30	~4	0	0	0	10.0	30	2.0	0	15	20.5	0.2	0.6	iv	v	i	ii	iii
4A	3.0	0 (5)	5.0	10-30	~4	0	0	0	15.0	30	2.0	0	20	25	0.2	0.6	iii	iv	v	i	ii
5A	2.0	0 (5)	5.0	15-30	~3	2.0	30-34	2	25.0	34	2.0	0	32	36	0.2	0.6	ii	iii	iv	v	i
5B	2.0	0 (5)	5.0	15-30	~3	2.0	30-34	2	25.0	34	2.0	0	32	36	0.2	0.6	i	ii	iii	iv	v
6A	2.0	0 (5)	5.0	15-30	~3	2.0	30-35	~2	30.0	35	2.0	0	37	41	0.2	0.8	v	i	ii	iii	iv
6B	2.0	0 (5)	5.0	15-30	~3	2.0	30-35	~2	30.0	35	2.0	0	37	41	0.2	0.8	iv	v	i	ii	iii
7A	1.0	0 (5)	5.0	15-30	~3	3.0	30-40	~3	32.0	40	2.0	0	40	43	0.2	0.8	iii	iv	v	i	ii
7B	1.0	0 (5)	5.0	15-30	~3	3.0	30-40	~3	32.0	40	2.0	0	40	43	0.2	0.8	ii	iii	iv	v	i
8A	1.0	0 (5)	5.0	15-30	~3	3.0	30-40	~3	32.0	40	2.0	0	40	43	0.4	0.8	i	ii	iii	iv	v
8B	1.0	0 (5)	5.0	15-30	~3	3.0	30-40	~3	32.0	40	2.0	0	40	43	0.4	0.8	v	i	ii	iii	iv
9A	1.0	0 (5)	5.0	15-30	~3	3.0	30-40	~3	32.0	40	2.0	0	40	43	0.4	1.0	iv	v	i	ii	iii
9B	1.0	0 (5)	5.0	15-35	~4	3.0	35-45	~3	32.0	45	2.0	0	40	43	0.4	1.0	iii	iv	v	i	ii
10A	1.0	0 (5)	5.0	15-35	~4	3.0	35-45	~3	32.0	45	2.0	0	40	43	0.4	1.0	ii	iii	iv	v	i
10B	1.0	0 (5)	5.0	15-35	~4	2.0	35-45	5	30.0	45	2.0	0	37	40	0.4	1.0	i	ii	iii	iv	v

Doc. Title:	**Rat Preconditioning on a Treadmill**			Project:	DEP2010-22205-C02-01
Doc. No.:	**QGR/101.055.001**	Doc. Type:	**Protocol**	Sector:	333(41)
Doc. Version:	2.1	Revision Date:	2013.06.26	DEV-1	Ginés Viscor
Version Date:	2013.06.26	Revision by:	J G Ríos	DEV-2:	J G Ríos
Editor:	J G Ríos	Next Revision:	2014.06.26	Page:	2 of 2
Procedure:	QGR/101.051.002				
Parameters:	d, day (d); a, acceleration (cm s^{-1} min^{-1}); t, time (min); u, velocity (cm s^{-1}); I, current (mA); T, temperature (°C)				

Guide

1. Register all settings, conditions, and initial parameters along with the Rat ID number for each cubicle.
2. Place each rats in its scheduled cubicle, and register the exact time when the exercise starts.
3. All changes in the current's intensity should be registered as: I(*mm:ss*) = x mA, where *mm:ss* are the minutes and seconds into the session of the actual change, and x is the new intensity value.
4. All observations that are considered necessary to register with respect to time should be registered as: t(*mm:ss*): *text*, where *mm:ss* are the minutes and seconds into the session of the actual occurrence, and "*text*" represents the actual observation.
5. During phase 0, have the motor unplugged and plugged it in to initiate phase I.
6. All velocity changes during phase I and phase II should be carried out as smoothly as possible.
7. During each session, the number of shocks (Number-S) for each rat should be registered after each phase, according to the exercise schedule, and about every 5 minutes during phase III, according to the registration table below.
8. Make notes on the running style of each rat during the session according protocol QGR/101.055.010.
9. At the end of phase III, after lowering the velocity, unplug the motor, and register the Distance (Dist.) and then the number of shock (Number-S).
10. After phase IV, press the red stop button on the treadmill monitor and register the number of shocks (Number-S), the total time of shocks (Time-S), the room temperature (T_f) and the relative humidity (RH_f), and register the intensity level as it is left after the session ($I_{4\,new}$).
11. Reward the rats that performed accordingly with a special food reward whilst in the treadmill cubicles linking the reward with the sound of the specified bell. (Protocol QGR/101.065.007).
12. Register how the rats reacted to the reward on the dedicated sheet QGR/101.066.013.
13. Place each rat in its cage and clean the treadmill. The treadmill needs to be cleaned between sessions A and B, as well as after the last session of each day.
14. Make sure all parameters necessary for the registration have been accounted for on the registration sheet and sign for the registration.

Registration Table

Day No.	1A/2A	3A	4A	5A/B	6A/B	7A/B, 8A/B, 9A/B, 10A	10B
phase 0	10.0	3.5	3.0	2.0	2.0	1.0	1.0
phase I	-	8.5	8.0	7.0	7.0	6.0	6.0
phase II	-	-	-	9.0	9.0	9.0	8.0
phase III	-	14.0	10.0	15.0	15.0	15.0	15.0
	-	18.5	15.0	20.0	20.0	20.0	20.0
	-	-	23.0	25.0	25.0	25.0	25.0
	-	-	-	30.0	30.0	30.0	30.0
	-	-	-	34.0	35.0	35.0	35.0
	-	-	-	-	39.0	41.0	38.0
phase IV	10.0	20.5	25.0	36.0	41.0	43.0	40.0

i The Registration Table explains at what minute a registration should be performed during each session. Note that that some patterns with respect to minutes is the same between some days – This however, does not mean that these time changes between certain days correspond to changes in, e.g., in velocity, acceleration, etc, according to the Exercise Schedule. Therefore, the setup for each session should be revised individually.

□

Appendix B.3 Treadmill Training Stage Protocol

Doc. Title:	**Rat Exercise Training on a Treadmill**			Project:	DEP2010-22205-C02-01
Doc. No.:	**QGR/101.055.002**	Doc. Type:	**Protocol**	Sector:	333(41)
Doc. Version:	2.1	Revision Date:	2013.06.26	DEV-1:	Ginés Viscor
Version Date:	2013.06.26	Revision by:	J G Ríos	DEV-2:	J G Ríos
Editor:	J G Ríos	Next Revision:	2014.06.26	Page:	1 of 2
Procedure:	QGR/101.051.002				
Parameters:	d, day (d); a, acceleration (cm s^{-1} min^{-1}); t, time (min); υ, velocity (cm s^{-1}); I, current (mA); T, temperature (°C).				

General Notes

A This protocol describes the exercise schedule of a single session but should be performed twice a day, with one session in the morning, session A, and one session in the afternoon, session B, where a strict minimum of 6 h rest between the end of session A and the beginning of session B should be included.

B All sort of registrations and observations must appear on this protocol's corresponding document, no. QGR/101.056.002, a part from the reward registration which must appear on a dedicated document no. QGR/101.066.013.

C The protocol is set up for a training lot of maximum five rats on a 5-channel treadmill, but can be used for one rat on a 1-channel treadmill as well without any changes.

D The day count continues from the last day of the preconditioning period (*protocol QGR/101.055.001*), only counting the days when the protocol is carried out.

E The exercise schedule should be followed precisely where changes in the intensity level of the current are the only ones allowed. The initial intensity (I_i) should be the same as the last change applied ($I_{u\,prev}$) in the previous session. Neither the initial intensity nor any other changes in the intensity during each session can be lower than I_{min} nor higher than I_{max} (with reference to the exercise schedule).

F It is necessary to be familiar with the protocol of running style classification (QGR/101.055.010), actions to difficult training (QGR/101.055.052), actions to treadmill malfunction (QGR/101.055.053), and rewarding rats (QGR/101.065.007) to carry out an exercise session successfully.

Exercise Schedule

	phase I			phase III		phase IV		summary		current	
Session	$(t_s)_1$	u_1	a_1	t_3	u_3	t_4	u_4	$t_{exerc.}$	t_{total}	I_{min}	I_{max}
	min	cm s^{-1}	cm s^{-1} min^{-1}	min	cm s^{-1}	min	cm s^{-1}	min	min	mA	mA
A & B	5	25-45	~ 5	30	45	1	0	35	36	0.8	1.8

Guide

1 Register all settings, conditions, and initial parameters along with the Rat ID number for each cubicle.

2 Place the rats in the cubicles, and register the exact time when the exercise starts.

3 All changes in the current's intensity should be registered as: I(*mm:ss*) = *x* mA, where *mm:ss* are the minutes and seconds into the session of the actual change, and *x* is the new intensity value.

4 All observations that are considered necessary to register with respect to time should be registered as: t(*mm:ss*): *text*, where *mm:ss* are the minutes and seconds into the session of the actual occurrence, and "*text*" represents the actual observation.

5 Make careful notes on the running style of each rat during the session according protocol QGR/101.055.010.

6 All velocity changes during phase I, according to step 7, should be carried out as smoothly as possible.

7 Carry out the following velocity changes during phase I:

[0 → 1] min: [5 → 25 → 30] cm s^{-1}
[1 → 2] min: 30 cm s^{-1}
[2 → 3] min: [30 → 35] cm s^{-1}
[3 → 4] min: [35 → 40] cm s^{-1}
[4 → 5] min: [40 → 45] cm s^{-1} ← *5th minute, End of phase I*
[5 → 35] min: 45 cm s^{-1}
[35 → 36] min: 0 cm s^{-1} ← *manually turn the velocity down before stopping it completely*

8 After phase I and every 5 minutes during phase III, register the number of shocks (Number-S) for each rat.

Doc. Title:	Rat Exercise Training on a Treadmill			Project:	DEP2010-22205-C02-01
Doc. No.:	QGR/**101.055.002**	Doc. Type:	Protocol	Sector:	333(41)
Doc. Version:	2.1	Revision Date:	2013.06.26	DEV-1:	Ginés Viscor
Version Date:	2013.06.26	Revision by:	J G Ríos	DEV-2:	J G Ríos
Editor:	J G Ríos	Next Revision:	2014.06.26	Page:	2 of 2
Procedure:	QGR/101.051.002				
Parameters:	d, day (d); a, acceleration (cm s^{-1} min^{-1}); t, time (min); u, velocity (cm s^{-1}); I, current (mA); T, temperature (ºC).				

9 At the end of phase III (35th minute), after lowering the velocity, unplug the motor, register the Distance (Dist.) and then the number of shocks (Number-S).

10 After phase IV (36th minute), press the red stop button on the treadmill monitor and register the number of shocks (Number-S), the total time of shocks (Time-S), the room temperature (T_r) and relative humidity (RH_r), and register the intensity level as it is left after the session ($I_{u,new}$).

11 Reward the rats that performed accordingly with the special food reward whilst in the treadmill cubicles, and link the reward with the sound of the specified bell. (Protocol QGR/101.065.007).

12 Register how the rats reacted to the reward on the dedicated sheet QGR/101.066.013.

13 Place each rat in its cage and clean the treadmill. The treadmill needs to be cleaned between sessions A and B, as well as after the last session of each day.

14 Make sure all parameters necessary for the registration have been accounted for on the registration sheet and sign for the registration.

Appendix B.4 Treadmill Muscle Damage Induction Protocol

Doc. Title:	**Rat Muscle Damage (Induced) on a Treadmill**			Project:	DEP2010-22205-C02-01
Doc. No.:	QGR/**101.055.003**	Doc. Type:	Protocol	Sector:	333(41)
Doc. Version:	2.1	Revision Date:	2013.06.26	DEV-1:	Ginés Viscor
Version Date:	2013.06.26	Revision by:	J G Ríos	DEV-2:	J G Ríos
Editor:	J G Ríos	Next Revision:	2014.06.26	Page:	1 of 2

Procedure:	QGR/101.051.002
Parameters:	d, day (d); a, acceleration (cm s^{-1} min^{-1}); t, time (min); u, velocity (cm s^{-1}); I, current (mA); T, temperature (ºC).

General Notes

A This protocol describes a single session of an eccentric exercise for rats on a treadmill to induce a muscle damage. It should be carried twice the same day; one session in the morning, session A, and one session in the afternoon, session B, with a strict minimum of 4-h rest between the end of session A and the beginning of session B.

B All sort of registrations and observations must appear on this protocol's corresponding document, no. QGR/101.056.003, a part from weight registration on document no. QGR/101.066.009 and the reward registration on document no. QGR/101.066.013.

C The protocol is set up for a training lot of maximum five rats on a 5-channel treadmill, but can be used for one rat on a 1-channel treadmill as well without any changes.

D The day of the muscle damage protocol is referred to as day D, for damage.

E The exercise schedule should be followed precisely with changes in the intensity level of the current depending on 'the fitness level' of the worst performer. Note that the first 5 minutes are used to adjust the slant level from 0° to −15°.

F Depending on the overall 'fitness level' of the rats trained together, the velocity can be increased to the range of 55 cm s^{-1} to 70 cm s^{-1} during the course of a session. Furthermore, if a session has reached ≈ 2 h, and the rats still do not show any sign of muscle damage, the velocity can be change constantly between 45 cm s^{-1} and 80 cm s^{-1}, oscillating between the two extremes. Both alternations need to be registered on the corresponding registration sheet if applied.

G The duration of the session depends on the rats individually. Once each rat (in its own time) is not able to continue running due to muscle damage it should be removed from the treadmill as quickly as possible.

H It is necessary to be familiar with the protocol of running style classification (QGR/101.055.010), actions to difficult training (QGR/101.055.052), actions to treadmill malfunction (QGR/101.055.053), and knowing of rewarding rats (QGR/101.065.007) to carry out an exercise session successfully.

Exercise Schedule

phase 0			phase I				phase III			current	
t_0	u_0	ϕ_0	$(t_a)_1$	a_1	u_1	ϕ_1	t_3	u_3	ϕ_3	I_{min}	I_{max}
min	cm s^{-1}	°	min	cm s^{-1} min^{-1}	cm s^{-1}	°	min	cm s^{-1}	°	mA	mA
1	0 (5)	0	5	5	20-50	0-(−15)	x	50	−15	1.2	1.8

Guide

1 Register all settings, conditions, and initial parameters along with the Rat ID number for each cubicle.

2 Each rat needs to be weighed before the session, registered on document QGR/101.066.009.

3 Place the rats in the cubicles, register the exact time when the exercise starts, and the room temperature (T_i) and the relative humidity (RH_i).

4 Carry out the first 100 minutes with reference to the black letters in the time-column of the registration document (QGR/101.056.003). After that start timing with a stop watch, as the controller has only the capacity of 99 min and 59 s, and continue the registry on an new sheet but with reference to the grey letters in the time-column of the document (QGR/101.056.003).

5 All changes in the current's intensity should be registered as: I(*mm:ss*) = x mA, where *mm:ss* are the minutes and seconds into the session of the actual change, and x is the new intensity value.

6 All changes in velocity should be registered as: v(*mm:ss*) = x cm s^{-1}, where *mm:ss* are the minutes and seconds into the session of the actual change, and x is the new intensity value. Oscillating changes should be registered as: v($mm_1 \rightarrow mm_2$) = $x_1 \rightarrow x_2$ cm s^{-1}, where the changes are carried out between minute mm_1 and mm_2 (with reference to the duration of the session) and changes in velocity are oscillating between x_1 and x_2 cm s^{-1}.

Doc. Title:	**Rat Muscle Damage (Induced) on a Treadmill**			Project:	DEP2010-22205-C02-01
Doc. No.:	QGR/**101.055.003**	Doc. Type:	Protocol	Sector:	333(41)
Doc. Version:	2.1	Revision Date:	2013.06.26	DEV-1:	Ginés Viscor
Version Date:	2013.06.26	Revision by:	J G Ríos	DEV-2:	J G Ríos
Editor:	J G Ríos	Next Revision:	2014.06.26	Page:	2 of 2

FEH·lab

Procedure: QGR/101.051.002

Parameters: d, day (d); a, acceleration (cm s^{-1} min^{-1}); t, time (min); u, velocity (cm s^{-1}); I, current (mA); T, temperature (°C).

7 All observations that are considered necessary to register with respect to time should be registered as: t(*mm:ss*): *text*, where *mm:ss* are the minutes and seconds into the session of the actual occurrence, and "*text*" represents the actual observation.

8 Make careful notes on the running style of each rat during the session according protocol QGR/101.055.010.

9 Whilst performing according to the exercise schedule, do the following in phase I:

t	u	ϕ	
[0 → 1] min:	0 cm s^{-1}	0°	← *1st minute, End of phase 0*
[1 → 2] min:	[5 → 25 → 30] cm s^{-1}	0°	
[2 → 3] min:	[30 → 35 → 40] cm s^{-1}	[0 → -5]°	
[3 → 4] min:	[40 → 45] cm s^{-1}	[-5 → -10]°	
[4 → 5] min:	[45 → 50] cm s^{-1}	[-10 → -15]°	
[5 → x] min:	50 cm s^{-1}	-15°	← *6th minute, End of phase I*

10 After phase I and every 10 minutes during phase III, register the number of shocks (Number-S) for each rat. It is absolutely necessary to force the rats to run with every trick possible, until muscle damage is clearly visible (and if not that, until an absolutely complete exhaustion).

11 When each rat (in its own time) cannot run anymore, quickly remove it from the treadmill, register the running time, the Distance (Dist.) and then the number of shock (Number-S).

12 When each rat has finished its session, it needs to be weighed again. (QGR/101.066.009).

13 Reward the rats that performed accordingly, several minutes after they have finished (or until they do not show sign of tiredness), with the special food reward whilst in their cages and link the reward with the sound of the specified bell. (Protocol QGR/101.065.007).

14 Register how the rats reacted to the reward on the dedicated sheet QGR/101.066.013.

15 Register the room temperature (T_f) and the relative humidity (RH_f).

16 After 'the last rat standing/running' has finished, clean the treadmill. The treadmill needs to be cleaned between sessions A and B, as well as after the last session of each day.

17 Make sure all parameters necessary for the registration have been accounted for on the registration sheet and sign for the registration.

□

Appendix B.5 Recovery Period's Intermittent Hypoxia Session Protocol

Doc. Title:	**Rat Intermittent Hypoxia Session**			Project:	DEP2010-22205-C02-01
Doc. No.:	QGR/**101.055.004**	Doc. Type:	Protocol	Sector:	332(40)
Doc. Version:	1.4	Revision Date:	2013.06.26	DEV-1:	Ginés Viscor
Version Date:	2013.06.26	Revision by:	J G Ríos	DEV-2:	J G Ríos
Editor:	J G Ríos	Next Revision:	2014.06.26	Page:	1 of 2
Procedure:	QGR/101.051.002				
Parameters:					

General Notes

A This protocol describes a single intermittent hypoxia treatment session of 4 hours in a hypobaric chamber, simulating the altitude of 4000 m (462 torr), and should be performed once a day (working day) until sampling.

B All sort of registrations and observations must appear on this protocol's corresponding document no. QGR/101.056.004.

C The day count starts one day after the induced muscle damage (*protocol QGR/101.055.003*) with H1, then H2, H3, etc., only counting the days when the protocol is carried out.

D The change from normal pressure (sea level) to 462 torr should be carried out according to the Delta Pressure Plan. This plan takes 15 min, however the allowed range for the time duration is from 12 to 18 min, ie, 15 (±3) min.

E The duration of the session is 15 min + 4 h + 15 min = 4.5 h in total, although the 15-minutes can vary according to the General Note D.

F Rat cages with control rats of the same lot should be placed on top of the hypobaric chamber whilst the session is ongoing.

Guide

1 Register all initial settings and parameters.

2 Remove water bottle from the cage/cages and replace it with small bowl of water.

3 If more than one cage needs to be in the chamber, then each cage has its own registration sheet.

4 Weigh the feed before the treatment and register.

5 Place the cage/cages inside the chamber.

6 The general operation procedure for a hypobaric session is described in protocol QGR/101.035.014, with the addition of The Delta Pressure Plans for this particular protocol (below).

7 Follow the Delta Pressure Plan I to perform pressure changes that simulate 0 m to 4000 m.

8 Register the initial time/hour in the end time for this pressure plan.

9 When the pressure of 462 torr has been reached, the 4 h session can begin.

10 Remember to place the cage/cages with the control rats of the same lot on top of the chamber.

11 When 4 h of the treatment have passed, turn off the pump and follow the Delta Pressure Plan II to perform pressure changes that simulate 4000 m to 0 m. (Use the ventilator valve to affect the pressure change)

12 Register the initial time/hour for Delta Pressure Plan II in the "end time" on the registration sheet.

13 Meanwhile the process of the Delta Pressure Plan II is taking place, the cages on top of the chamber can be removed and the straps that hold the lid can be loosened.

14 It is important to remove the ventilator valve, the filtration tube and the sensor after each session.

15 Remove the cage/cages form the inside of the chamber and clean the rubber floor with alcohol.

16 Replace the water bowl with the water bottle and clean the bowl.

17 Reweigh the feed for the rats that were inside the chamber and register.

18 Make sure all parameters necessary for the registration have been accounted for on the registration sheet and sign for the registration.

The Delta Pressure Plan

Next page ...

Doc. Title:	**Rat Intermittent Hypoxia Session**			Project:	DEP2010-22205-C02-01
Doc. No.:	QGR/**101.055.004**	Doc. Type:	Protocol	Sector:	332(40)
Doc. Version:	1.4	Revision Date:	2013.06.26	DEV-1:	Ginés Viscor
Version Date:	2013.06.26	Revision by:	J G Ríos	DEV-2:	J G Ríos
Editor:	J G Ríos	Next Revision:	2014.06.26	Page:	2 of 2
Procedure:	QGR/101.051.002				
Parameters:					

The Delta Pressure Plan

The subsequent table describes two plans to follow when controlling the pressure increase or decrease, where the decrease reflects a simulation of an altitude change from 0 m to 4000 m and is called the Delta Pressure Plan I (ΔP_I); and the increase reflects a simulation of an altitude change from 4000 m to 0 m and is called Delta Pressure Plan II (ΔP_{II}).

Δt	ΔP_i	Δt	ΔP_{ii}
[0 → 1] min:	[750-740 → 724] torr	[0 → 1] min:	[462 → 477] torr
[1 → 2] min:	[724 → 705] torr	[1 → 2] min:	[477 → 496] torr
[2 → 3] min:	[705 → 686] torr	[2 → 3] min:	[496 → 515] torr
[3 → 4] min:	[686 → 667] torr	[3 → 4] min:	[515 → 534] torr
[4 → 5] min:	[667 → 648] torr	[4 → 5] min:	[534 → 553] torr
[5 → 6] min:	[648 → 629] torr	[5 → 6] min:	[553 → 572] torr
[6 → 7] min:	[629 → 610] torr	[6 → 7] min:	[572 → 591] torr
[7 → 8] min:	[610 → 591] torr	[7 → 8] min:	[591 → 610] torr
[8 → 9] min:	[591 → 572] torr	[8 → 9] min:	[610 → 629] torr
[9 → 10] min:	[572 → 553] torr	[9 → 10] min:	[629 → 648] torr
[10 → 11] min:	[553 → 534] torr	[10 → 11] min:	[648 → 667] torr
[11 → 12] min:	[534 → 515] torr	[11 → 12] min:	[667 → 686] torr
[12 → 13] min:	[515 → 496] torr	[12 → 13] min:	[686 → 705] torr
[13 → 14] min:	[496 → 477] torr	[13 → 14] min:	[705 → 724] torr
[14 → 15] min:	[477 → 462] torr	[14 → 15] min:	[724 → 740-750] torr

Δt: The time frame in min
ΔP_i: The Delta Pressure Plan I in torr
ΔP_{ii}: The Delta Pressure Plan II in torr

Appendix B.6 Treadmill Recovery Period Protocol

Doc. Title:	**Rat Rehabilitation on a Treadmill**			Project:	DEP2010-22205-C02-01
Doc. No.:	QGR/**101.055.005**	Doc. Type:	Protocol	Sector:	333(41)
Doc. Version:	2.1	Revision Date:	2013.06.26	DEV-1:	Ginés Viscor
Version Date:	2013.06.26	Revision by:	J G Ríos	DEV-2:	J G Ríos
Editor:	J G Ríos	Next Revision:	2014.06.26	Page:	1 of 2

Procedure: QGR/101.051.002

Parameters: d, day (d); a, acceleration (cm s^{-1} min^{-1}); t, time (min); u, velocity (cm s^{-1}); I, current (mA); T, temperature (ºC).

General Notes

A This protocol describes a rehabilitation in the form of low impact concentric exercise for a rat, with an inclination, of a single session which should be applied immediately after intermittent hypoxia session (*protocol QGR/101.055.004*). If more than 30 minutes pass between the end of the hypoxia session and the beginning of this rehabilitation a deviation report needs to be written.

B All sort of registrations and observations must appear on this protocol's corresponding document, no. QGR/101.056.005, a part from the reward registration which must appear on a dedicated document no. QGR/101.066.013.

C The protocol is set up for a training lot of maximum five rats on a 5-channel treadmill, but can be used for one rat on a 1-channel treadmill as well without any changes.

D The day count follows the schedule of the intermittent hypoxia sessions.

E The exercise schedule should be followed precisely. Note that the first 5 minutes are used to adjust the slant level from 0° to +5°.

F Changes in the intensity level of the current are the only ones allowed. The initial intensity (I_i) should be the same as the last change applied ($I_{u,prev}$) in the previous session. Neither the initial intensity nor any other changes in the intensity during each session can be lower than I_{min} nor higher than I_{max} (with reference to the exercise schedule).

G It is necessary to be familiar with the protocol of running style classification (QGR/101.055.010), actions to difficult training (QGR/101.055.052), actions to treadmill malfunction (QGR/101.055.053), and rewarding rats (QGR/101.065.007) to carry out an exercise session successfully.

Exercise Schedule

phase 0			phase I				phase III			phase IV			current	
t_0	u_0	Φ_0	$(t_a)_1$	a_1	u_1	Φ_1	t_3	u_3	Φ_3	t_4	u_4	Φ_4	I_{min}	I_{max}
min	cm s^{-1}	°	min	cm s^{-1} min^{-1}	cm s^{-1}	°	min	cm s^{-1}	°	min	cm s^{-1}	°	mA	mA
1	0 (5)	0	5	~5	10-30	0-(+5)	15	30	+5	1	0 (5)	0	1.0	1.6

Guide

1 Register all settings, conditions, and initial parameters along with the Rat ID number for each cubicle.

2 Place the rats in the cubicles; register the time when the exercise starts, the room temperature (T_i) and the relative humidity (RH_i).

3 All changes in the current's intensity should be registered as: I(*mm:ss*) = *x* mA, where *mm:ss* are the minutes and seconds into the session of the actual change, and *x* is the new intensity value.

4 All observations that are considered necessary to register with respect to time should be registered as: t(*mm:ss*): *text*, where *mm:ss* are the minutes and seconds into the session of the actual occurrence, and "*text*" represents the actual observation.

5 Make careful notes on the running style of each rat during the session according protocol QGR/101.055.010.

6 Whilst performing according to the exercise schedule, do the following:

t	u	Φ	
[0 → 1] min:	0 cm s^{-1}	0°	← *1st minute, End of phase 0*
[1 → 2] min:	[5 → 10 → 20] cm s^{-1}	0°	
[2 → 3] min:	[20 → 25] cm s^{-1}	0°	
[3 → 4] min:	25 cm s^{-1}	[0 → +5]°	
[4 → 5] min:	[25 → 30] cm s^{-1}	+5°	
[5 → 6] min:	30 cm s^{-1}	+5°	← *6th minute, End of phase I*
[6 → 21] min:	30 cm s^{-1}	+5°	← *21st minute, End of phase III*
[21 → 22] min:	0 cm s^{-1}	0°	← *22nd minute, End of phase IV*

Doc. Title:	**Rat Rehabilitation on a Treadmill**			Project:	DEP2010-22205-C02-01
Doc. No.:	QGR/**101.055.005**	Doc. Type:	Protocol	Sector:	333(41)
Doc. Version:	2.1	Revision Date:	2013.06.26	DEV-1:	Ginés Viscor
Version Date:	2013.06.26	Revision by:	J G Ríos	DEV-2:	J G Ríos
Editor:	J G Ríos	Next Revision:	2014.06.26	Page:	2 of 2

FEH·lab

Procedure:	QGR/101.051.002
Parameters:	d, day (d); a, acceleration (cm s^{-1} min^{-1}); t, time (min); u, velocity (cm s^{-1}); I, current (mA); T, temperature (ºC).

7 After each phase I and every 5 minutes during phase III, register the number of shocks (Number-S) for every rat.

8 At the end of phase III (21st minute), after lowering the velocity and unplugging the motor, register the Distance (Dist.) and then the number of shocks (Number-S).

9 After phase IV (22nd minute), press the red stop button on the treadmill monitor and register the number of shock (Number-S), the total time of shocks (Time-S),

10 Register the room temperature (T_r) and relative humidity (RH_r), and register the intensity level as it is left after the session ($I_{d,new}$).

11 Reward the rats that performed accordingly with the special food reward whilst in the treadmill cubicles and link the reward with the sound of the specified bell. (Protocol QGR/101.065.007).

12 Register how the rats reacted to the reward on the dedicated sheet QGR/101.066.013.

13 Place each rat in its cage and clean the treadmill.

14 Make sure that all parameters necessary for the registration have been accounted for on the registration sheet and sign for the registration.

□

Appendix B.7 ELISA Protocols from Life Diagnostics

Appendix B.7.1 Creatine Kinase ELISA Protocol

RAT CK-MM ELISA KIT
Life Diagnostics, Inc., Catalog Number: 2112-2

ELISA for the Determination of Rat Creatine Kinase MM (CK-MM) in Serum or Plasma

Please Read All Instructions Before Starting The ELISA

INTRODUCTION

Creatine kinase (CK) is a key metabolic enzyme. It is a dimer of two subunits, each with molecular weights of approximately 43 kDa. Two different subunits occur, M and B. The CK holoenzyme therefore exists as MM and BB homodimers and an MB heterodimer. The MM and BB isoforms are expressed primarily in skeletal muscle and brain respectively while both MB and MM are expressed in heart. The relatively high expression levels of the MB isoform in heart explain its use as an established biomarker for heart disease. Likewise, CK-MM can be used as a specific biomarker for skeletal muscle injury.

PRINCIPLE OF THE TEST

The rat CK-MM ELISA is a solid phase enzyme-linked immunosorbent assay (ELISA). The assay uses affinity purified CK-MM antibodies for solid phase immobilization and a horseradish peroxidase (HRP) conjugated CK-MM monoclonal antibody for detection. Standards and diluted test samples are incubated in the microtiter wells for 45 minutes. The microtiter wells are subsequently washed and HRP conjugate is added and incubated for 45 minutes. As a result, CK-MM molecules are sandwiched between the immobilization and detection antibodies. The wells are then washed to remove unbound HRP-labeled antibodies and TMB Reagent is added and incubated for 20 minutes at room temperature. This results in the development of a blue color. Color development is stopped by the addition of Stop Solution, changing the color to yellow, and optical density is measured spectrophotometrically at 450 nm. The concentration of CK-MM is proportional to the optical density of the test sample and actual concentrations are determined by reference to a standard curve.

MATERIALS AND COMPONENTS

Materials provided with the kit:

- Anti-rat CK-MM antibody coated microtiter plate with 96 wells (provided as 12 detachable strips of 8)
- 2x HRP Conjugate, 6 ml
- Reference rat CK-MM stock (lyophilized)
- Wash Buffer (20x stock, 50 ml)
- Diluent (50 ml)
- TMB Reagent (One-Step) 11 ml
- Stop Solution (1N HCl), 11 ml

Materials required but not provided:

- Precision pipettes and tips
- Distilled or deionized water
- Polypropylene or glass tubes
- Vortex mixer
- Absorbent paper or paper towels
- Micro-Plate incubator/shaker mixing speed of ~150 rpm
- Plate reader with an optical density range of 0-4 at 450nm
- Graph paper (PC graphing software is optional)

STORAGE OF TEST KIT

The kit should be stored at 2-8°C and the microtiter strips should be kept in a sealed bag with desiccant to minimize exposure to damp air. Test kits will remain stable for six months from the date of purchase provided that the components are stored as described above.

GENERAL INSTRUCTIONS

All reagents should be allowed to reach room temperature (18-25°C) before use.

WASH SOLUTION PREPARATION

The wash solution is provided as a 20x stock. Prior to use dilute the contents of the bottle (50 ml) with 950 ml of distilled or deionized water.

HRP CONJUGATE PREPARATION

The HRP conjugate is provided as a 2x stock. Prior to use estimate the final volume of HRP conjugate required for your assay and dilute one (1) volume of the 2x stock with one (1) volume of diluent. Typically, we prepare 1 ml of conjugate for each 8-well strip used in the assay. This is prepared by mixing 0.5 ml of 2x HRP conjugate with 0.5 ml of diluent. Mix gently prior to use. Prepare the working conjugate no more than one hour in advance.

STANDARD PREPARATION

1. The reference CK-MM stock is provided in lyophilized form. Reconstitute with diluent as directed on the vial label and mix gently until dissolved. ***(the reconstituted standard remains stable for 1 day at 2-8°C)***.
2. Label 5 polypropylene or glass tubes as 50, 25, 12.5, 6.25 and 3.13 ng/ml.
3. Prepare the 50 ng/ml standard as described on the reference stock vial label.
4. Dispense 250 µl of diluent into the tubes labeled 25, 12.5, 6.25 and 3.13 ng/ml.
5. Pipette 250 µl of the 50 ng/ml CK-MM standard into the tube labeled 25 ng/ml and mix. This provides the working 25 ng/ml CK-MM standard.
6. Similarly prepare the 12.5, 6.25 and 3.13 ng/ml standards by serial dilution.

SAMPLE PREPARATION

General Note: CK-MM is usually below the detection level of the kit in samples from animals without skeletal muscle injury. However, after skeletal muscle injury levels can increase to

Life Diagnostics, Inc., P.O. Box 5205, West Chester, PA 19380
610-431-7707 – 610-431-7818 (Fax)
info@lifediagnostics.com – www.lifediagnostics.com

8000 ng/ml or greater. Undiluted serum or plasma must not be used in the ELISA. We recommend that samples be diluted at least 10-fold or more. This eliminates interference caused by serum/plasma components. Assuming that a dilution of 10-fold is used; samples should be treated as follows:

1. Dispense 225 µl of diluent into separate tubes.
2. Pipette and mix 25 µl of the serum/plasma sample into the tube containing 225 µl of diluent. This provides a 10 fold diluted sample.
3. Repeat this procedure for each sample to be tested.

Assay Procedure

1. Secure the desired number of coated wells in the holder.
2. Dispense 100 µl of standards and diluted samples into the wells (we recommend that samples be tested in duplicate).
3. Incubate on an orbital micro-plate shaker at 100-150 rpm at room temperature (18-25°C) for 45 minutes.
4. Remove the incubation mixture using either a plate washer or by flicking plate contents into an appropriate Bio-waste container.
5. Wash and empty the microtiter wells 5 times with 1x wash solution. This should preferentially be performed using a plate washer (400 µl/well). If a plate washer is not available use a squirt bottle. The entire wash procedure should be performed as quickly as possible.
6. Strike the wells sharply onto absorbent paper or paper towels to remove all residual droplets.
7. Add 100 µl of enzyme conjugate reagent into each well.
8. Incubate on an orbital micro-plate shaker at 100-150 rpm at room temperature (18-25°C) for 45 minutes.
9. Wash as detailed in 4 to 5 above.
10. Strike the wells sharply onto absorbent paper or paper towels to remove residual droplets.
11. Dispense 100 µl of TMB Reagent into each well.
12. Gently mix on an orbital micro-plate shaker at 100-150 rpm at room temperature (18-25°C) for 20 minutes.
13. Stop the reaction by adding 100 µl of Stop Solution to each well.
14. Gently mix. *It is important to make sure that all the blue color changes to yellow.*
15. Read the optical density at 450 nm with a microtiter plate reader *within 5 minutes*.

Calculation of Results

1. Calculate the average absorbance values (A_{450}) for each set of reference standards, and samples.
2. Construct a standard curve by plotting the mean absorbance obtained from each reference standard against its concentration in ng/ml on linear graph paper, with absorbance values on the vertical or Y-axis and concentrations on the horizontal or X-axis.
3. Using the mean absorbance value for each sample, determine the corresponding concentration of CK-MM in ng/ml from the standard curve.
4. Multiply the derived concentrations by the dilution factor to determine the actual concentration of CK-MM in the serum/plasma sample.
5. PC graphing software may be used for the above steps. We recommend a point-to-point "fit" of the data because of the concave shape of the standard curve. Alternatively, fitting to a polynomial second order equation may work well.
6. If the A_{450} values of samples exceed that of the high standard the samples should be further diluted and re-tested. Samples with absorbance values below the lowest standard should be assigned a value of $\leq 3.13 \times A$ ng/ml, where A represents the dilution factor used for the sample.

Typical Standard Curve

A typical standard curve with optical density readings at 450nm on the Y axis against CK-MM concentrations on the X axis is shown below. This curve is for the purpose of illustration only and should not be used to calculate unknowns. Each user should obtain his or her data and standard curve in each experiment.

CK-MM (ng/ml)	Absorbance (450 nm)
50	3.021
25	1.269
12.5	0.618
6.25	0.406
3.13	0.299

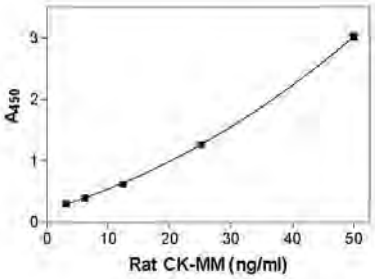

Limitations of the Procedure

1. Do not use samples at a dilution less than 10-fold (i.e., do not use a dilution of 5-fold). High serum content of the samples can interfere with the ELISA.
2. Reliable and reproducible results will be obtained when the assay procedure is carried out with a complete understanding of and in accordance with the instructions.
3. The wash procedure is critical. Insufficient washing will result in poor precision and falsely elevated absorbance readings.

Specificity

Rat CK-BB and rat CK-MB were not available when this kit was developed and specificity was therefore investigated using purified human CK-MM, CK-MB and CK-BB. Human CK-MM was strongly recognized but CK-BB was not recognized at concentrations up to 10 micrograms/ml. The ELISA was ~400-fold more selective for CK-MM compared to CK-MB.

Appendix B.7.2 Myoglobin ELISA Protocol

RAT MYOGLOBIN ELISA
Life Diagnostics, Inc., Catalog Number: 2110-2-N

ELISA for the Determination of Myoglobin in Rat Serum, Plasma & Urine[1]

STORAGE

Store standard at -20°C
STORE REMAINDER OF KIT AT 2 - 8°C

INTRODUCTION

Myoglobin is a heme protein found in both cardiac and skeletal muscle. Following myocardial necrosis associated with myocardial infarction (MI), myoglobin is one of the first markers to rise above normal levels. Studies with human subjects have shown that myoglobin increases measurably above baseline within 2-4 hours post-infarct, peaking at 9-12 hours, and returning to baseline within 24-36 hours. In the absence of skeletal muscle trauma or other factors associated with a noncardiac related increase in circulating myoglobin, myoglobin may used as a marker for MI. Similarly, in the absence of cardiac damage, myoglobin may be used as a marker of skeletal muscle injury.

PRINCIPLE OF THE TEST

The myoglobin test kit is based on the principle of a solid phase enzyme-linked immunosorbent assay (ELISA). A monoclonal anti-myoglobin antibody is used for solid phase immobilization (on the microtiter wells) and a polyclonal anti-myoglobin antibody conjugated to horseradish peroxidase (HRP) is used for detection. The test sample is allowed to react simultaneously with the two antibodies, and the myoglobin molecules are thus sandwiched between the solid phase and enzyme-linked antibodies. After one hour incubation at room temperature, the wells are washed to remove unbound labeled antibodies. TMB (tetramethylbenzidine) Reagent is added and incubated for 20 minutes, resulting in the development of a blue color. The color development is stopped with the addition of Stop Solution, changing the color to yellow. The concentration of myoglobin is proportional to the absorbance at 450 nm.

MATERIALS AND COMPONENTS

Materials provided with the kit:

- Anti-Myoglobin-coated microtiter wells, 96 wells
- Rat Myoglobin Stock (50 µl of 50 µg/ml) **Store at -20°C**
- Diluent, 12 ml
- HRP Conjugate Reagent, 11 ml
- 20x Wash Solution, 50 ml
- TMB Reagent (One-Step), 11 ml
- Stop Solution (1N HCl), 11 ml

Materials required but not provided:

- Precision pipettes
- Disposable pipette tips
- Distilled or deionized water
- Vortex mixer
- Absorbent paper or paper towels
- Graph paper (PC graphing software is optional but recommended)
- Plate shaker
- Microtiter plate reader with an optical density range of 0-4 OD at 450 nm wavelength

WASH SOLUTION PREPARATION

The wash solution is provided as a 20x stock. Prior to use dilute the contents of the bottle (50 ml) with 950 ml of distilled or deionized water.

STANDARD PREPARATION

1. Label 8 polypropylene tubes as 100, 50, 25, 12.5, 6.25, 3.125, 1.56 and 0 ng/ml.
2. Pipette 998 µl of diluent into the tube labeled 100 ng/ml.
3. Pipette 100 µl of diluent into the tubes labeled 50, 25, 12.5, 6.25, 3.125, 1.56 and 0 ng/ml.
4. Briefly centrifuge or flick the myoglobin stock tube to ensure that the liquid contents are at the bottom of the tube.
5. Dilute 2 µl of the 50 µg/ml myoglobin stock into the 998 µl of diluent in the tube labeled 100 ng/ml. This provides a 100 ng/ml solution of myoglobin.
6. Prepare a 50 ng/ml stock by diluting and mixing 100 µl of the 100 ng/ml stock with 100 µl of diluent in the tube labeled 50 ng/ml. Similarly prepare the 25, 12.5, 6.25, 3.125, 1.56 ng/ml stocks by serial dilution.

SAMPLE COLLECTION

Serum, plasma and urine should be collected using standard techniques. Remove serum or plasma from the coagulated or packed cells within 60 minutes after collection. Plasma samples may be collected into tubes containing EDTA. Samples that cannot be assayed within 3 hours of collection should be frozen at -20°C or lower. Samples should not be repeatedly frozen and thawed prior to testing.

SAMPLE PREPARATION

Samples may be tested undiluted or after dilution with diluent. The dilution factor should be determined empirically. On occasion a matrix effect may be observed with urine samples, slightly increasing or decreasing absorbance values, and we therefore strongly recommend that all urine samples within a particular study be similarly diluted. *Only 20 µl of sample is required per assay (2 x 20 µl, if samples are to be tested in duplicate).*

ASSAY PROCEDURE

1. Ensure that all reagents are at room temperature.
2. Secure the desired number of coated wells in the holder.
3. Dispense 100 µl of HRP Conjugate Reagent into each well.
4. Dispense 20 µl of myoglobin standards and samples (in duplicate) into the appropriate wells.
5. Incubate at room temperature (18-25°C) on a plate shaker for one hour. Mix Gently (~100-150 rpm)

[1] A matrix effect may be observed with urine samples, resulting in slight variances in absorbance values relative to dilution factor. It is therefore recommended that, wherever possible, all urine samples within a particular study be similarly diluted (with the provided diluent) prior to testing, thereby ensuring accurate determination of relative myoglobin levels.

Life Diagnostics, Inc., P.O. Box 5205, West Chester, PA 19380
610-431-7707 – 610-431-7818 (Fax)
info@lifediagnostics.com – www.lifediagnostics.com

6. Remove the incubation mixture either with a plate washer or by flicking plate contents into a waste container.
7. Wash and empty the microtiter wells 5 times with 1x wash solution. This may be performed using either a plate washer (400 µl/well) or a squirt bottle. The entire wash procedure should be performed as quickly as possible.
8. Strike the wells sharply onto absorbent paper or paper towels to remove all residual wash buffer.
9. Dispense 100 µl of TMB Reagent solution into each well. Gently mix for 5 seconds.
10. Incubate on a plate shaker at room temperature for 20 minutes. Mix Gently.
11. Stop the reaction by adding 100 µl of Stop Solution to each well.
12. Gently mix for 30 seconds. It is important to make sure that all the blue color changes to yellow color completely.
13. Read absorbance at 450 nm with a microtiter well reader within 5 minutes.

CALCULATION OF RESULTS

1. Calculate the mean absorbance value for each set of reference standards and samples.
2. Construct a standard curve by plotting the mean absorbance obtained for each reference standard against its concentration in ng/ml on graph paper, with absorbance values on the vertical or Y axis, and concentrations on the horizontal or X axis.
3. Use the mean absorbance values for each sample to determine the corresponding concentration of myoglobin in ng/ml from the standard curve.
4. Multiply the derived value by the appropriate dilution factor if the test samples were diluted.
5. Graphing software, if available, should be used.

TYPICAL STANDARD CURVE

Results of a typical standard run with optical density readings at 450 nm on the Y axis and myoglobin concentrations on the X axis are illustrated below. This standard curve is for illustrative purposes only, and should not be used to calculate unknowns. A standard curve should be run for each assay.

Myoglobin (ng/ml)	Absorbance (450 nm)
100	3.333
50	1.997
25	1.015
12.5	0.577
6.25	0.356
3.125	0.223
1.563	0.158
0	0.110

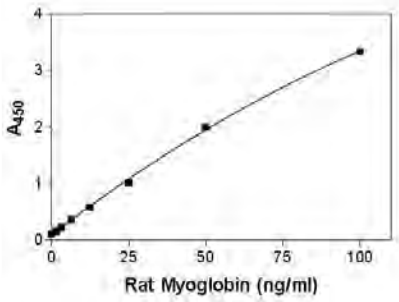

PROCEDURAL NOTES

1. Standards should be prepared immediately prior to use and should be used within 30 minutes of preparation.
2. Pipetting of conjugate, standards and samples into the microtiter plate should be completed within 10 minutes.
3. We recommend that standards and samples be run in duplicate.
4. It is recommended that the wells be read within 5 minutes following addition of Stop Solution.
5. Reliable and reproducible results will be obtained when the assay procedure is carried out with a complete understanding of the package insert instructions.
6. The wash procedure is critical. Insufficient washing will result in poor precision and falsely elevated absorbance readings.

Rev 123113

For technical assistance please email us at
techsupport@lifediagnostics.com

Appendix B.7.3 Troponin-I ELISA Protocol

RAT SKELETAL MUSCLE TROPONIN-I ELISA KIT*
Life Diagnostics, Inc., Cat. No. 2020-2-SK

RAT SKELETAL MUSCLE TROPONIN-I (SKM-TNI) ELISA

STORAGE CONDITIONS

- Store the SkM-TnI Stock vials at or below -20°C
- Store the remainder of the kit at 2-8°C
- Keep the microtiter plate in a sealed bag with desiccant to minimize exposure to damp air

EXPIRATION

The kit expiration date (six months from the date of shipment) is indicated on the package.

BACKGROUND

Troponin is the contractile regulating protein complex of striated muscle. It consists of three distinct polypeptides: troponin-I, troponin-C, and troponin-T. The troponin-I subunit exists in three distinct isoforms; one each in fast-twitch and slow-twitch skeletal muscle fibers, and one in cardiac muscle. Following muscle injury, troponin-I is released into the blood and measurement of troponin-I in serum or plasma provides a measurement of the extent of muscle injury. This ELISA kit uses a detection antibody that is specific for the fast twitch isoform of troponin-I, thereby allowing specific evaluation of skeletal muscle injury.

PRINCIPLE OF THE ASSAY

The assay uses two different affinity purified antibodies. One is used for solid phase immobilization (on the microtiter wells). The second is conjugated to horse radish peroxidase (HRP) and is used for detection. The test sample is diluted and incubated in the microtiter wells for 45 minutes after which the wells are washed and HRP conjugate is added and incubated for 45 minutes. This results in troponin-I molecules being sandwiched between the immobilization and detection antibodies. The wells are then washed to remove unbound HRP-labeled antibodies and TMB Reagent (HRP substrate solution) is added and incubated for 20 minutes. If troponin-I is present a blue color develops. Color development is stopped by the addition of Stop Solution, changing the color to yellow, and optical density is measured spectrophotometrically at 450 nm. The concentration of troponin-I is proportional to the optical density of the test sample.

REAGENTS AND MATERIALS PROVIDED

- Anti SkM-TnI Coated Wells (1 plate, 96 wells)
- SkM-TnI Stock (3 vials): Lyophilized rat SkM-TnI (reconstitute with 0.10 ml H_2O)
- Standard Diluent (50 ml)
- Sample Diluent (25 ml)
- Wash Buffer (20x stock, 50 ml)
- Anti SkM-TnI HRP Conjugate (11 ml)
- TMB Reagent (11 ml)
- Stop Solution (11 ml): 1N HCl

MATERIALS REQUIRED BUT NOT PROVIDED

- Distilled or deionized water
- Pipettes: P-10, P-200 & P-1000 or equivalent
- Disposable pipette tips
- Microtiter well reader capable of reading OD at 450 nm
- Vortex mixer
- Absorbent paper
- Graph paper or appropriate PC graphing software
- Polypropylene microcentrifuge tubes (1.5 ml)

WARNINGS AND PRECAUTIONS

- Avoid contact with 1N HCl (Stop Solution). It may cause skin irritation and burns. If contact occurs, wash with copious amounts of water and seek medical attention if irritation persists.
- Do not use reagents after expiration date and do not mix or use components from different kits.
- Replace caps on reagents immediately. Do not switch caps.

WASH SOLUTION PREPARATION

The wash solution is provided as a 20x stock. Prior to use dilute the contents of the bottle (50 ml) with 950 ml of distilled or deionized water.

STANDARD PREPARATION

1. Equilibrate kit components to room temperature before use.
2. Reconstitute one vial of the lyophilized SkM-TnI stock by addition of 100 µl of de-ionized or distilled water. Mix gently until dissolved – **USE WITHIN 30 MINUTES OF RECONSTITUTION**. The concentration of SkM-TnI in the reconstituted stock is indicated on the vial label.
3. Label 5 polypropylene tubes as 50, 25, 12.5, 6.25 and 3.125 ng/ml.
4. Into the tube labeled 50 ng/ml, pipette the volume of **Standard Diluent** detailed on the SkM-TnI stock vial label. Then add the indicated volume of SkM-TnI stock (shown on the SkM-TnI stock vial label) and mix gently. This provides the 50 ng/ml standard.
5. Pipette 0.25 ml of **Standard Diluent** into the tubes labeled 25, 12.5, 6.25 and 3.125 ng/ml
6. Prepare a 25 ng/ml standard by diluting and mixing 0.25 ml of the 50 ng/ml standard with 0.25 ml of standard diluent in the tube labeled 25 ng/ml. Similarly prepare the 12.5, 6.25 and 3.125 ng/ml standards by serial dilution.

NOTE: The reconstituted SkM-TnI standards should be used within 30 minutes of stock reconstitution. Discard the stock after use.

SAMPLE COLLECTION

Serum or plasma (EDTA) should be prepared as quickly as possible after blood collection and stored at 4°C. All samples should be similarly processed (i.e., storage times and temperatures should be the same for all samples). If samples cannot be assayed within 1-2

Life Diagnostics, Inc., P.O. Box 5205, West Chester, PA 19380
610-431-7707 – 610-431-7818 (Fax)
info@lifediagnostics.com – www.lifediagnostics.com

hours of collection they should be frozen at –70°C and thawed only once prior to use.

Sample Preparation

In studies at Life Diagnostics, Inc., we have encountered samples with very low (≤ 4 ng/ml) and high (> 500 ng/ml) levels of troponin-I. Depending on the level of troponin-I two different methods of sample preparation are recommended.

1. Low troponin-I levels: plasma or serum samples should be diluted with 1/3rd volume of **Sample Diluent** (i.e., 180 µl of serum or plasma should be diluted with 60 µl of sample diluent).
2. High troponin-I levels: If samples prepared as described in 1 above give absorbance values that exceed those of the 50 ng/ml standard, samples pre-diluted with Sample diluent as described above should be further diluted with **Standard diluent** (i.e., one volume of sample pre-diluted as described in 1 above, should be mixed directly with one or more volumes of Standard diluent).

We recommend that samples be assayed in duplicate. Wherever possible, all samples should be similarly diluted in order to avoid minor matrix differences.

Procedural Notes

1. Standards and diluted samples should be prepared immediately prior to use and used within 30 minutes.
2. Pipetting of all standards, samples and conjugate into the microtiter plate should be completed within 10 minutes.

Assay Procedure

1. Secure the desired number of coated wells in the holder.
2. Dispense 100 µl of standards and diluted samples into the wells (we recommend that samples be tested in duplicate).
3. Incubate on an orbital micro-plate shaker at 100-150 rpm at room temperature (18-25°C) for 45 minutes.
4. Remove the incubation mixture using either a plate washer or by flicking plate contents into an appropriate Bio-waste container.
5. Wash and empty the microtiter wells 5 times with 1x wash solution using a plate washer (400 µl/well). The entire wash procedure should be performed as quickly as possible.
6. Strike the wells sharply onto absorbent paper or paper towels to remove all residual droplets.
7. Add 100 µl of enzyme conjugate reagent into each well.
8. Incubate on an orbital micro-plate shaker at 100-150 rpm at room temperature (18-25°C) for 45 minutes.
9. Wash as detailed in 4 to 5 above.
10. Strike the wells sharply onto absorbent paper or paper towels to remove residual droplets.
11. Dispense 100 µl of TMB Reagent into each well.
12. Gently mix on an orbital micro-plate shaker at 100-150 rpm at room temperature (18-25°C) for 20 minutes.
13. Stop the reaction by adding 100 µl of Stop Solution to each well.
14. Gently mix. *It is important to make sure that all the blue color changes to yellow.*
15. Read the optical density at 450 nm with a microtiter plate reader *within 5 minutes*.
16. If absorbance values of samples exceed that of the 50 ng/ml standard, samples should be appropriately diluted and re-tested.

Calculation of Results

1. Calculate the mean absorbance value (A_{450}) for the standards and samples.
2. Construct a standard curve by plotting the A_{450} values obtained for each reference standard against its concentration in ng/ml on graph paper, with absorbance on the vertical (y) axis and concentration on the horizontal (x) axis.
3. Using the A_{450} values for each sample, determine the corresponding concentration of SkM-TnI (ng/ml) from the standard curve. If using graphing software, we suggest using a linear regression fit of the data.
5. Multiply the derived SkM-TnI concentrations by the dilution factor (i.e., 1.33, if the "low troponin-I level" dilution procedure was used) to obtain the actual SkM-TnI concentration.

Example of Standard Curve

Results of a typical standard curve with A_{450} plotted on the Y axis against cTnI concentrations on the X axis are shown below. **NOTE:** This standard curve is for the purpose of illustration only.

SkM-TnI (ng/ml)	Absorbance (450 nm)
50	1.576
25	0.781
12.5	0.421
6.25	0.263
3.125	0.197

Typical Rat SkM-TnI Standard Curve

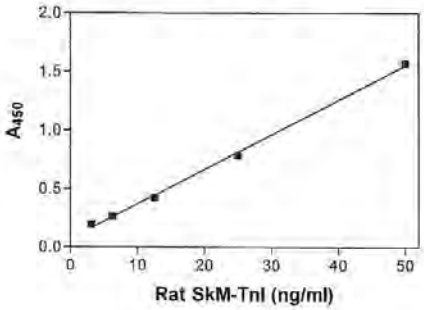

Limitations of the Procedure

Reliable and reproducible results will be obtained when the assay procedure is carried out with a complete understanding of the package insert instructions and with adherence to good laboratory practice.

**Patent application filed by Life Diagnostics, Inc.*

Appendix B.8 Adapted RNA Extraction Protocol from Qiagen

Doc. Title:	**RNAextraction of skeletal muscle w/ RNeasy Midi Kit**			Project:	DEP2010-22205-C02-01
Doc. No.:	QGR/**101.055.059**	Doc. Type:	Protocol	Sector:	323(26)
Doc. Version:	1.2	Revision Date:	2014.01.03	DEV-1:	G Viscor
Version Date:	2014.01.03	Revision by:	JG Ríos	DEV-2:	JG Ríos
Editor:	KM Kristjánsdóttir	Next Revision:	2014.01.10	Page:	1 of 3

FEH·lab

Procedure:
Parameters:

General Notes

A This protocol describes the RNAextraction of homogenised skeletal muscle tissue from protocol QAS/101.055.058 with RNeasy Fibrous Midi Kit.

B All sort of actions and observations should be registered on the corresponding QAS-soft programme.

C The procedure will start with a pre-part for re-initiating an interrupted procedure from QAS/101.055.059 ending with freezing the samples and storing having them stored at –80 °C. The main part of the procedure refers to from where discontinuous and continuous parts have joined.

D All steps in this protocol should be carried out at room temperature, but should be carried out as quickly as possible. Avoid prolonged incubation periods as it might compromise the RNA integrity.

E The spin columns cannot be overloaded with sample as it can significantly reduce the RNA yield and quality. Furthermore, bear in mind that incomplete homogenisation could cause clogging of the spin column and significantly reduce the RNA yield as well.

F Perform all centrifugation steps at 20-25 °C and 2800 g (preferably one minute less then listed in the protocol and at 3000-5000 g). Ensure that the centrifuge dos not cool below 20 °C.

G *Chemicals:* Kit material (*QGR/101.xxx.xxx*)
Material: [5-mL, 1000-µL, and 200-µL] micropipette, [5-mL, 1000-µL, and 200-µL] sterile micropipette tips, 25G sterile needles, 1-mL sterile 3-piece syringe, 15-mL sterile falcon tubes, 0.5-mL sterile cryogenic micro tube
Instrum.: Thermo bath (*QAS/101.111.021*), centrifuge (*QAS/101.111.xxx*), balance (*QAS/101.111.xxx*).

Guide

Preparation of material

1 Fill the thermo bath with distilled water and set it to 55 °C.
With a lid on, the set temperature should be reached after 30 min.

2 For each sample one of each of the following with its QAS-code:
Spin column (from kit)
Kit collection tube (from kit)
15-mL sterile falcon tube
0.5-mL sterile cryogenic micro tube
1-mL sterile syringe
25G needle case

3 Only have necessary sterile material on the RNase-free zone.

Preparation of solutions

4 Prepare the DNase I incubation mix according to protocol QAS/101.055.xxx.

5 Dilute the RPE buffer before using in the procedure:

5i Add 44 mL of EtOH into the 11 mL of the RPE concentrate that is in the bottle, and mix.
Put EtOH into 5x 15-mL sterile falcon tubes and use sterile 5-mL tips to transfer the volume of EtOH into the RPE concentrate bottle. Check the box on the cap that EtOH has been added.
The recipe is given on the bottle of the RPE concentrate, and is subject to change in accordance with different kit lot. Make sure to double check the recipe.

Pre-Part (for frozen samples)

0.1 Take the sample/samples processed with protocol QAS/101.055.058 out of –80 °C and put them at room temperature (T=20-25 °C)to thaw. Expect this to take about 1.5-2 h.
Do not put the tube in a water bath to hurry up the process, that might affect the end quality of the RNA.

Doc. Title:	**RNAextraction of skeletal muscle** w/ RNeasy Midi Kit			Project:	DEP2010-22205-C02-01
Doc. No.:	QGR/**101.055.059**	Doc. Type:	Protocol	Sector:	323(26)
Doc. Version:	1.2	Revision Date:	2014.01.03	DEV-1:	G Viscor
Version Date:	2014.01.03	Revision by:	JG Ríos	DEV-2:	JG Ríos
Editor:	KM Kristjánsdóttir	Next Revision:	2014.01.10	Page:	2 of 3

Procedure:
Parameters:

0.2 Once the samples have reached room temperature, add 4 mL of RNase free water with sterile tips. Change the tip if it touches any other surfaces than of the RNase free water container.

0.3 Swirl the sample around to have everything in it properly mixed.

0.4 Carry on to step 6.

Main Procedure

6 Add 65 µL of proteinase K solution. Mix thoroughly, with swirling.

7 Incubate the samples at 55 °C for exactly 20 min in the thermo bath.

8 Centrifuge at 20-25 °C for **6 min** at 2800 g
A small pellet of tissue debris will form after the centrifuge, sometimes accompanied by a thin layer or film on top of the supernatant.

9 Pipet the supernatant (approximately 6 mL) into a marked 15-mL sterile falcon tube.
Avoid transferring any of the pellet. If this is unavoidable, a small amount of pellete debris may be carried over without affecting the RNeasy procedure. Hold the pipet tip under the thin layer or film on top of the supernatant, if present. This layer will usually adhere to the outside of the pipet tip and should not be transferred.
The sample tube with the pellet can be discarded.

10 Add 0.5x the supernatant's volume (usually about 3 mL) of EtOH to the cleared lysate in the 15-mL falcon tube. Mix well by pipetting and/or swirling. Do not centrifuge.
Precipitates may be visible after addition of ethanol. This does not affect the procedure.

11 Transfer 3 mL of the sample, including any precipitate that may have formed, to an RNeasy Midi spin column placed in its 15-mL collection tube. Close the lid gently.

12 Centrifuge at 20-25 °C for **6 min** at 2800 g.

13 Discard the flow through but reuse the collection tube.

14 Repeat the cycle of step 11, 12 and 13 twice in order to transfer the total amount of about 9-mL sample through the column, always reusing the collection tube.
In the last cycle (the 3rd cycle) if there happens to be a little more liquid left, added to the column in that cycle.
The interesting part of the sample is now in the filter of the spin column, thus the flow through is discarded, but the collection tube will still be reused to collect and discard flow through.

15 Add 2 mL of RW1 buffer (wash buffer) on the spin column and close the lid gently.

16 Centrifuge at 20-25 °C for **6 min** at 2800 g.

17 Discard the flow through but reuse the collection tube.

18 Add 160 µL of the DNase I incubation mix directly onto the spin column membrane.
Be sure to add the DNase I incubation mix directly to the RNeasy spin column membrane. DNase digestion will be incomplete if part of the mix sticks to the walls or the O-ring of the spin column.

19 Incubate at 20-30 °C for exactly 15 min.
Do not centrifuge at this stage.

20 Add 2 mL of RW1 buffer onto the spin column. Close the lid gently.

21 Incubate at room temperature for exactly 5 min.

22 Centrifuge at 20-25 °C for **6 min** at 2800 g.

23 Discard the flow through but reuse the collection tube.

24 Add 2.5 mL of RPE-EtOH buffer onto the spin column. Close the lid gently.
The buffer is prepared according to step 5.

25 Centrifuge at 20-25 °C for **3 min** at 2800 g.

26 Discard the flow through but reuse the collection tube.

27 Add 2.5 mL of RPE-EtOH buffer (second cycle) onto the spin column. Close the lid gently.

Doc. Title:	**RNAextraction of skeletal muscle w/ RNeasy Midi Kit**			Project:	DEP2010-22205-C02-01
Doc. No.:	QGR/**101.055.059**	Doc. Type:	Protocol	Sector:	323(26)
Doc. Version:	1.2	Revision Date:	2014.01.03	DEV-1:	G Viscor
Version Date:	2014.01.03	Revision by:	JG Rios	DEV-2:	JG Rios
Editor:	KM Kristjánsdóttir	Next Revision:	2014.01.10	Page:	3 of 3

Procedure:
Parameters:

28 Centrifuge at 20-25 °C for **6 min** at 2800 g.

29 Carefully remove the spin column from the collection tube without it coming in contact with the flow through or the walls of the tube and place it in a new marked sterile collection tube.
Carryover of EtOH from the buffer cannot occur. The long centrifucation dries the spin column membrane, ensuring that no EtOH is carried over during the following RNA elution. Residual ethanol may interfere with downstream reactions.
Collection tube with the flow through and the flow through itself from step 25 can now be discarded.

30 Add 150 µL of RNase free water directly on the spin column membrane in the new collection tube. Close the lid gently.

31 Wait for 1 min to let the RNA elute.

32 Centrifuge at 20-25 °C for **4 min** at 2800 g.

33 Reuse the collection tube, but DO NOT discard the flow through.
The end sample is the flow through at this stage.

34 Repeat the cycle of steps 30, 31, 32 and 33 twice (total of 3 cycles) ending with accumulated 3x 150 µL sample solution as flow through in the collection tube.

35 Remove the spin column from the collection tube.

36 Transfer the sample solution (in the collection tube) with a 1-mL syringe (using the 25G needle) into dedicated 0.5-mL micro tube.

37 Place the micro tube into a –80 °C storage.

38 Register the time of freezing into QAS·soft.

□

Appendix C — Operational Diagrams

Appendix C.1 The Experimental Setup (Detailed), The Rat Handling Phase

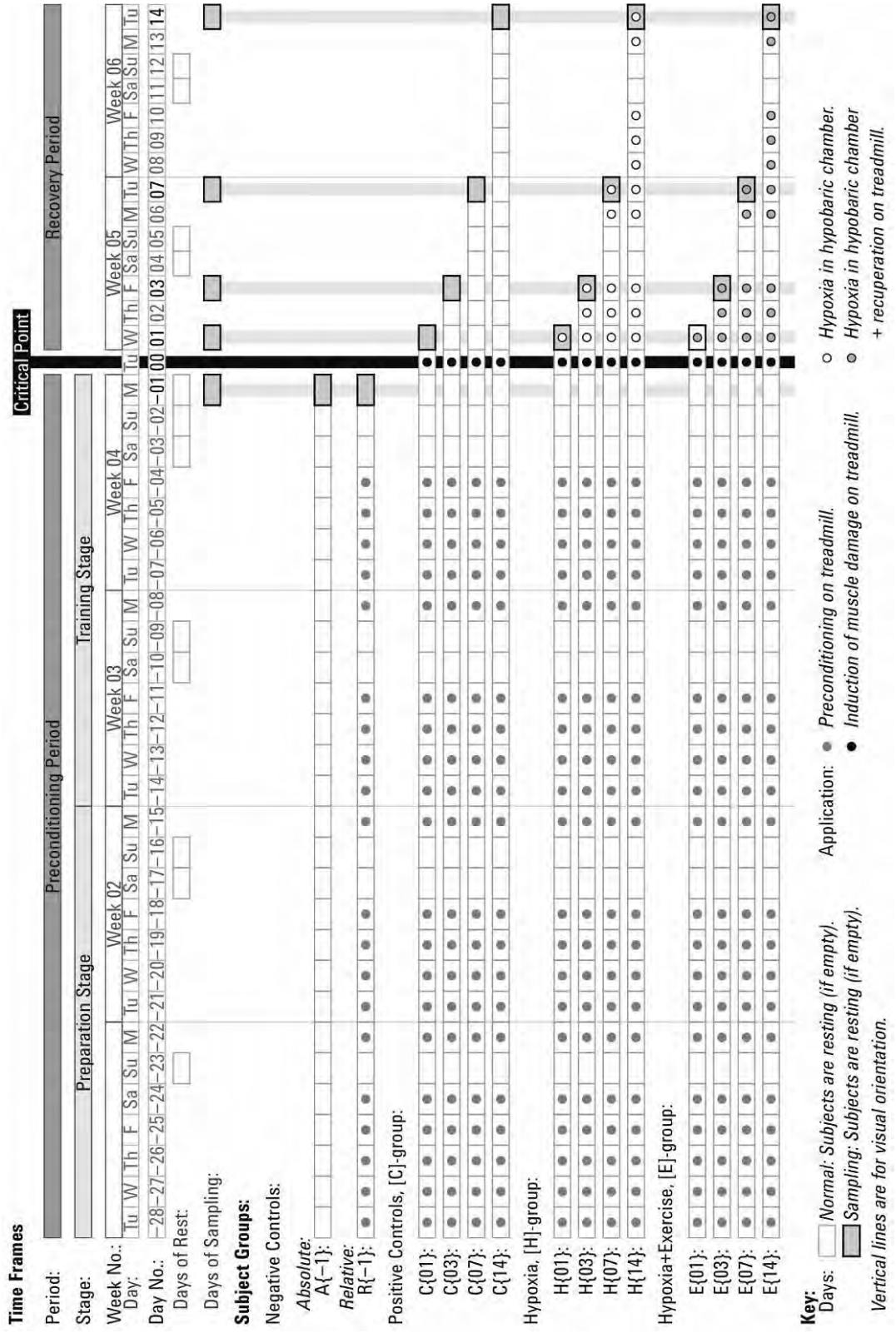

Appendix C.2 Overview of the S33+ Sampling Process

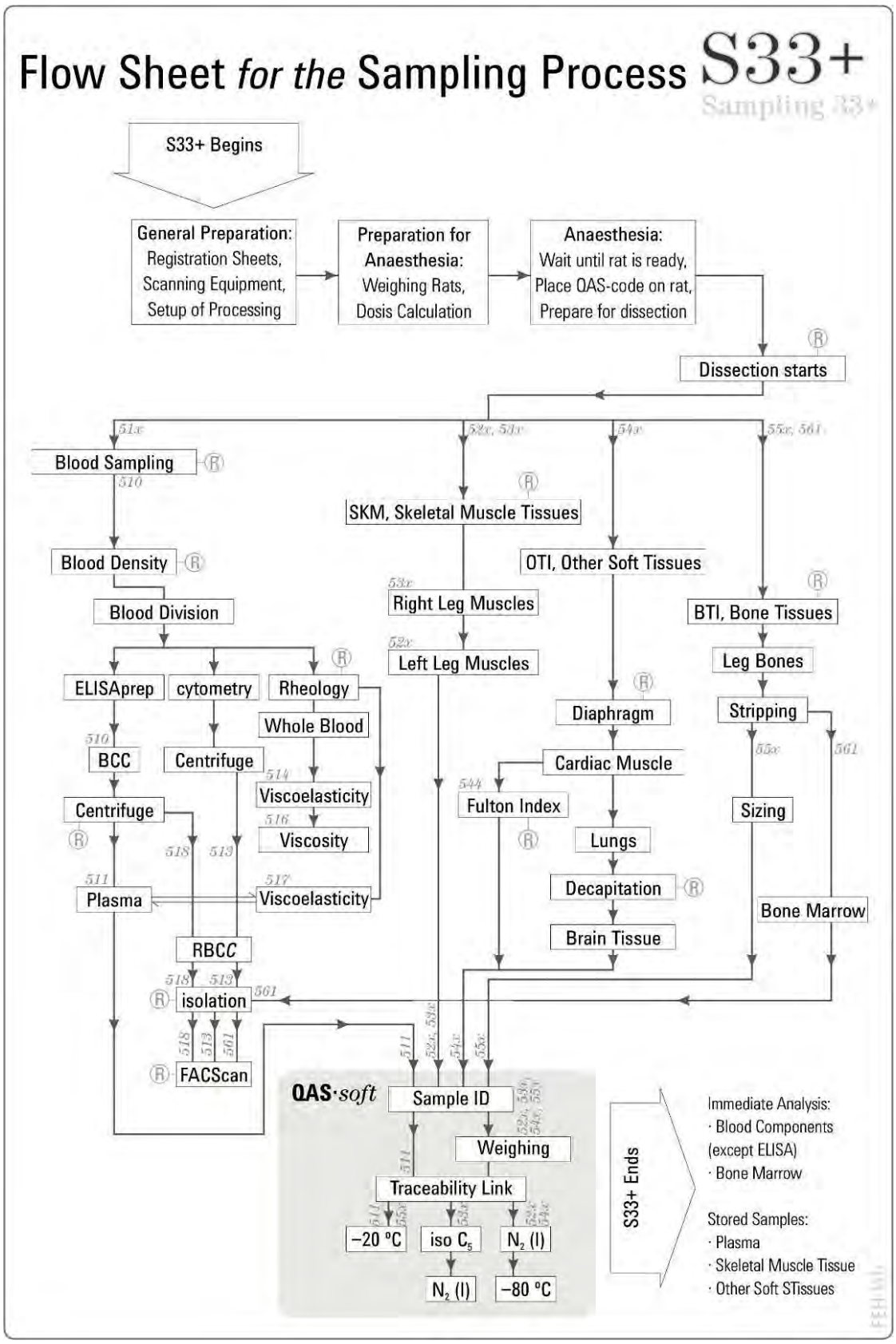

Appendix C.3 The AEY Rat-Performance Score (A-criteria)

AEY Performance Score; Schematic Setup.

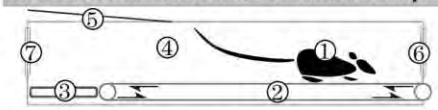

① A rat, running forward against the movement of ② the treadmill belt, with ③ an electric shock-providing metal grid at the back; in ④ an encased treadmill lane with ⑤ a hinge top lid, and ⑥ a front- and ⑦ a back air-opening to allow free air flow.

A-score Criteria with α score values.

Mark	Diagram	Description	Score
A	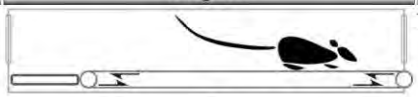	The rat runs continuously without touching the metal grid.	0.00
B	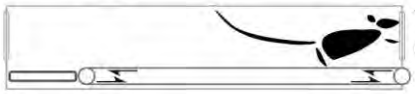	The rat runs but supports itself on the front wall with its fore limbs whilst only moving the hind limbs.	–0.70
C		The rat runs but continuously touches the metal grid.	–0.30
⊖D D ⊕D		The rat moves away from the metal grid to the front of the treadmill and stops until its has been moved back with the treadmill belt. Movement by: (–)D, running; D, galloping; (+)D, with a big jump.	⊖D –0.15 D –0.25 ⊕D –0.30
E		The rat hangs on to the front air-opening and therefore avoids running.	–0.50
F		The rat manages to slide in a brake against the movement of the treadmill belt and avoids running.	–0.50
G		The rat is somehow able to position itself (usually on its back) sliding still on the treadmill belt and avoids running.	–0.50
⊖H ⊕H	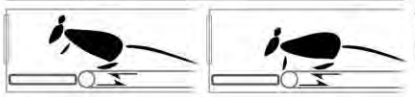	The rat walks backwards close (or really close) to the metal grid: (–)H, on hind limbs only; (+)H, on all four legs.	–0.80 (both)
I		The rat stands on the metal grid, receiving electric shock, and does not reposition itself onto the treadmill belt.	–0.90
J	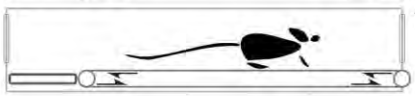	The rat runs forward but is really distracted at the same time.	–0.05
K		The rat rests the whole body on the treadmill belt whilst it runs or walks forward.	–0.40
L	*(front view)* *no image*	The rat uses the peripheral non-moving floor part (not covered by the treadmill belt) to avoid running. Essentially, one body-side is moving.	–0.50
M		The rat runs with only using the hind limbs to move and skating with the fore limbs.	–0.65
N		The rat runs with only using the fore limbs to move and dragging the hind limbs behind.	–0.65

Appendix C.4 The AEY Rat-Performance Score (E and Y-criteria)

AEY Performance Score; Schematic Setup.

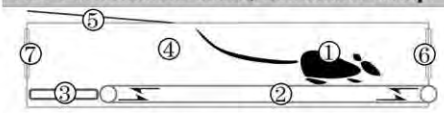

① A rat, running forward against the movement of ② the treadmill belt, with ③ an electric shock-providing metal grid at the back; in ④ an encased treadmill lane with ⑤ a hinge top lid, and ⑥ a front- and ⑦ a back air-opening to allow free air flow.

E-score Criteria with ϵ score values.

Mark	Diagram/Description	Score
(+)		1.00
(+/–)	Gradual changes in the position of tail from very lifted (+) to no lift at all (-).	0.75
(–/+)		0.50
(–)		0.25
(0)	Unfavourable A-criterion renders the position of the tail irrelevant or impossible.	0.00

Y-score Criteria with u score values.

Mark	Description	Score
ⓐ	The accumulative shock time increases due to: *- faeces or urine droplets 'stuck' on the metal grid.*	–0.15 (each)
ⓑ	*- no obvious reason.*	
ⓒ	The shock count increases due to: *- no obvious reason.*	
ⓓ	*- does not increase when touched.*	
ⓧ	Overwhelming count of artefacts.	–1.00

Note: Registry of ⓧ renders other u-score values redundant within the same registry period.

Appendix C.5 Representative AEY-Score Registry Notes with Calculations

1. *Create registration.*

2. *Quantify each registry period.*

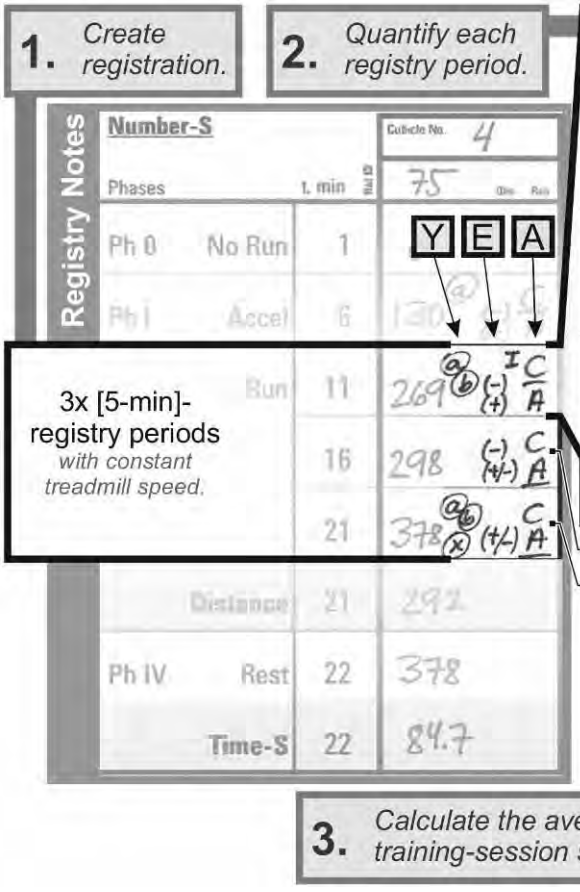

1st [5-min]-Registry period

	Marks	Quantify				Total	Calc./Score
A	C A I	C -0.3	C -0.3	A 0	I -0.9	n=4 Σ= -1.5	1 + (Σ / n) = 0.625
E	(–) (+)	(–) 0.25	(+) 1.00			n=2 Σ= 1.25	Σ / n = 0.625
Y	(a) (b)	(a) -0.15	(b) -0.15			* Σ= -0.30	1 + Σ = 0.700

* n_{max}=5: Each type of mark can only be noted once. If (x) is noted => Σ = -1.00.

2nd [5-min]-Registry period

3rd [5-min]-Registry period

3. *Calculate the average training-session score.*

Registry period	Score Category A	E	Y
1st	0.625	0.625	0.700
2nd	0.900	0.500	1.000
3rd	0.900	0.750	0.000
average	0.808	0.625	0.567

Appendix C.6 Plasma Preparation Procedure

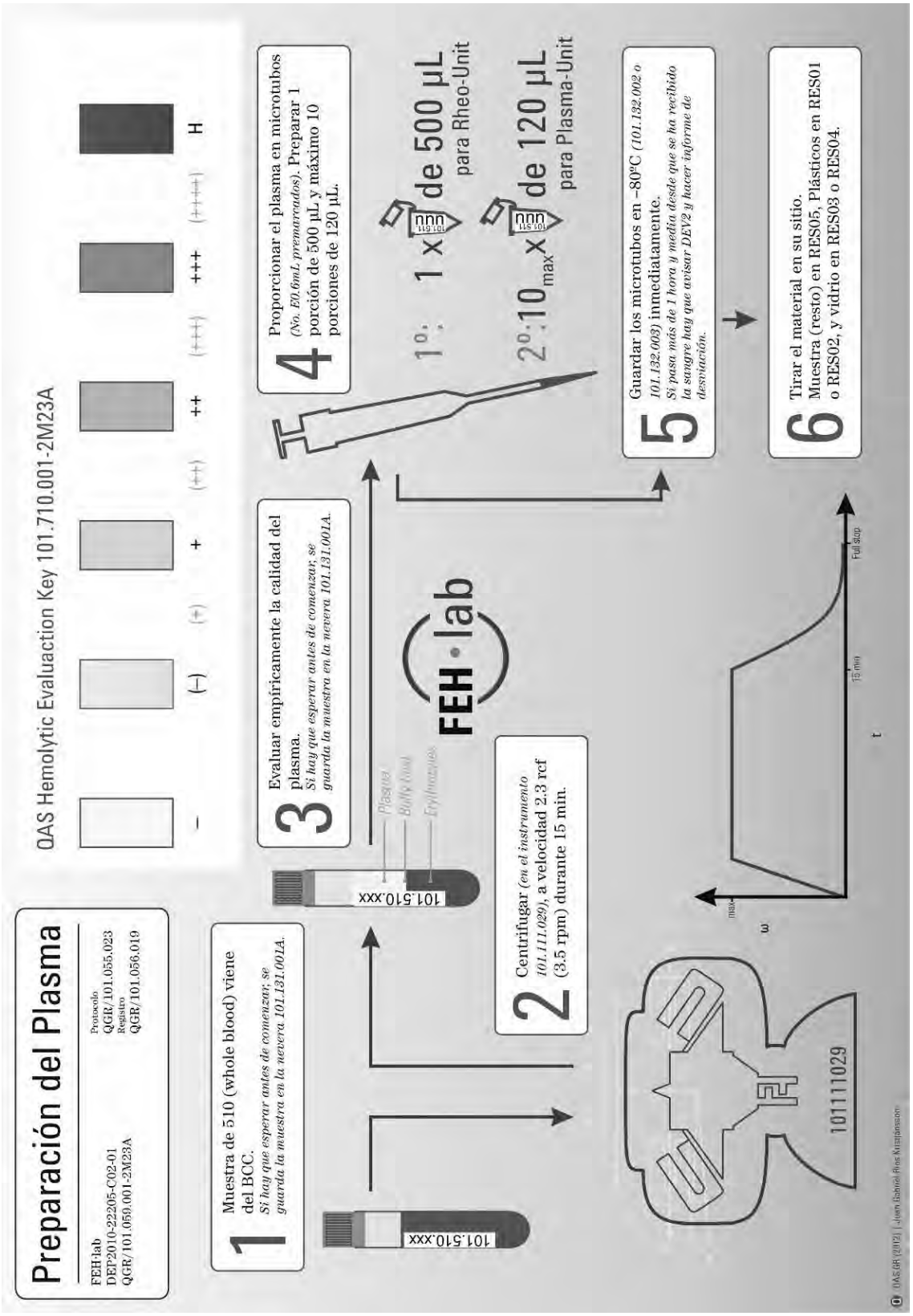

Appendix D — Supplementary Results

Appendix D.1 FEH·lab's In-house Haemolytic Scale with CMYK Colour Reference

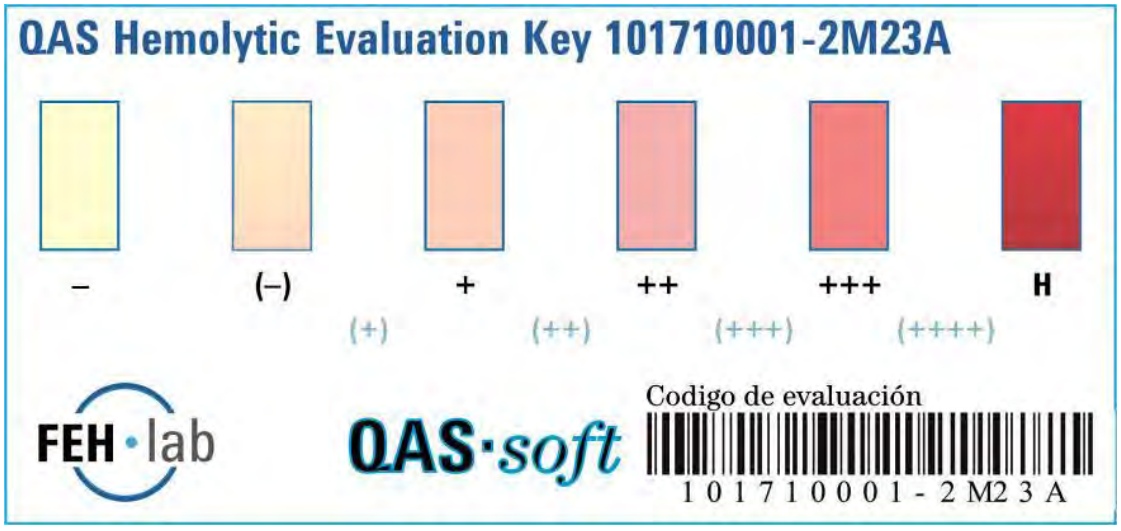

Fig. ApxD - 1. The in-house haemolytic evaluation key used to provide all fresh plasma samples with haemolytic status prior to freezing.

Table ApxD - 1. The in-house haemolytic evaluation key referenced with the CMYK colour model.

Order	Plasma Code	C	M	Y	K
1	-	0	0	20	0
2	(-)	0	9	20	0
3	(+)	-	-	-	-
4	+	0	20	20	0
5	(++)	-	-	-	-
6	++	2	36	17	0
7	(+++)	-	-	-	-
8	+++	0	60	33	0
9	(++++)	-	-	-	-
10	H	12-22	95	75	0-2

Appendix D.2 Full Gene List for False Discovery Rate Correction-Analysis

Complete Gene List for False Discovery Rate Correction Analysis (Part 1/4)

Code	Symbol	Code	Symbol	Code	Symbol	Code	Symbol
AY310138	Il6st	NM_001012357	Ccl9	NM_001100834	Ppa1	NM_001107296	Ercc6
AY325159	Plg	NM_001012359	Ang	NM_001100895	Atf1	NM_001107330	Irx4
BC081950	Mapk12	NM_001013045	Ccl24	NM_001100984	Ncf2	NM_001107407	Cdh5
D87927	Cxcl3	NM_001013062	Thbs1	NM_001105713	Prkca	NM_001107413	Irx3
NM_001002016	Lmna	NM_001013145	Ccr6	NM_001105725	Ccng2	NM_001107425	Nfat5
NM_001003959	Dnmt3b	NM_001013157	Nnt	NM_001105727	Psmb5	NM_001107588	Chuk
NM_001004100	Klk10	NM_001013413	Als2	NM_001105737	Tek	NM_001107737	Itga4
NM_001004202	Ccl6	NM_001013428	Pla2g2d	NM_001105738	Gpx5	NM_001107764	Pla2g4b
NM_001004250	Uqcrc1	NM_001014166	Il33	NM_001105749	Il16	NM_001107787	Pax1
NM_001004263	Itgb6	NM_001014199	Atp6v1c2	NM_001105822	Ccl12	NM_001107805	Nfatc2
NM_001005246	Dmd	NM_001014786	Ifna1	NM_001105829	Lpo	NM_001107869	Dysf
NM_001005534	Sdhc	NM_001015011	Il17f	NM_001105885	Hoxd4	NM_001107874	Xpc
NM_001005550	Ndufs1	NM_001024751	Sox6	NM_001105991	Atp6v1g3	NM_001107902	Sox17
NM_001005765	Rap1a	NM_001024897	Ehd2	NM_001105993	Glmn	NM_001107956	Car9
NM_001006961	Osm	NM_001025065	Angptl3	NM_001106007	Pgm2	NM_001108048	Rps6ka5
NM_001006970	Uqcrc2	NM_001025134	Uqcrq	NM_001106015	Pla2g3	NM_001108065	Shc2
NM_001006972	Ndufv1	NM_001025146	Ndufs4	NM_001106041	Ctsg	NM_001108069	Stk11
NM_001007612	Ccl7	NM_001025405	Ruvbl2	NM_001106148	Myot	NM_001108116	Hoxc5
NM_001007666	Bcs1l	NM_001025425	Map2k7	NM_001106153	Ndufa2	NM_001108118	Itga5
NM_001007684	Klf2	NM_001025695	Cops5	NM_001106259	Akt1s1	NM_001108216	Nck2
NM_001007729	Pf4	NM_001030023	Map2k4	NM_001106294	Ndufab1	NM_001108250	Foxp3
NM_001008324	Eif4b	NM_001033069	Eif4ebp2	NM_001106322	Ndufs8	NM_001108341	Ulk1
NM_001008384	Rac2	NM_001033699	Cox15	NM_001106360	Ndufb8	NM_001108392	Zic2
NM_001008525	Ndufs7	NM_001033883	Cxcl12	NM_001106361	Pax2	NM_001108400	Ankrd37
NM_001008724	Fga	NM_001034105	Tnnc1	NM_001106395	Foxo3	NM_001108442	Ndufb7
NM_001008767	Txnip	NM_001034125	Per1	NM_001106426	Ndufb5	NM_001108444	Gab1
NM_001008802	Krt1	NM_001034131	Foxp1	NM_001106489	Ndufs3	NM_001108447	Nfatc3
NM_001008888	Uqcrfs1	NM_001034164	Stat1	NM_001106641	Rragd	NM_001108517	Rps6ka4
NM_001009268	Actr2	NM_001037180	Fkbp8	NM_001106646	Ndufb6	NM_001108565	Pla2g12a
NM_001009290	Ndufc2	NM_001039539	Pax9	NM_001106673	Gpx7	NM_001108577	Ppp2r4
NM_001009480	Uqcrh	NM_001039849	Gpx4	NM_001106696	Pla2g2e	NM_001108604	Rbpjl
NM_001009623	Tnfsf13	NM_001044267	Mknk1	NM_001106704	Cox7a2l	NM_001108624	Ndufb2
NM_001009706	Lhpp	NM_001047858	Srxn1	NM_001106783	Myf5	NM_001108661	Ccl19
NM_001009964	Tbx5	NM_001047862	Ndufa8	NM_001106850	Sox14	NM_001108813	Ndufa1
NM_001010962	Rps6kb2	NM_001047880	Slc25a15	NM_001106897	Il17a	NM_001108836	Ccr10
NM_001010968	Eng	NM_001048184	Rragc	NM_001106912	Ndufb3	NM_001108943	Il21
NM_001011907	Ndufs2	NM_001080148	Dhcr24	NM_001106921	Prkag3	NM_001108978	Pik3cd
NM_001011917	Cab39l	NM_001082479	Igf1	NM_001106924	Cab39	NM_001108979	Atp6v1e2
NM_001011959	Ctsa	NM_001083911	Sepp1	NM_001106943	Foxo4	NM_001109112	Tnfsf13b
NM_001011964	Mapkap1	NM_001098241	Hras	NM_001106986	Noxo1	NM_001109181	Sox2
NM_001011972	Atp6v0d2	NM_001100171	Noxa1	NM_001107036	Mpo	NM_001109233	Hoxa9
NM_001011991	Ndrg1	NM_001100528	Rag2	NM_001107037	Epx	NM_001109269	Lin28a
NM_001012027	Serpinc1	NM_001100531	Dlx1	NM_001107039	Sgca	NM_001109383	Angptl1
NM_001012066	Sphk2	NM_001100539	Sdhb	NM_001107041	Hoxb13	NM_001109393	Timp4
NM_001012122	Tymp	NM_001100557	Olig2	NM_001107042	Hoxb3	NM_001109532	Mapk11
NM_001012127	Mapkapk3	NM_001100648	Foxn1	NM_001107094	Hoxd10	NM_001109587	Pla2g2f
NM_001012143	Jmjd6	NM_001100752	Ndufa9	NM_001107159	Mmp19	NM_001109615	Gys1
NM_001012147	Pxn	NM_001100781	Nanog	NM_001107264	Nfatc4	NM_001109884	Hoxc4

Complete Gene List for False Discovery Rate Correction Analysis (Part 2/4)

Code	Symbol	Code	Symbol	Code	Symbol	Code	Symbol
NM_001110334	Vegfa	NM_012628	Prkcg	NM_012982	Msx2	NM_017051	Sod2
NM_001115021	Qk	NM_012629	Prl	NM_012985	Ndufa5	NM_017058	Vdr
NM_001127294	Ndufb9	NM_012631	Prnp	NM_012998	P4hb	NM_017061	Lox
NM_001127553	Uqcrb	NM_012639	Raf1	NM_013001	Pax6	NM_017064	Stat5a
NM_001129878	Hoxa11	NM_012655	Sp1	NM_013005	Pik3r1	NM_017066	Ptn
NM_001130501	Zfpm2	NM_012671	Tgfa	NM_013010	Prkag1	NM_017071	Insr
NM_001130505	Ndufa6	NM_012675	Tnf	NM_013025	Ccl3	NM_017086	Egr3
NM_001130548	Col14a1	NM_012680	Tsc2	NM_013053	Ywhaq	NM_017093	Akt2
NM_001134499	Rptor	NM_012682	Ucp1	NM_013057	F3	NM_017102	Slc2a3
NM_001134530	Mmp1	NM_012689	Esr1	NM_013062	Kdr	NM_017104	Csf3
NM_001134979	Ezh2	NM_012715	Adm	NM_013070	Utrn	NM_017113	Grn
NM_001135009	Col4a1	NM_012735	Hk2	NM_013075	Hoxa1	NM_017115	Myog
NM_001135157	Myh2	NM_012742	Foxa1	NM_013076	Lep	NM_017116	Capn2
NM_001135158	Myh1	NM_012743	Foxa2	NM_013081	Ptk2	NM_017117	Capn3
NM_001135759	Col4a3	NM_012747	Stat3	NM_013085	Plau	NM_017143	F10
NM_001145367	Pparg	NM_012751	Slc2a4	NM_013096	Hba1	NM_017144	Tnni3
NM_001163168	Ntrk2	NM_012764	Gata1	NM_013102	Fkbp1a	NM_017160	Rps6
NM_001164060	Shc1	NM_012775	Tgfbr1	NM_013110	Il7	NM_017161	Adora2b
NM_001168641	Wars2	NM_012780	Arnt	NM_013123	Il1r1	NM_017168	Plcg2
NM_001170597	Bai1	NM_012797	Id1	NM_013129	Il15	NM_017169	Prdx2
NM_001172305	Prkcb	NM_012801	Pdgfa	NM_013135	Rasa1	NM_017171	Prkce
NM_001191052	Tcf7l2	NM_012802	Pdgfra	NM_013151	Plat	NM_017174	Pla2g5
NM_001191566	Mbnl1	NM_012806	Mapk10	NM_013156	Ctsl1	NM_017176	Pla2g10
NM_001191803	Tnfsf14	NM_012807	Smo	NM_013160	Mxi1	NM_017178	Bmp2
NM_001191845	Hey1	NM_012812	Cox6a2	NM_013167	Ucp3	NM_017183	Cxcr2
NM_001191923	Pik3r5	NM_012814	Cox6a1	NM_013172	Myf6	NM_017185	Tnni2
NM_001270665	Tnnt3	NM_012815	Gclc	NM_013174	Tgfb3	NM_017202	Cox4i1
NM_001270796	Pla2g6	NM_012817	Igfbp5	NM_013187	Plcg1	NM_017221	Shh
NM_001270931	Hnf4a	NM_012827	Bmp4	NM_013190	Pfkl	NM_017232	Ptgs2
NM_001276711	Nfkb1	NM_012842	Egf	NM_013195	Il2rb	NM_017256	Tgfbr3
NM_012492	Adrb2	NM_012846	Fgf1	NM_013199	Dnm2	NM_017258	Btg1
NM_012495	Aldoa	NM_012848	Fth1	NM_013216	Rheb	NM_017269	Ptprj
NM_012499	Apc	NM_012854	Il10	NM_016993	Bcl2	NM_017301	S1pr1
NM_012509	Atp4a	NM_012864	Mmp7	NM_017000	Nqo1	NM_017305	Gclm
NM_012510	Atp4b	NM_012870	Tnfrsf11b	NM_017001	Epo	NM_017309	Ppp3r1
NM_012520	Cat	NM_012880	Sod3	NM_017003	Erbb2	NM_017322	Mapk9
NM_012548	Edn1	NM_012881	Spp1	NM_017017	Hgf	NM_017322	Mapk9
NM_012551	Egr1	NM_012886	Timp3	NM_017019	Il1a	NM_017325	Runx1
NM_012557	Fancc	NM_012908	Faslg	NM_017020	Il6r	NM_017339	Isl1
NM_012561	Fst	NM_012922	Casp3	NM_017022	Itgb1	NM_017344	Gsk3a
NM_012580	Hmox1	NM_012925	Cd59	NM_017025	Ldha	NM_017347	Mapk3
NM_012581	Hoxa2	NM_012931	Bcar1	NM_017034	Pim1	NM_019127	Ifnb1
NM_012588	Igfbp3	NM_012935	Cryab	NM_017039	Ppp2ca	NM_019130	Ins2
NM_012589	Il6	NM_012945	Hbegf	NM_017041	Ppp3ca	NM_019142	Prkaa1
NM_012603	Myc	NM_012948	Emd	NM_017042	Ppp3cb	NM_019143	Fn1
NM_012611	Nos2	NM_012951	Fgf10	NM_017043	Ptgs1	NM_019147	Jag1
NM_012615	Odc1	NM_012953	Fosl1	NM_017045	Rb1	NM_019151	Mstn
NM_012620	Serpine1	NM_012969	Irs1	NM_017050	Sod1	NM_019155	Cav3

Complete Gene List for False Discovery Rate Correction Analysis (Part 3/4)

Code	Symbol	Code	Symbol	Code	Symbol	Code	Symbol
NM_019156	Vtn	NM_022214	Cxcl5	NM_030989	Tp53	NM_031643	Map2k1
NM_019183	Actc1	NM_022266	Ctgf	NM_030992	Pld1	NM_031716	Wisp1
NM_019185	Gata6	NM_022269	Cd55	NM_030994	Itga1	NM_031761	Figf
NM_019191	Smad2	NM_022381	Pcna	NM_031004	Acta2	NM_031785	Atp6ap1
NM_019205	Ccl11	NM_022404	Mlst8	NM_031012	Anpep	NM_031832	Lgals3
NM_019212	Acta1	NM_022503	Cox7a2	NM_031018	Atf2	NM_031970	Hspb1
NM_019218	Neurod1	NM_022525	Gpx3	NM_031020	Mapk14	NM_031976	Prkab1
NM_019223	Ndufs6	NM_022528	Hif3a	NM_031021	Csnk2b	NM_031977	Src
NM_019231	Mapk13	NM_022531	Des	NM_031051	Mif	NM_031985	Rps6kb1
NM_019232	Sgk1	NM_022532	Araf	NM_031054	Mmp2	NM_032080	Gsk3b
NM_019233	Ccl20	NM_022540	Prdx3	NM_031055	Mmp9	NM_032085	Col3a1
NM_019247	Pitx3	NM_022542	Rhob	NM_031056	Mmp14	NM_033230	Akt1
NM_019305	Fgf2	NM_022584	Txnrd2	NM_031061	Musk	NM_033299	Pld2
NM_019306	Flt1	NM_022597	Ctsb	NM_031064	Ndufv2	NM_033359	Ngb
NM_019310	Cxcr1	NM_022605	Hpse	NM_031081	Pdpk1	NM_053290	Pgam1
NM_019333	Pfkfb4	NM_022611	Il12b	NM_031107	Rps6ka1	NM_053291	Pgk1
NM_019334	Pitx2	NM_022627	Prkab2	NM_031116	Ccl5	NM_053295	Cast
NM_019353	Tpo	NM_022631	Wnt5a	NM_031131	Tgfb2	NM_053297	Pkm
NM_019354	Ucp2	NM_022677	Zic1	NM_031139	Usf2	NM_053303	Cxcr5
NM_019360	Cox6c	NM_022698	Bad	NM_031140	Vim	NM_053304	Col1a1
NM_019363	Aox1	NM_022712	Tfrc	NM_031317	Pdgfc	NM_053328	Bhlhe40
NM_019371	Egln3	NM_022714	Crhr2	NM_031334	Cdh1	NM_053353	Cd40lg
NM_019383	Atp5h	NM_022922	Tpi1	NM_031347	Ppargc1a	NM_053355	Ikbkb
NM_019905	Anxa2	NM_022924	F2	NM_031353	Vdac1	NM_053356	Col1a2
NM_019906	Mtor	NM_022938	Htr7	NM_031507	Egfr	NM_053357	Ctnnb1
NM_020082	Rnase4	NM_022958	Pik3c3	NM_031507	Egfr	NM_053364	Prl7d1
NM_020542	Ccr1	NM_023090	Epas1	NM_031510	Idh1	NM_053390	Il12a
NM_021578	Tgfb1	NM_023092	Myo1c	NM_031511	Igf2	NM_053415	Cxcr3
NM_021588	Mb	NM_023093	Atp5a1	NM_031512	Il1b	NM_053420	Bnip3
NM_021592	Hand1	NM_023098	Nup62	NM_031513	Il3	NM_053423	Tert
NM_021655	Chga	NM_023963	Cdx2	NM_031515	Kras	NM_053425	Ccs
NM_021689	Ereg	NM_023981	Csf1	NM_031517	Met	NM_053429	Fgfr3
NM_021698	F13a1	NM_023991	Prkaa2	NM_031524	Pdgfb	NM_053450	Hdac5
NM_021701	Ppp3r2	NM_024141	Duox2	NM_031530	Ccl2	NM_053472	Cox4i2
NM_021760	Col5a3	NM_024148	Apex1	NM_031534	Wt1	NM_053481	Pik3cb
NM_021834	Il5	NM_024160	Cyba	NM_031534	Wt1	NM_053488	Col5a2
NM_021835	Jun	NM_024161	Dnajc5	NM_031549	Tagln	NM_053489	Col18a1
NM_021838	Nos3	NM_024358	Notch2	NM_031550	Cdkn2a	NM_053512	Prdx4
NM_021854	Tsc1	NM_024359	Hif1a	NM_031554	Acvr2b	NM_053524	Nox4
NM_021866	Ccr2	NM_024400	Adamts1	NM_031560	Ctsk	NM_053540	Cox17
NM_021989	Timp2	NM_030826	Gpx1	NM_031575	Akt3	NM_053545	Tie1
NM_022182	Fgf7	NM_030834	Slc16a3	NM_031585	Pla2g1b	NM_053546	Angpt1
NM_022185	Pik3r2	NM_030836	Erap1	NM_031591	Pecam1	NM_053549	Vegfb
NM_022194	Il1rn	NM_030845	Cxcl1	NM_031598	Pla2g2a	NM_053551	Pdk4
NM_022196	Lif	NM_030846	Grb2	NM_031606	Pten	NM_053552	Tnfsf4
NM_022197	Fos	NM_030854	Lect1	NM_031614	Txnrd1	NM_053576	Prdx6
NM_022209	Ppp2r2b	NM_030859	Mdk	NM_031632	Casp9	NM_053586	Cox5b
NM_022213	Pik3r3	NM_030869	Nrp2	NM_031633	Foxm1	NM_053595	Pgf

Complete Gene List for False Discovery Rate Correction Analysis (Part 4/4)

Code	Symbol	Code	Symbol	Code	Symbol	Code	Symbol
NM_053599	Efna1	NM_057149	Tnfsf11	NM_134454	Angpt2	NM_184051	Prkag2
NM_053602	Atp5j	NM_057151	Ccl17	NM_134455	Cx3cl1	NM_198788	Sdhd
NM_053610	Prdx5	NM_057193	Il10ra	NM_138503	Map3k2	NM_199115	Angptl4
NM_053645	Il5ra	NM_057203	Ccl22	NM_138528	Ero1l	NM_199495	Ndufa10
NM_053647	Cxcl2	NM_058213	Atp2a1	NM_138827	Slc2a1	NM_201270	Il4
NM_053652	Flt4	NM_080399	Ddit4l	NM_138828	Apoe	NM_206847	Pfkp
NM_053653	Vegfc	NM_080481	Atp5i	NM_138832	Slc38a1	NM_207592	Gpi
NM_053697	Dag1	NM_080766	Nras	NM_138854	Slc38a5	NM_207605	Sh2d2a
NM_053708	Gbx2	NM_080769	Lta	NM_138880	Ifng	NM_212505	Ier3
NM_053710	Pax3	NM_080778	Nr2f2	NM_138883	Atp5o	NM_212507	Ltb
NM_053713	Klf4	NM_080888	Bnip3l	NM_139089	Cxcl10	NM_212516	Atp5l
NM_053725	Itga6	NM_080889	Il2rg	NM_139104	Egfl7	NM_212517	Ndufa11
NM_053734	Ncf1	NM_080903	Trim63	NM_139105	Rnh1	X02610	Eno1
NM_053756	Atp5g3	NM_080906	Ddit4	NM_139106	Atp5d	XM_001069410	Hoxc6
NM_053757	Aimp1	NM_130417	Hey2	NM_139192	Scd1	XM_001076610	Ep300
NM_053769	Dusp1	NM_130428	Sdha	NM_144737	Fmo2	XM_001079130	RGD1561905
NM_053775	Atp6v0a2	NM_130744	Cygb	NM_144744	Adipoq	XM_003749164	Mef2c
NM_053789	Il17b	NM_130755	Cs	NM_145095	Kcnh8	XM_003750414	Hoxc10
NM_053792	Ift172	NM_131908	Fgf6	NM_145098	Nrp1	XM_235733	Amot
NM_053800	Txn1	NM_133386	Sphk1	NM_145672	Cxcl9	XM_575155	Ttn
NM_053819	Timp1	NM_133386	Sphk1	NM_145681	Tnfsf10		
NM_053824	Csnk2a1	NM_133399	Pik3ca	NM_145783	Cox5a		
NM_053825	Atp5c1	NM_133409	Ilk	NM_147139	Itgb5		
NM_053826	Pdk1	NM_133418	Slc25a10	NM_147165	Gpx6		
NM_053828	Il13	NM_133424	Actn3	NM_153629	Hspa4		
NM_053829	Mapk8	NM_133517	Atp12a	NM_153720	Itgb3		
NM_053836	Il2	NM_133519	Il11	NM_153721	Ppbp		
NM_053842	Mapk1	NM_133521	Fbxo32	NM_153739	Duox1		
NM_053852	Csf2	NM_133523	Mmp3	NM_171992	Ccnd1		
NM_053857	Eif4ebp1	NM_133524	Tcfe2a	NM_171994	Cdc42		
NM_053858	Ccl4	NM_133532	Ccr4	NM_172055	Cited1		
NM_053883	Dusp6	NM_133551	Pla2g4a	NM_172062	P4ha1		
NM_053887	Map3k1	NM_133556	Atp5g2	NM_172068	Surf1		
NM_053906	Gsr	NM_133601	Cblb	NM_173120	Vimp		
NM_053918	Cga	NM_133605	Camk2g	NM_175754	Agrn		
NM_053958	Ccr3	NM_133651	Cav1	NM_175761	Hsp90aa1		
NM_053960	Ccr5	NM_134326	Alb	NM_175843	Sqstm1		
NM_053965	Slc25a20	NM_134345	Cox8a	NM_176075	Ppargc1b		
NM_053972	RragB	NM_134352	Plaur	NM_176079	Myod1		
NM_053973	Rraga	NM_134355	Pou4f2	NM_177927	Serpinf1		
NM_053974	Eif4e	NM_134364	Atp5b	NM_177928	Nampt		
NM_057108	Serpinb5	NM_134365	Atp5f1	NM_178102	Mapkapk2		
NM_057114	Prdx1	NM_134366	Rac1	NM_181371	Gstk1		
NM_057120	Nudt1	NM_134367	Ppp3cc	NM_182667	Myocd		
NM_057128	Rps6ka2	NM_134388	Tnnt1	NM_182819	Cox7b		
NM_057132	Rhoa	NM_134443	Creb1	NM_182952	Cxcl11		
NM_057135	Pfkfb3	NM_134443	Creb1	NM_183055	Cox8c		
NM_057143	Park7	NM_134452	Col5a1	NM_183403	Gpx2		

Appendix D.3 RNA Extraction Assessment (from m. Soleus Samples)

Appendix D.3.1 RNA Quality and Quantity

Nº	Name	28S/18S Ratio	RIN	Chip	Conc. Nano (ng/ul)	A260/280	A260/230
1	101521178	1,9	6,8	R6K Screen Tape	314,97	2,01	1,94
2	101521259	2,7	7,1	R6K Screen Tape	131,12	1,85	1,92
3	101521265	2,1	7,9	R6K Screen Tape	257,67	1,81	2,03
4	101521094	3	6,7	R6K Screen Tape	210,48	2,06	2,14
5	101521102	2,5	6,9	R6K Screen Tape	357,47	1,92	2,13
6	101521140	2,4	6,9	R6K Screen Tape	162,2	1,87	1,95
7	101521187	1,2	7,5	R6K Screen Tape	180,59	2,08	2,07
8	101521192	1,9	6,3	R6K Screen Tape	109,3	2,07	2,05
9	101521524	2,2	7,1	R6K Screen Tape	554,81	2,08	2,13
10	101521205	2,3	6,7	R6K Screen Tape	340,04	1,95	2,06
11	101521209	2,4	7	R6K Screen Tape	332,67	1,84	2,1
12	101521334	2,2	6,9	R6K Screen Tape	313,49	2,05	2,2
13	101521287	2,2	7	R6K Screen Tape	515,5	2,11	2,11
14	101521344	2,5	7,1	R6K Screen Tape	296,67	2,03	2,15
15	101521544	2,3	7,2	R6K Screen Tape	547,43	2,09	2,04
16	101521151	2,3	7,1	R6K Screen Tape	320,15	2,04	1,97
17	101521410	2,3	7,3	R6K Screen Tape	573,92	2,06	2,09
18	101521473	2,6	7,4	R6K Screen Tape	313,76	1,89	2,16
19	101521122	2,5	7,8	R6K Screen Tape	235,84	1,99	2
20	101521196	2,3	7,1	R6K Screen Tape	412,37	1,87	2,05
21	101521278	2,7	7	R6K Screen Tape	430,99	2,05	2,18
22	101521066	2,1	8,2	R6K Screen Tape	229,75	1,95	2,03
23	101521513	2,7	6,9	R6K Screen Tape	328,79	2,07	2,07
24	101521534	2,8	7,2	R6K Screen Tape	456,2	2,04	2,21
25	101521297	2,6	7,1	R6K Screen Tape	398,5	2,04	2,23
26	101521539	2,5	7,5	R6K Screen Tape	411,2	2,03	2,23
27	101521549	2,6	7,3	R6K Screen Tape	462,34	2,01	2,23
28	101521162	2,6	7,2	R6K Screen Tape	240,85	1,91	2,12
29	101521308	1,6	7	R6K Screen Tape	467,12	2,03	2,19
30	101521555	2,6	7	R6K Screen Tape	420,76	2,02	2,18
31	101521222	2	6,6	R6K Screen Tape	128,16	2,02	1,98
32	101521227	2,2	7,5	R6K Screen Tape	326,01	1,83	2,03
33	101521273	2,7	7,1	R6K Screen Tape	396,41	2,06	2,19
34	101521072	2,7	7,5	R6K Screen Tape	277,29	1,96	2,17
35	101521327	2,6	7,1	R6K Screen Tape	423,3	2,07	2,21
36	101521508	2,6	7,3	R6K Screen Tape	315,12	1,97	2,16
37	101521229	2,2	7	R6K Screen Tape	325,1	2,03	2,14
38	101521292	2,5	7	R6K Screen Tape	427,01	2,01	2,18
39	101521389	2,5	7,1	R6K Screen Tape	442,78	2,04	2,18
40	101521254	2,5	6,8	R6K Screen Tape	224,9	2,05	2,05
41	101521302	1,9	5,8	R6K Screen Tape	385,33	2,06	2,16
42	101521463	2,5	7	R6K Screen Tape	442,95	2,04	2,22
43	101521174	2	7,1	R6K Screen Tape	307,31	2,04	2,08
44	101521268	2,2	7	R6K Screen Tape	340,16	2,07	2,18
45	101521107	2,3	6,8	R6K Screen Tape	307,68	1,94	2,17
46	101521109	1,8	7,2	R6K Screen Tape	102,31	1,73	1,57
47	101521283	2,1	7,3	R6K Screen Tape	413,11	2,04	2,25
48	101521497		-	R6K Screen Tape	392,25	1,95	2,18
49	101521198	1,5	6,9	R6K Screen Tape	375,69	1,8	2,24
50	101521202	2,3	7,3	R6K Screen Tape	303,88	1,76	2,15
51	101521457	2,1	6,9	R6K Screen Tape	438,05	2,03	2,16
52	101521154	1,8	8,1	R6K Screen Tape	300,02	1,78	2,13
53	101521372	2,1	7,3	R6K Screen Tape	381	2,04	2,21
54	101521488	2,3	7,3	R6K Screen Tape	384,13	2,05	2,19
55	101521426	1,7	7,2	R6K Screen Tape	329,1	2,01	2,16
56	101521394	2,2	7,7	R6K Screen Tape	142,1	2,03	2,05
57	101521362	2,3	7,3	R6K Screen Tape	382,46	2,05	2,21
58	101521126	2,3	7,8	R6K Screen Tape	298,42	1,77	1,99
59	101521131	2,3	6,8	R6K Screen Tape	119,38	1,74	1,49
60	101521377	1,8	6,9	R6K Screen Tape	437,53	2	2,2
61	101521529	2,5	7,2	R6K Screen Tape	366,53	2,04	2,22
62	101521075	2,3	7,3	R6K Screen Tape	139,27	1,88	2,08
63	101521238	2,3	7,3	R6K Screen Tape	283,81	1,94	2,07
64	101521446	2,2	7,3	R6K Screen Tape	407,88	2,04	2,18
65	101521452	2,5	7,6	R6K Screen Tape	360,64	2,05	2,14
66	101521318	2,8	7,2	R6K Screen Tape	331,63	2	2,24
67	101521357	2,7	7,2	R6K Screen Tape	422,99	2,05	2,22
68	101521420	2,6	7	R6K Screen Tape	319,75	2,08	2,2

Appendix D.3.2 Sample's Dye-Proportions Prior to the Microarray Analysis Procedure

Nº	Name	Starting Qty. (ug)	ng/ul	Cy5 pmol/ul	Cy3 pmol/ul	RNA ratio (260/280)	Yield (ug)	Spec. Act. Cy5	Spec. Act. Cy3
1	101521205	0,2	217,93	5,09	0	2,27	6,5379	23,3561235	0
2	101521192	0,2	230,21	0	4,53	2,27	6,9063	0	19,6776856
3	101521344	0,2	308	7,14	0	2,27	9,24	23,1818182	0
4	101521334	0,2	224,72	0	4,79	2,19	6,7416	0	21,3154147
5	101521410	0,2	271,16	6,29	0	2,19	8,1348	23,1966367	0
6	101521544	0,2	217,09	0	4,84	2,29	6,5127	0	22,2949007
7	101521524	0,2	273,08	6,19	0	2,25	8,1924	22,6673502	0
8	101521473	0,2	298,26	0	6,74	2,26	8,9478	0	22,5977335
9	101521287	0,2	316,49	7,49	0	2,23	9,4947	23,6658346	0
10	101521187	0,2	152,69	0	2,68	2,16	4,5807	0	17,5519025
11	101521151	0,2	268,58	5,91	0	2,35	8,0574	22,0046169	0
12	101521209	0,2	248,69	0	4,7	2,11	7,4607	0	18,8990309
13	10152166	0,2	288,57	6,66	0	2,26	8,6571	23,0793222	0
14	101521196	0,2	153,95	0	3,02	2,24	4,6185	0	19,6167587
15	101521297	0,2	311,26	7,44	0	2,24	9,3378	23,9028465	0
16	101521534	0,2	247,13	0	5,35	2,2	7,4139	0	21,6485251
17	101521308	0,2	274,65	6,33	0	2,2	8,2395	23,047515	0
18	101521549	0,2	208,38	0	3,63	2,15	6,2514	0	17,4200979
19	101521278	0,2	320,33	7,21	0	2,22	9,6099	22,5080386	0
20	101521555	0,2	257,11	0	5,15	2,19	7,7133	0	20,0303372
21	101521539	0,2	305,17	6,42	0	2,21	9,1551	21,0374545	0
22	101521122	0,2	264,95	0	4,96	2,17	7,9485	0	18,7205133
23	101521162	0,2	248,94	5,29	0	2,22	7,4682	21,2501004	0
24	101521513	0,2	248,66	0	4,81	2,12	7,4598	0	19,3436821
25	10152172	0,2	216,94	4,23	0	2,16	6,5082	19,4984788	0
26	101521227	0,2	135,34	0	1,98	2,16	4,0602	0	14,6298212
27	101521229	0,2	279,06	5,56	0	2,2	8,3718	19,9240307	0
28	101521508	0,2	146,06	0	2,68	2,18	4,3818	0	18,3486239
29	101521357	0,2	301,56	5,88	0	2,2	9,0468	19,4986072	0
30	101521389	0,2	236,8	0	4,02	2,23	7,104	0	16,9763514
31	101521273	0,2	266,58	5,41	0	2,18	7,9974	20,2940956	0
32	101521463	0,2	241,47	0	4,29	2,22	7,2441	0	17,7661821
33	101521292	0,2	311,71	6,65	0	2,26	9,3513	21,3339322	0
34	101521222	0,2	217,05	0	4,02	2,31	6,5115	0	18,5210781
35	101521254	0,2	211,58	4,44	0	2,27	6,3474	20,9849702	0
36	101521327	0,2	317,47	0	8,7	2,29	9,5241	0	27,4041642
37	101521178	0,2	161,68	3,13	0	2,23	4,8504	19,3592281	0
38	10152194	0,2	320,98	0	8,92	2,24	9,6294	0	27,7898935
39	101521102	0,2	177,82	3,59	0	2,35	5,3346	20,1889551	0
40	101521259	0,2	266,19	0	7,61	2,37	7,9857	0	28,5886021
41	101521265	0,2	191,5	3,76	0	2,3	5,745	19,6344648	0
42	101521140	0,2	256,03	0	5,82	2,27	7,6809	0	22,7317111

Appendix D.4 The Differential Gene Expression Profiles

Appendix D.4.1 The Skeletal Muscle (Myogenesis & Myopathy) Pathway

Table ApxD - 2. The Skeletal Muscle Contractility – Dystrophin-Glycoprotein Complex Gene Profile of Significant Differential Fold Changes (log_2(FC)).

Timing	Reference	Objective	Gene (Symbol)							
			Capn3	Emd	Lmna	Cav3	Dmd	Dysf	Dag1	Camk2g
Day −1	A{−1}	R{−1}								
Day 1	A{−1}	C{01}	**−0.59***	*0.28*	**0.57***	*−0.23*		**0.49***		
	R{−1}		**−0.52***	*0.24*	**0.48***			*0.30*		
	A{−1}	H{01}	**−0.56***	**0.36***	**0.72***	**−0.41***	*−0.39*	**0.50***		
	R{−1}		**−0.49***	**0.31***	**0.64***	*−0.29*	*−0.44*	*0.31*		
	A{−1}	E{01}	**−0.64***	**0.32***	**0.59***	**−0.39***		*0.41*	*−0.26*	
	R{−1}		**−0.57***	*0.27*	**0.50***	*−0.26*			*−0.24*	
	C{01}									*−0.61*
Day 3	A{−1}	C{03}			*0.48*			*0.48*		
	R{−1}				*0.39*					
	C{01}		**0.52***							
	A{−1}	H{03}			*0.36*			*0.33*		
	H{01}		*0.44*	*−0.29*	*−0.36*	*0.30*	*0.53*			
	A{−1}	E{03}			*0.49*			*0.33*		
	R{−1}				*0.41*					
	E{01}		*0.39*			*0.28*				
Day 7	C{03}	C{07}			*−0.28*					
	A{−1}	H{07}					*0.44*			
	R{−1}						*0.39*			
	H{01}		**0.70***	**−0.42***	**−0.57***	**0.36***	**0.84***			
	C{07}						*0.38*			
	E{01}	E{07}	**0.61***	*−0.27*	**−0.40***	*0.27*		*−0.38*		*0.46*
	E{03}				*−0.30*			*−0.29*		
	H{07}						*−0.37*			
Day 14	R{−1}	C{14}	*0.33*							*0.48*
	A{−1}	H{14}							*−0.24*	
	R{−1}		*0.34*						*−0.23*	
	H{01}		**0.84***	**−0.30***	**−0.52***	**0.36***	**0.71***	*−0.30*		
	H{03}		*0.39*							
	E{01}	E{14}	**0.62***	**−0.35***	**−0.44***	*0.21*	*0.37*	*−0.39*		
	E{03}				*−0.34*			*−0.30*		

Fold change values marked with an asterisk and in boldface letters are significant ($p \leq 0.05$) with an adjusted p-value (false discovery rate corrected). Positive fold change values are in white letters on dark background. Genes within this pathway line with no significant differential expression are: Mapk1, Sgca.

Table ApxD - 3. The Skeletal Muscle Contractility – Titin Complex Gene Profile of Significant Differential Fold Changes (log_2(FC)).

Timing	Reference	Objective	Gene (Symbol)											
			Actn3	Capn3	Lmna	Myot	Cryab	Tnnt3	Tnni2	Trim63	Acta1	Des	Ttn	Myh1	Myh2
Day −1	A{−1}	R{−1}								*−0.48*	*0.25*				
Day 1	A{−1}	C{01}	*−3.10*	**−0.59***	**0.57***	**−0.75***		*−2.05*	*−2.78*	**−0.67***					
	R{−1}		*−3.82*	**−0.52***	**0.48***	*−0.62*					*−0.39*				
	A{−1}	H{01}		**−0.56***	**0.72***	**−0.56***	*0.42*			*−0.51*				*−2.40*	
	R{−1}			**−0.49***	**0.64***	*−0.43*	*0.43*				*−0.36*			*−2.11*	
	A{−1}	E{01}	*−3.25*	**−0.64***	**0.59***	**−0.68***							*−0.51*		
	R{−1}		**−3.98***	**−0.57***	**0.5***	*−0.56*					*−0.40*				
	C{01}							*2.35*	*3.31*	*0.49*			*−0.51*		*2.72*
Day 3	A{−1}	C{03}	*−2.54*		*0.48*							*0.38*			
	R{−1}		*−3.27*		*0.39*							*0.31*			
	C{01}			**0.52***		*0.59*	*−0.59*	**2.52***	**3.33***			*0.32*			*2.66*
	A{−1}	H{03}			*0.36*										
	R{−1}									*0.49*					
	H{01}			*0.44*	*−0.36*	*0.38*	**−0.64***			*0.53*				*2.14*	
	C{03}		*2.92*												
	A{−1}	E{03}			*0.49*							*0.27*			
	R{−1}		*−2.63*		*0.41*					*0.54*					
	E{01}			*0.39*		*0.53*					*0.35*				
Day 7	C{03}	C{07}			*−0.28*							*−0.31*			
	R{−1}												*0.64*		
	H{01}	H{07}		**0.70***	**−0.57***	*0.54*	*−0.47*				*0.28*		*0.67*		
	H{03}												*0.48*		
	R{−1}		*−3.14*							**0.83***					
	E{01}			**0.61***	**−0.40***	*0.52*				*0.54*					
	E{03}	E{07}			*−0.30*										
	C{07}									*0.56*					
	H{07}									*0.51*					
Day 14	A{−1}	C{14}												*−2.16*	
	R{−1}		*−2.65*	*0.33*									*0.51*		
	A{−1}	H{14}						*−2.21*	*−2.31*						*−2.27*
	R{−1}			*0.34*											
	H{01}			**0.84***	**−0.52***	**0.55***					*0.31*				
	H{03}			*0.39*				*−2.35*	*−2.64*						*−2.70*
	R{−1}		*−2.68*							*0.46*					
	E{01}	E{14}		**0.62***	**−0.44***	*0.41*			*−1.97*						
	E{03}				*−0.34*							*−0.25*			

Fold change values marked with an asterisk and in boldface letters are significant ($p \leq 0.05$) with an adjusted p-value (false discovery rate corrected). Positive fold change values are in white letters on dark background. Genes within this pathway line with no significant differential expression are: Mapk1, Mstn, Neb, Sgca, Tnnt1.

Table ApxD - 4. The Skeletal Muscle Contractility – Energy Metabolism Gene Profile of Significant Differential Fold Changes (log_2(FC)).

Timing	Reference	Objective	Gene (Symbol)			
			Hk2	Slc2a4	Cs	Pdk4
Day −1	A{−1}	R{−1}				
Day 1	A{−1}	C{01}		*0.46*	*0.24*	
	R{−1}			*0.47*		
	C{01}	H{01}			*−0.25*	
	A{−1}	E{01}	**0.54***			*0.89*
	R{−1}		*0.39*			*0.96*
	C{01}		**0.67***			
	H{01}		*0.47*			
Day 3	C{01}	C{03}	*0.38*	**−0.53***		
	H{01}	H{03}		*−0.33*		
	E{01}	E{03}	*−0.49*			
Day 7	A{−1}	C{07}	*−0.42*			
	R{−1}		*−0.57*			
	C{03}		*−0.67*			
	A{−1}	H{07}	*−0.69*			
	R{−1}		**−0.85***			
	H{01}		**−0.77***			
	H{03}		*−0.70*		*−0.21*	
	A{−1}	E{07}				*0.87*
	R{−1}					*0.84*
	E{01}		**−0.66***			
	C{07}					*0.89*
	H{07}		*0.57*			
Day 14	A{−1}	H{14}			*−0.19*	
	R{−1}		*−0.37*		*−0.29*	
	H{01}				*−0.19*	
	H{03}				*−0.32*	
	H{07}		*0.47*			
	A{−1}	E{14}	*−0.39*			
	R{−1}		*−0.54*		*−0.20*	
	E{01}		**−0.93***		**−0.29***	
	E{03}		*−0.44*		*−0.26*	

Fold change values marked with an asterisk and in boldface letters are significant (p≤0.05) with an adjusted p-value (false discovery rate corrected). Positive fold change values are in white letters on dark background. Genes within this pathway line with no significant differential expression are: none.

Table ApxD - 5. The Skeletal Muscle Contractility – Fast-Twitch Fibres Gene Profile of Significant Differential Fold Changes (log_2(FC)).

Timing	Reference	Objective	Gene (Symbol)				
			Atp2a1	Tnnt3	Tnni2	Myh1	Myh2
Day −1	A{−1}	R{−1}					
Day 1	A{−1}	C{01}	**−0.72***	*−2.05*	*−2.78*		
	A{−1}	H{01}	*−0.60*			*−2.4*	
	R{−1}					*−2.11*	
	C{01}	E{01}	**0.80***	*2.35*	*3.31*		*2.72*
	H{01}		*0.67*				
Day 3	R{−1}	C{03}	*0.54*				
	C{01}		**0.93***	**2.52***	**3.33***		*2.66*
	R{−1}	H{03}	*0.67*				
	H{01}		**0.83***			*2.14*	
	C{03}	E{03}	*−0.46*				
	H{03}		*−0.59*				
Day 7	H{03}	H{07}	*−0.57*				
Day 14	A{−1}	C{14}				*−2.16*	
	A{−1}	H{14}	*−0.51*	*−2.21*	*−2.31*		*−2.27*
	H{03}		*−0.85*	*−2.35*	*−2.64*		*−2.70*
	E{01}	E{14}	*−0.44*		*−1.97*		

Fold change values marked with an asterisk and in boldface letters are significant (p≤0.05) with an adjusted p-value (false discovery rate corrected). Positive fold change values are in white letters on dark background. Genes within this pathway line with no significant differential expression are: none.

Table ApxD - 6. The Skeletal Muscle Contractility – Slow-Twitch Fibres Gene Profile of Significant Differential Fold Changes (log_2(FC)).

Timing	Reference	Objective	Gene (Symbol)		
			Mb	Myh1	Tnnc1
Day −1	A{−1}	R{−1}			
Day 1	R{−1}	C{01}	*−0.32*		
	A{−1}	H{01}		*−2.4*	
	R{−1}		*−0.29*	*−2.11*	
Day 3	H{01}	H{03}		*2.14*	
Day 7	H{03}	H{07}			*0.45*
Day 14	A{−1}	C{14}		*−2.16*	
	H{03}	H{14}			*0.43*
	E{01}	E{14}			*0.40*

Fold change values marked with an asterisk and in boldface letters are significant (p≤0.05) with an adjusted p-value (false discovery rate corrected). Positive fold change values are in white letters on dark background. Genes within this pathway line with no significant differential expression are: Tnnt1.

Table ApxD - 7. The Skeletal Muscle Contractility – Other Genes Gene Profile of Significant Differential Fold Changes (log_2(FC)).

Timing	Reference	Objective	Gene (Symbol)
			Rps6kb1
Day −1	A{−1}	R{−1}	
Day 1	A{−1}	C{01}	−0.33
	R{−1}		−0.36
	A{−1}	H{01}	**−0.39***
	R{−1}		**−0.42***
	R{−1}	E{01}	−0.29
Day 3	E{01}	E{03}	0.26
Day 7	A{−1}	H{07}	−0.27
	R{−1}		−0.30
Day 14	H{01}	H{14}	0.30
	E{01}		0.32

Fold change values marked with an asterisk and in boldface letters are significant (p≤0.05) with an adjusted p-value (false discovery rate corrected). Positive fold change values are in white letters on dark background. Genes within this pathway line with no significant differential expression are: Dmpk, Ikbkb.

Table ApxD - 8. The Skeletal Myogenesis Gene Profile of Significant Differential Fold Changes (log_2(FC)).

Timing	Reference	Objective	Gene (Symbol)																				
			Myod1	Mef2c	Hdac5	Myog	Adrb2	Dmd	Rps6kb1	Agrn	Igfbp5	Cast	Utrn	Cav1	Bmp4	Capn2	Acta1	Myf5	Igfbp3	Igf1	Mbnl1	Myf6	Ppp3ca
Day −1	A{−1}	R{−1}										0.44					0.25						
Day 1	A{−1}	C{01}	0.74	−0.48			−0.45		−0.33				0.24			−0.29							
	R{−1}		0.88	−0.44					−0.36			**−0.60***				−0.36	−0.39						
	A{−1}	H{01}	**1.10***	**−0.55***	−0.39	0.59	−0.57	−0.39	**−0.39***	**−0.41***	−0.81			−0.33									−0.33
	R{−1}		**1.24***	**−0.51***	**−0.46***		−0.53	−0.44	**−0.42***	**−0.44***				−0.39			−0.36						
	C{01}									−0.42	−0.96		−0.21	−0.39		0.34					0.43		
	A{−1}	E{01}	**1.32***	**−0.65***	**−0.6***	0.61	−0.48			−0.31	−0.96												
	R{−1}		**1.46***	**−0.61***	**−0.68***		−0.45		−0.29	−0.33				−0.31			−0.40						
	C{01}				−0.45					−0.31	−1.12	0.46	−0.3	−0.31									
Day 3	R{−1}	C{03}																	−0.48				
	C{01}			**0.54***								0.33						0.24					
	A{−1}	H{03}											0.26										
	R{−1}																		−0.51				
	H{01}		−0.88	**0.70***		**−0.72***		0.53		**0.41***			0.24		0.34								
	A{−1}	E{03}																	−0.45				
	R{−1}				−0.34														−0.52				
	E{01}		−1.04	**0.75***	0.33	−0.48	0.66		0.26				0.22				0.35	0.27					
	C{03}				−0.32																		
Day 7	A{−1}	C{07}													0.34								
	R{−1}					−0.59						−0.44		−0.29		−0.30							
	A{−1}	H{07}						0.44	−0.27				0.31	−0.38	0.34								
	R{−1}					−0.67		0.39	−0.30	−0.27		−0.47	0.26	−0.43				0.27					
	H{01}		**−1.16***	0.45	0.34	**−0.94***	0.42	**0.84***		−0.28	0.90		**0.29***		0.39		0.28						
	C{07}							0.38		−0.31			0.21					0.26					
	A{−1}	E{07}								−0.34				−0.50		−0.26							
	R{−1}					−0.61						−0.56		**−0.56***		−0.33							
	E{01}		**−1.65***	**0.59***	**0.44***	**−0.90***	**0.74***				0.95	−0.43											
	E{03}										0.68			−0.28									
	C{07}									−0.35					−0.37								
	H{07}							−0.37							−0.37								
Day 14	A{−1}	C{14}											0.26										
	R{−1}					−0.57						−0.41				−0.24							
	A{−1}	H{14}											0.22										
	R{−1}					−0.51						−0.37						0.26					
	H{01}		**−1.52***		0.31	**−0.78***	**0.69***	**0.71***	0.30	0.25	0.72				0.33		0.31						
	H{03}			−0.42																			
	C{14}																	0.26					
	A{−1}	E{14}								−0.39				−0.36									
	R{−1}					−0.66				−0.41		−0.41		−0.42	−0.38	−0.28				−0.57			
	E{01}		**−1.53***	0.38	**0.43***	**−0.95***	**0.71***	0.37	0.32		**1.00***				−0.32								
	E{03}			−0.36		−0.47				−0.25	0.73				−0.31							−0.52	
	C{14}									−0.28				−0.28	−0.48								
	H{14}														−0.49			−0.24					

Fold change values marked with an asterisk and in boldface letters are significant (p≤0.05) with an adjusted p-value (false discovery rate corrected). Positive fold change values are in white letters on dark background. Genes within this pathway line with no significant differential expression are: Bcl2, Ctnnb1, Mstn, Musk, Pax3, Rhoa.

Table ApxD - 9. The Skeletal Muscle Hypertrophy Gene Profile of Significant Differential Fold Changes (log_2(FC)).

Timing	Reference	Objective	Gene (Symbol)							
			Myod1	Adrb2	Acvr2b	Rps6kb1	Igfbp5	Acta1	Igf1	Myf6
Day −1	A{−1}	R{−1}						0.25		
Day 1	A{−1}	C{01}	0.74	−0.45		−0.33				
	R{−1}		0.88			−0.36		−0.39		
	A{−1}	H{01}	**1.10***	−0.57		**−0.39***	−0.81			
	R{−1}		**1.24***	−0.53		**−0.42***		−0.36		
	C{01}						−0.96			
	A{−1}	E{01}	**1.32***	−0.48			−0.96			
	R{−1}		**1.46***	−0.45		−0.29		−0.40		
	C{01}						−1.12			
Day 3	H{01}	H{03}	−0.88		0.62					
	E{01}	E{03}	−1.04	0.66				0.35		
Day 7	A{−1}	H{07}				−0.27				
	R{−1}					−0.30				
	H{01}		**−1.16***	0.42	0.63		0.90	0.28		
	E{01}	E{07}	**−1.65***	**0.74***		0.26	0.95			
	E{03}						0.68			
Day 14	H{01}	H{14}	**−1.52***	**0.69***	**0.75***	0.30	0.72	0.31		
	R{−1}								−0.57	
	E{01}	E{14}	**−1.53***	**0.71***	0.50	0.32	**1.00***			
	E{03}						0.73			−0.52

Fold change values marked with an asterisk and in boldface letters are significant (p≤0.05) with an adjusted p-value (false discovery rate corrected). Positive fold change values are in white letters on dark background. Genes within this pathway line with no significant differential expression are: Mstn.

Table ApxD – 10. The Skeletal Muscle Autocrine Signalling Gene Profile of Significant Differential Fold Changes (log_2(FC)).

Timing	Reference	Objective	Gene (Symbol)					
			Il6	Tgfb1	Igf2	Adipoq	Fgf2	Igf1
Day −1	A{−1}	R{−1}				1.90		
Day 1	A{−1}	C{01}		0.71*				
	R{−1}			0.49				
	A{−1}	H{01}		0.86*				
	R{−1}			0.64*		−1.56		
	A{−1}	E{01}	1.06*	0.56	−0.53			
	R{−1}		1.00*		−0.57		0.50	
	C{01}		0.91					
	H{01}		0.75					
Day 3	A{−1}	C{03}		0.70				
	R{−1}			0.48				
	C{01}				0.54			
	A{−1}	H{03}		0.55		1.92		
	R{−1}						0.59	
	H{01}				0.67	1.58		
	A{−1}	E{03}		0.61		1.79		
	R{−1}						0.45	
	E{01}		−0.89		0.71			
Day 7	A{−1}	C{07}			0.66			
	R{−1}				0.63			
	H{01}	H{07}		−0.65*	0.90*			
	E{01}	E{07}	−0.98*		0.77*			
Day 14	C{07}	C{14}			−0.69			
	H{07}	H{14}		−0.58*	−0.60			
	R{−1}	E{14}					0.50	−0.57
	E{01}		−1.04*	−0.55				
	E{03}			−0.60				

Fold change values marked with an asterisk and in boldface letters are significant ($p \leq 0.05$) with an adjusted p-value (false discovery rate corrected). Positive fold change values are in white letters on dark background. Genes within this pathway line with no significant differential expression are: Lep, Mstn.

Table ApxD – 11. The Diabetes/Metabolic Syndrome Gene Profile of Significant Differential Fold Changes (log_2(FC)).

Timing	Reference	Objective	Gene (Symbol)						
			Ppargc1a	Prkaa1	Slc2a4	Prkab2	Ppargc1b	Adipoq	Pparg
Day −1	A{−1}	R{−1}				−0.64		1.90	
Day 1	A{−1}	C{01}			0.46				
	R{−1}				0.47	0.80			
	A{−1}	H{01}		0.53*				−1.56	−0.54
	R{−1}						−0.71		−0.55
	C{01}						−0.71		
	A{−1}	E{01}	1.65*	0.44					
	R{−1}		1.77*			0.89			
	C{01}		1.27				−0.97		
	H{01}		1.51						
Day 3	A{−1}	C{03}		0.52					
	C{01}				−0.53*	−0.71			
	A{−1}	H{03}				−0.71		1.92	
	H{01}				−0.33	−0.68		1.58	
	A{−1}	E{03}	1.42	0.73*				1.79	
	R{−1}		1.54	0.46					
	C{03}		1.45						
	H{03}		1.17						
Day 7	C{03}	C{07}		−0.38					−0.53
	R{−1}	H{07}					0.80		
	H{01}								
	A{−1}	E{07}	2.18*						
	R{−1}		2.30*				0.71		
	E{01}								
	E{03}			−0.56					
	C{07}		2.16*						
	H{07}		1.90*						
Day 14	R{−1}	H{14}		−0.43		0.91	0.88		
	H{01}						0.65		
	H{03}					0.98			
	C{14}					0.78			
	A{−1}	E{14}	1.45						
	R{−1}		1.56			0.79			
	E{01}						0.63		
	E{03}			−0.39					
	C{14}		1.20						
	H{14}		1.30						

Fold change values marked with an asterisk and in boldface letters are significant ($p \leq 0.05$) with an adjusted p-value (false discovery rate corrected). Positive fold change values are in white letters on dark background. Genes within this pathway line with no significant differential expression are: Lep, Prkag1, Prkag3.

Table ApxD - 12. The Skeletal Muscle Wasting/Atrophy – Autophagy Gene Profile of Significant Differential Fold Changes (log_2(FC)).

Timing	Reference	Objective	Gene (Symbol)								
			Fbxo32	Casp3	Nos2	Rps6kb1	Ppargc1a	Trim63	Foxo3	Capn2	Ppargc1b
Day −1	A{−1}	R{−1}	−0.58					−0.48			
Day 1	A{−1}	C{01}	0.42	0.52		−0.33		**−0.67***		−0.29	
	R{−1}		**1.01***			−0.36			0.28	−0.36	
	A{−1}	H{01}		0.61	−0.36	**−0.39***		−0.51			
	R{−1}		**0.62***	0.42		−0.42			0.31		
	C{01}									0.34	−0.71
	A{−1}	E{01}		0.64			1.65				−0.71
	R{−1}			0.45		−0.29	1.77				
	C{01}		−0.66				1.27	0.49			−0.97
	H{01}						1.51				
Day 3	A{−1}	C{03}		**0.43***	−0.33						
	R{−1}		0.59								
	C{01}		−0.41						−0.33		
	A{−1}	H{03}		**0.43***							
	R{−1}		**0.92***					0.49			
	H{01}							0.53	−0.36		
	A{−1}	E{03}					1.42				
	R{−1}		0.47				1.54	0.54			
	E{01}					0.26					
	C{03}						1.45				
	H{03}		−0.45				1.17				
Day 7	R{−1}	C{07}	0.66							−0.30	
	A{−1}	H{07}	0.46			−0.27					
	R{−1}		**1.05***			−0.3					
	H{01}		0.42	**−0.53***	0.26				−0.27		0.80
	A{−1}	E{07}					2.18			−0.26	
	R{−1}		**0.95***				2.30	**0.83***		−0.33	
	E{01}		**0.61***	**−0.60***				0.54			0.71
	E{03}		0.48						0.23		
	C{07}						2.16	0.56			
	H{07}						1.90	0.51			
Day 14	R{−1}	C{14}	**0.92***							−0.24	
	R{−1}	H{14}	**0.96***								
	H{01}			−0.59		0.30					0.88
	H{03}			**−0.42***							0.65
	A{−1}	E{14}	0.50				1.45				
	R{−1}		**1.08***				1.56	0.46	0.31	−0.28	
	E{01}		**0.74***	−0.70		0.32					0.63
	E{03}		0.61						0.30		
	C{14}						1.20		0.25		
	H{14}						1.30				

Fold change values marked with an asterisk and in boldface letters are significant (p≤0.05) with an adjusted p-value (false discovery rate corrected). Positive fold change values are in white letters on dark background. Genes within this pathway line with no significant differential expression are: Mstn.

Table ApxD - 13. The Skeletal Muscle Wasting/Atrophy – Dystrophy Gene Profile of Significant Differential Fold Changes (log_2(FC)).

Timing	Reference	Objective	Gene (Symbol)										
			Fbxo32	Akt2	Il1b	Trim63	Mapk8	Utrn	Mapk14	Tnf	Akt1	Mapk3	Nfkb1
Day −1	A{−1}	R{−1}	−0.58			−0.48							
Day 1	A{−1}	C{01}	0.42	−0.45		**−0.67***	−0.38	0.24	−0.29	−0.64			
	R{−1}		**1.01***	−0.50			−0.34			−0.78			
	A{−1}	H{01}		**−0.51***		−0.51	**−0.49***						
	R{−1}		**0.62***	**−0.55***			−0.45			−0.62			
	C{01}							−0.21					
	A{−1}	E{01}		−0.44	**1.18***		−0.39						
	R{−1}			−0.48	0.76		−0.34				−0.43		
	C{01}		−0.66		0.84	0.49		−0.30		0.59			
Day 3	A{−1}	C{03}							−0.29				
	R{−1}		0.59										
	C{01}		−0.41	**0.55***						0.69			
	A{−1}	H{03}					−0.4	0.26	−0.27				
	R{−1}		**0.92***			0.49	−0.35						
	C{01}												
	H{01}					0.53		0.24					
	A{−1}	E{03}							−0.36				
	R{−1}		0.47			0.54					−0.48		−0.30
	E{01}				−0.83			0.22	−0.33				
	C{03}			−0.36									
	H{03}		−0.45										
Day 7	A{−1}	C{07}					−0.39						
	R{−1}		0.66				−0.34						
	A{−1}	H{07}	0.46					0.31	−0.32				
	R{−1}		**1.05***					0.26					
	H{01}		0.42	**0.49***	−0.75			**0.29***					
	C{07}							0.21					
	A{−1}	E{07}							−0.33				
	R{−1}		**0.95***			**0.83***							
	E{01}		**0.61***		−0.90	0.54			−0.29				
	E{03}		0.48										
	C{07}					0.56							
	H{07}					0.51							
Day 14	A{−1}	C{14}						0.26					
	R{−1}		**0.92***										
	A{−1}	H{14}						0.22					
	R{−1}		**0.96***										
	H{01}			0.44									
	A{−1}	E{14}	0.50										
	R{−1}		**1.08***			0.46							
	E{01}		**0.74***		**−1.05***								
	E{03}		0.61										
	H{14}											−0.29	

Fold change values marked with an asterisk and in boldface letters are significant (p≤0.05) with an adjusted p-value (false discovery rate corrected). Positive fold change values are in white letters on dark background. Genes within this pathway line with no significant differential expression are: Mapk1, Mmp9.

Appendix D.4.2 The Hypoxia Signalling Pathway

Table ApxD - 14. The Hypoxia Signalling – Angiogenesis Gene Profile of Significant Differential Fold Changes (log_2(FC)).

Timing	Reference	Objective	Gene (Symbol)												
			Hmox1	Btg1	Adora2b	Anxa2	Plau	Serpine1	Lox	Pgf	Vegfa	Jmjd6	Angptl4	F3	Gpi
Day −1	A{−1}	R{−1}													
Day 1	A{−1}	C{01}					0.69	1.21	1.29			−0.38			
	R{−1}							1.16							
	A{−1}	H{01}	1.26	**0.57***	0.52	**1.33***	**1.05***	**1.99***	**2.03***		**−1.11***				
	R{−1}		1.23	**0.46***		0.99	0.73	**1.94***	**1.46***		−0.62				
	C{01}			0.35											
	A{−1}	E{01}	**1.96***	**0.89***	**0.72***	**1.09***	**1.29***	**2.24***	**1.90***		−0.62				
	R{−1}		**1.93***	**0.79***	0.50	0.76	**0.97***	**2.20***	1.34	0.74					
	C{01}		**1.59***	**0.68***			0.60	1.03		0.59			2.92		
	H{01}			0.32						0.56					
Day 3	A{−1}	C{03}				0.87		0.97	1.94						
	R{−1}							0.92	1.38						
	A{−1}	H{03}				0.83	0.56		1.77		−1.02				
	R{−1}								1.20			−0.33			
	H{01}		−0.98	−0.30	−0.45			**−1.51***							
	A{−1}	E{03}				0.82	0.56	**1.85***	1.59		−0.98				
	R{−1}							1.80	1.02						
	E{01}		**−1.51***	**−0.80***	**−0.72***		−0.72			−0.73			−2.49		
	H{03}							1.37							
Day 7	C{03}	C{07}						−0.97	−1.04						
	A{−1}	H{07}								−0.63		−0.36			
	R{−1}											−0.43			
	H{01}		**−1.38***	**−0.69***	−0.53	**−1.32***	−0.66	**−1.59***	−1.17						
	H{03}			−0.39		−0.81									
	A{−1}	E{07}					0.57	1.14							
	R{−1}							1.09							
	E{01}		**−1.82***	**−1.07***	**−0.66***	**−1.12***	−0.71	−1.10	−1.21	−0.73			−2.84		
	E{03}					−0.84					0.91				
	C{07}							1.14							
Day 14	R{−1}	C{14}												−0.74	
	H{01}	H{14}	**−1.39***	**−0.69***	**−0.62***	**−1.22***	**−0.81***	**−1.44***	**−1.46***		0.68				
	H{03}			−0.39		−0.72			−1.20		0.59				
	H{07}									0.55					
	A{−1}	E{14}						1.02							−0.29
	R{−1}							0.97							
	E{01}		**−1.84***	**−1.01***	**−0.79***	**−1.27***	**−0.94***	−1.22	**−1.84***	**−0.77***					
	E{03}					−1.00			−1.52		0.62				

Fold change values marked with an asterisk and in boldface letters are significant (p≤0.05) with an adjusted p-value (false discovery rate corrected). Positive fold change values are in white letters on dark background. Genes within this pathway line with no significant differential expression are: Egr1, Edn1, Epo, Mmp9.

Table ApxD - 15. The Hypoxia Signalling – HIF1 & Co-Transcription Factors Gene Profile of Significant Differential Fold Changes (log_2(FC)).

Timing	Reference	Objective	Gene (Symbol)				
			Arnt	Per1	Hif1a	Cops5	Hif3a
Day −1	A{−1}	R{−1}		−0.57			
Day 1	A{−1}	C{01}	−0.30	−0.78	−1.11	−0.25	
	R{−1}		−0.22				
	A{−1}	H{01}		−0.64			
	A{−1}	E{01}		−0.58			
	C{01}		**0.37***		1.32		
Day 3	R{−1}	C{03}		0.52			
	C{01}		0.22	0.72			
	A{−1}	H{03}		−0.66			
	C{03}			−0.61			
	A{−1}	E{03}		−0.53			
Day 7	A{−1}	C{07}	−0.23	−0.63			
	C{03}			−0.57			
	A{−1}	H{07}	−0.24	−0.53			
	H{03}		−0.20				
	A{−1}	E{07}		−0.69			
	C{07}		0.26				
	H{07}		0.27				
Day 14	A{−1}	C{14}	−0.22	−0.66			
	C{07}						0.24
	A{−1}	H{14}	−0.36	−0.68			
	R{−1}		−0.28				
	H{01}		−0.23				
	H{03}		−0.31				
	A{−1}	E{14}		−0.56			
	C{14}		0.25				
	H{14}		0.38				

Fold change values marked with an asterisk and in boldface letters are significant (p≤0.05) with an adjusted p-value (false discovery rate corrected). Positive fold change values are in white letters on dark background. Genes within this pathway line with no significant differential expression are: Hnf4a.

Table ApxD - 16. The Hypoxia Signalling – Other HIF1 Interactors Gene Profile of Significant Differential Fold Changes (log_2(FC)).

Timing	Reference	Objective	Gene (Symbol)					
			Egln3	P4hb	Tp53	Apex1	P4ha1	Nfkb1
Day −1	A{−1}	R{−1}						
Day 1	A{−1}	C{01}	**−1.98***	*0.51*			*−0.83*	
	R{−1}		**−2.10***				*−0.95*	
	A{−1}	H{01}	**−1.49***	**0.80***	**0.44***	*0.30*		
	R{−1}		**−1.62***	**0.61***	**0.44***	*0.27*		
	A{−1}	E{01}	**−0.88***	*0.50*				
	R{−1}		**−1.00***					
	C{01}		**1.09***				*0.96*	
	H{01}		*0.61*					
Day 3	A{−1}	C{03}		*0.60*	*0.36*			
	R{−1}			*0.41*	*0.36*			
	C{01}		**2.18***					
	A{−1}	H{03}		*0.49*				
	H{01}		**1.33***		*−0.39*	**−0.37***		
	C{03}				*−0.31*			
	R{−1}	E{03}						*−0.30*
	E{01}		*0.88*			*−0.29*		
	C{07}				*−0.37*			
Day 7	A{−1}	C{07}		*0.36*				
	A{−1}	H{07}					*−0.80*	
	R{−1}		*−0.64*				*−0.92*	
	H{01}		**0.97***	**−0.73***	*−0.31*			
	H{03}			*−0.42*			*−0.67*	
	E{01}	E{07}	*0.78*	*−0.39*				
	H{07}						*0.89*	
Day 14	R{−1}	C{14}	*−0.61*				*−0.64*	
	R{−1}	H{14}	*−0.66*					
	H{01}		**0.95***	**−0.55***	*−0.28*			
	E{01}	E{14}	*0.68*	*−0.45*	**−0.42***			
	E{07}				*−0.28*			
	C{14}						*0.65*	
	H{14}				*−0.34*			

Fold change values marked with an asterisk and in boldface letters are significant (p≤0.05) with an adjusted p-value (false discovery rate corrected). Positive fold change values are in white letters on dark background. Genes within this pathway line with no significant differential expression are: Cdkn2a, Egln1.

Table ApxD - 17. The Hypoxia Signalling – Coagulation Gene Profile of Significant Differential Fold Changes (log_2(FC)).

Timing	Reference	Objective	Gene (Symbol)					
			Anxa2	Plau	Serpine1	Aldoa	F10	F3
Day −1	A{−1}	R{−1}						
Day 1	A{−1}	C{01}		*0.69*	*1.21*		*0.27*	
	R{−1}				*1.16*			
	A{−1}	H{01}	**1.33***	**1.05***	**1.99***			
	R{−1}		*0.99*	*0.73*	**1.94***	*−0.45*		
	A{−1}	E{01}	**1.09***	**1.29***	**2.24***			
	R{−1}		*0.76*	**0.97***	**2.20***			
	C{01}			*0.60*	*1.03*			
Day 3	A{−1}	C{03}	*0.87*		*0.97*			
	R{−1}				*0.92*			
	C{01}					*0.54*		
	A{−1}	H{03}	*0.83*	*0.56*		*0.41*		
	H{01}				**−1.51***	**0.68***		
	A{−1}	E{03}	*0.82*	*0.56*	**1.85***			
	R{−1}				*1.80*			
	E{01}			*−0.72*				
	H{03}				*1.37*			
Day 7	C{03}	C{07}			*−0.97*			
	H{01}	H{07}	**−1.32***	*−0.66*	**−1.59***			
	H{03}		*−0.81*			*−0.44*		
	A{−1}	E{07}		*0.57*	*1.14*			
	R{−1}				*1.09*			
	E{01}		**−1.12***	*−0.71*	*−1.1*			
	E{03}		*−0.84*					
	C{07}				*1.14*			
Day 14	R{−1}	C{14}						*−0.74*
	H{01}	H{14}	**−1.22***	**−0.81***	**−1.44***			
	H{03}		*−0.72*			*−0.49*		
	A{−1}	E{14}			*1.02*			
	R{−1}				*0.97*			
	E{01}		**−1.27***	**−0.94***	*−1.22*			
	E{03}		*−1.00*			*−0.41*	*−0.26*	

Fold change values marked with an asterisk and in boldface letters are significant (p≤0.05) with an adjusted p-value (false discovery rate corrected). Positive fold change values are in white letters on dark background. Genes within this pathway line with no significant differential expression are:

Table ApxD - 18. The Hypoxia Signalling – DNA Damage Signalling & Repair Gene Profile of Significant Differential Fold Changes (log_2(FC)).

Timing	Reference	Objective	Gene (Symbol)		
			Mif	Ndrg1	Ruvbl2
Day −1	A{−1}	R{−1}			
Day 1	R{−1}	C{01}	*−0.27*		
	A{−1}	E{01}	*−0.32*		
	R{−1}		**−0.42***		
	C{01}			*0.48*	
Day 3	A{−1}	E{03}			*−0.23*
	R{−1}		*−0.30*		
Day 7	R{−1}	H{07}	*−0.25*		
	H{01}			*−0.52*	
	H{03}			*−0.46*	
	E{01}	E{07}	*0.23*	*−0.55*	
Day 14	H{07}	H{14}	*0.22*		
	R{−1}		*−0.23*		
	E{01}			*−0.60*	

Fold change values marked with an asterisk and in boldface letters are significant (p≤0.05) with an adjusted p-value (false discovery rate corrected). Positive fold change values are in white letters on dark background. Genes within this pathway line with no significant differential expression are: LOC367198.

Table ApxD - 19. The Hypoxia Signalling – Metabolism Gene Profile of Significant Differential Fold Changes (log_2(FC)).

Timing	Reference	Objective	Gene (Symbol)														
			Pdk1	Pfkl	Ero1l	Hk2	Pgam1	Slc2a1	Aldoa	Ldha	Pkm	Ddit4	Pgm2	Pfkp	Gpi	Gys1	Tpi1
Day −1	A{−1}	R{−1}															
Day 1	A{−1}	C{01}	−0.39	**−0.84***				−0.67		−0.5	−0.54	**1.18***					−0.28
	R{−1}		**−0.60***	**−0.62***				−0.85		−0.49	−0.39	0.72					
	A{−1}	H{01}	**−0.58***	**−0.43***							**−0.54***						
	R{−1}		**−0.78***						−0.45		−0.39						
	C{01}			0.41			0.61	0.70				−0.70					
	A{−1}	E{01}	**−0.72***	**−0.48***		**0.54***		0.75			−0.41						
	R{−1}		**−0.93***			0.39											
	C{01}			0.36		**0.67***	0.60	**1.42***				−0.91					
	H{01}					0.47		0.72									
Day 3	R{−1}	C{03}	−0.40														
	C{01}			**0.57***		0.38		0.61	0.54	**0.79***	0.56	−0.74				0.40	
	A{−1}	H{03}							0.41								
	H{01}		**0.6***				−0.51		**0.68***	0.42	0.41						
	A{−1}	E{03}		−0.34								0.83					
	E{01}		**0.59***			−0.49		**−1.23***				0.57	−0.40				
Day 7	A{−1}	C{07}		−0.40		−0.42											
	R{−1}					−0.57		−0.62									
	C{03}		0.34			−0.67											
	A{−1}	H{07}		−0.42		−0.69		−0.58									
	R{−1}					**−0.85***		−0.77					−0.43				
	H{01}		**0.58***		**−0.60***	**−0.77***	**−0.66***	−0.62					−0.39				
	C{07}				−0.40												
	A{−1}	E{07}										0.60					
	R{−1}							−0.65					−0.48				
	E{01}		**0.85***			**−0.66***											
	H{03}				−0.49	−0.70			−0.44	−0.40							
	E{03}							−0.70									
	H{07}					0.57											
Day 14	A{−1}	C{14}		−0.35													
	R{−1}							−0.61					−0.37				
	A{−1}	H{14}		−0.43							−0.40						
	R{−1}				−0.40	−0.37		−0.70					−0.36	−0.54			
	H{01}		**0.83***		**−0.62***								−0.32				
	H{07}					0.47											
	A{−1}	E{14}		−0.39		−0.39				−0.41		0.73	−0.35		−0.29		
	R{−1}					−0.54		−0.70		−0.39			−0.54	−0.55			
	E{01}		**0.86***			**−0.93***	−0.58	**−1.27***					**−0.46***	−0.49			
	H{03}				−0.51				−0.49								
	E{03}					−0.44		−0.74	−0.41	−0.41			−0.37				

Fold change values marked with an asterisk and in boldface letters are significant ($p \leq 0.05$) with an adjusted p-value (false discovery rate corrected). Positive fold change values are in white letters on dark background. Genes within this pathway line with no significant differential expression are: Eno1, Pfkfb3, Pfkfb4, Pfkl, Slc2a3.

Table ApxD - 20. The Hypoxia Signalling – Regulation of Apoptosis Gene Profile of Significant Differential Fold Changes (log_2(FC)).

Timing	Reference	Objective	Gene (Symbol)								
			Bnip3	Btg1	Pim1	Mif	Ddit4	Ier3	Bnip3l	Adm	Nos3
Day −1	A{−1}	R{−1}									
Day 1	A{−1}	C{01}	**−1.52***		0.38		**1.18***	1.23			
	R{−1}		**−1.53***		0.36	−0.27	0.72	1.21			
	A{−1}	H{01}	**−1.40***	**0.57***	**0.94***						
	R{−1}		**−1.41***	**0.46***	**0.92***				−0.37		
	C{01}			0.35	0.56		−0.7				
	A{−1}	E{01}	**−1.18***	**0.89***	**0.99***	−0.32		1.01			
	R{−1}		**−1.19***	**0.79***	**0.98***	**−0.42***		1.00			
	C{01}			**0.68***	**0.61***		−0.91				0.42
	H{01}			0.32							0.36
Day 3	R{−1}	C{03}	**1.26***				−0.74	−0.98	−0.31		
	C{01}				0.33			0.90			
	A{−1}	H{03}			0.31			0.88			
	R{−1}		**1.12***	−0.30	**−0.61***				0.30		
	H{01}				**0.59***		0.83				
	A{−1}	E{03}			0.58	−0.30					
	R{−1}		**0.79***	**−0.8***	−0.4		0.57				−0.45
	E{01}				0.41						
	C{03}										
Day 7	R{−1}	H{07}	**1.36***	**−0.69***	**−0.83***	−0.25			−0.34		
	H{01}			−0.39					−0.27		
	H{03}				0.43		0.60				
	A{−1}	E{07}			0.41				−0.31	−0.55	
	R{−1}		**1.00***	**−1.07***	**−0.56***	0.23				−0.61	
	E{01}				0.39					−0.59	
	H{07}										
Day 14	R{−1}	C{14}							−0.35		
	C{07}				−0.41						
	A{−1}	H{14}						0.93			
	R{−1}							0.91			
	H{01}		**1.35***	**−0.69***	**−0.8***						
	H{03}			−0.39		0.22					
	H{07}							0.90			
	C{14}						0.73				
	A{−1}	E{14}				−0.23			−0.32		
	R{−1}										
	E{01}		**1.07***	**−1.01***	**−0.96***						
	E{03}				−0.56						
	E{07}				−0.40						

Fold change values marked with an asterisk and in boldface letters are significant ($p \leq 0.05$) with an adjusted p-value (false discovery rate corrected). Positive fold change values are in white letters on dark background. Genes within this pathway line with no significant differential expression are: none.

Table ApxD - 21. The Hypoxia Signalling – Regulation of Cell Proliferation Gene Profile of Significant Differential Fold Changes (log_2(FC)).

Timing	Reference	Objective	Gene (Symbol)											
			Btg1	Pim1	Mxi1	Ccng2	Mif	Pgf	Odc1	Igfbp3	Met	Adm	Nampt	Nos3
Day −1	A{−1}	R{−1}												
Day 1	A{−1}	C{01}		0.38	−0.37	0.37			−0.73					
	R{−1}			0.36	−0.40	**0.56***	−0.27		−0.77					
	A{−1}	H{01}	**0.57***	**0.94***	**−0.47***				−0.68					
	R{−1}		**0.46***	**0.92***	**−0.50***				−0.72					
	C{01}		0.35	0.56		−0.38								
	A{−1}	E{01}	**0.89***	**0.99***	−0.39		−0.32						0.42	
	R{−1}		**0.79***	**0.98***	−0.42		**−0.42***	0.74						
	C{01}		**0.68***	**0.61***		−0.47		0.59					0.51	0.42
	H{01}		0.32	0.56				0.56						0.36
Day 3	R{−1}	C{03}								−0.48				
	C{01}				0.29									
	A{−1}	H{03}		0.33					−0.58					
	R{−1}			0.31					−0.62	−0.51				
	H{01}		−0.30	**−0.61***	0.42									
	A{−1}	E{03}		**0.59***					−0.61	−0.45	0.22		0.45	
	R{−1}			0.58			−0.30		−0.65	−0.52	0.22			
	E{01}		**−0.80***	−0.40				−0.73						−0.45
	C{03}			0.41										
Day 7	A{−1}	H{07}						−0.63						
	R{−1}					0.35	−0.25							
	H{01}		**−0.69***	**−0.83***							−0.24			
	H{03}		−0.39											
	C{07}			−0.25							−0.25			
	A{−1}	E{07}		0.43										
	R{−1}			0.41		0.36						−0.55		
	E{01}		**−1.07***	**−0.56***	0.31		0.23	−0.73				−0.61		
	E{03}										−0.22			
	H{07}			0.33								−0.59		
Day 14	R{−1}	C{14}				0.41								
	C{07}			−0.41										
	H{01}	H{14}	**−0.69***	**−0.80***	0.38				0.68					
	H{03}		−0.39						0.57					
	H{07}						0.22	0.55						
	A{−1}	E{14}				0.38								
	R{−1}					0.56	−0.23							
	E{01}		**−1.01***	**−0.96***	**0.44***	**0.48***		**−0.77***	0.65					
	E{03}			−0.56		0.41			0.82					
	E{07}			−0.40					0.58					

Fold change values marked with an asterisk and in boldface letters are significant (p≤0.05) with an adjusted p-value (false discovery rate corrected). Positive fold change values are in white letters on dark background. Genes within this pathway line with no significant differential expression are: Blm, Egr1, Txnip.

Table ApxD - 22. The Hypoxia Signalling – Transcription Factors Gene Profile of Significant Differential Fold Changes (log_2(FC)).

Timing	Reference	Objective	Gene (Symbol)		
			Usf2	Bhlhe40	Fos
Day −1	A{−1}	R{−1}			
Day 1	A{−1}	E{01}	−0.26		
	R{−1}		−0.26		
	C{01}			0.60	
Day 3	C{01}	C{03}	0.28		
Day 7	R{−1}	H{07}		0.62	
	H{01}				−1.42
	E{01}	E{07}	**0.34***	−0.62	
	E{03}		0.23		
	H{07}			−0.67	
Day 14	H{01}	H{14}	0.30		
	H{03}		0.27		
	H{07}			−0.67	
	E{01}		0.31		

Fold change values marked with an asterisk and in boldface letters are significant (p≤0.05) with an adjusted p-value (false discovery rate corrected). Positive fold change values are in white letters on dark background. Genes within this pathway line with no significant differential expression are: Rbpjl.

Table ApxD - 23. The Hypoxia Signalling – Transporters, Channels & Receptors Gene Profile of Significant Differential Fold Changes (log_2(FC)).

Timing	Reference	Objective	Gene (Symbol)			
			Tfrc	Slc16a3	Slc2a1	Vdac1
Day −1	A{−1}	R{−1}				
Day 1	A{−1}	C{01}		−0.94	−0.67	
	R{−1}				−0.85	
	A{−1}	H{01}		**−1.78***		−0.40
	R{−1}			**−1.57***		−0.43
	C{01}			−0.83	0.70	
	A{−1}	E{01}		−0.88	0.75	
	C{01}				**1.42***	
	H{01}			0.89	0.72	0.31
Day 3	A{−1}	C{03}	−1.10			−0.34
	R{−1}		−0.85			−0.37
	C{01}		−0.85	0.98	0.61	
	A{−1}	H{03}	**−1.54***			−0.31
	R{−1}		**−1.29***			−0.34
	H{01}		**−1.12***	**1.67***		
	A{−1}	E{03}	−0.60			
	H{03}		0.94			
Day 7	A{−1}	C{07}	−0.97			
	R{−1}		−0.72		−0.62	
	A{−1}	H{07}	−1.23		−0.58	
	R{−1}		−0.98		−0.77	
	H{01}		**−0.81***	**1.09***	−0.62	
	A{−1}	E{07}	**−1.34***	−0.87		
	R{−1}		−1.09		−0.65	
	E{01}		**−1.10***		**−1.23***	
	E{03}		−0.74		−0.70	
Day 14	A{−1}	C{14}	−0.98	−0.97		
	R{−1}		−0.73		−0.61	
	A{−1}	H{14}	−1.19	−1.00		
	R{−1}		−0.93	−0.79	−0.70	
	H{01}		−0.77	0.77		0.31
	H{03}			−0.89		
	A{−1}	E{14}	−1.20	−1.18		
	R{−1}		−0.94	−0.97	−0.7	
	E{01}		**−0.95***		**−1.27***	
	E{03}		−0.60		−0.74	0.29

Fold change values marked with an asterisk and in boldface letters are significant ($p \leq 0.05$) with an adjusted p-value (false discovery rate corrected). Positive fold change values are in white letters on dark background. Genes within this pathway line with no significant differential expression are: Slc2a3.

Table ApxD - 24. The Hypoxia Signalling – Other Responsive Genes Gene Profile of Significant Differential Fold Changes (log_2(FC)).

Timing	Reference	Objective	Gene (Symbol)						
			Lgals3	Ctsa	Ankrd37	Car9	Dnajc5	Eif4ebp1	Map3k1
Day −1	A{−1}	R{−1}							
Day 1	A{−1}	C{01}	**1.79***	**1.02***	**−1. 20***	−0.25			
	R{−1}		1.17	0.75	**−1.03***				
	A{−1}	H{01}	**2.51***	**1.10***	−0.82	−0.24			
	R{−1}		**1.88***	**0.84***	−0.64				
	A{−1}	E{01}	**2.10***	0.77					
	R{−1}		**1.47***						
	C{01}				0.60				
Day 3	A{−1}	C{03}	1.31	0.66					
	C{01}				0.72	0.23			
	A{−1}	H{03}	1.49	0.75	−0.65			0.57	
	R{−1}		0.87						
	H{01}		−1.01			0.21			
	A{−1}	E{03}	**1.79***	0.55					
	R{−1}		1.16						
	E{01}						0.31		
Day 7	C{03}	C{07}	−0.94						
	A{−1}	H{07}	0.86						−0.49
	H{01}		**−1.64***	**−0.81***		0.24			
	H{03}						−0.26	−0.58	
	E{01}	E{07}	**−1.47***	−0.57					
	E{03}		−1.16						
Day 14	A{−1}	H{14}	1.26						
	H{01}		**−1.24***	**−0.79***		0.23			
	E{01}	E{14}	**−1.48***	−0.54					
	E{03}		−1.17				−0.31	−0.45	

Fold change values marked with an asterisk and in boldface letters are significant ($p \leq 0.05$) with an adjusted p-value (false discovery rate corrected). Positive fold change values are in white letters on dark background. Genes within this pathway line with no significant differential expression are: none.

Appendix D.4.3 The VEGF Pathway

Table ApxD - 25. The VEGF – Small G-Protein Signalling Gene Profile of Significant Differential Fold Changes (log_2(FC)).

Timing	Reference	Objective	Gene (Symbol)						
			Nras	Raf1	Rac1	Rac2	Shc2	Src	Hras
Day −1	A{−1}	R{−1}							
Day 1	A{−1}	C{01}	*0.40*	**−0.52***					
	R{−1}			**−0.6***					
	A{−1}	H{01}	**0.53***	*−0.39*	**0.43***	**1.14***	*0.33*		
	R{−1}		*0.36*	**−0.47***	*0.37*	*0.92*	*0.29*		
	A{−1}	E{01}	**0.53***	**−0.51***	*0.28*	**1.16***			
	R{−1}		*0.37*	**−0.6***		*0.94*			
Day 3	A{−1}	C{03}	*0.44*		*0.29*		*0.41*	*0.37*	
	R{−1}						*0.38*	*0.27*	
	C{01}			**0.45***			*0.33*		
	A{−1}	H{03}					*0.38*		*−0.51*
	R{−1}						*0.35*		*−0.38*
	H{01}			*0.32*					
	E{01}	E{03}		*0.34*		*−0.82*			
Day 7	A{−1}	C{07}						*0.24*	
	H{01}	H{07}	**−0.64***	**0.42***	**−0.40***	**−1.08***			
	H{03}		*−0.38*						
	E{01}	E{07}	**−0.67***	**0.44***		**−1.27***			
	E{03}		*−0.46*						
Day 14	A{−1}	H{14}					*0.30*		
	R{−1}						*0.26*		
	C{14}						*0.29*		
	H{01}		**−0.53***	**0.46***	*−0.31*	**−1.22***			
	R{−1}		*−0.36*						
	E{01}	E{14}	**−0.74***	**0.39***	*−0.31*	**−1.28***			
	E{03}		*−0.52*						

Fold change values marked with an asterisk and in boldface letters are significant (p≤0.05) with an adjusted p-value (false discovery rate corrected). Positive fold change values are in white letters on dark background. Genes within this pathway line with no significant differential expression are: Kras.

Table ApxD - 26. The VEGF – Growth Factors & Receptors Gene Profile of Significant Differential Fold Changes (log_2(FC)).

Timing	Reference	Objective	Gene (Symbol)								
			Vegfc	Kdr	Flt1	Pgf	Vegfa	Vegfb	Pdgfc	Figf	Nrp1
Day −1	A{−1}	R{−1}									
Day 1	A{−1}	C{01}		*−0.70*							
	R{−1}			*−0.49*							
	A{−1}	H{01}	*−0.47*	**−1.11***			**−1.11***				
	R{−1}		**−0.65***	**−0.90***			*−0.62*				
	C{01}		*−0.38*								*−0.37*
	A{−1}	E{01}	**−0.57***	*−0.59*			*−0.62*				
	R{−1}		**−0.76***		*0.39*	*0.74*					
	C{01}		*−0.49*			*0.59*					*−0.47*
	H{01}			*0.51*	*0.41*	*0.56*					
Day 3	A{−1}	C{03}		*−0.72*							
	R{−1}			*−0.51*				*2.18*			
	A{−1}	H{03}		*−0.85*	*−0.38*		*−1.02*	*2.19*			
	R{−1}			*−0.64*				*2.43*			
	H{01}		*0.36*								
	A{−1}	E{03}		*−0.76*			*−0.98*				
	R{−1}		*−0.39*	*−0.55*							
	C{03}							*−3.18*			
	H{03}							*−3.43*			
	E{01}		*0.36*		*−0.45*	*−0.73*		*−2.91*			
Day 7	A{−1}	H{07}		*−0.56*	*−0.33*	*−0.63*		*2.20*			
	R{−1}		*−0.46*					*2.44*			
	H{01}			*0.55*							
	A{−1}	E{07}	*−0.61*								
	R{−1}		**−0.80***								
	C{07}		*−0.64*								
	E{01}				*−0.37*	*−0.73*					
	E{03}		*−0.40*				*0.91*	*3.07*			
Day 14	R{−1}	C{14}							*−0.25*		
	R{−1}							*2.31*			
	C{14}								*0.24*		
	H{01}	H{14}	**0.51***	**0.88***			*0.68*			*−0.34*	
	H{03}			*0.62*			*0.59*				
	H{07}					*0.55*				*−0.37*	
	R{−1}	E{14}	*−0.52*								
	C{14}								*0.26*		
	H{14}		*−0.38*								
	E{01}				**−0.52***	**−0.77***					
	E{03}						*0.62*	*3.15*			

Fold change values marked with an asterisk and in boldface letters are significant (p≤0.05) with an adjusted p-value (false discovery rate corrected). Positive fold change values are in white letters on dark background. Genes within this pathway line with no significant differential expression are: Flt4, Nrp2.

Table ApxD - 27. The VEGF – Akt & PI-3-Kinase Signalling Gene Profile of Significant Differential Fold Changes (log_2(FC)).

Timing	Reference	Objective	Gene (Symbol)									
			Pik3r1	Pik3ca	Akt2	Pik3r3	Pik3r2	Akt3	Pik3r5	Akt1	Pik3cb	Pik3cd
Day −1	A{−1}	R{−1}										
Day 1	A{−1}	C{01}	**0.92***	**−0.79***	*−0.45*				*−0.41*			
	R{−1}		**0.84***	**−0.67***	*−0.5*				*−0.38*			
	A{−1}	H{01}		**−0.79***	**−0.51***							
	R{−1}			**−0.67***	**−0.55***							
	C{01}								*0.34*			
	A{−1}	E{01}	**1.18***	**−0.63***	*−0.44*		*−0.44*					
	R{−1}		**1.09***	**−0.51***	*−0.48*		*−0.33*			*−0.43*		
	C{01}					*−0.59*	**−0.58***					
	H{01}		*0.67*				*−0.38*					
Day 3	C{01}	C{03}	**−0.82***	**0.52***	**0.55***							
	A{−1}	H{03}		*−0.41*								
	H{01}		*−0.60*	*0.38*								
	A{−1}	E{03}		*−0.34*								
	R{−1}									*−0.48*		
	C{03}				*−0.36*		*−0.43*					
	H{03}						*−0.34*					
	E{01}		**−1.00***									
Day 7	A{−1}	H{07}		*−0.30*		*0.50*						
	R{−1}							*−0.34*				
	H{01}			**0.49***	**0.49***	**0.63***		*−0.36*			*−0.29*	
	H{03}					*0.53*		*−0.35*				*−0.31*
	C{07}	E{07}	*0.52*				*−0.38*					
	H{07}					*−0.52*						
	E{01}		**−0.85***	*0.34*								
Day 14	A{−1}	C{14}		*−0.34*								
	R{−1}							*−0.31*				
	A{−1}	H{14}		*−0.40*								
	R{−1}							*−0.33*				
	H{01}		**−0.76***	*0.39*	*0.44*	*0.47*		*−0.34*				
	H{03}							*−0.34*				
	H{07}		*−0.49*									
	A{−1}	E{14}		*−0.34*								
	H{14}		*0.59*									
	E{01}		**−0.85***									

Fold change values marked with an asterisk and in boldface letters are significant (p≤0.05) with an adjusted p-value (false discovery rate corrected). Positive fold change values are in white letters on dark background. Genes within this pathway line with no significant differential expression are: Pik3cg.

Table ApxD - 28. The VEGF – Heat Shock Proteins Gene Profile of Significant Differential Fold Changes (log_2(FC)).

Timing	Reference	Objective	Gene (Symbol)	
			Hspb1	Hsp90aa1
Day −1	A{−1}	R{−1}		
Day 1	A{−1}	H{01}	**0.84***	
	R{−1}		*0.70*	
	C{01}			*0.89*
	A{−1}	E{01}	*0.72*	**1.08***
	R{−1}		*0.58*	*0.93*
	C{01}			**1.35***
Day 3	H{01}	H{03}	*−0.58*	
	A{−1}	E{03}	*0.64*	*0.80*
	C{03}			*0.94*
	H{03}			*0.83*
Day 7	C{03}	C{07}	*−0.64*	
	A{−1}	H{07}		*−0.91*
	R{−1}			*−1.06*
	H{01}		**−1.01***	**−1.54***
	H{03}			*−0.88*
	H{07}			*1.04*
	E{01}	E{07}	**−0.91***	*−0.95*
	E{03}		*−0.84*	
Day 14	H{01}	H{14}	**−1.24***	**−1.15***
	H{03}		*−0.65*	
	A{−1}	E{14}	*−0.68*	
	R{−1}		*−0.82*	
	E{01}		**−1.41***	*−0.93*
	E{03}		**−1.33***	

Fold change values marked with an asterisk and in boldface letters are significant (p≤0.05) with an adjusted p-value (false discovery rate corrected). Positive fold change values are in white letters on dark background. Genes within this pathway line with no significant differential expression are: none.

Table ApxD - 29. The VEGF – MAP Kinase Signalling Gene Profile of Significant Differential Fold Changes (log_2(FC)).

Timing	Reference	Objective	Gene (Symbol)				
			Map2k1	Mapk11	Mapk14	Mapkapk3	Mapk3
Day −1	A{−1}	R{−1}					
Day 1	A{−1}	C{01}		**−0.52***	−0.29		
	R{−1}			−0.40			
	A{−1}	H{01}	**0.53***	**−0.67***			
	R{−1}		**0.47***	**−0.55***			
	C{01}		0.49				
	A{−1}	E{01}		**−0.70***			
	R{−1}			**−0.58***			
	H{01}		−0.29				
Day 3	A{−1}	C{03}		**−0.70***	−0.29		
	R{−1}			−0.58		0.45	
	A{−1}	H{03}		−0.62	−0.27		
	R{−1}			−0.50			
	H{01}		−0.36				
	A{−1}	E{03}		**−0.62***	−0.36		
	R{−1}			−0.50			
	C{03}					−0.43	
	E{01}				−0.33		
Day 7	A{−1}	C{07}		−0.46			
	R{−1}			−0.35			
	A{−1}	H{07}		−0.48	−0.32		
	R{−1}			−0.36			
	H{01}		**−0.46***				
	A{−1}	E{07}		−0.55	−0.33		
	R{−1}			−0.44			
	E{01}				−0.29		
Day 14	A{−1}	H{14}		−0.64		−0.51	
	R{−1}			−0.53			
	C{14}			−0.33			
	H{01}		**−0.39***				
	H{03}					−0.46	
	A{−1}	E{14}		−0.56			
	R{−1}			−0.44			
	H{14}						−0.29
	E{01}		−0.29				
	E{03}		−0.28				

Fold change values marked with an asterisk and in boldface letters are significant (p≤0.05) with an adjusted p-value (false discovery rate corrected). Positive fold change values are in white letters on dark background. Genes within this pathway line with no significant differential expression are: Map2k2, Mapk11, Mapk12, Mapk13, Mapkapk2.

Table ApxD - 30. The VEGF – Nfat Signalling Gene Profile of Significant Differential Fold Changes (log_2(FC)).

Timing	Reference	Objective	Gene (Symbol)		
			Nfatc2	Nfatc3	Nfatc4
Day −1	A{−1}	R{−1}			
Day 1	A{−1}	C{01}	−0.36		
	A{−1}	H{01}			0.38
	C{01}	E{01}	0.46		
	H{01}		0.33		
Day 3	A{−1}	C{03}			0.42
	A{−1}	H{03}			0.52
	A{−1}	E{03}			0.50
	C{03}		0.38		
Day 7	H{03}	H{07}		−0.35	
Day 14	E{01}	E{14}	−0.39		
	E{03}		−0.36		−0.56

Fold change values marked with an asterisk and in boldface letters are significant (p≤0.05) with an adjusted p-value (false discovery rate corrected). Positive fold change values are in white letters on dark background. Genes within this pathway line with no significant differential expression are: Nfat5, RGD1560225.

Table ApxD - 31. The VEGF – Phospholipase A2 & C Gene Profile of Significant Differential Fold Changes (log_2(FC)).

Timing	Reference	Objective	Gene (Symbol)										
			Pla2g2d	Pla2g2e	Pla2g1b	Pla2g6	Pla2g12a	Pla2g2a	Pla2g4a	Pla2g3	Pla2g5	Pla2g2f	Pla2g10
Day −1	A{−1}	R{−1}	0.85										
Day 1	A{−1}	C{01}	**1.33***		**−0.39***					−0.36			
	R{−1}				−0.34					−0.29			
	A{−1}	H{01}	**2.05***		**−0.37***		−0.92	1.29		−0.33			
	R{−1}		1.20		−0.32					−0.26			
	C{01}												
	A{−1}	E{01}	**1.53***		−0.26	−0.2	**−1.10***	1.30	0.53				
	R{−1}						−0.71						
	C{01}					−0.2							
Day 3	A{−1}	C{03}	1.67		−0.29	0.22	−0.77			−0.33			
	R{−1}					0.33				−0.26			
	C{01}					0.22							
	A{−1}	H{03}	**1.98***			0.19	−0.93			−0.26			
	R{−1}		1.13			0.31							
	C{03}											0.50	
	H{01}					**0.34***							
	A{−1}	E{03}	**1.65***					1.33	0.53				
	R{−1}												−0.23
	C{03}					−0.22		1.20					
	H{03}					−0.19							
	E{01}					0.20							
Day 7	A{−1}	C{07}	0.85			0.24							
	R{−1}												
	C{03}		−0.82										
	A{−1}	H{07}	0.94				−0.83						
	R{−1}					0.24					−0.26		
	C{07}										−0.33		
	H{01}		−1.11		0.22	**0.27***		−1.42	−0.65				
	H{03}		−1.03						−0.55			−0.33	
	R{−1}					0.20							
	C{07}	E{07}									−0.29		
	E{01}			**0.34***		**0.29***		−1.27	−0.58				
	E{03}		−0.84	0.28				−1.30	−0.58				
Day 14	A{−1}	C{14}	0.99		−0.24								
	R{−1}					0.21							
	C{07}										−0.30		
	A{−1}	H{14}	1.05										−0.23
	R{−1}												
	H{01}		−1.00	0.22	0.26	0.21		−1.08	−0.62				
	H{03}		−0.92	0.23					−0.52			−0.42	
	E{01}	E{14}	−0.95			0.20	0.80	−1.14					
	E{03}		−1.07					−1.17					

Fold change values marked with an asterisk and in boldface letters are significant (p≤0.05) with an adjusted p-value (false discovery rate corrected). Positive fold change values are in white letters on dark background. Genes within this pathway line with no significant differential expression are: Pla2g12b, Pla2g4b, Plcg1, Plcg2.

Table ApxD - 32. The VEGF – Protein Kinase C Gene Profile of Significant Differential Fold Changes (log_2(FC)).

Timing	Reference	Objective	Gene (Symbol) Prkca	Prkcb
Day −1	A{−1}	R{−1}		
Day 1	A{−1}	C{01}	**−0.58***	*0.89*
	R{−1}		**−0.70***	
	A{−1}	H{01}	**−0.68***	*0.92*
	R{−1}		**−0.81***	
	A{−1}	E{01}	**−0.47***	*0.86*
	R{−1}		**−0.59***	
Day 3	C{01}	C{03}	*0.45*	
	R{−1}	H{03}	*−0.39*	
	H{01}		*0.41*	
	R{−1}	E{03}	*−0.31*	
	E{01}		*0.28*	
Day 7	A{−1}	C{07}	*−0.3*	
	R{−1}		*−0.43*	
	R{−1}	H{07}	*−0.35*	
	H{01}		**0.45***	*−0.95*
	H{03}			*−0.82*
	R{−1}	E{07}	*−0.36*	
	E{01}			*−0.90*
Day 14	R{−1}	C{14}	*−0.38*	
	A{−1}	H{14}	*−0.36*	
	R{−1}		*−0.48*	
	H{01}		*0.32*	
	A{−1}	E{14}	*−0.52*	
	R{−1}		*−0.64*	
	E{01}			*−1.07*
	E{03}		*−0.33*	*−0.94*

Fold change values marked with an asterisk and in boldface letters are significant (p≤0.05) with an adjusted p-value (false discovery rate corrected). Positive fold change values are in white letters on dark background. Genes within this pathway line with no significant differential expression are: Prkcg.

Table ApxD - 33. The VEGF – Protein Phosphatases Gene Profile of Significant Differential Fold Changes (log_2(FC)).

Timing	Reference	Objective	Gene (Symbol) Ppp3cc	Ppp3r1	Ppp3cb	Ppp3ca	Ppp3r2
Day −1	A{−1}	R{−1}					
Day 1	A{−1}	C{01}			*−0.55*		
	R{−1}			*0.50*			
	A{−1}	H{01}			*−0.49*	*−0.33*	
	C{01}			*−0.44*			
	R{−1}	E{01}	*−0.25*				
	C{01}			*−0.46*			
Day 3	C{01}	C{03}		*−0.45*			
	C{03}	H{03}					*−0.25*
Day 7	A{−1}	H{07}	*−0.32*				
	R{−1}		*−0.34*				
	H{03}		*−0.26*				
	H{07}	E{07}	*0.22*				

Fold change values marked with an asterisk and in boldface letters are significant (p≤0.05) with an adjusted p-value (false discovery rate corrected). Positive fold change values are in white letters on dark background. Genes within this pathway line with no significant differential expression are: none.

Table ApxD - 34. The VEGF – Transcription Factors Gene Profile of Significant Differential Fold Changes (log_2(FC)).

Timing	Reference	Objective	Gene (Symbol) Arnt	Nfatc2	Nfatc4	Hif1a	Nfatc3
Day −1	A{−1}	R{−1}					
Day 1	A{−1}	C{01}	*−0.30*	*−0.36*		*−1.11*	
	R{−1}		*−0.22*				
	A{−1}	H{01}			*0.38*		
	C{01}	E{01}	**0.37***	*0.46*		*1.32*	
	H{01}			*0.33*			
Day 3	A{−1}	C{03}			*0.42*		
	C{01}		*0.22*				
	A{−1}	H{03}			*0.52*		
	A{−1}	E{03}			*0.50*		
	C{03}			*0.38*			
Day 7	A{−1}	C{07}	*−0.23*				
	A{−1}	H{07}	*−0.24*				
	H{03}		*−0.20*				*−0.35*
	C{07}	E{07}	*0.26*				
	H{07}		*0.27*				
Day 14	A{−1}	C{14}	*−0.22*				
	A{−1}	H{14}	*−0.36*				
	R{−1}		*−0.28*				
	H{01}		*−0.23*				
	H{03}		*−0.31*				
	C{14}	E{14}	*0.25*				
	H{14}		*0.38*				
	E{01}			*−0.39*			
	E{03}			*−0.36*	*−0.56*		

Fold change values marked with an asterisk and in boldface letters are significant (p≤0.05) with an adjusted p-value (false discovery rate corrected). Positive fold change values are in white letters on dark background. Genes within this pathway line with no significant differential expression are: Nfat5, RGD1560225.

Table ApxD - 35. The VEGF – Apoptosis & Cell Cycle Gene Profile of Significant Differential Fold Changes (log_2(FC)).

Timing	Reference	Objective	Gene (Symbol)	
			Bad	Casp9
Day −1	A{−1}	R{−1}		
Day 1	A{−1}	C{01}	0.24	0.30
	R{−1}		0.30	
	A{−1}	H{01}	**0.35***	0.26
	R{−1}		**0.41***	
	R{−1}	E{01}	0.24	
Day 3	R{−1}	C{03}	0.21	
	A{−1}	H{03}	0.21	
	R{−1}		0.27	
Day 7	R{−1}	C{07}	0.24	
	H{01}	H{07}	−0.23	
Day 14	A{−1}	C{14}		0.22
	A{−1}	H{14}	0.29	
	R{−1}		0.36	
	C{14}		0.19	
	R{−1}	E{14}	0.24	

Fold change values marked with an asterisk and in boldface letters are significant (p≤0.05) with an adjusted p-value (false discovery rate corrected). Positive fold change values are in white letters on dark background. Genes within this pathway line with no significant differential expression are: Cdc42.

Table ApxD - 36. The VEGF – Cell Motility, Migration & Morphology Gene Profile of Significant Differential Fold Changes (log_2(FC)).

Timing	Reference	Objective	Gene (Symbol)	
			Ptk2	Pxn
Day −1	A{−1}	R{−1}		
Day 1		C{01}		−0.23
		H{01}	**−0.33***	
			−0.28	
		E{01}	**−0.31***	
			−0.25	
Day 3	H{01}	H{03}	0.20	
Day 14	H{01}	H{14}	**0.28***	
	H{07}			0.24

Fold change values marked with an asterisk and in boldface letters are significant (p≤0.05) with an adjusted p-value (false discovery rate corrected). Positive fold change values are in white letters on dark background. Genes within this pathway line with no significant differential expression are: none.

Table ApxD - 37. The VEGF – Other Related Genes Gene Profile of Significant Differential Fold Changes (log_2(FC)).

Timing	Reference	Objective	Gene (Symbol)					
			Grb2	Sh2d2a	Cav1	Sphk2	Nos3	Ptgs2
Day −1	A{−1}	R{−1}						
Day 1	A{−1}	C{01}	**0.42***	0.30				
	R{−1}		**0.37***	0.25				
	A{−1}	H{01}	**0.35***	**0.47***	−0.33			
	R{−1}		0.29	**0.42***	−0.39			
	C{01}				−0.39			
	A{−1}	E{01}	0.31	0.26				
	R{−1}		0.26		−0.31			
	C{01}				−0.31		0.42	
	H{01}						0.36	
Day 3	A{−1}	C{03}	0.24			0.24		
	R{−1}			0.34				
	A{−1}	H{03}		0.30		0.24		
	R{−1}						−0.45	
	E{01}	E{03}	−0.23					
Day 7	R{−1}	C{07}			−0.29			
	C{03}		−0.21					
	A{−1}	H{07}			−0.38			
	R{−1}				−0.43			
	H{01}		−0.28	**−0.35***				
	A{−1}	E{07}			−0.50			
	R{−1}				**−0.56***	0.29		
	E{03}				−0.28			
Day 14	R{−1}	C{14}				0.37		
	A{−1}	H{14}		0.39				
	R{−1}			0.35		0.37		
	C{14}			0.38				
	H{01}		**−0.30***					
	H{07}			0.27				
	A{−1}	E{14}			−0.36			
	R{−1}				−0.42	0.34		
	C{14}				−0.28			0.22
	H{14}			−0.35				
	E{01}		**−0.32***					

Fold change values marked with an asterisk and in boldface letters are significant (p≤0.05) with an adjusted p-value (false discovery rate corrected). Positive fold change values are in white letters on dark background. Genes within this pathway line with no significant differential expression are: Sphk1.

Appendix D.4.4 The Wound Healing Pathway

Table ApxD - 38. The Wound Healing Extracellular Matrix & Cell Adhesion – Remodelling Enzymes Gene Profile of Significant Differential Fold Changes (log_2(FC)).

Timing	Reference	Objective	Gene (Symbol)										
			Plaur	Ctsl1	F13a1	Plau	Mmp7	Fga	Ctsk	Mmp2	Ctsg	F3	Plg
Day −1	A{−1}	R{−1}			1.08		0.92						
Day 1	A{−1}	C{01}			**1.49***	0.69							
	R{−1}						**−0.84***						
	A{−1}	H{01}	**0.96***	**0.90***	**1.81***	**1.05***							
	R{−1}		**0.90***	0.60		0.73	**−0.76***						
	C{01}		0.51	0.54									
	A{−1}	E{01}	**1.38***	0.75	**1.54***	**1.29***		0.45					
	R{−1}		**1.33***			**0.97***	**−0.79***	0.48					
	C{01}		**0.93***			0.60		0.54					
	H{01}							0.55					
Day 3	A{−1}	C{03}			1.07								
	R{−1}						−1.05						
	A{−1}	H{03}			1.50	0.56			0.76	0.87			
	R{−1}						**−1.06***						
	H{01}		−0.70	−0.50					0.67				
	A{−1}	E{03}	0.71		1.44	0.56							
	R{−1}		0.66				−0.57						
	C{03}						0.48						
	H{03}						0.48						
	E{01}		−0.66			−0.72		−0.39					
Day 7	A{−1}	C{07}							0.80	0.83			
	R{−1}						**−1.07***						
	C{03}												
	R{−1}	H{07}					−0.84						
	H{01}		**−1.12***	**−0.98***	**−1.42***	−0.66							
	H{03}				−1.11								
	A{−1}	E{07}				0.57							
	R{−1}						−0.78						
	C{07}												
	E{01}		**−1.14***	**−0.88***	−1.12	−0.71		−0.41					
	E{03}				−1.02								
Day 14	A{−1}	C{14}					0.58						
	R{−1}											−0.74	
	C{07}						0.73		−0.83				
	R{−1}	H{14}					−0.48						
	C{14}										−0.25		
	H{01}		**−0.88***	**−0.96***	**−1.20***	**−0.81***							
	H{03}				−0.89		0.57						
	A{−1}	E{14}						0.51					
	R{−1}			−0.58			−0.59	0.54					
	C{14}							0.54					
	H{14}							0.55					−0.63
	E{01}		**−1.27***	**−1.04***	**−1.30***	**−0.94***							
	E{03}		−0.60	−0.58	−1.21			0.45	−0.64				
	E{07}							0.47					

Fold change values marked with an asterisk and in boldface letters are significant ($p \leq 0.05$) with an adjusted p-value (false discovery rate corrected). Positive fold change values are in white letters on dark background. Genes within this pathway line with no significant differential expression are: Mmp1, Mmp9, Plat, Serpine1, Timp1.

Table ApxD - 39. The Wound Healing Extracellular Matrix & Cell Adhesion – ECM Components Gene Profile of Significant Differential Fold Changes (log_2(FC)).

Timing	Reference	Objective	Gene (Symbol)									
			Col14a1	Col4a1	Col1a2	Col5a2	Col5a1	Col3a1	Col1a1	Col5a3	Col4a3	Vtn
Day −1	A{−1}	R{−1}			0.87							
Day 1	A{−1}	C{01}		0.41								
	A{−1}	H{01}									−0.22	
	R{−1}											−0.43
	C{01}											−0.49
Day 3	A{−1}	C{03}	0.79		1.04	1.12	0.97	1.07	1.17			
	R{−1}					0.82	0.71			0.72		
	C{01}		0.57				0.60			0.87		
	A{−1}	H{03}	0.95		1.38	1.21	0.93	1.19	1.48			
	R{−1}		0.59			0.91	0.68					
	H{01}		**0.86***		1.09			0.76	1.05			
	A{−1}	E{03}	0.62		1.45	0.99		1.07	1.12			
	C{03}									−0.81		
	E{01}		0.62		0.98							
Day 7	A{−1}	C{07}	0.75				0.66		1.15			
	A{−1}		0.59									
	H{01}	H{07}		−0.52								
	H{03}					−0.77						
	C{07}										0.22	
	E{01}	E{07}		**−0.63***								
	E{03}			−0.37	−1.25	−0.81		−0.85				
Day 14	R{−1}	C{14}			−0.96							
	C{07}		−0.53		−0.99		−0.61					
	A{−1}	H{14}		−0.39								
	R{−1}			−0.44								
	H{01}			**−0.66***								
	H{03}		−0.58			−1.02	−0.77	−1.00				
	A{−1}	E{14}		−0.56								
	R{−1}			−0.61								
	E{01}			**−0.86***		−0.77						
	E{03}		−0.59	−0.60	−1.37	−1.18	−0.77	−1.06	−0.97			

Fold change values marked with an asterisk and in boldface letters are significant ($p \leq 0.05$) with an adjusted p-value (false discovery rate corrected). Positive fold change values are in white letters on dark background. Genes within this pathway line with no significant differential expression are: none.

Table ApxD - 40. The Wound Healing Extracellular Matrix & Cell Adhesion – Cellular Adhesion Gene Profile of Significant Differential Fold Changes (log_2(FC)).

Timing	Reference	Objective	Itga1	Itgb1	Itga6	Cdh1	Itga5	Itgb5	Itga4	Itgb3
Day −1	A{−1}	R{−1}						1.44		
Day 1	A{−1}	C{01}		2.91*		−2.23	1.75	1.94		
	R{−1}			2.59*						
	A{−1}	H{01}	−1.62*	2.33*	−1.67*	−2.36	2.00			
	R{−1}		−1.97*	2.01		−2.68	1.58			
	C{01}		−1.41		−1.66					
	A{−1}	E{01}		1.64	−1.62*		1.96		4.79	1.05
	R{−1}					−2.13			5.33	
	C{01}				−1.61			−1.67		
	H{01}		1.35							
Day 3	A{−1}	C{03}		2.25			2.70	2.36		
	R{−1}			1.83			2.28			
	C{01}					1.92				
	A{−1}	H{03}		1.62	−1.68	−2.69	1.79	2.67		1.21
	R{−1}					−3.01				
	C{03}					−2.71				
	H{01}		1.60					1.51		
	A{−1}	E{03}			−1.81	−2.4	2.24	1.77		1.16
	R{−1}					−2.73	1.82			
	C{03}					−2.42				
	E{01}							1.51	−3.93	
Day 7	A{−1}	C{07}						2.08		
	R{−1}					−2.21				
	C{03}					−1.90	−1.61			
	A{−1}	H{07}			−1.45	−2.41				
	R{−1}					−2.74				
	H{01}		1.43							
	R{−1}	E{07}	−1.29					−1.51		
	C{07}								−4.08	−1.08
	E{01}									−1.18
	E{03}				0.97					
Day 14	A{−1}	C{14}			−1.13					
	A{−1}	H{14}			−1.17	−2.97				1.05
	R{−1}					−3.3				
	H{01}		1.66*							
	H{03}							−1.59		
	A{−1}	E{14}			−1.21					
	R{−1}					−2.12				
	C{14}								4.33	
	E{01}			−1.49			−1.90			
	E{03}						−2.18			−0.94

Fold change values marked with an asterisk and in boldface letters are significant (p≤0.05) with an adjusted p-value (false discovery rate corrected). Positive fold change values are in white letters on dark background. Genes within this pathway line with no significant differential expression are: Itga2, Itga3, Itgav, Itgb6.

Table ApxD - 41. The Wound Healing Extracellular Matrix & Cell Adhesion – Cytoskeleton Gene Profile of Significant Differential Fold Changes (log_2(FC)).

Timing	Reference	Objective	Rac1	Actc1	Tagln
Day −1	A{−1}	R{−1}		4.76	1.53
Day 1	A{−1}	C{01}		4.92	
	A{−1}	H{01}	1.74*	5.03	
	R{−1}		1.51		−1.59
	A{−1}	E{01}	1.14		
	R{−1}				−1.64
Day 3	A{−1}	C{03}	1.17	4.21	1.84
	A{−1}	H{03}		5.07	1.42
	H{01}				1.48
	A{−1}	E{03}		7.09	
	E{01}			4.34	
Day 7	H{01}	H{07}	−1.63*		
	R{−1}	E{07}			−1.68
	E{03}			−5.44	
Day 14	R{−1}	C{14}		−5.58	
	H{01}	H{14}	−1.25	−4.21	
	H{03}			−4.25	
	E{01}	E{14}	−1.26		
	E{03}			−5.82	

Fold change values marked with an asterisk and in boldface letters are significant (p≤0.05) with an adjusted p-value (false discovery rate corrected). Positive fold change values are in white letters on dark background. Genes within this pathway line with no significant differential expression are: Acta2, Rhoa.

Table ApxD - 42. The Wound Healing – Inflammatory Cytokines & Chemokines Gene Profile of Significant Differential Fold Changes (log_2(FC)).

Timing	Reference	Objective	Ccl7	Ccl12	Il6	Il1b	Cxcl3	Il10	Cxcl1	Ifng	Il4
Day −1	A{−1}	R{−1}									
Day 1	A{−1}	H{01}	10.47*	5.27							
	R{−1}		8.04								
	C{01}		6.90	4.92							
	A{−1}	E{01}	13.85*	7.40*	4.25*	4.74*	3.51	1.18			
	R{−1}		11.42*	6.07	4.02*	3.07	3.83				
	C{01}		10.28*	7.05*	3.64	3.36	3.47	1.26			
	H{01}				3.00						
Day 3	C{03}	H{03}									−0.72
	H{01}		−8.69*								
	C{03}	E{03}							4.07	0.72	
	H{03}									0.65	
	E{01}		−11.41*	−7.60*	−3.59	−3.35	−3.13				
Day 7	C{03}	C{07}									−0.72
	H{01}	H{07}	−11.58*	−6.21*		−3.02	−2.54				
	E{01}	E{07}	−13.44*	−8.73*	−3.93*	−3.63	−3.86*	−1.12	−4.21		
Day 14	H{01}	H{14}	−11.03*	−6.73*							
	E{01}	E{14}	−13.40*	−9.21*	−4.18*	−4.21*	−3.29	−1.22	−4.13		
	E{03}									−0.66	

Fold change values marked with an asterisk and in boldface letters are significant (p≤0.05) with an adjusted p-value (false discovery rate corrected). Positive fold change values are in white letters on dark background. Genes within this pathway line with no significant differential expression are: Cd40lg, Cxcl11, Cxcl5, Il2.

Table ApxD - 43. The Wound Healing – Growth Factors Gene Profile of Significant Differential Fold Changes (log_2(FC)).

Timing	Reference	Objective	Gene (Symbol)										
			Pdgfa	Csf3	Hbegf	Mif	Fgf7	Hgf	Angpt1	Fgf2	Fgf10	Ctgf	Igf1
Day −1	A{−1}	R{−1}											
Day 1	A{−1}	C{01}	−1.49	**−3.12***				1.25					
	R{−1}		−1.26	**−2.47***		−1.09		1.10	2.28				
	A{−1}	H{01}											
	R{−1}			1.99	3.96				−1.80		1.06		
	C{01}					−1.29							
	A{−1}	E{01}	1.34			**−1.70***				2.01			
	R{−1}		1.56										
	C{01}		**2.83***	**3.14***	4.20								
	H{01}		2.04										
Day 3	A{−1}	C{03}		−2.22				1.09					
	R{−1}			−1.57				0.93					
	C{01}												
	A{−1}	H{03}								2.36			
	R{−1}										−0.97		
	H{01}												
	A{−1}	E{03}				−1.22				1.80			
	R{−1}												
	C{03}			2.07									
	E{01}		**−2.18***										
Day 7	A{−1}	C{07}		−2.33			1.50						
	R{−1}			−1.68			1.51						
	A{−1}	H{07}					1.58						
	R{−1}				−4.18	−1.02	1.58						
	H{01}				−4.44								
	H{03}							−0.95					
	R{−1}	E{07}			−4.36				2.11				
	C{07}			1.92									
	E{01}		**−2.45***		−4.86	0.93							
	E{03}				−4.57								
Day 14	A{−1}	C{14}		−2.01			1.62		2.08				
	R{−1}						1.62						
	A{−1}	H{14}					1.76						
	R{−1}				−5.21		1.77						
	H{01}				**−5.47***							4.48	
	H{03}							−1.04					
	H{07}					0.91							
	A{−1}	E{14}					2.66						
	R{−1}				−5.52	−0.93	2.67		2.28	2.01			−2.30
	C{14}			1.58									
	E{01}		**−1.69***		**−6.02***		1.95						
	E{03}				−5.74		1.79						
	E{07}						1.83						

Fold change values marked with an asterisk and in boldface letters are significant (p≤0.05) with an adjusted p-value (false discovery rate corrected). Positive fold change values are in white letters on dark background. Genes within this pathway line with no significant differential expression are: Csf2, Egf, Tgfa, Tgfb1, Tnf, Vegfa.

Table ApxD - 44. The Wound Healing Signal Transduction – TGF Gene Profile of Significant Differential Fold Changes (log_2(FC)).

Timing	Reference	Objective	Gene (Symbol)	
			Tgfb1	Stat3
Day −1	A{−1}	R{−1}		
Day 1	A{−1}	C{01}	**2.87***	
	R{−1}		1.99	
	A{−1}	H{01}	**3.46***	
	R{−1}		**2.58***	1.94
	A{−1}	E{01}	2.25	**2.14***
	R{−1}			**2.69***
	C{01}			1.87
Day 3	A{−1}	C{03}	2.80	
	R{−1}		1.92	
	A{−1}	H{03}	2.22	
	H{01}			−1.68
	A{−1}	E{03}	2.45	
	E{01}			−1.61
Day 7	H{01}	H{07}	**−2.61***	−1.81
	E{01}	E{07}		−2.00
Day 14	H{01}	H{14}	**−2.33***	−1.54
	E{01}	E{14}	−2.21	**−2.62***
	E{03}		−2.42	

Fold change values marked with an asterisk and in boldface letters are significant (p≤0.05) with an adjusted p-value (false discovery rate corrected). Positive fold change values are in white letters on dark background. Genes within this pathway line with no significant differential expression are: Tgfbr3.

Table ApxD - 45. The Wound Healing Signal Transduction – WNT Gene Profile of Significant Differential Fold Changes (log_2(FC)).

Timing	Reference	Objective	Gene (Symbol)	
			Wnt5a	Wisp1
Day −1	A{−1}	R{−1}		
Day 1	A{−1}	H{01}	**−1.91***	
	R{−1}		**−1.81***	
	C{01}		−1.68	
	A{−1}	E{01}	−1.38	
	R{−1}		−1.29	
	C{01}		−1.15	
Day 3	A{−1}	C{03}		3.82
	A{−1}	H{03}	−1.11	
	A{−1}	E{03}	−1.33	
	R{−1}		−1.23	
Day 7	A{−1}	H{07}	−1.07	
Day 14	C{07}	C{14}		−3.06
	A{−1}	H{14}	−1.06	

Fold change values marked with an asterisk and in boldface letters are significant (p≤0.05) with an adjusted p-value (false discovery rate corrected). Positive fold change values are in white letters on dark background. Genes within this pathway line with no significant differential expression are: Ctnnb1.

Table ApxD - 46. The Wound Healing Signal Transduction – Phosphorylation Gene Profile of Significant Differential Fold Changes (log_2(FC)).

Timing	Reference	Objective	Gene (Symbol)	
			Pten	Mapk3
Day −1	A{−1}	R{−1}		
Day 3	C{01}	C{03}	−1.24	
Day 7	R{−1}	H{07}	−1.19	
	H{01}		−1.13	
Day 14	R{−1}	C{14}	−1.07	
	H{14}	E{14}		−1.16

Fold change values marked with an asterisk and in boldface letters are significant (p≤0.05) with an adjusted p-value (false discovery rate corrected). Positive fold change values are in white letters on dark background. Genes within this pathway line with no significant differential expression are: Mapk1.

Table ApxD - 47. The Wound Healing Signal Transduction – Receptors Gene Profile of Significant Differential Fold Changes (log_2(FC)).

Timing	Reference	Objective	Gene (Symbol)
			Il6st
Day −1	A{−1}	R{−1}	
Day 7	R{−1}	H{07}	−1.23

Fold change values marked with an asterisk and in boldface letters are significant (p≤0.05) with an adjusted p-value (false discovery rate corrected). Positive fold change values are in white letters on dark background. Genes within this pathway line with no significant differential expression are: Egfr.

The Wound Healing **Signal Transduction – Other Related Gene Profile of Ptgs2** did not demonstrate any significant differential fold changes.